Medicinal Chemistry Techniques to Gain Selectivity at G Protein-Coupled Receptors Targeting the CNS:

M_4 Muscarinic Acetylcholine Receptor Positive Allosteric Modulators, Dopamine D_2 Receptor Biased Ligands, M_1/D_2 Merged Ligands and D_2 Fluorescently Labelled Ligands.

A thesis submitted for the degree of Doctor of Philosophy

By

Monika Szabo

Department of Medicinal Chemistry and Drug Discovery Biology
Faculty of Pharmacy and Pharmaceutical Sciences
Monash University
2014

MONASH University
Pharmacy and Pharmaceutical Sciences

Copyright Notices

Notice 1

Notice 2

We shall not cease from exploration,
And the end of all our exploring
Will be to arrive where we started
And know the place for the first time.

-T.S. Eliot

Table of contents

Statement of Originality

I hereby declare that this thesis contains no material which has been accepted for the award of any other degree or diploma at any university or equivalent institution and that, to the best of my knowledge and belief, this thesis contains no material previously published or written by another person, except where due reference is made in the text of the thesis.

Monika Szabo

General Declaration

In accordance with Monash University Doctorate Regulation 17 Doctor of Philosophy and Research Master's regulations the following declarations are made:

I hereby declare that this thesis contains no material which has been accepted for the award of any other degree or diploma at any university or equivalent institution and that, to the best of my knowledge and belief, this thesis contains no material previously published or written by another person, except where due reference is made in the text of the thesis.

This thesis includes 1 original paper published in a peer reviewed journal, 1 submitted paper and 2 unpublished publications currently in manuscript format. This thesis explores medicinal chemistry techniques that may be used to gain selectivity at G protein-coupled receptors targeting the CNS. This involves the development of positive allosteric modulators for the M_4 muscarinic acetylcholine receptor, dopamine D_2 receptor biased ligands, M_1/D_2 merged ligands and D_2 fluorescently labelled ligands.

The ideas, development and writing up of all the papers in the thesis were the principal responsibility of myself, the candidate, working within Monash University under the supervision of Dr Ben Capuano and Prof. Arthur Christopoulos. The inclusion of co-authors reflects the fact that the work came from active collaboration between researchers and acknowledges input into team-based research.

In the case of chapters 2-5 my contribution to the work involved the following:

Thesis Chapter	Publication title	Publication status	Nature and extent of candidates contribution
2	A SAR Study of the Positive Allosteric Modulator LY2033298 at	Unpublished	Synthesis, characterisation and testing of compounds. Writing and preparation of the

Thesis Chapter	Publication title	Publication status	Nature and extent of candidates contribution
	the M_4 Muscarinic Acetylcholine Receptor		manuscript. Main author of the manuscript. 65% contribution.
3	Structure-Activity Relationships of Privileged Structures Lead to the Discovery of Novel Biased Ligands at the Dopamine D_2 Receptor	Published	Synthesis, characterisation and testing of all compounds. Writing and preparation of the manuscript. Main author of the manuscript. 85% contribution.
4	Designed Multiple Ligands Targeting the Dopamine D_2 and Muscarinic M_1 Receptors	Submitted	Synthesis, characterisation and testing of compounds. Writing and preparation of the manuscript. Main author of the manuscript. 80% contribution.
5	Fluorescently Labelled Ligands for the Dopamine D_2 Receptor	Unpublished	Synthesis, characterisation and testing of all compounds. 85% contribution.

I have not renumbered sections of published papers or unpublished manuscripts within the thesis. Every chapter stands on its own and therefore the numbering of the chemical structures, figures, schemes, tables and references commences in each chapter from 1.

Signed:

Date:

Acknowledgments

There is often a great deal more behind a PhD than the research. Being independent takes on a deeper level and your tenacity is sought to its fullest. When I look back on how far I've come as a scientist and the breadth of knowledge that I've learned, I know that I would not have got there had it not been for some fundamental people.

First and foremost I would like to express my sincere gratitude to my two supervisors Dr Ben Capuano and Prof. Arthur Christopoulos. Ben thank you for believing in me as a student all those years back when I started honours with you and for all the chemistry wisdom you have given me. Your optimism is really something that I've appreciated, especially when things didn't always work out the way we planned. Arthur thank you for always pushing me to take my research to the highest level possible. Your level of detail and knowledge on everything from pharmacology to writing manuscripts is definitely something that you have imparted on me. I would equally like to thank Dr Robert Lane who started out teaching me all the pharmacology but quickly acquired a central role in my PhD. Your ideas and feedback on all aspects of my projects has really been paramount and I don't think my research would have been at the level it is had it not been for your involvement. I really could not have asked for someone better as a mentor throughout my time at Monash.

To all the members of labs 103/106 both past and present: Manuela Jorg, Anitha Kopinathan, Jeremy Shonberg, Vladimir Moudretski, Tracey Huynh, Fiona McRobb, Dragan Krsta and Tim Fyfe. I have so many great memories with each of you from all the conferences we attended together, travelling overseas to Europe, office fun (fashion parades and grasshoppers), trivia nights, postgrad balls, lunchtimes in the sun and so much more. Having you all around at various stages to trouble-shoot chemistry ideas or just to have a laugh after a stressful day made my PhD life so much better. To all my fellow medchem PhD students and post-docs that I've met along

the way (there are too many to be named) thank you for your advice and friendship. Special mention to Briana Davie who has shared this journey with me from first year undergrad right up to the end of our PhDs.

There are numerous PhD students and post-docs in DDB that I would also like to thank. You all made me feel welcome and were always willing to help me out when I needed it. In particular thank you to all members in the dopamine group: Carmen Klein Herenbrink, Chris Draper-Joyce and Herman Lim. I am likewise grateful to Dr Meri Canals and Dr Michelle Halls for your suggestions and feedback during our group meetings. Particular thanks to Cameron Nowell for all your expertise and assistance with achieving such great results with the confocal microscopy. Thank you to my PhD panel members Prof. Peter Scammells and Dr Daniel Malone for your advice and input on my projects over the course of my PhD. I would also like to thank Dr Jason Dang for running various characterisation data for me.

As with everything in life, you must always have down time and the friends in my life made that transition so easy for me. I am so blessed to have such a beautiful support network of friends who never fail to bring me back to center and constantly make me smile, especially at the times when I needed it the most. In particular: Tash, Ange, Andrea, Emma, Maria, Dian, Sheryn, Haset and Nat, thank you for being the most amazing group of friends I could ever ask for.

Lastly, I would like to thank my Dad, Mum and Laci for being supportive of me no matter what path I've chosen to take in life and the decisions I've made along the way. This is of course mirrored for my extended family who have always shown how proud they are of me and always go out of their way to make sure I'm happy and doing okay. I love you and appreciate you all so much.

As I close this chapter in my life I am not fearful of what will come next, rather I am ready for the new challenges that await me. Change is beautiful if you let it be.

Abbreviations

^0C	degrees celsius
2-MPP	2-methoxyphenyl piperazine
5-HT	5- hydroxytrptamine
AC	adenylate cyclase
ACh	acetylcholine
ADME	absorption, distribution, metabolism and excretion
aq.	aqueous
BBB	blood brain barrier
Boc	*tert*-butyloxycarbonyl
BODIPY	boron-dipyrromethene
BOP	(benzotriazol-1-yloxy)tris(dimethylamino)phosphonium hexafluorophosphate.
cAMP	cyclic adenosine monophosphate
$CDCl_3$	deuterated chloroform
CH_3CN	acetonitrile
$CHCl_3$	chloroform
CHO	Chinese hamster ovary
CNS	central nervous system
Compd	compound
D_{2L}	dopamine D_2 receptor long
D_2R	dopamine D_2 receptor
d_6-DMSO	deuterated dimethyl sulfoxide
DCE	dichloroethane
DCM	dichloromethane
DIBAL-H	diisobutylaluminium hydride
DIPEA	*N*,*N*-diisopropylethylamine
DMAP	4-dimethylaminopyridine
DMEM	Dulbecco's Modified Eagle Medium
DMF	dimethylformamide
DML	designed multiple ligand
DMSO	dimethyl sulfoxide
EC_{50}	half maximal effective concentration

E_{max}	maximal stimulation in the control condition
EPS	extrapyramidal side effects
equiv.	equivalent
ERK	extracellular-regulated kinase
ESI	electrospray ionisation
EtOAc	ethyl acetate
EtOH	ethanol
FBS	fetal bovine serum
FDA	The food and drug administration
FITC	fluorescein isothiocyanate
FSK	forskolin
GIRK	G protein-coupled inwardly-rectifying potassium channels
GPCR	G protein-coupled receptor
h	hours
HEPES	2-[4-(2-hydroxyethyl)-1-piperazinyl]ethanesulfonic acid
hERG	human ether-a-go-go related gene
HPLC	high performance liquid chromatography
HRMS	high resolution mass spectrometry
HTS	high throughput screen
IC_{50}	half maximal inhibitory constant
K_B	functional equilibruim binding constant
K_i	inhibitory constant
LCMS	liquid chromatography mass spectrometry
LRB	lissamine rhodamine B
M	molar concentration
mAChR	muscarinic acetylcholine receptor
MAPK	mitogen-activated protein kinase
MeOH	methanol
MHz	megahertz
min	minutes
mp	melting point
MS	mass spectrometry
MW	molecular weight

NAM	negative allosteric modulator
nm	nanometer
nM	nanomolar
NMR	nuclear magnetic resonance
NMS	*N*-methylscopolamine
PAM	positive allosteric modulator
PBS	phosphate-buffered saline
pM	picomolar
PREP-HPLC	preparative high performance liquid chromatography
RT	room temperature
SAR	structure activity relationship
SEM	standard error of the mean
TFA	trifluoroacetic acid
THF	tetrahydrofuran
TLC	thin layer chromatography
TM	transmembrane
t_R	retention time
UV	ultraviolet
α	affinity modulation
αβ	cooperativity
β	efficacy modulation
δ	chemical shift
λ	wavelength
μM	micromolar
μm	micron

Abstract

The study of G protein-coupled receptors (GPCRs) and their role in central nervous system (CNS) disorders and/or disease states is integral to drug discovery. For schizophrenia, a favourable polypharmacology profile is useful to effectively treat all symptom domains of the disorder. However, GPCRs can be difficult to gain subtype selectivity in order to avoid binding to receptors in the same family and to various off-target receptors. This thesis explores multiple medicinal chemistry approaches to achieve subtype selectivity or pathway specificity, and tools to screen for new compounds and/or scaffolds.

Chapter 2 investigates the use of positive allosteric modulators (PAMs) for the M_4 muscarinic acetylcholine receptor (mAChR). A comprehensive structure activity relationship (SAR) study around the PAM, LY2033298, was conducted, which investigates different linkage points, halogen replacements and different substitution combinations on the thienopyridine scaffold. The compounds are evaluated via the use of an operational model of allosterism to determine values of functional affinity (K_B), cooperativity ($\alpha\beta$) and intrinsic agonism (τ_B) for all compounds. These parameters allowed the elucidation of the molecular determinants of allostery that may be important for certain functional changes.

Chapter 3 explores the concept of biased agonism as an approach to gain pathway-specific selectivity at the dopamine D_2 receptor (D_2R). The determinants of efficacy, affinity and bias for three privileged structures for the D_2R were explored by focusing on changes to linker length and incorporation of a heterocyclic unit. By quantifying bias at two signalling pathways (cAMP and pERK1/2), distinct bias patterns were observed associated with the substitution of certain phenylpiperazine structures. Subtle structural changes to the heterocycle resulted in significant effects on bias that over-ruled the effect of the phenylpiperazine substitution pattern. As such the series of compounds may represent useful tools to gain further insight into the contribution of biased agonism to antipsychotic efficacy.

Chapter 4 uses a "designed multiple ligand" approach, to rationally synthesise compounds with a favourable polypharmacology profile. Specifically, D_2/5-HT_{2A} activity has been implicated as useful for antipsychotic efficacy and activity at M_1 mAChRs is highlighted as an important target for the cognitive deficits in key CNS disorders. The hybridisation process makes use of substituted piperazine or pipridine privileged structures with D_2 or D_2/5-HT_{2A} activity in combination with the putative M_1 mAChR allosteric agonist LuAE51090. The focused library of compounds was profiled in both radioligand binding assays in addition to functional assays at the M_1 mAChR, D_2R and 5-HT_{2A}R. From this we identified a compound which retained activity at all three receptors and therefore represents an ideal starting point for further optimisation.

Chapter 5 explores the use of fluorescently labelled ligands as pharmacological tools for the D_2R of which there is a notable lack thereof in the literature. A series of ligands based on two clinical compounds, clozapine and ropinirole, in addition to a negative allosteric modulator, SB269652, and its high-affinity variant 2-MPP-SB269652, were selected to create a series of fluorescently labelled ligands. The ligands were tethered to a spectrum of fluorophores (BODIPY 630/650-X, Cy5, Cy3, FITC and LRB) as each of the fluorophores varied in spectral properties and chemical scaffolds. Three of the four series maintained functionality at the D_2R, with the derivatives of 2-MPP-SB269652 maintaining high binding affinities. Three novel fluorescent ligands demonstrated rather specific cell membrane binding and very weak non-specific binding. These fluorescent ligands represent useful tools to be adapted towards multiple applications for the D_2R and a starting point for further optimisation.

Finally, chapter 6 provides a brief summary of the outcomes from this thesis, as well as directions for future prospects.

Chapter 1- Introduction and Thesis Aims

Introduction

1. G protein-coupled receptors as central nervous system drug targets

1.1. GPCR structure and function

G protein-coupled receptors (GPCRs) are a dynamic class of cell-surface proteins that consist of seven transmembrane α helices. Five families exist (rhodopsin (family A), secretin (family B), glutamate (family C), adhesion and frizzled/ taste2) of which several members contain their own receptor families and subtypes. GPCRs can be activated by a variety of different ligands such as small molecules, peptides, hormones, neurotransmitters and light. The mechanism of action of these receptors stems initially from the activation of the receptor via these ligands binding to the receptor. This in turn initiates a conformational change in the receptor and subsequently triggers a response by the heterotrimeric G proteins. These G proteins, consisting of α, β and γ subunits, undergo a change that results in guanosine diphosphate (GDP) being exchanged for guanosine triphosphate (GTP). The Gα and Gβγ subunit can then go on to activate effector molecules.[1-3] In particular, this thesis explores the signaling of GPCRs coupled to either $G_{q/11}$ or $G_{i/o}$ G proteins (Figure 1). Coupling to the $G_{q/11}$ family of G proteins results in the activation of phospholipase C (PLC) which will then release inositol-1,4,5-trisphosphate (IP_3) and therefore mobilise intracellular calcium (Ca^{2+}). IP_3 can also signal to IP_2 and consequently IP_1. Conversely coupling to the $G_{i/o}$ family of G proteins results in the inhibition of adenylate cyclase (AC) and therefore the inhibition of cyclic adenosine monophosphate (cAMP). Additionally, both pathways lead to the activation of ERK1/2, which is significantly more downstream in the signaling cascade. The involvement of effector molecules to second messengers and ultimately a biological response in the signaling transduction cascade is complex. In many cases it can be represented as a linear process however it is now known that this is not the case and a biological response can be attributed to cross-talk between other GPCRs and other signaling pathways, and also signaling

pathways that are not dependent on G protein activation.[4] These receptors are important drug targets, as approximately 30% of FDA approved drugs act at GPCRs,[5] the largest of any class.

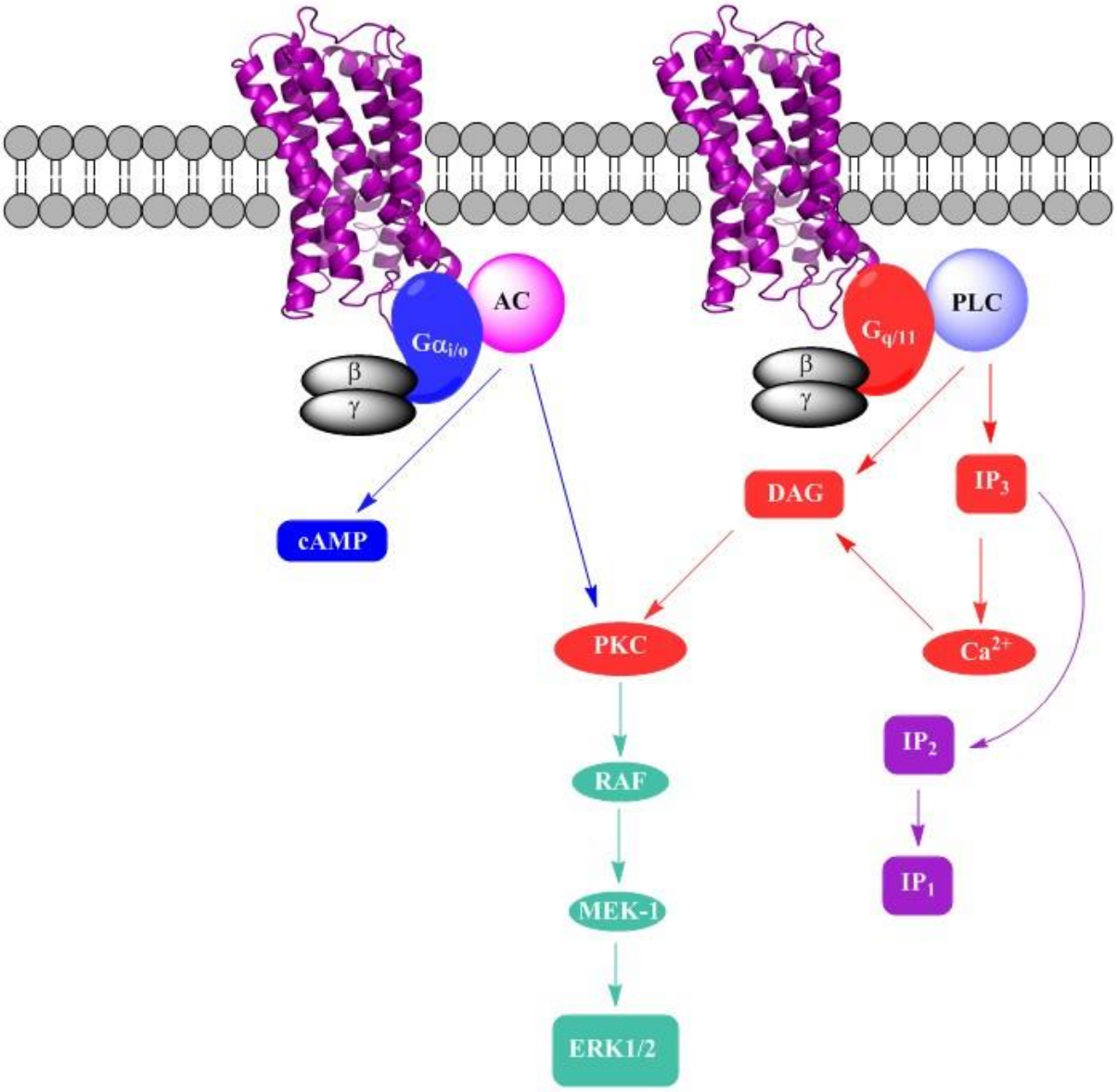

Figure 1. Simplified signal transduction pathway of $G_{q/11}$ and $G_{i/o}$ coupled GPCRs to key pathways explored in this thesis (Ca^{2+}, IP_1, cAMP and ERK1/2).

1.2. Targeting the CNS

Drug design for the central nervous system (CNS) is notoriously difficult due to the requirement for the drug to cross the blood-brain barrier (BBB). The BBB consists of three important

components, endothelial cells, astrocyte end feet and pericytes; all imperative for function and maintenance. Tight junctions are also a crucial part of the BBB, as they form a diffusion barrier that allows for tight control of what can pass through to the brain.[6] The overall passage of drugs through the BBB is dependent on several factors and will usually occur through either lipid-mediated free diffusion or carrier/receptor mediated transport.[7] There are multiple intrinsic properties of a drug/ligand that determine BBB penetration. Quantitative structure-activity relationship (QSAR) descriptors include lipophilicity, molecular weight, hydrogen bonding, polar surface area, molecular volume and flexibility, charge, pharmacokinetics, metabolic stability and liability, permeability, protein binding and hERG inhibition.[8] Lipinski's 'rule of 5' are a set of guidelines common to medicinal chemists to determine if a drug will be permeable and/or water soluble. They focus solely on the physical characteristics of the ligand, i.e. molecular weight, logP, hydrogen bond donors and acceptors and number of rotatable bonds.[9] Ligands generally must be more lipophilic than hydrophilic. As a consequence, there is a fine line between a drug having good absorption, distribution, metabolism and excretion (ADME) properties and also being able to pass the BBB. Coupled with selectivity for a GPCR target, targeting the CNS makes for a challenging undertaking.

1.3. Involvement of Class A GPCRs in CNS disorders

The involvement of class A GPCRs in the CNS is quite extensive. By examining six CNS disorders and/or disease states, we can observe that multiple different receptors and their respective subtypes are implicated (Table 1) and their contribution can be both direct and/or indirect. For example, the use of an antagonist can act directly on the dopamine D_2 receptor to decrease the hyperactivity of dopamine in the brain for the treatment of schizophrenia.[10] Whereas M_1 agonists can have direct action in the cognitive aspect of Alzheimer's disease but may also be involved indirectly, as activation of M_1 receptors stimulates the release of the

amyloid precursor protein, which plays an important part in the complex cascade of the disease.[11]

When considering the design of a drug for a particular disorder or disease state, it is important to consider which receptors are viable targets. Receptor profiling in this regard can reveal a great deal about a disease state. For example, by examining the implicated receptors in Table 1, it is evident that certain areas of the brain contain multiple GPCRs from different families in addition to subtypes belonging to the same family (Figure 2). The top three areas most affected are the hippocampus, hypothalamus and amygdala. The hippocampus, the most highly affected area, is responsible for memory, spatial navigation and emotional responses. The hypothalamus is particularly important for synthesizing and secreting hormones, one of these being dopamine. In addition, it also has many regulatory functions such as motor function control, body temperature, thirst, sleep and many more. The amygdala is associated with emotional responses, memory and secretion of hormones. As such, the functions of these three areas have a direct impact on all the disease states mentioned in Table 1, i.e. schizophrenia (negative symptoms: emotional, regulation of dopamine and cognitive: memory), Parkinson's disease (motor function and control), Alzheimer's disease (cognitive; memory), depression (emotional), epilepsy (motor function and control) and anxiety (emotional). Therefore it is evident that drugs that exhibit favourable polypharmacology may be beneficial for disorders and/or disease states targeting the CNS.

Table 1. CNS disorders and disease states and some key GPCRs involved.

CNS disorder and/or disease state	GPCRs involved[a]
Schizophrenia	$D_{1\text{-}4}$, 5-$HT_{1A/2A/2C}$, $M_{1/4}$, $mGlu_{2/3/5}$, H_3
Parkinson's disease	D_2, A_{2A}, M_1,
Alzheimer's disease	A_{2A}, $M_{1/3}$, $mGlu_{1/2/3/5}$, 5-$HT_{2A/2C/4/6}$
Depression	5-$HT_{1A/2C/6/7}$, $mGlu_{2/3/5}$
Epilepsy	5-HT_7, $GalR_{1\text{-}3}$
Anxiety	5-HT_{1A}, $mGlu_{2/3}$

[a]The GPCRs in this table are not limited to the ones listed, but represent the ones with the most substantial evidence for involvement in the disorder and/or disease state.

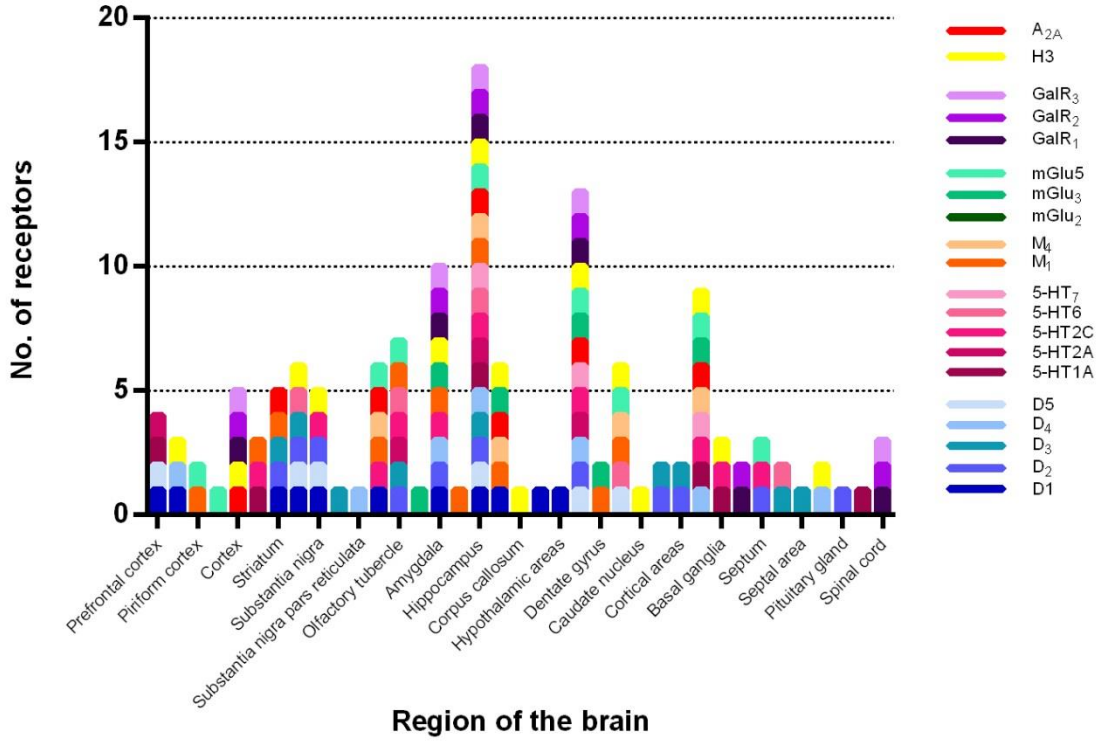

Figure 2. Receptor profiling for CNS disorders listed in Table 1: Results are a combination of human and/or rat studies. References: dopamine[12,13], serotonin[14-18], muscarinic[19], glutamate[20-22], adenosine[23], histamine[24], galanin.[25]

2. Schizophrenia

2.1. Background

Schizophrenia is a severe mental illness that results in a person being unable to express rational ideas/thoughts or to experience normal emotions, thereby making it difficult to maintain a

normal life and healthy relationships.[26] There is no single symptom that characterises schizophrenia, but rather a complex set of interrelated symptoms (Figure 3). The positive symptoms refer to hallucinations, delusions, disordered thoughts and irrational behavior whereas the negative symptoms are defined as avolition (lack of motivation), apathy (lack of interest), alogia (poverty of speech) and anhedonia (absence of pleasure).[27] The cognitive dysfunctions that arise in schizophrenic patients include poor performance in a variety of mental tasks involving perception, memory, problem solving, reasoning and judgment.[28] Previous research has demonstrated that the cognitive dysfunction prevalent in patients suffering from schizophrenia is as much an important aspect in the etiology of schizophrenia as the positive and negative symptoms.[29,30]

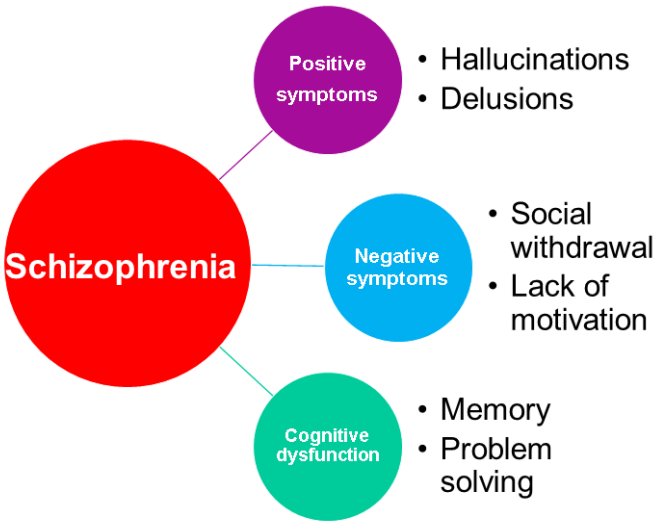

Figure 3. The interrelated set of symptoms that defines schizophrenia.

The onset of schizophrenia is usually in the late teens and early twenties (16-25 years old), just before the commencement of adulthood and currently affects 24 million people worldwide.[31,32] The most widely known theory contributing to the cause of schizophrenia is the dopamine hypothesis. The hypothesis states that schizophrenia is a result of hyper-activity of dopamine in the mesolimbic system (containing dopaminergic projections from the ventral tegmental area (VTA) to the limbic region). The dopamine hypothesis also incorporates that disruption to the

mesocortical system in schizophrenic patients inhibits the negative feedback loop to the VTA. This leads to an increase in VTA firing and, consequently, an increase in dopamine activity in the mesolimbic system.[33,34] Evidence supporting the hypothesis stems from research in which drugs known to increase dopamine activity (L-Dopa and amphetamines) induce psychotic-like symptoms.[35,36] Post-mortem brain studies of schizophrenic patients, which show an increase in dopamine receptor sensitivity and concentration, also allude to the involvement of dopamine in schizophrenia.[37,38] Furthermore, most current antipsychotics have a high affinity towards the dopamine receptor family, in particular the D_2 receptor (D_2R) subtype, in which D_2R antagonists are able to reduce psychotic symptoms in schizophrenic patients by blocking the levels of excessive dopamine in the brain.[10]

2.2. Antipsychotics

The antipsychotics used in the treatment of schizophrenia cover two main classes; typical and atypical, and span three generations (Figure 4). Typical antipsychotics, such as haloperidol (**1**) are considered the first generation antipsychotics (FGAs), which are all commonly D_2 antagonists that decrease the positive symptoms associated with schizophrenia. The consequences however, are that FGAs are only effective against the positive symptoms of schizophrenia and cause extrapyramidal side-effects (EPS). EPS are defined as muscle tremors/rigidity and the general parkinsonian side effects, which are detrimental to a person's motor control and function. As a result of this, FGAs are seldom used, as second generation antipsychotics (SGAs) offer more beneficial outcomes in the treatment of schizophrenia. SGAs such as clozapine (**2**), are not only virtually devoid of EPS and have no significant effect on prolactin levels, but have favourable polypharmacology binding profiles and therefore help to improve the positive and to some extent the negative symptoms associated with schizophrenia. For example, clozapine's atypical activity is thought to come through its antagonism of

dopamine D_2 and serotonin 5-HT_{2A} receptors. Blockade of serotonin receptors have been shown to be beneficial towards the improvement of negative symptoms associated with schizophrenia.[39,40] Aripiprazole (**3**), a third generation antipsychotic (TGA) has a unique pharmacological profile, as it is a potent partial agonist at both presynaptic and postsynaptic D_2 receptors and the serotonin 5-HT_{1A} receptor.[41-43] The clinical relevance of partial agonists in the treatment of schizophrenia and other related psychoactive disorders is highlighted by Tamminga et al.[44] Partial agonists for the D_2R have an affinity for the receptor but have limited intrinsic activity. They display the ability to act as an agonist or antagonist depending on the receptor population and the concentration of the endogenous ligand, dopamine. Particularly at the postsynaptic receptor, where there are regions of high dopamine concentration, partial dopamine agonists behave as antagonists. Consequently, a potent partial agonist can effectively block the action of dopamine at receptors and can be useful as an antipsychotic drug. Since dopamine neurons all contain autoreceptors responsive to agonists such as dopamine, activation of these autoreceptors may function to decrease dopamine synthesis, release and neuronal firing pertaining to certain instances. A partial agonist may be beneficial in that it still retains some agonism at autoreceptors and can therefore help to decrease dopamine synthesis and release. Alternatively, dopamine concentrations can also be low in some regions of the brain and as a consequence a partial agonist can occupy receptors in order to cause partial activation.[45] Due to their multifaceted functionality at the D_2R, partial agonists can help to decrease the side effects profile that is still evident in many SGAs by accommodating situations of both low and high concentrations of dopamine in the brain.

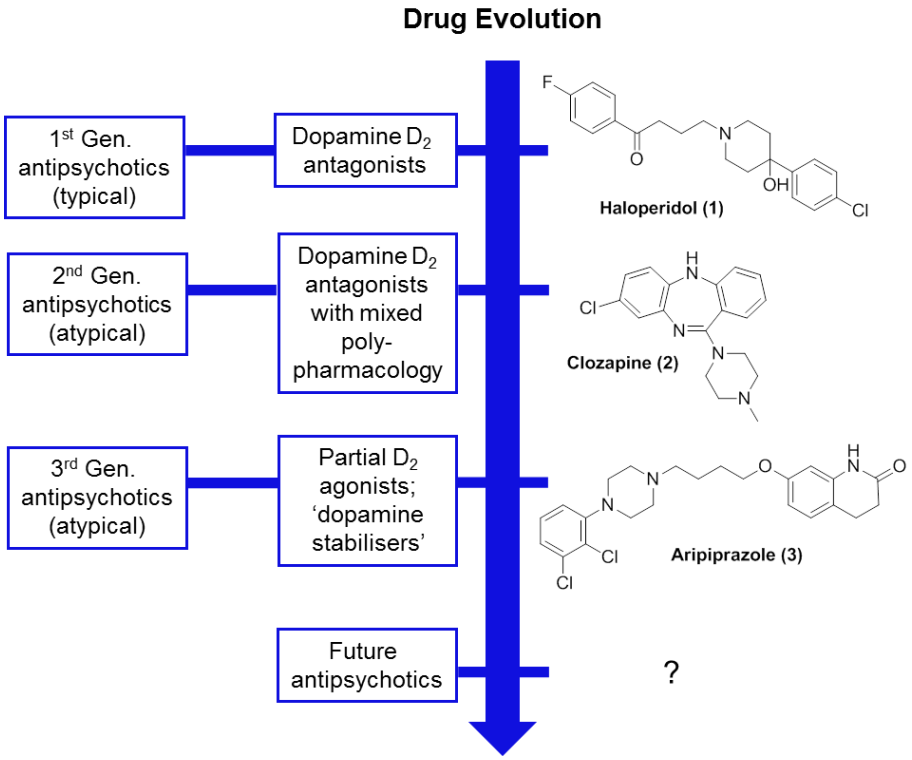

Figure 4. The evolution of drugs for the treatment of schizophrenia.

While there have been significant advances in the design of antipsychotics from the FGAs to the TGAs, the same issues remain today. Gaining selectivity for particular receptor subtypes remains an ongoing challenge. This problem of selectivity accounts for the extensive side effects profiles observed with antipsychotics as there are often many off target GPCRs that the ligands binds to, which can include GPCRs from the same receptor family or external ones. The other major limitation to current antipsychotics is that whilst they are successfully able to treat the positive symptoms and to some extent the negative symptoms of schizophrenia, there remains an ongoing need to address the cognitive aspect of schizophrenia. In this respect, we can therefore ask, what medicinal chemistry approaches can we employ to address both these limitations for the future development of antipsychotics?

3. Techniques for subtype selectivity at GPCRs

3.1. Targeting allosteric sites

3.1.1. Modes of action

The activation of GPCRs traditionally occurs through the orthosteric site, which is the site of binding for the endogenous ligand. However, due to the highly conserved residues in the orthosteric site across receptor subtypes, it makes it difficult to gain subtype selectivity. Therefore, in order to design a subtype selective ligand, the ligand must target an area that is distinct from other receptors belonging to the same family. Allosteric sites on GPCRs offer a region that is topographically different to the orthosteric site.

An allosteric ligand can have multiple modes of action as demonstrated in Figure 5. An orthosteric ligand binds to the orthosteric site with a binding affinity defined by the equilibrium dissociation constant (K_A) and similarly the allosteric ligand can bind to the allosteric site with its binding affinity defined by K_B. The efficacy produced by the orthosteric ligand is defined by τ_A, the intrinsic agonism of the ligand, and an allosteric ligand can also produce a response in its own right, defined by τ_B and can occur regardless of whether there is a ligand present in the orthosteric site. Allosteric ligands can also modulate the binding and/or signaling of the orthosteric ligand.[46] Affinity modulation (α) refers to a change in the orthosteric site upon binding of a ligand to the allosteric site. Changes to the orthosteric site may involve a change in the association or dissociation rate of the ligand. Efficacy modulation (β) occurs when the allosteric ligand has an effect on the response elicited by the ligand in the orthosteric site. It may result in a greater or lesser response in intrinsic efficacy.[46,47]

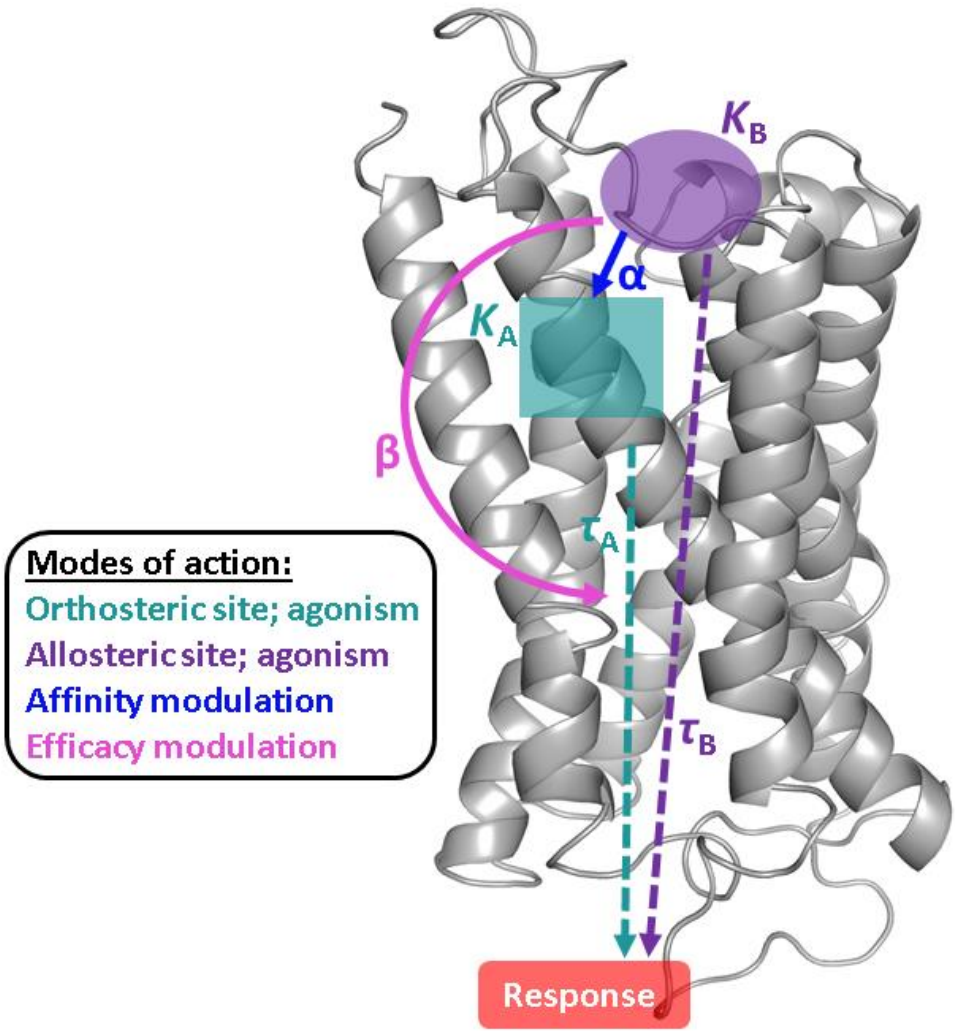

Figure 5. Modes of action of orthosteric and allosteric ligands.

An orthosteric antagonist (Figure 6, A) will directly compete with the ligand in the orthosteric site thus never reaching a saturation point. Alternatively, when an allosteric ligand is co-administered with an orthosteric ligand in a functional signalling assay (Figure 6, B&C) it can be defined as a negative allosteric modulator (NAM), if it decreases the response produced by the ligand in the orthosteric site or a positive allosteric modulator (PAM) if it enhances it. In both cases a NAM and PAM will eventually reach a saturation point. Additionally, an allosteric ligand can also be neutral in that it will have no effect on the ligand present in the orthosteric site at equilibrium. For a detailed review of the effects a NAM and PAM can have on the affinity and/or efficacy of the ligand in the orthosteric site, see the review by Kenakin.[48]

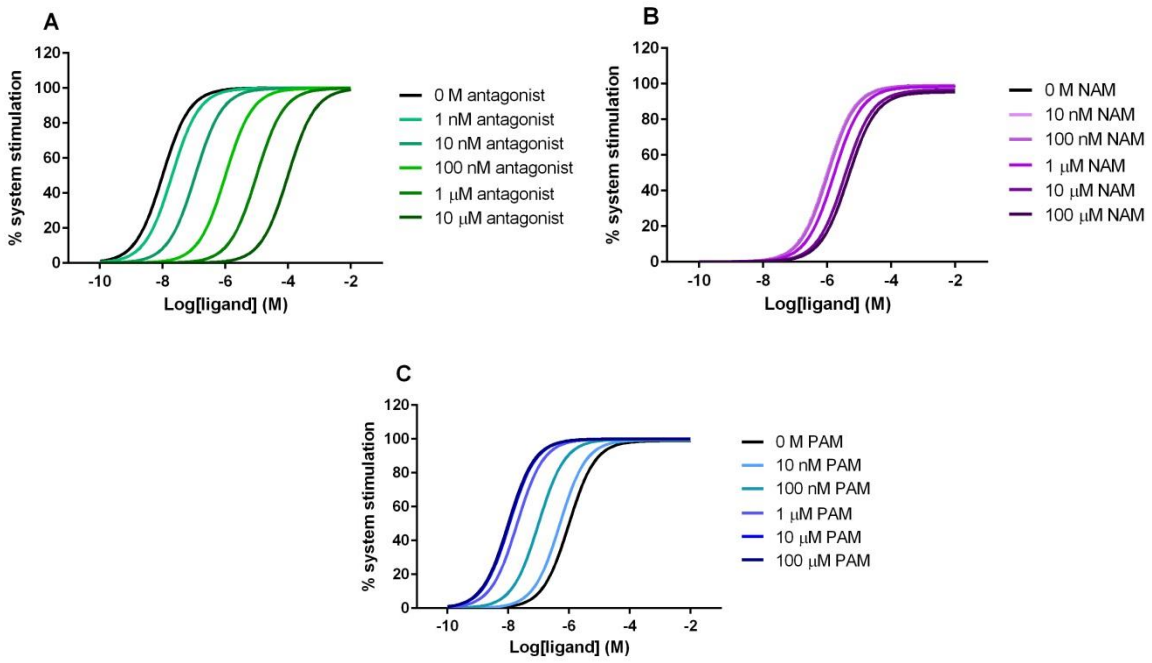

Figure 6. A) Orthosteric antagonist in competition with an orthosteric ligand. B) Orthosteric ligand in the presence of a negative allosteric modulator (NAM). C) Orthosteric ligand in the presence of a positive allosteric modulator (PAM).

3.1.2. Muscarinic acetylcholine receptors

The muscarinic acetylcholine receptors (mAChRs) belong to the class A family of GPCRs and are divided into five receptor subtypes M_1-M_5, with acetylcholine (ACh) as the endogenous ligand. The M_1, M_3 and M_5 receptors preferentially couple to G_{q11} G proteins, whereas the M_2 and M_4 receptors preferentially couple to pertussis toxin sensitive $G_{i/o}$ G proteins.[49] The five mAChRs are all expressed abundantly in certain regions of the brain. Of particular interest are the M_1 and M_4 mAChR subtypes. The M_1 mAChR is mostly expressed post-synaptically, and found in the cerebral cortex, hippocampus and striatum,[50] whereas the M_4 mAChR is mostly found presynaptically in the striatum, hippocampus, cortex and thalamus.[50] Cholinergic transmission plays a vast role in the CNS and is responsible for regulating many processes such as motor function, cognitive control, memory, motivation, psychosis and mood, which cover all three subsets of symptoms that are affected in schizophrenic patients.[51] Cholinergic transmission is also heavily involved in the peripheral system, which makes designing drugs for mAChRs

difficult due to the multiple side effects that can arise. Antagonists for the mAChRs have shown to severely worsen the cognitive deficits associated with schizophrenia, whereas the development of agonists have shown to be beneficial for positive and/or cognitive aspects of schizophrenia.[52] Xanomeline (**4**), which was discovered to be a selective M_1/M_4 preferring orthosteric agonist, was an important breakthrough for the association of the mAChRs with schizophrenia. This compound showed improvements in cognitive functions and positive symptoms in patients affected with schizophrenia[53], thus proving that the M_1 mAChR and M_4 mAChR are valid target sites for schizophrenia. Since the discovery of **4**, which didn't progress any further as a drug candidate due to peripheral side effects, there has been the development of many ligands targetting these receptors, particularly allosteric and/or bitopic agonists for the M_1 and allosteric agonists and/or modulators for the M_4 mAChR.

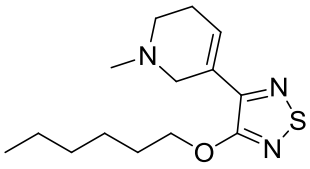

Xanomeline (4)

3.1.3. M_1 allosteric and/or bitopic agonists

The design of M_1 agonists to particularly benefit the cognitive deficits[54] in CNS disorders such as schizophrenia has mostly focused on allosteric ligands for achieving subtype selectivity, in addition to bitopic ligands. A bitopic binding mode is the bridging of two topographically distinct binding domains, i.e. the orthosteric and allosteric sites via a single molecule.[55,56] A bitopic ligand may therefore offer improved affinity and selectivity for the receptor target. Additionally, whilst an allosteric ligand may be dependent on the endogenous agonist to be present in the orthosteric site, a bitopic ligand already interacts with the orthosteric site on its own.[57] Many bitopic ligands such as AC-42 (**5**), 77-LH-28-1 (**6**) and TBPB (**7**) were initially characterised as allosteric agonists for the M_1 mAChR but have since been re-characterised as interacting with both allosteric and orthosteric binding sites.[58,59]

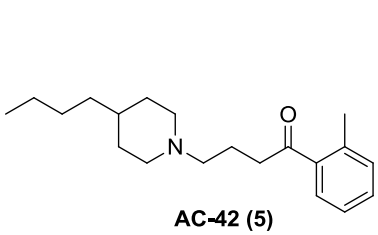

AC-42 (5)

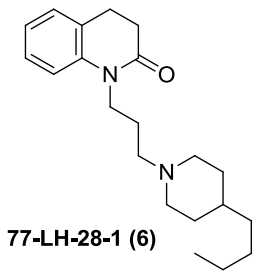

77-LH-28-1 (6)

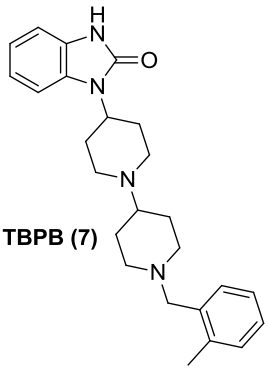

TBPB (7)

All three bitopic ligands (**5**, **6** and **7**) display common structural features. For instance all three contain an ionisable piperidine and an elongated linear scaffold. Ligands **5** and **6** both have a 3-carbon alkyl chain/spacer and a butyl alkyl chain subsitituted at the 4′ position of the piperidine. Furthermore ligands **6** and **7** both consist of a heterocyclic ring system and **5** and **7** have an aromatic ring substituted with a methyl at the ortho position. As the ionisable piperidine is key to all three structures and the endogenous agonist ACh, is also permanently charged upon binding to the orthosteric site, we could assume that this region of each of the ligands resides in the orthosteric site and the remainder of the molecule binds in the secondary site. However, to date, no definite orthosteric and allosteric portions of the agonists have been confirmed, thus it still remains speculation. Another ligand that displays similar features to those of **5**, **6** and **7**, is the putative M_1 allosteric agonist LuAE51090 (**8**). There has been no work to determine whether this ligand acts via a bitopic binding mode, however the authors have characterised its allosteric action through both mutagenesis data and Schild regression analysis.[60] Compound **8** had a favourable M_1 profile (EC_{50}= 61 nM, E_{max}= 83%; intracellular Ca^{2+} mobilization assay) and was selective over the other mAChR subtypes.

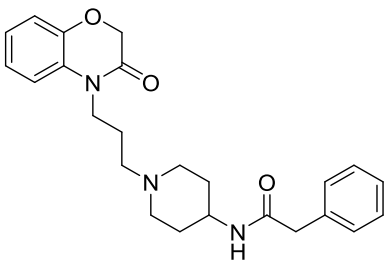

Lu AE51090 (8)

3.1.4. M_4 positive allosteric modulators

The first PAM for the M_4 mAChR, thiochrome (**9**), was able to enhance the affinity of ACh by 3-5 fold.[61] Although it was a relatively weak PAM, it showed promise for the development of future PAMs for this receptor. The structure activity-relationships (SAR) for PAMs targeting the M_4 mAChR have solely centered around one structural scaffold, the thienopyridine core. Various derivatives have been made in attempts to optimize this scaffold, with the current 'best in field' being LY2033298 (**10**) in terms of positive allosteric modulation of ACh affinity and efficacy at the M_4 mAChR.[62,63]

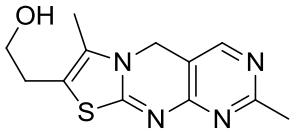

Thiochrome (9)

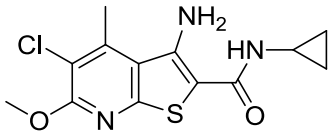

LY2033298 (10)

Key PAMs targeting the M_4 mAChR are summarised in Table 2. The first novel series of PAMs to move away from the structural core of **10** came from Shirey et al.[64], who replaced the 5-chloro-4-methyl-6-methoxy substitution from **10** with a 4,6-dimethyl substitution. Their standout compound, VU10010 (**11**) was able to potentiate both the efficacy and affinity of ACh, but had poor physiochemical properties (logP ~ 4.5) and therefore could not be used for subsequent *in vivo* models. The next series of compounds by Brady et al.[65] worked on alternative scaffolds and variations of **11** to improve physiochemical properties and to lower the logP. The two novel compounds that emerged from their SAR study were both based on the structure of **11** but with a benzodioxolylmethyl, VU152099 (**12**) and the other with a *p*-methoxybenzyl, VU152100 (**13**) in place of the *p*-chlorobenzyl. Both exhibited a similar pharmacological profile to **11** and had vastly improved physiochemical and pharmacokinetic profiles that contributed to their CNS penetrability. In a model for psychosis, both **12** and **13** were able to reduce amphetamine induced hyperlocomotion in rats, therefore validating their use as potential CNS agents for the M_4 mAChR. SAR work by Kennedy et al.[66] focussed on varying both the right and

left hand side of the thienopyridine scaffold. Substitution from the left hand side (LHS) of the analogues occurred at the 6′ position on the pyridine ring. Compound sets looked at substituting at this position with alkylamine-linked analogues and ether-linked analogues, with the latter more tolerable. Noteable compounds **14** and **15** showed modest decreases in amphetamine induced hyperlocomotion in rats and were able to modulate the EC_{50} of ACh similar to lead compounds **11-13**. Despite further improvements, particularly in the stability of the compounds, both **14** and **15** had decreased potency (2-4 μM), which is thought to account for its reduced *in vivo* efficacy. Additionally, this work highlighted that the thienopyridine scaffold is able to tolerate longer and bulkier groups from both the left and right hand side. In attempts to move away from the 4,6-dimethyl thienopyridine substitution pattern, Uyen et al.[67] combined this scaffold with that of **10** to give a new 4-methyl-5-chloro-6-methyl substitution. Through conducting a comprehensive SAR study for potential groups for the RHS of the scaffold, they eventually produced ML253 (**16**), which caused a 106-fold shift in the EC_{50} of ACh using a fluorescence-based calcium assay. The pharmacokinetics and CNS penetrability were also enhanced as compared to previous Vanderbilt University (VU) compounds. In addition, **16** maintained subtype selectivity, showed a dose-dependent reversal of amphetamine-induced hyperlocomotion and exhibited less species variability than its predecessors. Finally, as a comprehensive means to characterising the modular activity of PAMs, Huynh et al.[68] synthesised a series of compounds based upon the VU-derived 4,6-dimethyl thienopyridine scaffold. Specifically, they looked at alternative fluorine, methoxy and the combination of both substitutions to the scaffold of **15**, and applying the operational model of allosterism. Noteable compounds from their SAR studies were the 3-fluoro- (**17**) and the 3-fluoro-4-methoxy- (**18**) substituted analogues.

Table 2. SAR summary of key PAMs for the M_4 mAChR.

Reference	Key compound(s)	Structural modifications/features	Significance
Shirey, J.K et al.[64]	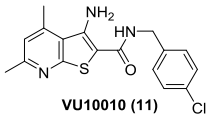 VU10010 (11)	- 4,6-Dimethyl thienopyridine substitution - Varied substituents on the amide; both alkyl and aryl systems	- Emergence of an alternative substitution on the thienopyridine scaffold to **10**
Brady, A.E et al.[65]	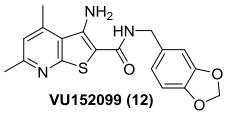 VU152099 (12) 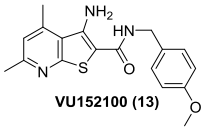 VU152100 (13)	- 4,6-Dimethyl thienopyridine substitution - Exploring alternative amides to improve physicochemical properties and logP	- Improved physiochemical and pharmacokinetic properties; CNS penetrant - Showed potential in *in vivo* models for psychosis
Kennedy, J. P et al.[66]	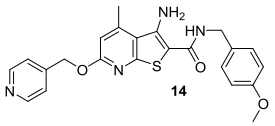 14 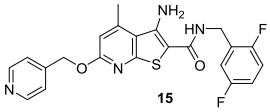 15	- Varying groups on the LHS and RHS of the thienopyridine core scaffold	- Showed potential in *in vivo* models for psychosis - Compounds showed species variability (rat vs human)
Uyen, L et al.[67]	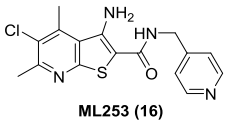 ML253 (16)	- Hybridising scaffolds of **10** and **11**	- Good pharmacokinetic profile and CNS penetrant - Limited species variability
Huynh, T et al.[68]	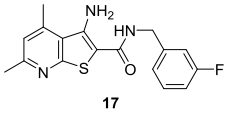 17 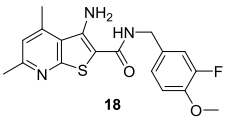 18	- 4,6-Dimethyl thienopyridine substitution, focusing on varied substitutions on the benzyl ring	- Compounds are profiled using the operational model of allosterism

3.2. Designed multiple ligands

The term designed multiple ligands (DMLs) stems from Morphy et al., describing compounds that are designed to modulate multiple targets of relevance to the disease, with the main goal of enhancing efficacy and or improving safety.[69] There are a number of terms to describe ligands which have multiple activities; dual, binary, bivalent, dimeric, mixed, triple or balanced are usually used in addition with ligand, inhibitor, agonist, antagonist, conjugate or blocker. DMLs involve incorporating two separate pharmacophores and slowly increasing the integration between the two until the ligand progresses from a conjugate to a merged structure (Figure 7). A DML drug may offer additional benefits over fixed dose combination (FDC) drugs (multiple drugs in one tablet), as the physiochemical properties for FDC drugs may differ between the two drugs. For example, one drug may have a different pharmacokinetic profile over the other, hence possible problems with bioavailability, toxicity and optimal time required for each drug at the target of interest may arise. In addition, it may be costly and time-consuming to synthesise and pharmacologically characterise two separate compounds both in an *in vitro* and *in vivo* setting.[70] Despite these advantages there are limitations in finding the optimum combination of pharmacophores for a desirable activity profile and the different framework combinations for DMLs (conjugates, fused and merged), each have their own advantages and disadvantages as outlined in Table 3.

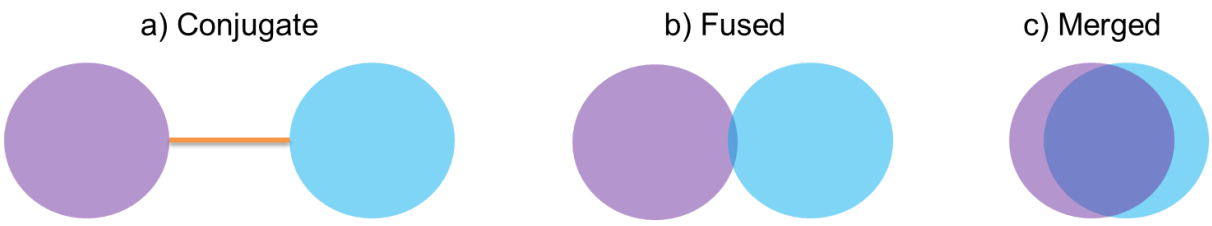

Figure 7. Classification of designed multiple ligands by combining two separate pharmacophores (purple and blue) either with a linker (a; orange) or without (b, c).

Table 3. Characteristics and advantages/disadvantages of designed multiple ligands.

Type	Characteristics	Advantages	Disadvantages
Conjugates / bivalents	• Pharmacophores remain completely intact • Separated by a linker • Depending on size, may be bitopic or span a dimer	• Structure of original pharmacophore remains intact • Useful for use as pharmacological tools rather than drugs, eg. studying GPCR dimerization	• Molecular weight and size is usually large • Lipophilicity increases; may not pass the BBB • Requires SAR knowledge on type of linker/spacer to be used and the length required • Significant work is needed to find a suitable linkage point
Fused	• Pharmacophores slightly integrated	• No linker required • Smaller molecular weight	• A suitable linker point for integration must be known or investigated • Closer proximity of pharmacophores may affect activity profile
Merged	• Pharmacophores integrated via overlapping common functional groups or by the use of isosteres	• More favourable pharmacokinetics profile; likely to be more drug like • Size of the molecule remains a similar size to the previous pharmacophore	• Isostere may completely abolish activity • Important functional groups from the original pharmacophore may be overridden, hence loss in activity

Conjugate DMLs usually contain two distinct pharmacophores that are well separated by a linker group that is not common to either of the original structures. The linker in most cases is stable, however some structures can employ a cleavable linker that upon being metabolized, releases two ligands that are free to act at separate targets.[71] Portoghese is one of the leaders in terms of homo and hetero- conjugates, in which he investigated a variety of different linker lengths for the study at opioid receptors.[72] Since then, a variety of other ligands have emerged for the D_2R, including homobivalent ligands utilizing the antipsychotic clozapine and the antiparkinson drug

ropinirole.[73,74] In particular, the clozapine homobivalent (**19**) showed a 79-fold increase in binding affinity and a 5-fold increase in inhibitory potency measured in an ERK1/2 phosphorylation assay compared to clozapine for the D_2R; thus representing a pharmacological tool for numerous applications such as the study of GPCR dimers.

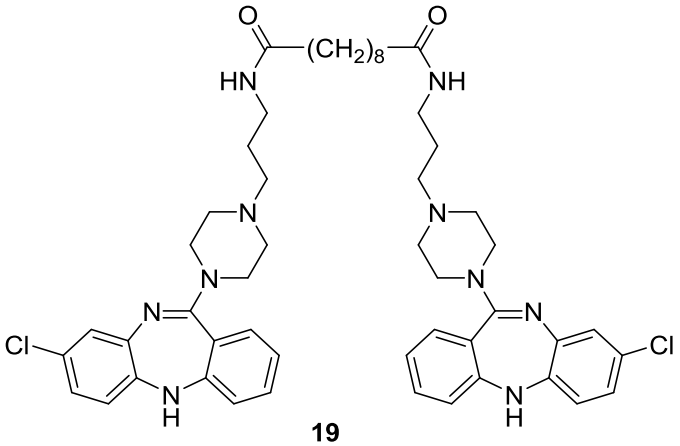

19

Fused structures are usually employed when there are not enough common structural features in both pharmacophores to allow the structure to be more highly integrated. An example of this method is the research by Kawanishi et al. that combined a gastrin antagonist (**20**) with a histamine H_2 antagonist (**21**) to give analogue **22** (Figure 8). The fused DML had improved dual activity at the target receptors in addition to selectivity for the gastrin receptor antagonist site compared to the cholecystokinin A receptor.[75]

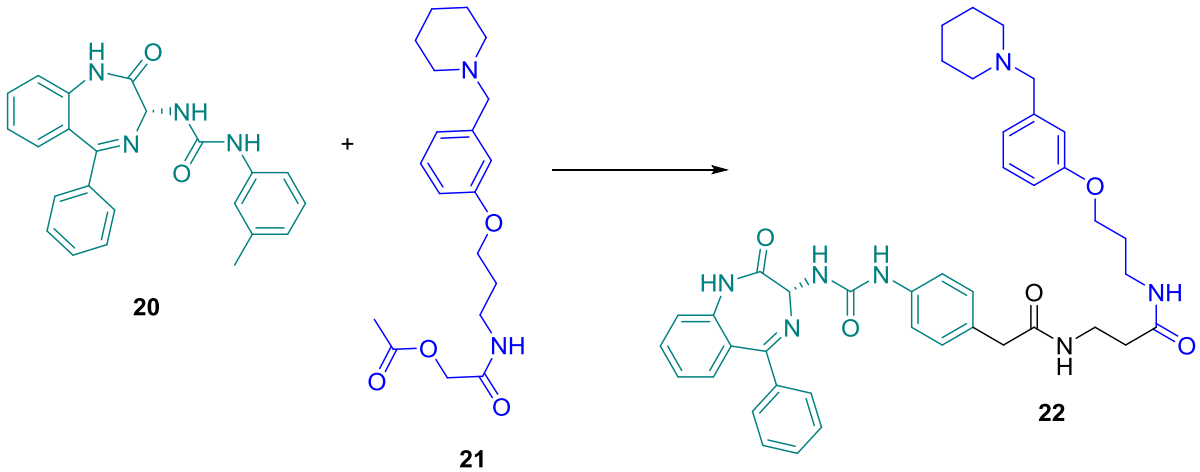

20 **21** **22**

Figure 8. Example of a fused gastrin antagonist- histamine H_2 antagonist DML, **22**.

Merged DMLs are considered highly integrated, which is favorable, as merged structures can provide smaller and less complex molecules that may even fit into Lipinski's rule of 5, giving it the best chance of becoming drug-like.[9,76] An example of a merged structure comes from the design of the D_2/5-HT_{2A} antipsychotic ziprasidone. Lowe et al.[77] at Pfizer merged the endogenous orthosteric agonist dopamine (**23**) with a serotonin ligand (**24**) to give compound **25** (Figure 9). The indole was used in **25** in order to mimic any hydrogen bond interactions that may come about from the catechol present in dopamine's structure. Further optimization of **25** gave the final structure **26**, which increased potency, making it comparable to the very potent D_2 antagonist haloperidol and a good ratio of D_2/5-HT_{2A} activity, also comparable to the atypical antipsychotic clozapine.[78] Ziprasidone was found to be efficacious in clinical trials pertaining to schizophrenia, with particular advantages such as no weight gain and rarely any effects on prolactin levels or causing EPS,[79] thus validating the DML approach as a useful technique for drug discovery.

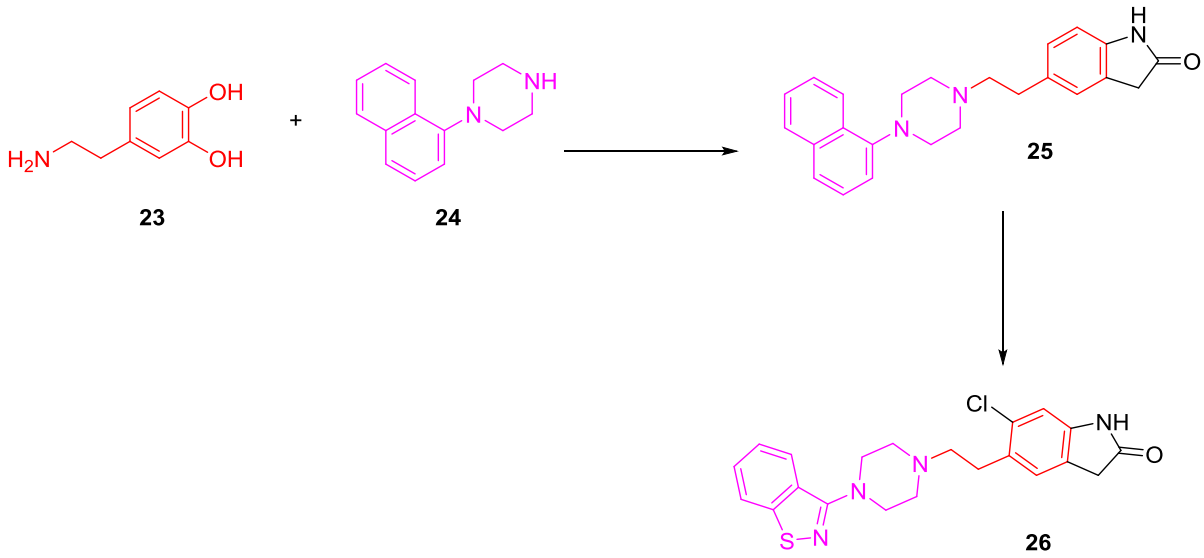

Figure 9. Development of the antipsychotic ziprasidone (**26**) using a merged DML approach.

DMLs therefore offer an approach to design ligands that can be used as pharmacological tools to study receptor structure and/or function (conjugates), or towards drugs that offer a

polypharmacology profile (fused and merged). This makes them ideal starting points for targeting many CNS disorders due to the involvement of multiple receptors in the brain, particularly for schizophrenia.

3.3. Privileged structures

The earliest definition of a privileged structure by Evans et al.[80] was "a single molecular framework able to provide ligands for diverse receptors." While this definition implies that privileged structures can be used to create ligands with a polypharmacology profile, they can also be used to produce ligands that may be selective for a class of receptors and, more ideally, a single receptor target.[81] For GPCRs in particular, drug design can be challenging for numerous reasons, but especially due to difficulties in achieving subtype selectivity due to highly conserved residues across receptor families. Indeed a privileged structure can be used to impart the selectivity on its own or through subsequent functionalization.[82] Therefore privileged structures can be "built in" to a molecule by replacing certain functional groups or can be used as the starting scaffold, where one can "build out" to create an optimized ligand.

There are multiple ways to identify privileged structures for the chosen receptor target.[83] The most obvious way is by observing already identified molecules for the receptor target to identify key scaffolds that may be repeated. In the search for novel antipsychotics, it is beneficial to look at both clinical and non-clinical compounds to not only identify privileged structures but also to develop pharmacophores that can help towards functionalizing the privileged structures initially determined. Computational techniques are often utilized for the identification of privileged structures, as programs and/or databases can be designed to identify certain privileged structures for leads and molecular modelling can provide insight into why some structure motifs are favored over others at a particular receptor target.[83] For example the ZINC database contains over 21 million commercially available compounds with compounds available in 3D 'ready to

dock' formats. While finding novel scaffolds is an equally important aspect in drug design development, the program can be used to identify common or known privileged structures by allowing to search for structures via multiple different categories such as: commercial availability, lead/fragment/drug-like molecules, specific bioactivity, potential drug-like properties and specific targets.[84,85] Additionally, privileged structures can be used to guide combinatorial chemistry for the generation of libraries for high throughput screening (HTS).[86] Privileged structures are therefore powerful tools for drug design and can be exploited in the early stages such as the generation of libraries for HTS or in the later stage as building blocks for a drug itself.

3.4. Biased agonism

3.4.1. Definition

Biased agonism (sometimes termed "functional selectivity" or "stimulus bias") refers to the phenomenon by which different agonists acting at the same receptor can stabilize distinct receptor conformations linked to different functional responses (Figure 10).[87-89] The characterisation of ligands in terms of selectivity is predominantly by the affinity of the drug for the receptor (the dissociation constant of the ligand, K_A) and across similar receptor families and subtypes. The efficacy of the ligand is nonetheless an equally important part in determining the overall physiological response of the ligand at the receptor target.[90] Therefore biased agonism offers a way to connect both parameters (efficacy and affinity) for an agonist to determine if it may favour one functional pathway over another at a particular receptor target. The main advantage of biased agonism is the promise of desirable therapeutic outcomes, in that a biased ligand may avoid potential on-target side-effects that may be associated with the disease state of interest and therefore offer an alternative approach to the design of selective drugs.

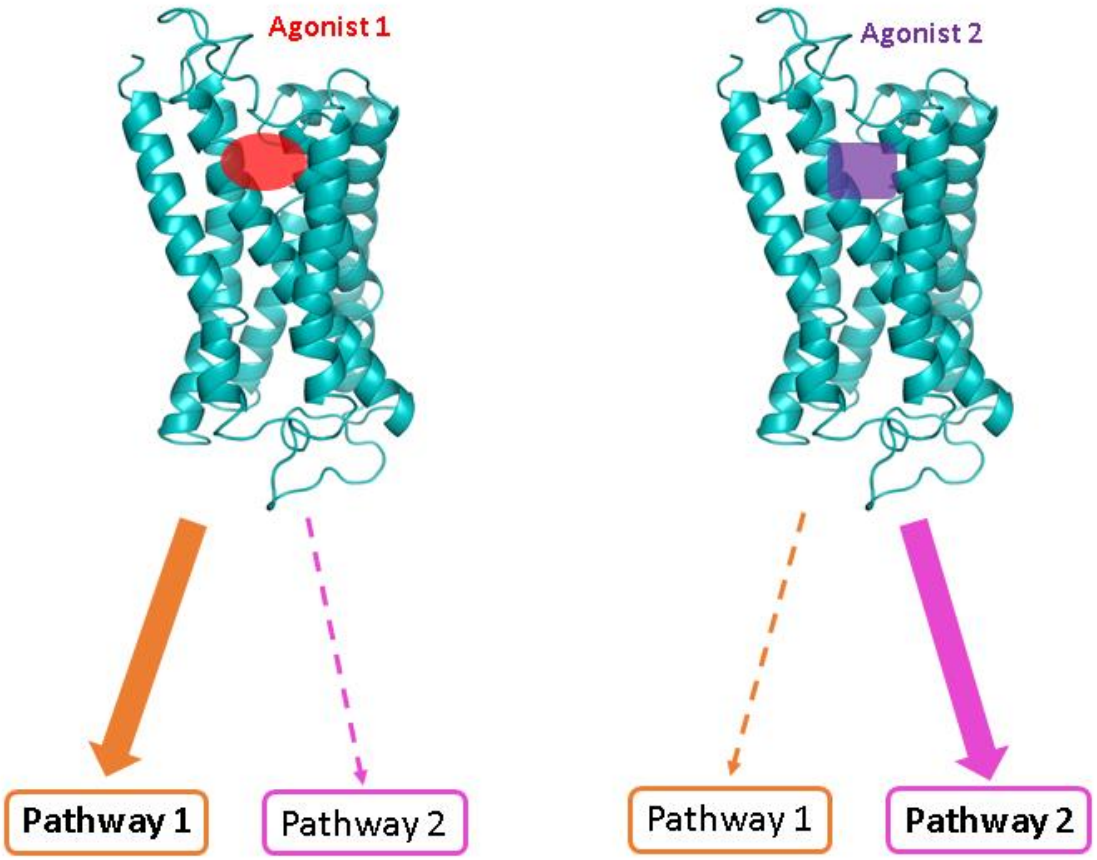

Figure 10. Biased agonism- different ligands can activate distinct conformations of GPCRs that make them biased towards one signalling pathway over another.

3.4.2. Quantifying bias

To quantify biased agonism, the operational model of agonism originally developed by Black and Leff,[91] can be utilized. The model firstly requires calculation of the transduction coefficient, log (τ/K_A), for all ligands. This parameter incorporates τ, which is used to describe the efficacy of the ligand. More specifically, τ takes into account the intrinsic efficacy of the activated ligand-receptor complex (K_E) and the receptor density [R_t]. The transduction coefficient also involves K_A, the equilibrium dissociation constant, which describes the functional affinity of the ligand for the receptor. The value of log (τ/K_A) determined can then be normalized to a reference agonist to account for differences between the two assay endpoints in the same cellular background such as coupling efficiency or signal amplification giving a value of $\Delta\log(\tau/K_A)$. The

final step is to subtract one pathway from the other to give the bias factor $\Delta\Delta\log(\tau/K_A)$ (pathway 1-pathway 2).[88] The equations associated with each of these transformations and calculations of errors will be described in greater detail in Chapter 3.

3.4.3. Biased agonism at the dopamine D_2 receptor

Since the emergence of partial agonists for the treatment of schizophrenia, there has been considerable effort towards understanding more about how partial agonists impart their therapeutic effects and whether the lack of side effects compared to some of the atypical antipsychotics can be explained by bias. Table 4 summarises some key ligands for the D_2R that have shown bias towards a downstream signalling pathway. Some of the first molecules to show bias at the D_2R were dihydrexidine (DHX, **27**) and a structurally homologous analogue dinapsoline (DNS, **28**). While **27** was able to stimulate GTPγS binding in rat substantia nigral tissue,[92] it was unable to inhibit the synthesis and release of dopamine in rat striatum, which is common for D_2 agonists. This therefore led to the further characterisation of **27** and multiple analogues in three functional pathways; inhibition of cAMP synthesis, MAPK phosphorylation and GIRK activation. The results showed that **27** and **28** displayed particular rank orders of potency at the first two pathways and only partially activated GIRK channels. Although a quantitative value for bias was not determined, this still lead the authors to believe that the results were indicative of functional selectivity occurring at the D_2R.[93] Furthermore, Shonberg et al.[90] reanalysed the data from compounds **27**, **28** and various other analogues and applied the operational model of agonism to generate bias factors which confirmed that both analogues were biased towards MAPK over cAMP relative to the full agonist quinpirole. This not only confirmed the authors' conclusions, but demonstrated the power of using this model.

Aripiprazole was the first clinical antipsychotic to show functional selectivity at the D_2R by showing a preference towards potentiation of arachidonic acid (AA) release.[94] Since then there has been considerable work towards designing ligands that may also exhibit a bias profile and also to understanding the SAR around these compounds to determine what factors may be important for bias at the D_2R. Analogues **29**-**32** were discovered by exploring multiple structural features in aripiprazole's structure such as looking at different mono- and di-substituted phenyls, various cyclic amines, diverse linkers including more conformationally restrained and different bicyclic heterocycles. These compounds showed a large bias towards β-arrestin-2 recruitment. Specifically, compounds **30** and **31** were able to show antipsychotic activity *in vivo* and induce catalepsy in β-arrestin-2 knockout mice, thus suggesting the importance of the β-arrestin recruitment in the role of antipsychotic efficacy.[95,96] As an extension from the scaffold of aripiprazole and as an attempt to develop some novel ligands based on 1,4-disubstituted phenyl piperazine ligands, compound **33** was synthesised containing a 2,3-dihydrobenzofuran scaffold with a pyrazolo[1,5-*a*]pyridine scaffold. This ligand showed a bias towards the ERK signalling pathway over cAMP, but more significantly, the authors identified $His393^{6.55}$ to be an important residue in influencing ligand-biased signalling and confirming that slight changes in the overall conformation or binding site interactions at the D_2R can have an impact on bias.[97] To further expand on these findings, analogues based on cariprazine,[98] a partial agonist currently in clinical trials, were synthesised. Key analogue **34** showed a bias towards cAMP over ERK which was quantified via generating a bias factor, $\Delta\Delta\log(\tau/K_A)$, by the use of the operational model of agonism. Compound **34** and multiple other analogues from their study represent useful tools towards the study of biased agonism and antipsychotic efficacy at the D_2R and the usefulness of applying the operational model of agonism. Finally, compound **35**, which features the same 2,3-dichlorophenylpiperazine present in many earlier compounds and an (*E*)-oxime pyrazolo[1,5-*a*]pyridine heterocycle was found to have a bias for the GTPγS pathway over β-arrestin-2

recruitment. Compound **35** was also functionally selective for one specific G protein over another ($G\alpha_{01}$ over $G\alpha_{i2}$), which is thought to increase synaptic plasticity and possibly benefit the negative symptoms of schizophrenia. Such information from compound **35**, in addition to all analogues outlined in Table 4 provides invaluable insight towards understanding potential underlying mechanisms and SAR of biased ligands at the D_2R. In particular, there are common structural features in many of the biased compounds and all these ligands can be further exploited to gain a better understanding of antipsychotic efficacy at the D_2R.

Table 4. SAR summary of key biased ligands for the dopamine D_2 receptor.

Reference	Key compound(s)	Signalling pathways	Significance
Gay, E. A et al.[93]	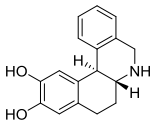 DHX (**27**) 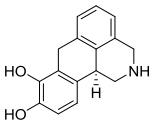 DNS (**28**)	Inhibition of cAMP synthesis, MAPK phosphorylation, GIRK activation; distinct rank orders of potency	First evidence of functional selectivity at the D_2R
Urban, J.D et al.[94]	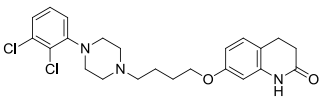 Aripiprazole (3)	MAPK phosphorylation: 170 ± 35 nM [^{3}H]AA release: 1.53 ± 0.39 nM	First evidence of a clinical antipsychotic showing functional selectivity for the D_2R
Allen, J.A et al.[95]	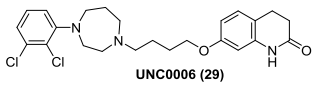 UNC0006 (29) 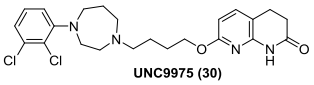 UNC9975 (30) 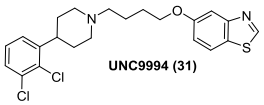 UNC9994 (31)	cAMP: **29**-**31**: Inactive β-arrestin-2, EC_{50}, E_{max}: **29**: 17 nM, 47% **30**: 6.0 nM, 20% **31**: >1,000 nM, >50%	Derivatives of aripiprazole show bias towards the β-arrestin signalling pathway. Compound **30** and **31** displayed antipsychotic-like activity
Chen, X et al.[96]	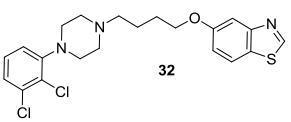 32	cAMP: Inactive β-arrestin-2, EC_{50}, E_{max}: 126 nM, 88%	Use of medicinal chemistry and pharmacological profiling to generate multiple selective biased ligands towards β-arrestin

Reference	Key compound(s)	Signalling pathways	Significance
Tschammer, N et al.[97]	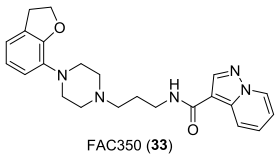 FAC350 (**33**)	cAMP: Inactive ERK phosphorylation, EC_{50}, E_{max}: 35 nM, 55%	Residue His393$^{6.55}$ was found to influence ligand-biased signalling at the D_2R
Shonberg, J et al.[99]	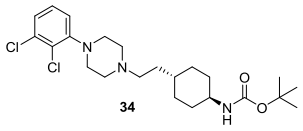 **34**	cAMP, EC_{50}, E_{max}: 7.9 nM, 84% ERK phosphorylation, EC_{50}, E_{max}: 25 nM, 30%	SAR study of cariprazine based analogues via the use of the operational model of agonism Minor structural changes can lead to significant changes in bias
Möller, D et al.[100]	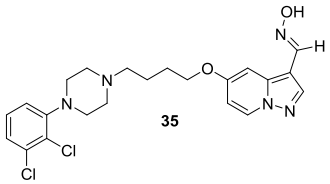 **35**	[^{35}S]GTPγS, EC_{50}, E_{max}: $D_{2S}G\alpha_{01}$ 1.3 nM, 65% $D_{2S}G\alpha_{i2}$ 234 nM, 27% β-arrestin-2: Inactive	Identified ligands that have a bias for a specific G-protein ($G\alpha_{01}$ over $G\alpha_{i2}$)

3.5. Fluorescently labelled ligands

3.5.1. Rationale

As the importance of GPCRs, in not only CNS disorders but multiple other disease states, continues to rise so do the techniques used to study them. Fluorescently labelled ligands offer the opportunity to study the structure and function of GPCRs and to be used as tools for screening new analogues. Selecting an agonist or antagonist for a particular receptor and tethering a fluorophore to this structure can be useful in a variety of different applications. There are multiple challenges in making fluorescently labelled ligands and the major draw-back is that the fluorophore has the potential to interfere with the ligand binding to either the orthosteric or allosteric sites. In addition to this, it can change the functionality of the ligand. For example a ligand that may have previously been an agonist may become an antagonist via the addition of

the fluorophore to its structure. There are also multiple structural aspects to consider in the design of fluorescently labelled ligands. The length of the linker/spacer used between the ligand and the fluorophore is a very important structural feature. This can affect where the fluorophore sits in the binding site, if it's present within extracellular space or even if it's able to bind at all. The composition of the linker may also be important for the properties of the ligand.[101] One may explore the possibility of more rigid linkers to avoid flexibility in the binding site, such as introducing a greater degree of unsaturation to the linker. An increase in hydrophillicity, such as a poly-ethyleneglycol (PEG) linker may also be useful for greater water solubility, particularly later on for use in biological applications. Another important consideration in the design of fluorescently labelled ligands is a suitable point on the ligand where a linker may be attached. Adding to the wrong position of the structure can cause a loss in efficacy and/or affinity of the ligand or even a complete loss of activity.

3.5.2. Fluorophores

Fluorophores are synthetically derived compounds or dyes that usually consist of a conjugated system that results in them being able to emit light. They can be excited at a particular wavelength and the emission produced can be detected. Many fluorophores are now commercially available with key components optimised so that they can be useful over a variety of different wavelengths, different degrees of brightness, promote photostability and reduction in self-quenching. Table 5 highlights the optical properties that are of importance for fluorescent compounds and some of which should be considered before use in particular applications. Optimisation of these fluorophores has been achieved through increasing or decreasing the extent of conjugation of the molecules and also creating more rigid structures through incorporation of extra rings and also introducing electron-withdrawing or charged substituents such as fluorines or sulfonates, respectively.[102] There are other labelling molecules that can be

used for specific applications that provide other beneficial outcomes and display alternative properties over organic fluorophores such as: lanthanide chelates[103], quantum dots[104] and self-luminescent organic nanoparticles.[105,106] However, not all of these labels are suitable for attachment to a ligand and due to the commercial availability of many organic fluorophores this makes them more suitable for the development of initial fluorescently labelled ligands.

Table 5. Optical properties of importance to fluorescent compounds.[107,108]

Molar absorption coefficient (ε)	Absorbance divided by the absorption path length and the specific concentration
Quantum yield (Φ_f)	Number of emitted photons occurring per number of absorbed photons
Brightness	Extinction coefficient × quantum yield of fluorescence
Bleaching	Loss of excited fluorophore as a result of photosensitized generation of reactive oxygen species
Fluorescence lifetime	The total time the fluorophore may remain in the excited state before it releases a photon and decays back to a ground state
pH dependence	The ability of a fluorophore to function in a specific pH environment or become effected by large changes to pH
Quenching	Loss of fluorescence signal due to interactions with the environment
Stokes shift	The difference between the absorbance and emission maxima

There a number of traditional fluorophores based on the scaffolds of fluorescein (**36**), rhodamine (**37**), BODIPY (**38**) and cyanine (**39**) (Figure 11) from which further derivatives have been developed and optimized that have excitation and emission profiles in suitable regions in the visible spectrum for use in imaging techniques (Figure 12). Fluorophores based on the structural core of fluorescein are commonly used due to displaying high molar absorptivity and good water solubility and fluorescence quantum yield that makes them suitable for confocal microscopy imaging and flow cytometry.[109] However, these dyes do possess various drawbacks such as being susceptible to photobleaching[110] and quenching and also have some pH sensititvity.[111] Rhodamine-based fluorophores, whilst structurally similar to the fluoresceins have greater pH stability and less photodegradation,[112,113] therefore depending on the fluorescent derivative, may

have increased sensitivity which is particularly beneficial for imaging purposes. Cyanine fluorophores move away from the central xanthene core that is present in many fluorescein and rhodamine based derivatives. They instead consist of two aromatic or heterocyclic rings that are connected through a conjugated carbon-carbon system.[109] Sulfonate derivatives of cyanine fluorophores have been especially advantageous towards increasing the solubility in an aqueous environment and also contribute to an increase in brightness.[114] The structures of BODIPY fluorophores are based upon a 4,4-difluoro-4-bora-3a,4a-diaza-*s*-indacene core which can then be further substituted. BODIPY fluorescent derivatives offer many benefical properties for use in biological labelling as they are highly fluorescent and are insensitive to solvent polarity and pH.[115] Additionally, their large absorption coefficent and high fluorescence quantum yields make them suitable for a variety of different applications and particularly for imaging purposes.[116]

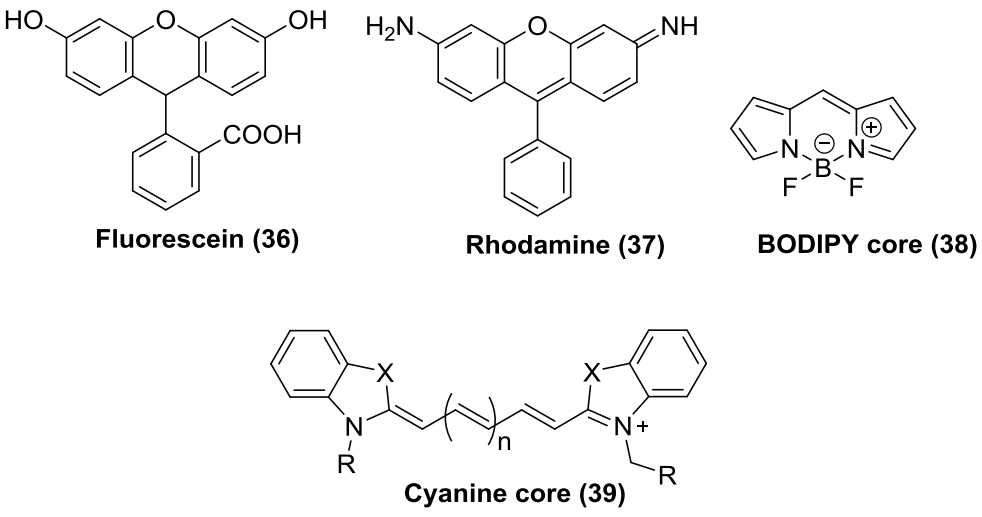

Figure 11. Scaffolds of xanthene based fluorophores fluorescein and rhodamine, representation of the BODIPY 4,4-difluoro-4-bora-3a,4a-diaza-*s*-indacene core and the general substitution pattern of cyanine based fluorophores.

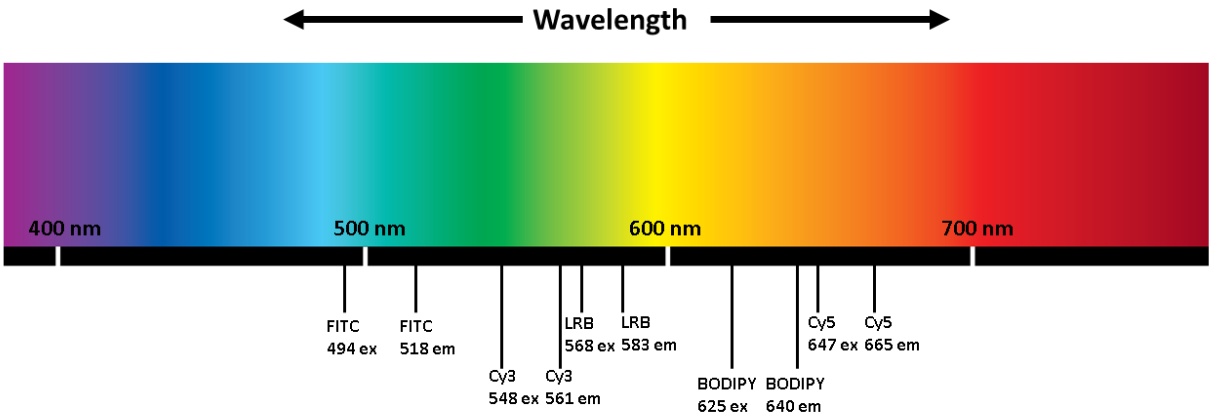

Figure 12. Visible spectrum showing the excitation and emission wavelengths of the following fluorophores: Cy5 (647/665), Cy3 (548/561), BODIPY 630/650-X (625/640), LRB (568/583) and FITC (494/518).

3.5.3. Applications of fluorescently labelled ligands

There are multiple receptors implicated in CNS disorders as indicated in section 1.3, in particular, certain receptor subtypes. As a result of this, there have been countless efforts towards the synthesis of fluorescently labelled ligands for class A GPCRs that are subtype selective in addition to being suited towards a certain application.[117] Some of these targets include histamine receptors,[118] mAChRs,[119] and serotonin receptors.[120] The following will provide a brief review on the development of fluorescently labelled ligands for dopamine D_2 and adenosine A_1 and A_3 receptors and how they have been utilised using a variety of different techniques.

Fluorescently labelled ligands that target the D_2R has been relatively limited. Initial work focused on the development of fluorescently labelled antagonists of *N*-(p-aminophenethyl)spiperone (NAPS, **40**, Figure 13) which is a structural derivative of spiperone (a first generation antipsychotic). Analogues of NAPS were able to maintain nanomolar binding affinities at the D_2R when BODIPY, fluorescein, rhodamine texas red, coumarin and cascade blue fluorophores were attached.[121,122] When attached to the fluorescent probes biotin or 7-nitrobenz-2-oxa-1,3-diazole-4-yl (NBD), both fluorescently labelled ligands had binding

affinities of 0.58 and 0.66 nM and had 190- and 150-fold D_2/D_1 selectivity respectively.[123,124] In a follow up study, some of the fluorescently labelled ligands such as NAPS -BODIPY, -rhodamine and -fluorescein were used to identify the localisation of dopamine D_2 receptors in neuronal tissue such as the striatum and also show specific binding.[125] The work on fluorescently labelled ligands of NAPS particularly highlights that antagonists for the D_2R are able to tolerate fluorescent dyes and still maintain high binding affinity. Furthermore, it has also been demonstrated that fluorophores can be coupled to a D_2R agonist, 2-(*N*-phenthyl-*N*-propyl)amino-5-hydroxytetralin, and still retain full agonist efficacy.[122]

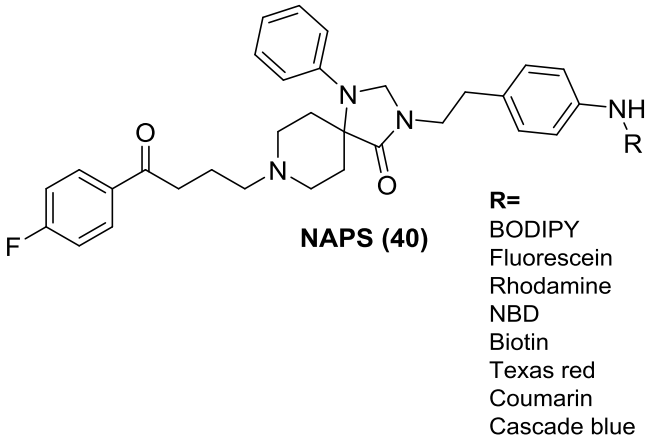

Figure 13. Structure of NAPS (**40**) and various fluorophores that were attached.

The development of fluorescently labelled ligands for adenosine receptors has included assessing the SAR of both antagonist and agonist derivatives. Work on the agonist adenosine 5′-*N*-ethyl caboxamide (NECA) showed that attachment of the fluorophore BODIPY 630/650-X to give compound **41** (Figure 14) was able to maintain full agonist efficacy. Confocal imaging showed clear cell membrane binding of the adenosine A_1 receptor (Figure 14) and measurements using fluorescence correlation spectroscopy (FCS), a technique used to record the fluctuations in fluorescence intensity that can be used to quantify ligand-receptor interactions[126], revealed the presence of two agonist-receptor complexes.[127] Subsequent optimisation of **41** lead to detailed SAR around the linker composition and length of the spacer between NECA and BODIPY for utilisation as a selective A_1R fluorescently labelled agonist.[101,128]

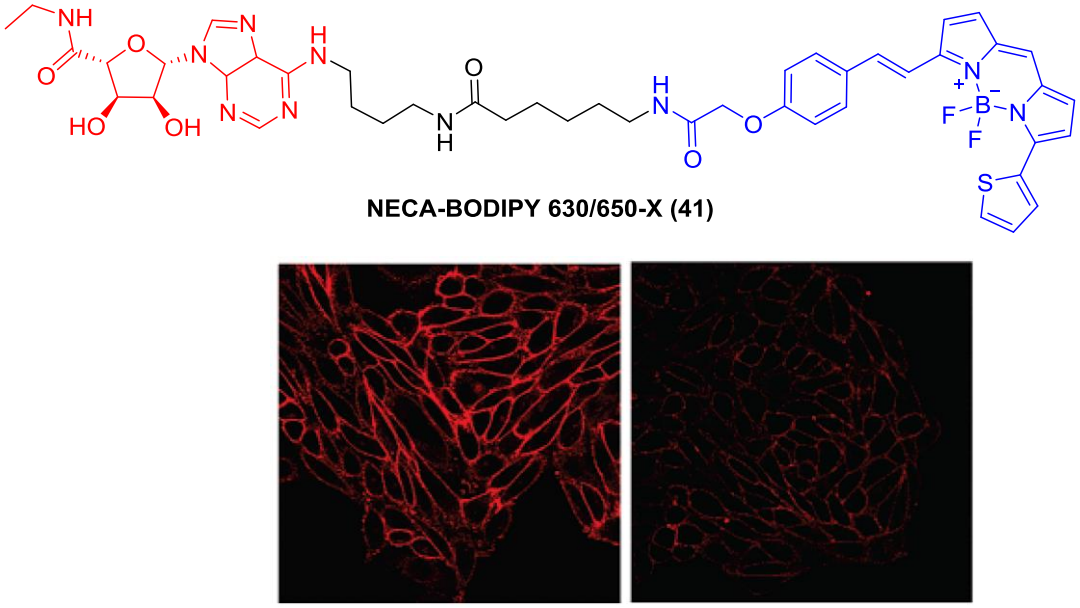

Figure 14. The structure of the A_1R fluorescently labelled ligand NECA-BODIPY 630/650-X and confocal images of the ligand in the control condition (LEFT) and with pre-incubation with the non-fluorescent antagonist DPCPX to show the degree of non-specific binding (RIGHT) at the A_1R.

Previous research using antagonists for the A_3R based on the 1,2,4-triazolo[4,3-*a*]quinoxalin-1-one scaffold (**42**) and attaching different fluorophores (Figure 15) showed that most fluorescent derivatives were able to maintain relatively high binding affinities for the A_3R. In most cases the affinity was maintained or enhanced in comparison to the congeners (the ligands which have been functionalised with a linker but don't yet have the fluorophore attached). Of this series, the BODIPY 630/650-X derivative of **42** was able to demonstrate clear and specific membrane labelling for the A_3R using confocal microscopy.[129]

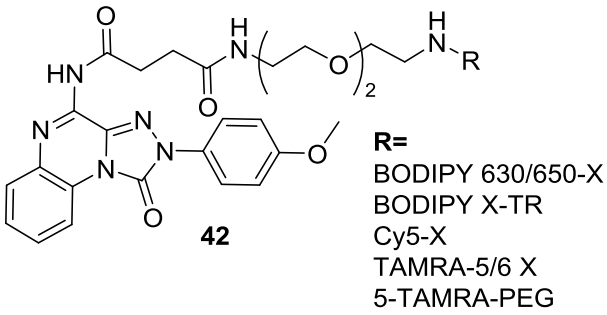

Figure 15. Fluorescent derivatives of the A_3R antagonist **42**.

While there are multiple applications for uses of fluorescently labelled ligands, such as the expression and localisation of GPCRs, receptor ligand interactions (eg. kinetics) and trafficking (internalisation and recycling; agonists), a particular advantage is that fluorescently labelled ligands can be adapted towards competitive binding assays. The distinct advantage of fluorescently labelled ligands over radioligand binding approaches is that it avoids the use of radioactive materials. Fluorescent approaches are also highly sensitive and can be performed in suitable time scales. Compared to radioligand binding assays, the visualisation of what is happening is possible, often down to a single cell level. For assays that involve receptor purification or the isolation of membranes for radioligand approaches, this can be avoided with fluorescent binding assays as they can be performed directly on live cells in real-time.[130,131]

Stoddart et al.[132] developed a fluorescent based binding assay using CA200645 (**43**, Figure 16), which is based on a modified xanthine fluorescent probe which has previously been utilised in confocal microscopy and FCS studies for the A_1R.[133] The assay uses confocal microscopy which performs automated capture to take images of the ligand binding to live cells. The amount of bound fluorophore is quantified via intensity at different concentration ranges (Figure 16A). This can then be used to construct competition curves which can be used to accurately determine affinity values (Figure 16B). The authors showed that this technique could be applied towards the screening of a fragment library in which the assay could evaluate the binding of low-affinity compounds, thus highlighting its potential to be used as a HTS approach.

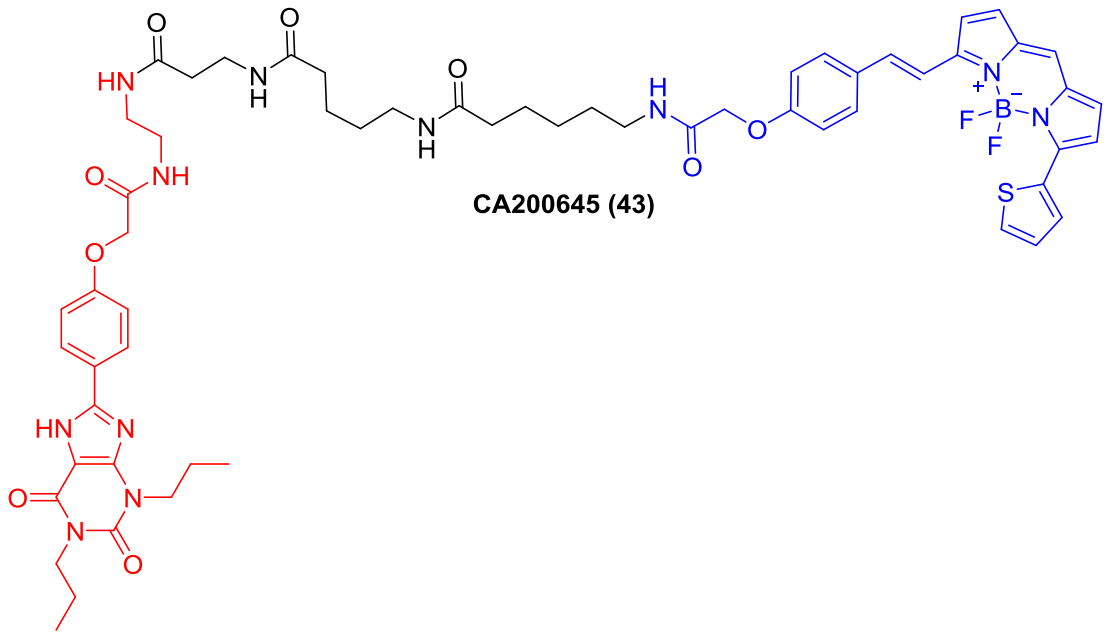

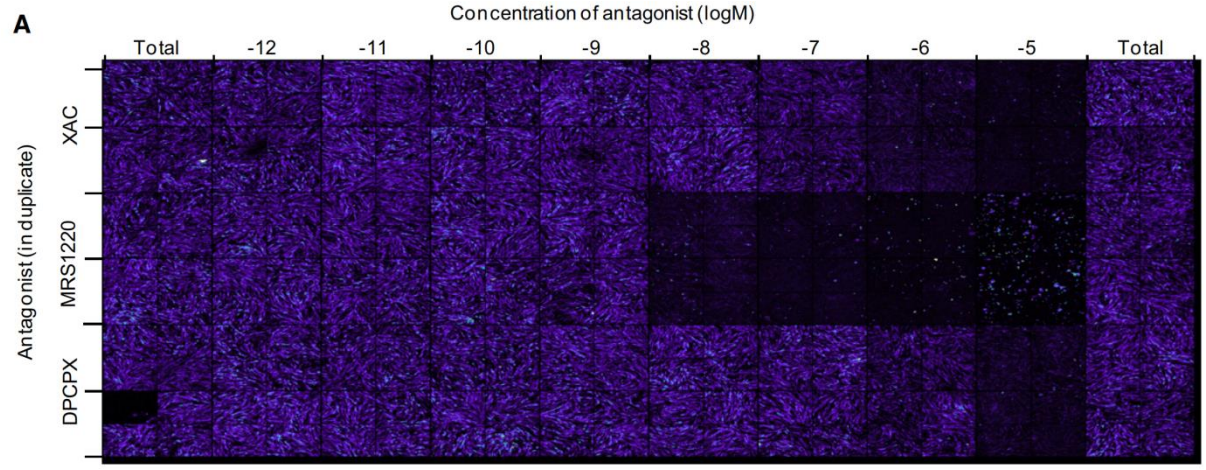

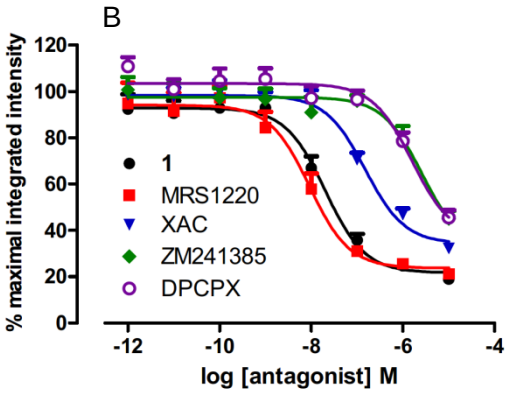

Figure 16. Fluorescence binding assay using BODIPY 630/650-X labelled ligand CA200645 (**43**). A) Images captured on the confocal microscope of antagonists XAC, MRS1220 and DPCPX at the A_3R. The results of quantifying the intensity over the concentration range tested (10 μM to 1 pM) is translated to a competition curve in (B) along with two other antagonists (1 and ZM241385).

Due to the highly successful advances in the development of fluorescently labelled agonists and antagonists, this provides the scope to achieve similar applications in confocal microscopy and FCS for the D_2R. The involvement of the D_2R in multiple CNS disorders makes the idea of a fluorescent based competition binding assay an attractive concept in order to screen for new drugs and/or fragments.

3.6. Other techniques

Medicinal chemistry approaches to achieve polypharmacology and/or subtype selectivity at GPCRs is a vast field that takes advantage of many different techniques. It is not always possible to use every technique and some techniques can rely on the use of others before progressing towards a potential drug candidate or lead. Therefore, while this thesis explores some key techniques/approaches as previously described, medicinal chemists are not limited to these techniques.

Computational modelling is often a powerful tool that is usually used in parallel with another technique. Specifically, it can be used to model how certain ligands may be interacting with the receptor of interest. Therefore it may help to deduce a mechanism of binding, how certain ligands may be selective over non-selective ligands and the SAR around compounds. One of the main uses of computational modelling comes from its ability to predict the structure of GPCRs through homology modelling based on x-ray crystal structures of known GPCRs. This therefore allows the ligands to be docked directly into the predicted model of the desired receptor target. The success of computational modelling does in many circumstances rely on biological data to confirm results or predictions. The success of computational modelling has also allowed *in silico* methods such as virtual screening as a HTS avenue.[134] This approach can search through sometimes very large chemical libraries to generate a variety of "hits" that can be used to synthetically guide a medicinal chemist.

In many cases, working on previous drugs or chemical scaffolds can be very advantageous in developing new drugs because a great deal of SAR is already known for that receptor target. However, there is always the need to develop new drugs based on new chemical structures that may enhance activity or may lack certain side-effects that may be associated with previous chemical scaffolds. In this regard, chemogenomics is a useful approach in identifying new scope for exisiting receptor targets in addition to developing drugs with favourable polypharmacology. For example, the construction of phylogenetic trees for the classification of GPCRs is useful for revealing relationships between GPCRs that may not be immediately obvious through a sequence-based approach.[135] Thus this is particularly useful for the design of ligands with a polypharmacology profile. Subsequently, construction of ligand- and sequence-based dendrograms for GPCRs can be used to identify ligands that may be linked distantly via sequence but are neighbours by ligand similarity.[136]

4. Summary

It has become evident that drug design for the CNS can no longer follow a simple one receptor target approach.[137] In particular for the design of antipsychotics, there are multiple receptors that are implicated and in order to have the best possible chance of addressing all three subsets of symptoms for schizophrenia, considering multiple receptor targets is paramount. In order to do this, this thesis looks at using multiple different medicinal chemistry approaches as a way to gain subtype or pathway specific selectivity (allosteric approaches and biased agonism) in addition to synthesising merged DMLs via the use of privileged structures and finally the use of fluorescently labelled ligands to create a 'toolbox' of ligands that may be applied towards a HTS approach via the development of a fluorescence competition binding assay.

Thesis aims

Aim 1- Allosteric modulators based on LY2033298

LY2033298 still remains the 'best in class' for PAMs targeting the M_4 mAChR, therefore the aim was to utilise LY203398 as part of a DML approach to make use of its allosteric mode of action in combination with a D_2 antagonist or partial agonist. Before doing this it was essential to perform a comprehensive SAR study of LY2033298 to determine what structural features are essential for its activity and where there may be suitable tethering points. The proposed structural changes are outlined in Figure 17. To assess whether it was possible to link off LY203398, there were two linkage points for exploration; *N*-alkyl substituents from the right hand side and *O*-alkyl substituents from the left hand side by gradually increasing the chain length from 2-6 carbon atoms in length. This information could not only reveal whether linkers are tolerable at these positions, but it could also inform the degree of space available in the allosteric binding site at these positions. As a third linkage point, substitution off the primary amine with acyl linkers was also a synthetically viable option to investigate. The last position was the 5′ position on the thienopyridine scaffold. Replacing the chlorine with larger halogens with concomitantly reduced electronegativity (Br and I) could provide useful SAR knowledge about not only the size but electronic effects at this position. The compounds were to be profiled using the operational model of allosterism to obtain values of functional affinity (K_B), the cooperativity of the compounds with ACh ($\alpha\beta$) and the intrinsic agonism (τ_B). To gain more insight into the allosteric modulatory properties of certain compounds of interest, profiling of the compounds in a radioligand binding assay to obtain values of affinity modulation (α), could then be used to generate a value for the efficacy modulation (β).

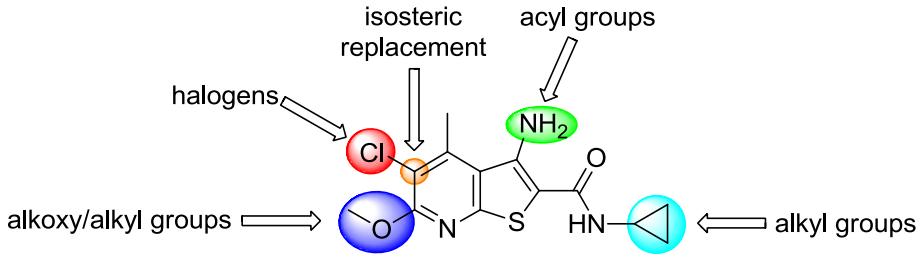

Figure 17. Structural diversification of LY2033298 (**10**).

Aim 2- Biased ligands for the dopamine D_2 receptor

The concept of biased agonism and what may influence ligands to be biased towards certain signalling pathways over others is becoming an increasingly important topic. In view of the possible relationship between bias and antipsychotic efficacy at the D_2R, further investigation of this topic may prove useful in the design of new antipsychotics. The series of ligands intended for synthesis are based on the model pharmacophore in Figure 18. Three distinct privileged structures for the D_2R were chosen, namely 2-methoxyphenylpiperazine, 2,3-dichlorophenylpiperazine and 4,4-chlorophenyl-4-hydroxypiperidine. These privileged structures were linked with variable length spacers to thienopyridine heterocycles (which are structurally similar to many of the lipophilic appendages of D_2 ligands), providng a number of analogues for SAR analysis into the structural requirements of biased agonism at the D_2R. Ligands that displayed partial agonism were then to be calculated using a method for quantifying bias.[138]

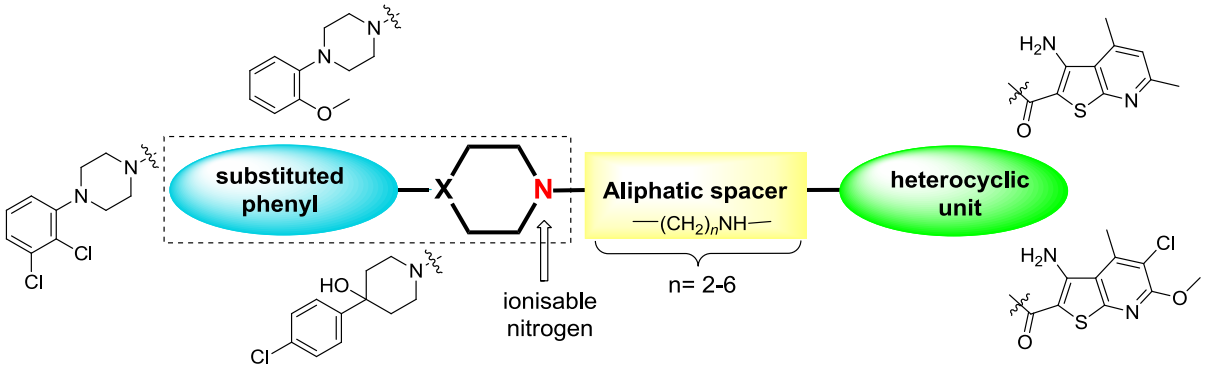

Figure 18. Model pharmacophore for the development of novel D_2R antagonists and/or partial agonists.

Aim 3- Merged DMLs for the M_1 muscarinic acetylcholine receptor and dopamine D_2 receptor

Utilising both the merged DML approach and the use of privileged structures, the aim was to synthesise a focused group of compounds that involved incorporating privileged structures for the D_2R and merging them with the putatative M_1 allosteric agonist LuAE51090 (**8**). In particular, D_2 antagonism or partial agonism in combination with activity at serotonin 5-HT_{2A} receptors, have been shown to be beneficial towards antipsychotic efficacy. The intended synthesised ligands were designed to incorporate a putative M_1 allosteric functionality, for both subtype selectivity and because agonism of the M_1 mAChR has been shown to be beneficial towards the cognitive deficits that are present in key CNS disorders. There were common features inherent in the structure of **8** that made it ideal for incorporating D_2 privileged structures as highlighted in Figure 19. Privileged structures were selected from the D_2R based on three groups; (i) phenylpiperazines, (ii) antipsychotics and (iii) partial agonists.

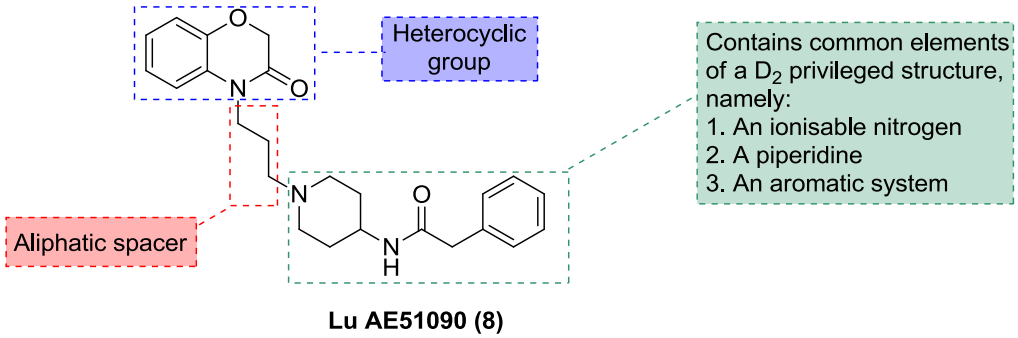

Figure 19. Structure of **8** highlighting key dopaminergic D_2 structural characteristics; a motif containing features of common privileged structures namely an aryl system and ionisable nitrogen atom, an aliphatic spacer/linker and a heterocyclic group.

Aim 4- Fluorescently labelled ligands for the dopamine D_2 receptor

To design a "toolbox" of fluorescently labelled ligands for the D_2R that could be optimised for a HTS approach for the identification of novel and selective ligands in addition to new scaffolds for further optimisation. To do this, four ligands each with their own unique structural characteristics and functionality were chosen (Figure 20). The first ligand, SB269652 is a NAM

for D_2/D_3 receptors.[139] As there are limited NAMs for the D_2R, a fluorescent derivative may aid in confirming this mechanism of action and give more insight into the location of the allosteric pocket of the D_2R. There is also sufficient evidence that supports SB269652 extends from the orthosteric site into a secondary pocket at the D_2R, with the indole moiety being the most suitable point for attachment of a fluorophore.[140] The second ligand, 2-MPP-SB269652, is a structural derivative of SB269652 identified in-house, that was found to be a high affinity ligand for the D_2R. The high affinity, in combination with its novelty made it a suitable ligand, as attachment of a fluorophore was postulated to be at a similar position to that of SB269652. The third ligand was the antipsychotic clozapine for which previous SAR has already been generated.[73] The final ligand ropinirole, a D_2R agonist has also been profiled extensively.[74] This provided valuable insight into a suitable tethering point for the attachment of fluorophores to both clozapine and ropinirole.

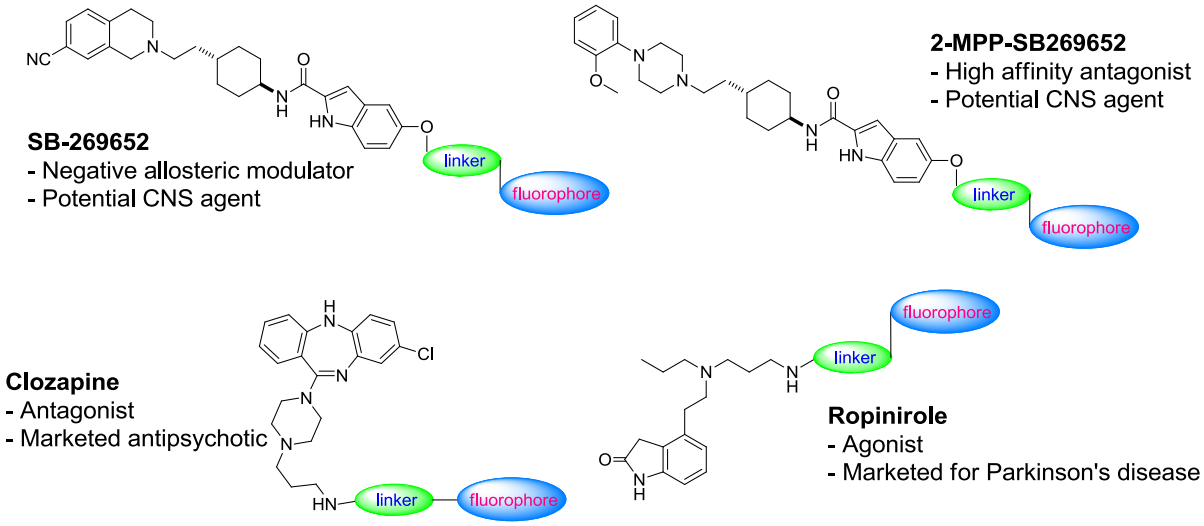

Figure 20. Proposed ligands and their structural modifications for development as fluorescently labelled ligands.

As this is intended to be an initial SAR screen of the compounds, the aim was to explore a variety of fluorophores for attachment to the four chosen ligands (Figure 21). Fluorophore

choices were based on the diversity in the region of the electromagnetic spectrum they emit, as well as their structural diversity and cost.

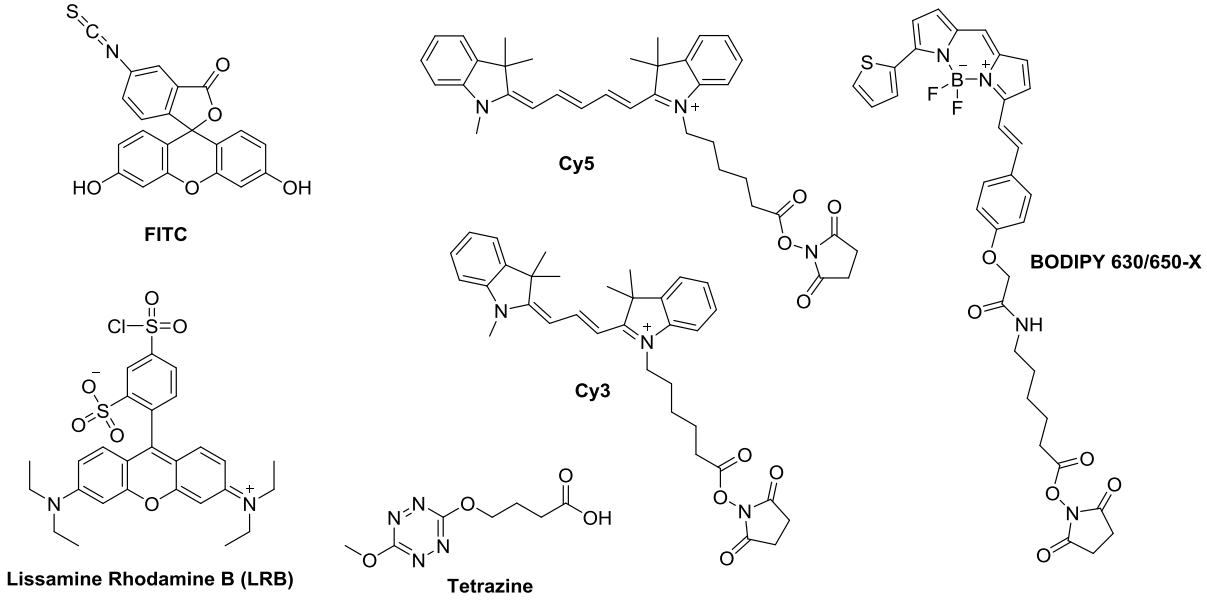

Figure 21. Commercially available activated fluorophores (excluding the tetrazine analogue which is activated in situ) for the generation of fluorescently labelled ligands.

References

1. Rosenbaum, D. M.; Rasmussen, S. G. F.; Kobilka, B. K. The structure and function of G-protein-coupled receptors. *Nature* **2009,** *459*, 356-363.

2. Oldham, W. M.; Hamm, H. E. Heterotrimeric G protein activation by G-protein-coupled receptors. *Nat. Rev. Mol. Cell Biol.* **2008,** *9*, 60-71.

3. Marinissen, M. J.; Gutkind, J. S. G-protein-coupled receptors and signaling networks: Emerging paradigms. *Trends Pharmacol. Sci.* **2001,** *22*, 368-376.

4. Hur, E.-M.; Kim, K.-T. G protein-coupled receptor signalling and cross-talk: Achieving rapidity and specificity. *Cell. Signalling* **2002,** *14*, 397-405.

5. Overington, J. P.; Al-Lazikani, B.; Hopkins, A. L. How many drug targets are there? *Nat. Rev. Drug. Discov.* **2006,** *5*, 993-996.

6. Ballabh, P.; Braun, A.; Nedergaard, M. The blood–brain barrier: An overview: Structure, regulation, and clinical implications. *Neurobiol. Dis.* **2004,** *16*, 1-13.

7. Pardridge, W. M. Drug transport across the blood-brain barrier. *J. Cereb. Blood Flow Metab.* **2012,** *32*, 1959-1972.

8. Pajouhesh, H.; Lenz, G. R. Medicinal chemical properties of successful central nervous system drugs. *NeuroRx* **2005,** *2*, 541-553.

9. Lipinski, C. A.; Lombardo, F.; Dominy, B. W.; Feeney, P. J. Experimental and computational approaches to estimate solubility and permeability in drug discovery and development settings. *Adv. Drug Delivery Rev.* **2001,** *46*, 3-26.

10. Seeman, P. Targeting the dopamine D_2 receptor in schizophrenia. *Expert Opin. Ther. Targets* **2006,** *10*, 515-531.

11. Thathiah, A.; De Strooper, B. The role of G protein-coupled receptors in the pathology of Alzheimer's disease. *Nat. Rev. Neurosci.* **2011,** *12*, 73-87.

12. Missale, C.; Nash, S. R.; Robinson, S. W.; Jaber, M.; Caron, M. G. Dopamine receptors: From structure to function. *Physiol. Rev.* **1998,** *78*, 189-225.

13. Catapano, L. A.; Manji, H. K. G protein-coupled receptors in major psychiatric disorders. *Biochim. Biophys. Acta, Biomembr.* **2007,** *1768*, 976-993.

14. Burnet, P. W. J.; Eastwood, S. L.; Lacey, K.; Harrison, P. J. The distribution of 5-HT_{1A} and 5-HT_{2A} receptor MRNA in human brain. *Brain Res.* **1995,** *676*, 157-168.

15. Hamon, M.; Doucet, E.; Lefevre, K.; Miquel, M.-C.; Lanfumey, L.; Insausti, R.; Frechilla, D.; Del Rio, J.; Verge, D. Antibodies and antisense oligonucleotide for probing the distribution and putative functions of central 5-HT_6 receptors. *Neuropsychopharmacology* **1999,** *21*, 68S-76S.

16. Hedlund, P. B.; Sutcliffe, J. G. Functional, molecular and pharmacological advances in 5-HT_7 receptor research. *Trends Pharmacol. Sci.* **2004,** *25*, 481-486.

17. Ito, H.; Halldin, C.; Farde, L. Localization of 5-HT_{1A} receptors in the living human brain using [Carbonyl-11C]WAY-100635: Pet with anatomic standardization technique. *J. Nucl. Med.* **1999,** *40*, 102-109.

18. Pompeiano, M.; Palacios, J. M.; Mengod, G. Distribution of the serotonin 5-HT_2 receptor family MRNAs: Comparison between 5-HT_{2A} and 5-HT_{2C} receptors. *Mol. Brain Res.* **1994,** *23*, 163-178.

19. Buckley, N. J.; Bonner, T. I.; Brann, M. R. Localization of a family of muscarinic receptor MRNAs in rat brain. *J. Neurosci.* **1988,** *8*, 4646-4652.

20. Herman, E. J.; Bubser, M.; Conn, P. J.; Jones, C. K., Metabotropic glutamate receptors for new treatments in schizophrenia. In *Novel antischizophrenia treatments*, Geyer, M. A.; Gross, G., Eds. Springer Berlin Heidelberg: 2012; Vol. 213, pp 297-365.

21. Romano, C.; Sesma, M. A.; McDonald, C. T.; O'Malley, K.; van den Pol, A. N.; Olney, J. W. Distribution of metabotropic glutamate receptor $mGluR_5$ immunoreactivity in rat brain. *J. Comp. Neurol.* **1995,** *355*, 455-469.

22. Ohishi, H.; Shigemoto, R.; Nakanishi, S.; Mizuno, N. Distribution of the mrna for a metabotropic glutamate receptor ($mGluR_3$) in the rat brain: An in situ hybridization study. *J. Comp. Neurol.* **1993,** *335*, 252-266.

23. Dixon, A. K.; Gubitz, A. K.; Sirinathsinghji, D. J. S.; Richardson, P. J.; Freeman, T. C. Tissue distribution of adenosine receptor MRNAs in the rat. *Brit. J. Pharmacol.* **1996,** *118*, 1461-1468.

24. Esbenshade, T. A.; Browman, K. E.; Bitner, R. S.; Strakhova, M.; Cowart, M. D.; Brioni, J. D. The histamine H3 receptor: An attractive target for the treatment of cognitive disorders. *Brit. J. Pharmacol.* **2008,** *154*, 1166-1181.

25. Waters, S. M.; Krause, J. E. Distribution of Galanin-1, -2 and -3 receptor messenger RNAs in central and peripheral rat tissues. *Neuroscience* **1999,** *95*, 265-271.

26. Andreasen, N. C. Schizophrenia: The fundamental questions. *Brain. Res. Rev.* **2000,** *31*, 106-112.

27. Rosen, W. G.; Mohs, R. C.; Johns, C. A.; Small, N. S.; Kendler, K. S.; Horvath, T. B.; Davis, K. L. Positive and negative symptoms in schizophrenia. *Psychiatry Res.* **1984,** *13*, 277-284.

28. Lublin, H. Cognitive dysfunction in schizophrenia. *Acta. Psychiatr. Scand.* **2001,** *104*, 5-9.

29. Heinrichs, R. W.; Zakzanis, K. K. Neurocognitive deficit in schizophrenia: A quantitative review of the evidence. *Neuropsychology* **1998,** *12*, 426-445.

30. Saykin, A. J.; Gur, R. C.; Gur, R. E.; Mozley, P. D.; Mozley, L. H.; Resnick, S. M.; Kester, D. B.; Stafiniak, P. Neuropsychological function in schizophrenia: Selective impairment in memory and learning. *Arch Gen Psychiatry* **1991,** *48*, 618-624.

31. Andreasen, N. C. Symptoms, signs, and diagnosis of schizophrenia. *Lancet* **1995,** *346*, 477-481.

32. Orgainisation, W. H. Schizophrenia, http://www.who.int (accessed June, 2014).

33. Capuano, B.; Crosby, I. T.; Lloyd, E. J. Schizophrenia: Genesis, receptorology and current therapeutics. *Curr. Med. Chem.* **2002,** *9*, 521-548.

34. Toda, M.; Abi-Dargham, A. Dopamine hypothesis of schizophrenia: Making sense of it all. *Current. Psychiat. Rep.* **2007,** *9*, 329-336.

35. Tomiyama, G. Chronic schizophrenia-like states in methamphetamine psychosis. *Psychiatry Clin. Neurosci.* **1990,** *44*, 531-539.

36. Janowsky, D.; Risch, C. Amphetamine psychosis and psychotic symptoms. *Psychopharmacology* **1979,** *65*, 73-77.

37. Owen, F.; Crow, T. J.; Poulter, M.; Cross, A. J.; Longden, A.; Riley, G. J. Increased dopamine-receptor sensitivity in schizophrenia. *Lancet* **1978,** *312*, 223-226.

38. Mackay, A. V. P.; Iversen, L. L.; Rossor, M.; Spokes, E.; Bird, E.; Arregui, A.; Creese, I.; Snyder, S. H. Increased brain dopamine and dopamine receptors in schizophrenia. *Arch. Gen. Psychiatry* **1982,** *39*, 991-997.

39. Meltzer, H. Y. The role of serotonin in antipsychotic drug action. *Neuropsychopharmacology* **1999,** *21*, 106S-115S.

40. Meltzer, H. Y.; Massey, B. W. The role of serotonin receptors in the action of atypical antipsychotic drugs. *Curr. Opin. Pharmacol.* **2011,** *11*, 59-67.

41. Inoue, T.; Domae, M.; Yamada, K.; Furukawa, T. Effects of the novel antipsychotic agent 7-(4-[4-(2,3-dichlorophenyl)-1-piperazinyl]butyloxy)-3,4-dihydro -2(1H)-quinolinone (OPC-14597) on prolactin release from the rat anterior pituitary gland. *J. Pharmacol. Exp. Ther.* **1996,** *277*, 137-143.

42. Jordan, S.; Koprivica, V.; Chen, R.; Tottori, K.; Kikuchi, T.; Altar, C. A. The antipsychotic aripiprazole is a potent, partial agonist at the human 5-HT_{1A} receptor. *Eur. J. Pharmacol.* **2002,** *441*, 137-140.

43. Shapiro, D. A.; Renock, S.; Arrington, E.; Chiodo, L. A.; Liu, L.-X.; Sibley, D. R.; Roth, B. L.; Mailman, R. Aripiprazole, a novel atypical antipsychotic drug with a unique and robust pharmacology. *Neuropsychopharmacology* **2003,** *28*, 1400-1411.

44. Tamminga, C. A. Partial dopamine agonists in the treatment of psychosis. *J. Neural. Transm.* **2002,** *109*, 411-420.

45. Mailman, R. B.; Murthy, V. Third generation antipsychotic drugs: Partial agonism or receptor functional selectivity? *Curr. Pharm. Design* **2010,** *16*, 488-501.

46. Jeffrey Conn, P.; Christopoulos, A.; Lindsley, C. W. Allosteric modulators of GPCRs: A novel approach for the treatment of CNS disorders. *Nat. Rev. Drug. Discov.* **2009,** *8*, 41-54.

47. May, L. T.; Leach, K.; Sexton, P. M.; Christopoulos, A. Allosteric modulation of G protein-coupled receptors. *Annu. Rev. Pharmacol. Toxicol.* **2007,** *47*, 1-51.

48. Kenakin, T. P. Biased signalling and allosteric machines: New vistas and challenges for drug discovery. *Brit. J. Pharmacol.* **2012,** *165*, 1659-1669.

49. Gregory, K. J.; Sexton, P. M.; Christopoulos, A. Allosteric modulation of muscarinic acetylcholine receptors. *Curr. Neuropharmacol.* **2007,** *5*, 157-167.

50. Levey, A.; Kitt, C.; Simonds, W.; Price, D.; Brann, M. Identification and localization of muscarinic acetylcholine receptor proteins in brain with subtype-specific antibodies. *J. Neurosci* **1991,** *11*, 3218-3226.

51. Langmead, C. J.; Watson, J.; Reavill, C. Muscarinic acetylcholine receptors as CNS drug targets. *Pharmacol. Ther.* **2008,** *117*, 232-243.

52. Raedler, T. J.; Bymaster, F. P.; Tandon, R.; Copolov, D.; Dean, B. Towards a muscarinic hypothesis of schizophrenia. *Mol. Psychiatry* **2007,** *12*, 232-246.

53. Shekhar, A.; Potter, W. Z.; Lightfoot, J.; Lienemann, J.; Dube, S.; Mallinckrodt, C.; Bymaster, F. P.; McKinzie, D. L.; Felder, C. C. Selective muscarinic receptor agonist xanomeline as a novel treatment approach for schizophrenia. *Am. J. Psychiatry* **2008,** *165*, 1033-1039.

54. Davie, B. J.; Christopoulos, A.; Scammells, P. J. Development of M_1 mAChR allosteric and bitopic ligands: Prospective therapeutics for the treatment of cognitive deficits. *ACS Chem. Neurosci.* **2013,** *4*, 1026-1048.

55. Valant, C.; Sexton, P. M.; Christopoulos, A. Orthosteric/allosteric bitopic ligands going hybrid with gpcrs. *Mol. Interventions* **2009,** *9*, 125-135.

56. Mohr, K.; Tränkle, C.; Kostenis, E.; Barocelli, E.; De Amici, M.; Holzgrabe, U. Rational design of dualsteric GPCR ligands: Quests and promise. *Brit. J. Pharmacol.* **2010,** *159*, 997-1008.

57. Lane, J. R.; Sexton, P. M.; Christopoulos, A. Bridging the gap: Bitopic ligands of G-protein-coupled receptors. *Trends Pharmacol. Sci.* **2013,** *34*, 59-66.

58. Avlani, V. A.; Langmead, C. J.; Guida, E.; Wood, M. D.; Tehan, B. G.; Herdon, H. J.; Watson, J. M.; Sexton, P. M.; Christopoulos, A. Orthosteric and allosteric modes of interaction of novel selective agonists of the M_1 muscarinic acetylcholine receptor. *Mol. Pharmacol.* **2010,** *78*, 94-104.

59. Keov, P.; Valant, C.; Devine, S. M.; Lane, J. R.; Scammells, P. J.; Sexton, P. M.; Christopoulos, A. Reverse engineering of the selective agonist TBPB unveils both orthosteric and allosteric modes of action at the M_1 muscarinic acetylcholine receptor. *Mol. Pharmacol.* **2013,** *84*, 425-437.

60. Sams, A. G.; Hentzer, M.; Mikkelsen, G. K.; Larsen, K.; Bundgaard, C.; Plath, N.; Christoffersen, C. T.; Bang-Andersen, B. Discovery of *N*-{1-[3-(3-oxo-2,3-dihydrobenzo[1,4]oxazin-4-yl)propyl]piperidin-4-yl}-2-phenylacetamide (Lu AE51090):

An allosteric muscarinic M_1 receptor agonist with unprecedented selectivity and procognitive potential. *J. Med. Chem.* **2010,** *53*, 6386-6397.

61. Lazareno, S.; Doležal, V.; Popham, A.; Birdsall, N. J. M. Thiochrome enhances acetylcholine affinity at muscarinic M_4 receptors: Receptor subtype selectivity via cooperativity rather than affinity. *Mol. Pharmacol.* **2004,** *65*, 257-266.

62. Chan, W. Y.; McKinzie, D. L.; Bose, S.; Mitchell, S. N.; Witkin, J. M.; Thompson, R. C.; Christopoulos, A.; Lazareno, S.; Birdsall, N. J. M.; Bymaster, F. P.; Felder, C. C. Allosteric modulation of the muscarinic M_4 receptor as an approach to treating schizophrenia. *P. Natl. Acad. Sci. USA* **2008,** *105*, 10978-10983.

63. Leach, K.; Loiacono, R. E.; Felder, C. C.; McKinzie, D. L.; Mogg, A.; Shaw, D. B.; Sexton, P. M.; Christopoulos, A. Molecular mechanisms of action and in vivo validation of an M_4 muscarinic acetylcholine receptor allosteric modulator with potential antipsychotic properties. *Neuropsychopharmacology* **2010,** *35*, 855-869.

64. Shirey, J. K.; Xiang, Z.; Orton, D.; Brady, A. E.; Johnson, K. A.; Williams, R.; Ayala, J. E.; Rodriguez, A. L.; Wess, J.; Weaver, D.; Niswender, C. M.; Conn, P. J. An allosteric potentiator of M_4 mAChR modulates hippocampal synaptic transmission. *Nat. Chem. Biol.* **2008,** *4*, 42-50.

65. Brady, A. E.; Jones, C. K.; Bridges, T. M.; Kennedy, J. P.; Thompson, A. D.; Heiman, J. U.; Breininger, M. L.; Gentry, P. R.; Yin, H.; Jadhav, S. B.; Shirey, J. K.; Conn, P. J.; Lindsley, C. W. Centrally active allosteric potentiators of the M_4 muscarinic acetylcholine receptor reverse amphetamine-induced hyperlocomotor activity in rats. *J. Pharmacol. Exp. Ther.* **2008,** *327*, 941-953.

66. Kennedy, J. P.; Bridges, T. M.; Gentry, P. R.; Brogan, J. T.; Kane, A. S.; Jones, C. K.; Brady, A. E.; Shirey, J. K.; Conn, P. J.; Lindsley, C. W. Synthesis and structure-activity relationships of allosteric potentiators of the M_4 muscarinic acetylcholine receptor. *ChemMedChem* **2009,** *4*, 1600-1607.

67. Le, U.; Melancon, B. J.; Bridges, T. M.; Vinson, P. N.; Utley, T. J.; Lamsal, A.; Rodriguez, A. L.; Venable, D.; Sheffler, D. J.; Jones, C. K.; Blobaum, A. L.; Wood, M. R.; Daniels, J. S.; Conn, P. J.; Niswender, C. M.; Lindsley, C. W.; Hopkins, C. R. Discovery of a selective M_4 positive allosteric modulator based on the 3-amino-thieno[2,3-*b*]pyridine-2-carboxamide scaffold: Development of ML253, a potent and brain penetrant compound that is active in a preclinical model of schizophrenia. *Bioorg. Med. Chem. Lett.* **2013,** *23*, 346-350.

68. Huynh, T.; Valant, C.; Crosby, I. T.; Sexton, P. M.; Christopoulos, A.; Capuano, B. Probing structural requirements of positive allosteric modulators of the M_4 muscarinic receptor. *J. Med. Chem.* **2013,** *56*, 8196-8200.

69. Morphy, R.; Kay, C.; Rankovic, Z. From magic bullets to designed multiple ligands. *Drug Discovery Today* **2004,** *9*, 641-651.

70. Morphy, R.; Rankovic, Z., Lead generation approaches in drug discovery. John Wiley & Sons, Inc., 2010.

71. Morphy, R.; Rankovic, Z. Designed multiple ligands. An emerging drug discovery paradigm. *J. Med. Chem.* **2005,** *48*, 6523-6543.

72. Portoghese, P. S. From models to molecules: Opioid receptor dimers, bivalent ligands, and selective opioid receptor probes. *J. Med. Chem.* **2001,** *44*, 2259-2269.

73. McRobb, F. M.; Crosby, I. T.; Yuriev, E.; Lane, J. R.; Capuano, B. Homobivalent ligands of the atypical antipsychotic clozapine: Design, synthesis, and pharmacological evaluation. *J. Med. Chem.* **2012,** *55*, 1622-1634.

74. Jorg, M.; Kaczor, A. A.; Mak, F. S.; Lee, K. C. K.; Poso, A.; Miller, N. D.; Scammells, P. J.; Capuano, B. Investigation of novel ropinirole analogues: Synthesis, pharmacological evaluation and computational analysis of dopamine D_2 receptor functionalized congeners and homobivalent ligands. *MedChemComm* **2014,** *5*, 891-898.

75. Kawanishi, Y.; Ishihara, S.; Tsushima, T.; Seno, K.; Miyagoshi, M.; Hagishita, S.; Ishikawa, M.; Shima, N.; Shimamura, M.; Ishihara, Y. Synthesis and pharmacological evaluation of highly potent dual histamine H_2 and gastrin receptor antagonists. *Bioorg. Med. Chem. Lett.* **1996,** *6*, 1427-1430.

76. Lipinski, C. A. Drug-like properties and the causes of poor solubility and poor permeability. *J. Pharmacol. Toxicol. Methods* **2000,** *44*, 235-249.

77. Lowe, J. A.; Seeger, T. F.; Nagel, A. A.; Howard, H. R.; Seymour, P. A.; Heym, J. H.; Ewing, F. E.; Newman, M. E.; Schmidt, A. W. 1-Naphthylpiperazine derivatives as potential atypical antipsychotic agents. *J. Med. Chem.* **1991,** *34*, 1860-1866.

78. Howard, H. R.; Lowe, J. A.; Seeger, T. F.; Seymour, P. A.; Zorn, S. H.; Maloney, P. R.; Ewing, F. E.; Newman, M. E.; Schmidt, A. W.; Furman, J. S.; Robinson, G. L.; Jackson, E.; Johnson, C.; Morrone, J. 3-Benzisothiazolylpiperazine derivatives as potential atypical antipsychotic agents. *J. Med. Chem.* **1996,** *39*, 143-148.

79. Greenberg, W. M.; Citrome, L. Ziprasidone for schizophrenia and bipolar disorder: A review of the clinical trials. *CNS Drug Rev.* **2007,** *13*, 137-177.

80. Evans, B. E.; Rittle, K. E.; Bock, M. G.; DiPardo, R. M.; Freidinger, R. M.; Whitter, W. L.; Lundell, G. F.; Veber, D. F.; Anderson, P. S. Methods for drug discovery: Development of potent, selective, orally effective cholecystokinin antagonists. *J. Med. Chem.* **1988,** *31*, 2235-2246.

81. Costantino, L.; Barlocco, D. Privileged structures as leads in medicinal chemistry. *Curr. Med. Chem.* **2010,** *5*, 381-422.

82. Bondensgaard, K.; Ankersen, M.; Thøgersen, H.; Hansen, B. S.; Wulff, B. S.; Bywater, R. P. Recognition of privileged structures by G-protein coupled receptors. *J. Med. Chem.* **2004,** *47*, 888-899.

83. DeSimone, R. W.; Currie, K. S.; Mitchell, S. A.; Darrow, J. W.; Pippin, D. A. Privileged structures: Applications in drug discovery. *Comb. Chem. High Throughput Screening* **2004,** *7*, 473-493.

84. Irwin, J. J.; Shoichet, B. K. ZINC − a free database of commercially available compounds for virtual screening. *J. Chem. Inf. Model.* **2004,** *45*, 177-182.

85. Irwin, J. J.; Sterling, T.; Mysinger, M. M.; Bolstad, E. S.; Coleman, R. G. ZINC: A free tool to discover chemistry for biology. *J. Chem. Inf. Model.* **2012,** *52*, 1757-1768.

86. Guo, T.; Hobbs, D. W. Privileged structure-based combinatorial libraries targeting G protein-coupled receptors. *Assay Drug Dev. Technol.* **2003,** *1*, 579-592.

87. Kenakin, T. Functional selectivity and biased receptor signaling. *J. Pharmacol. Exp. Ther.* **2011,** *336*, 296-302.

88. Kenakin, T.; Christopoulos, A. Signalling bias in new drug discovery: Detection, quantification and therapeutic impact. *Nat. Rev. Drug. Discov.* **2013,** *12*, 205-216.

89. Stallaert, W.; Christopoulos, A.; Bouvier, M. Ligand functional selectivity and quantitative pharmacology at G protein-coupled receptors. *Expert Opin. Drug Discovery* **2011,** *6*, 811-825.

90. Shonberg, J.; Lopez, L.; Scammells, P. J.; Christopoulos, A.; Capuano, B.; Lane, J. R. Biased agonism at G protein-coupled receptors: The promise and the challenges—a medicinal chemistry perspective. *Med. Res. Rev.* **2014**, n/a-n/a.

91. Black, J. W.; Leff, P. Operational models of pharmacological agonism. *Proc. R. Soc. Lond. B* **1983,** *220*, 141-162.

92. Mottola, D. M.; Kilts, J. D.; Lewis, M. M.; Connery, H. S.; Walker, Q. D.; Jones, S. R.; Booth, R. G.; Hyslop, D. K.; Piercey, M.; Wightman, R. M.; Lawler, C. P.; Nichols, D. E.; Mailman, R. B. Functional selectivity of dopamine receptor agonists. I. Selective activation of postsynaptic dopamine D_2 receptors linked to adenylate cyclase. *J. Pharmacol. Exp. Ther.* **2002,** *301*, 1166-1178.

93. Gay, E. A.; Urban, J. D.; Nichols, D. E.; Oxford, G. S.; Mailman, R. B. Functional selectivity of D_2 receptor ligands in a chinese hamster ovary hD_{2L} cell line: Evidence for induction of ligand-specific receptor states. *Mol. Pharmacol.* **2004,** *66*, 97-105.

94. Urban, J. D.; Vargas, G. A.; von Zastrow, M.; Mailman, R. B. Aripiprazole has functionally selective actions at dopamine D_2 receptor-mediated signaling pathways. *Neuropsychopharmacology* **2006,** *32*, 67-77.

95. Allen, J. A.; Yost, J. M.; Setola, V.; Chen, X.; Sassano, M. F.; Chen, M.; Peterson, S.; Yadav, P. N.; Huang, X.-p.; Feng, B.; Jensen, N. H.; Che, X.; Bai, X.; Frye, S. V.; Wetsel, W. C.; Caron, M. G.; Javitch, J. A.; Roth, B. L.; Jin, J. Discovery of β-arrestin–biased dopamine D_2 ligands for probing signal transduction pathways essential for antipsychotic efficacy. *P. Natl. Acad. Sci. USA* **2011,** *108*, 18488-18493.

96. Chen, X.; Sassano, M. F.; Zheng, L.; Setola, V.; Chen, M.; Bai, X.; Frye, S. V.; Wetsel, W. C.; Roth, B. L.; Jin, J. Structure–functional selectivity relationship studies of β-arrestin-biased dopamine D_2 receptor agonists. *J. Med. Chem.* **2012,** *55*, 7141-7153.

97. Tschammer, N.; Bollinger, S.; Kenakin, T.; Gmeiner, P. Histidine 6.55 is a major determinant of ligand-biased signaling in dopamine D_{2L} receptor. *Mol. Pharmacol.* **2011,** *79*, 575-585.

98. Kiss, B.; Horváth, A.; Némethy, Z.; Schmidt, É.; Laszlovszky, I.; Bugovics, G.; Fazekas, K.; Hornok, K.; Orosz, S.; Gyertyán, I.; Ágai-Csongor, É.; Domány, G.; Tihanyi, K.; Adham, N.; Szombathelyi, Z. Cariprazine (RGH-188), a dopamine D_3 receptor-preferring, D_3/D_2 dopamine receptor antagonist–partial agonist antipsychotic candidate: In vitro and neurochemical profile. *J. Pharmacol. Exp. Ther.* **2010,** *333*, 328-340.

99. Shonberg, J.; Herenbrink, C. K.; López, L.; Christopoulos, A.; Scammells, P. J.; Capuano, B.; Lane, J. R. A structure–activity analysis of biased agonism at the dopamine D_2 receptor. *J. Med. Chem.* **2013,** *56*, 9199-9221.

100. Möller, D.; Kling, R. C.; Skultety, M.; Leuner, K.; Hübner, H.; Gmeiner, P. Functionally selective dopamine D_2, D_3 receptor partial agonists. *J. Med. Chem.* **2014,** *57*, 4861-4875.

101. Baker, J. G.; Middleton, R.; Adams, L.; May, L. T.; Briddon, S. J.; Kellam, B.; Hill, S. J. Influence of fluorophore and linker composition on the pharmacology of fluorescent adenosine A_1 receptor ligands. *Brit. J. Pharmacol.* **2010,** *159*, 772-786.

102. Giepmans, B. N. G.; Adams, S. R.; Ellisman, M. H.; Tsien, R. Y. The fluorescent toolbox for assessing protein location and function. *Science* **2006,** *312*, 217-224.

103. Hemmilä, I.; Laitala, V. Progress in lanthanides as luminescent probes. *J. Fluoresc.* **2005,** *15*, 529-542.

104. Chan, W. C. W.; Maxwell, D. J.; Gao, X.; Bailey, R. E.; Han, M.; Nie, S. Luminescent quantum dots for multiplexed biological detection and imaging. *Curr. Opin. Biotechnol.* **2002,** *13*, 40-46.

105. Fu, H.-B.; Yao, J.-N. Size effects on the optical properties of organic nanoparticles. *J. Am. Chem. Soc.* **2001,** *123*, 1434-1439.

106. An, B.-K.; Kwon, S.-K.; Park, S. Y. Photopatterned arrays of fluorescent organic nanoparticles. *Angew. Chem., Int. Ed.* **2007,** *46*, 1978-1982.

107. Resch-Genger, U.; Grabolle, M.; Cavaliere-Jaricot, S.; Nitschke, R.; Nann, T. Quantum dots versus organic dyes as fluorescent labels. *Nat. Methods* **2008,** *5*, 763-775.

108. Invitrogen, The molecular probes handbook: A guide to fluorescent probes and labeling technologies 11th ed., 2010.

109. Gonçalves, M. S. T. Fluorescent labeling of biomolecules with organic probes. *Chem. Rev.* **2008,** *109*, 190-212.

110. Song, L.; Varma, C. A.; Verhoeven, J. W.; Tanke, H. J. Influence of the triplet excited state on the photobleaching kinetics of fluorescein in microscopy. *Biophys. J.* **1996,** *70*, 2959-2968.

111. Martin, M. M.; Lindqvist, L. The pH dependence of fluorescein fluorescence. *J. Lumin.* **1975,** *10*, 381-390.

112. Brandtzaeg, P. Rhodamine conjugates: Specific and nonspecific binding properties in immunohistochemistry. *Ann. N. Y. Acad. Sci.* **1975,** *254*, 35-53.

113. McKay, I. C.; Forman, D.; White, R. G. A comparison of fluorescein isothiocyanate and lissamine rhodamine (RB 200) as labels for antibody in the fluorescent antibody technique. *Immunology* **1981,** *43*, 591-602.

114. Wessendorf, M. W.; Brelje, T. C. Which fluorophore is brightest? A comparison of the staining obtained using fluorescein, tetramethylrhodamine, lissamine rhodamine, texas red, and cyanine 3.18. *Histochemistry* **1992,** *98*, 81-85.

115. Karolin, J.; Johansson, L. B. A.; Strandberg, L.; Ny, T. Fluorescence and absorption spectroscopic properties of dipyrrometheneboron difluoride (BODIPY) derivatives in liquids, lipid membranes, and proteins. *J. Am. Chem. Soc.* **1994,** *116*, 7801-7806.

116. Ulrich, G.; Ziessel, R.; Harriman, A. The chemistry of fluorescent BODIPY dyes: Versatility unsurpassed. *Angew. Chem., Int. Ed.* **2008,** *47*, 1184-1201.

117. Vernall, A. J.; Hill, S. J.; Kellam, B. The evolving small-molecule fluorescent-conjugate toolbox for class A GPCRs. *Brit. J. Pharmacol.* **2014,** *171*, 1073-1084.

118. Tomasch, M.; Schwed, J. S.; Paulke, A.; Stark, H. Bodilisant—a novel fluorescent, highly affine histamine H_3 receptor ligand. *ACS Med. Chem. Lett.* **2012,** *4*, 269-273.

119. Daval, S. B.; Valant, C.; Bonnet, D.; Kellenberger, E.; Hibert, M.; Galzi, J.-L.; Ilien, B. Fluorescent derivatives of AC-42 to probe bitopic orthosteric/allosteric binding mechanisms on muscarinic M_1 receptors. *J. Med. Chem.* **2012,** *55*, 2125-2143.

120. Alonso, D.; Vázquez-Villa, H.; Gamo, A. M.; Martínez-Esperón, M. F.; Tortosa, M.; Viso, A.; Fernández de la Pradilla, R.; Junquera, E.; Aicart, E.; Martín-Fontecha, M.; Benhamú, B.; López-Rodríguez, M. L.; Ortega-Gutiérrez, S. Development of fluorescent ligands for the human 5-HT_{1A} receptor. *ACS Med. Chem. Lett.* **2010,** *1*, 249-253.

121. Monsma, F. J.; Barton, A. C.; Chol Kang, H.; Brassard, D. L.; Haugland, R. P.; Sibley, D. R. Characterization of novel fluorescent ligands with high affinity for D_1 and D_2 dopaminergic receptors. *J. Neurochem* **1989,** *52*, 1641-1644.

122. Barton, A. C.; Kang, H. C.; Rinaudo, M. S.; Monsma Jr, F. J.; Stewart-Fram, R. M.; Macinko Jr, J. A.; Haugland, R. P.; Ariano, M. A.; Sibley, D. R. Multiple fluorescent ligands for dopamine receptors. I. Pharmacological characterization and receptor selectivity. *Brain Res.* **1991,** *547*, 199-207.

123. Madras, B. K.; Canfield, D. R.; Pfaelzer, C.; Vittimberga, F. J.; Difiglia, M.; Aronin, N.; Bakthavachalam, V.; Baindur, N.; Neumeyer, J. L. Fluorescent and biotin probes for dopamine receptors: D_1 and D_2 receptor affinity and selectivity. *Mol. Pharmacol.* **1990,** *37*, 833-839.

124. Bakthavachalam, V.; Baindur, N.; Madras, B. K.; Neumeyer, J. L. Fluorescent probes for dopamine receptors: Synthesis and characterization of fluorescein and 7-nitrobenz-2-oxa-1,3-diazol-4-yl conjugates of D_1 and D_2 receptor ligands. *J. Med. Chem.* **1991,** *34*, 3235-3241.

125. Ariano, M. A.; Hee Chol, K.; Haugland, R. P.; Sibley, D. R. Multiple fluorescent ligands for dopamine receptors. II. Visualization in neural tissues. *Brain Res.* **1991,** *547*, 208-222.

126. Briddon, S. J.; Hill, S. J. Pharmacology under the microscope: The use of fluorescence correlation spectroscopy to determine the properties of ligand–receptor complexes. *Trends Pharmacol. Sci.* **2007,** *28*, 637-645.

127. Middleton, R. J.; Briddon, S. J.; Cordeaux, Y.; Yates, A. S.; Dale, C. L.; George, M. W.; Baker, J. G.; Hill, S. J.; Kellam, B. New fluorescent adenosine A_1-receptor agonists that allow quantification of ligand−receptor interactions in microdomains of single living cells. *J. Med. Chem.* **2007,** *50*, 782-793.

128. Dale, C. L.; Hill, S. J.; Kellam, B. New potent, short-linker BODIPY-630/650 labelled fluorescent adenosine receptor agonists. *MedChemComm* **2012,** *3*, 333-338.

129. Vernall, A. J.; Stoddart, L. A.; Briddon, S. J.; Hill, S. J.; Kellam, B. Highly potent and selective fluorescent antagonists of the human adenosine A_3 receptor based on the 1,2,4-triazolo[4,3-a]quinoxalin-1-one scaffold. *J. Med. Chem.* **2012,** *55*, 1771-1782.

130. Bohme, I.; Beck-Sickinger, A. Illuminating the life of GPCRs. *Cell Commun. Signaling* **2009,** *7*, 16.

131. Cottet, M.; Faklaris, O.; Zwier, J. M.; Trinquet, E.; Pin, J.-P.; Durroux, T. Original fluorescent ligand-based assays open new perspectives in G-protein coupled receptor drug screening. *Pharmaceuticals* **2011,** *4*, 202-214.

132. Stoddart, Leigh A.; Vernall, Andrea J.; Denman, Jessica L.; Briddon, Stephen J.; Kellam, B.; Hill, Stephen J. Fragment screening at adenosine-A_3 receptors in living cells using a fluorescence-based binding assay. *Chemistry & Biology* **2012,** *19*, 1105-1115.

133. Briddon, S. J.; Middleton, R. J.; Cordeaux, Y.; Flavin, F. M.; Weinstein, J. A.; George, M. W.; Kellam, B.; Hill, S. J. Quantitative analysis of the formation and diffusion of A_1-adenosine receptor-antagonist complexes in single living cells. *P. Natl. Acad. Sci. USA* **2004,** *101*, 4673-4678.

134. Shoichet, B. K. Virtual screening of chemical libraries. *Nature* **2004,** *432*, 862-865.

135. van der Horst, E.; Peironcely, J. E.; Ijzerman, A. P.; Beukers, M. W.; Lane, J. R.; van Vlijmen, H. W. T.; Emmerich, M. T. M.; Okuno, Y.; Bender, A. A novel chemogenomics analysis of G protein-coupled receptors (GPCRs) and their ligands: A potential strategy for receptor de-orphanization. *BMC Bioinf.* **2010,** *11*.

136. Lin, H.; Sassano, M. F.; Roth, B. L.; Shoichet, B. K. A pharmacological organization of G protein-coupled receptors. *Nat. Methods* **2013,** *10*, 140-146.

137. Roth, B. L.; Sheffler, D. J.; Kroeze, W. K. Magic shotguns versus magic bullets: Selectively non-selective drugs for mood disorders and schizophrenia. *Nat. Rev. Drug. Discov.* **2004,** *3*, 353-359.

138. Kenakin, T.; Watson, C.; Muniz-Medina, V.; Christopoulos, A.; Novick, S. A simple method for quantifying functional selectivity and agonist bias. *ACS Chem. Neurosci.* **2011,** *3*, 193-203.

139. Stemp, G.; Ashmeade, T.; Branch, C. L.; Hadley, M. S.; Hunter, A. J.; Johnson, C. N.; Nash, D. J.; Thewlis, K. M.; Vong, A. K. K.; Austin, N. E.; Jeffrey, P.; Avenell, K. Y.; Boyfield, I.; Hagan, J. J.; Middlemiss, D. N.; Reavill, C.; Riley, G. J.; Routledge, C.; Wood, M. Design and synthesis of *trans*-*N*-[4-[2-(6-cyano-1,2,3,4-tetrahydroisoquinolin-2- yl)ethyl]cyclohexyl]-4-quinolinecarboxamide (SB-277011): A potent and selective dopamine D_3 receptor antagonist with high oral bioavailability and cns penetration in the rat. *J. Med. Chem.* **2000,** *43*, 1878-1885.

140. Lane, J. R.; Donthamsetti, P.; Shonberg, J.; Draper-Joyce, C. J.; Dentry, S.; Michino, M.; Shi, L.; López, L.; Scammells, P. J.; Capuano, B.; Sexton, P. M.; Javitch, J. A.; Christopoulos, A. A new mechanism of allostery in a G protein–coupled receptor dimer. *Nat. Chem. Biol.* **2014,** *10*, 745-752.

Chapter 2- A SAR Study of the Positive Allosteric Modulator LY2033298 at the M_4 Muscarinic Acetylcholine Receptor

Declaration for Thesis Chapter 2

The data presented in Chapter 2 contains research which is in manuscript format for submission to *ACS Medicinal Chemistry Letters*.

Declaration by candidate

In the case of Chapter 2, the nature and extent of my contribution to the work was the following:

Nature of contribution	**Contribution (%)**
Design, synthesis, purification, characterisation and pharmacological testing of all analogues in Table 1 Main author of manuscript.	65

The following co-authors contributed to the work. Co-authors who are students at Monash University must also indicate the extent of their contribution in percentage terms:

Name	**Nature of contribution**	**Contribution (%)***
Tracey Huynh	Design, synthesis, purification, characterisation and pharmacological testing of all analogues in Scheme 2	20
Celine Valant	Supervised project	
J. Robert Lane	Co-author of manuscript	
Patrick M. Sexton	Supervised project	
Arthur Christopoulos	Co-author of manuscript	
Ben Capuano	Co-author of manuscript	

*Percentage contribution only shown for co-authors who were students at Monash University at the time of their contribution to this work.

Candidate's Signature: 01/12/2014

Monika Szabo

Declaration by co-authors

The undersigned hereby certify that:

1. The above declaration correctly reflects the nature and extent of the candidate's contribution to this work, and the nature of the contribution of each of the co-authors.
2. They meet the criteria for authorship in that they have participated in the conception, execution, or interpretation, of at least that part of the publication in their field of expertise;
3. They take public responsibility for their part of the publication, except for the responsible author who accepts overall responsibility for the publication;
4. There are no other authors of the publication according to these criteria;
5. Potential conflicts of interest have been disclosed to (a) granting bodies, (b) the editor or publisher of journals or other publications, and (c) the head of the responsible academic unit; and
6. The original data are stored at the following location(s) and will be held for at least five years from the date indicated below:

   Department of Medicinal Chemistry, Monash Institute of Pharmaceutical Sciences, 381 Royal Parade, Parkville, Victoria, 3052, Australia

Co-author signatures:

Tracey Huynh: [redacted] 01/12/2014

Celine Valant: [redacted] 01/12/2014

J. Robert Lane: [redacted] 01/12/2014

Patrick M. Sexton: [redacted] 01/12/2014

Arthur Christopoulos: [redacted] 01/12/2014

Ben Capuano: [redacted] 01/12/2014

A SAR Study of the Positive Allosteric Modulator LY2033298 at the M_4 Muscarinic Acetylcholine Receptor

Monika Szabo[†‡], *Tracey Huynh*[†], *Celine Valant*[‡], *J. Robert Lane*[‡], *Patrick M. Sexton*[‡], *Arthur Christopoulos*[‡,*], *Ben Capuano*[†,*]

[†]Medicinal Chemistry, [‡]Drug Discovery Biology, Monash Institute of Pharmaceutical Sciences, Monash University, 381 Royal Parade, Parkville 3052, Victoria, Australia.

KEYWORDS: M_4 muscarinic acetylcholine receptor, positive allosteric modulator, PAM, allosteric, CNS, LY2033298.

Abstract

Positive allosteric modulators (PAMs) targeting the M_4 muscarinic acetylcholine receptor (mAChR) offer greater subtype selectivity and unique potential as central nervous system agents through their novel mode of action to traditional orthosteric ligands. In an attempt to elucidate the molecular determinants of allostery mediated by the exemplar thienopyridine M_4 mAChR PAM, LY2033298, we report herein a systematic SAR study investigating different linkage points, halogen replacements to examine size and electronic effects, and different substitution combinations on the thienopyridine scaffold. We applied an operational model of allosterism to determine values of functional affinity (K_B), cooperativity ($\alpha\beta$) and intrinsic agonism (τ_B) for all compounds.

Introduction

The muscarinic acetylcholine receptors (mAChRs) are a class of G protein-coupled receptors (GPCRs) consisting of five subtypes (M_1-M_5) and are expressed in the central nervous system (CNS) and the periphery. The M_4 mAChR is of clinical interest as it has demonstrated an involvement in CNS disorders such as schizophrenia.[1] Specifically, the M_4 mAChR has been shown to alleviate the positive symptoms (hallucinations, delusions) and potentially benefit the cognitive deficits (memory, learning) associated with schizophrenia.[2,3]

A significant problem associated with clinically prescribed antipsychotics designed to target a designated GPCR orthosteric site is their promiscuity and therefore lack of receptor selectivity. This phenomenon often results in an extensive side effect profile. Allosteric ligands offer a potential solution to this problem by targeting a topographically distinct site to the orthosteric site. While orthosteric sites tend to be conserved across receptor subtypes, allosteric sites can differ, making subtype selectivity a more eminent possibility.[4] Previous work on the M_4 mAChR has focused on positive allosteric modulators (PAMs), whereby they can exhibit several possible

modes of action: potentiation of the binding of the endogenous ligand, acetylcholine (ACh); potentiation of the downstream efficacy upon binding of the endogenous ligand; and/or direct activation by the allosteric ligand itself.[5] Earlier studies have deduced parameters for allosterism via implementing the operational model of allosterism. This model quantifies the magnitude and direction of the parameters of allosterism including modulator binding affinity, K_B, modulation of binding affinity of the orthosteric ligand, α, modulation of downstream efficacy upon binding of the orthosteric ligand, β, and intrinsic allosteric agonism, τ_B.[6]

There has been considerable research conducted in the field of M_4 PAMs, all of which focus on the thienopyridine scaffold.[7-9] Whilst significant progress has been made, none have matched the pharmacological profile to that of LY2033298 (Figure 1; **8a**). In attempts to move away from the 5-chloro-6-methoxy-4-methyl substitution pattern on **8a**, researchers at Vanderbilt University (VU) developed a number of analogues based on a 4,6-dimethyl substitution pattern on the thienopyridine motif, such as VU100010 (Figure 1; **1**). We have also published work on this scaffold investigating the pharmacological impact of incorporating modifications to the substitution pattern of the arylmethyl motif.[10]

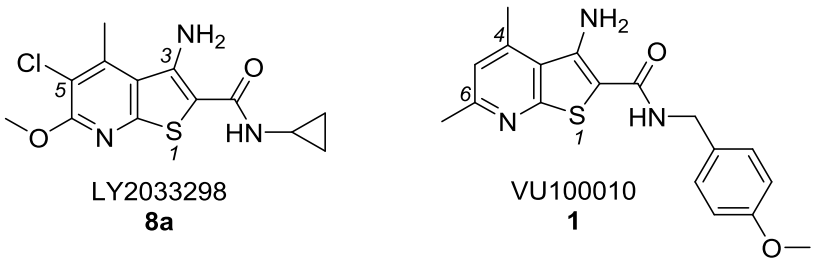

Figure 1. Muscarinic M_4 positive allosteric modulators LY2033298 (**8a**) and VU100010 (**1**) with numbering systems.

To explore the structure activity relationship (SAR) of **8a**, we synthesised a focussed series of compounds that involved alkyl chain extensions from several points on **8a** (Figure 2). The aim was to determine suitable tethering points and to observe if larger groups may be tolerated at these positions, with the future aim of structurally extending derivatives that incorporate either

an orthosteric mAChR moiety to generate bitopic ligands[11] or dual acting ligands that incorporate a pharmacophore selective for another protein target.[12] This information may also be useful in determining the size of the allosteric binding pocket at the M_4 mAChR and therefore the scope for structural diversification. We also assessed the importance of the halogen at the 5′ position in relation to both size and electronic effects by substituting with larger halogens (Br and I). In addition, we investigated an isosteric replacement of the C-Cl moiety for N to yield a thienopyrimidine bicyclic system in place of the thienopyridine. Although, the new scaffold is lacking a chlorine atom, it is predicted that the incorporation of an additional nitrogen atom will maintain a relatively electron-deficient six-membered ring of the bicyclic system comparable to that of LY2033298. We also explored different combinations of substituents on the thienopyridine ring of **8a** to ascertain which substitution pattern is optimal and/or essential for a PAM profile at the M_4 mAChR. To do this we looked at the following substitution patterns of the thienopyridine core, namely 6-methoxy-4-methyl, 5-chloro-4,6-dimethyl and 4,6-dimethyl. Although these substitutions have been previously reported[9,13], the underlying operational parameters describing their allosteric effects were not determined. All compounds were characterised in functional M_4 mAChR-mediated ERK1/2 phosphorylation (pERK1/2) assays and compounds that showed significant differences compared to **8a**, were further profiled in radioligand binding assays.

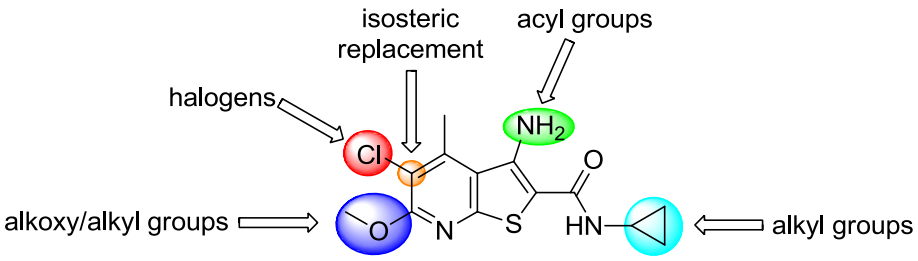

Figure 2. Structural diversification of LY2033298 (**8a**).

Results and discussion

Chemistry. The synthesis of derivatives with alkyl chains extending from the 6′ position of the methoxy (*O*-alkyl derivatives) are represented in Scheme 1. We commenced the sequence with the monocyclic pyridinone (**2**); the chemistry of which has been previously described.[14] In one step, we combined **2** with the required primary alkyl iodide under mild basic conditions to effect *O*-alkylation then subsequently added a stronger base (1 M aqueous KOH) to convert to the monocyclic intermediates to bicyclic analogues (**3a-d**).[10] The primary aromatic amine of all analogues was protected as the phthalimide (**4a-d**) in good yield using phthalic anhydride prior to halogenating the 5′ position (**5a-f**) with the appropriate *N*-halosuccinimide, to circumvent *N*-halogentaion. Subsequent phthalimide deprotection under standard conditions of hydrazine monohydrate afforded **6a-f** in good to excellent yield (46-89%). Base-promoted ester hydrolysis furnished the carboxylic acids **7a-f** following acid work-up in similar yields. A BOP-mediated amide coupling reaction was then employed between cyclopropylamine and carboxylic acids (**7a-f**) to generate the final *O*-alkyl analogues (**8a-f**). The *N*-alkyl analogues (**9a-c**) were furnished by simply coupling the intermediate carboxylic acid **7a** with the required acyclic alkanamines. Synthesis of the amine modified analogues was carried out using LY2033298 (**8a**) and the required acid chlorides to give the carboxamide derivatives (**10a-c**). Synthesis of des-chloro-LY2033298 was achieved by firstly converting the bicyclic ethyl ester (**3a**) to the free carboxylic acid (**11**) via base hydrolysis, followed by a BOP-mediated coupling reaction to install the cyclopropyl moiety to give the target analogue (**12**).

Scheme 1. Synthesis of *O*-alkyl, *N*-alkyl, *N*-acyl and des-chloro derivatives of LY2033298[a]

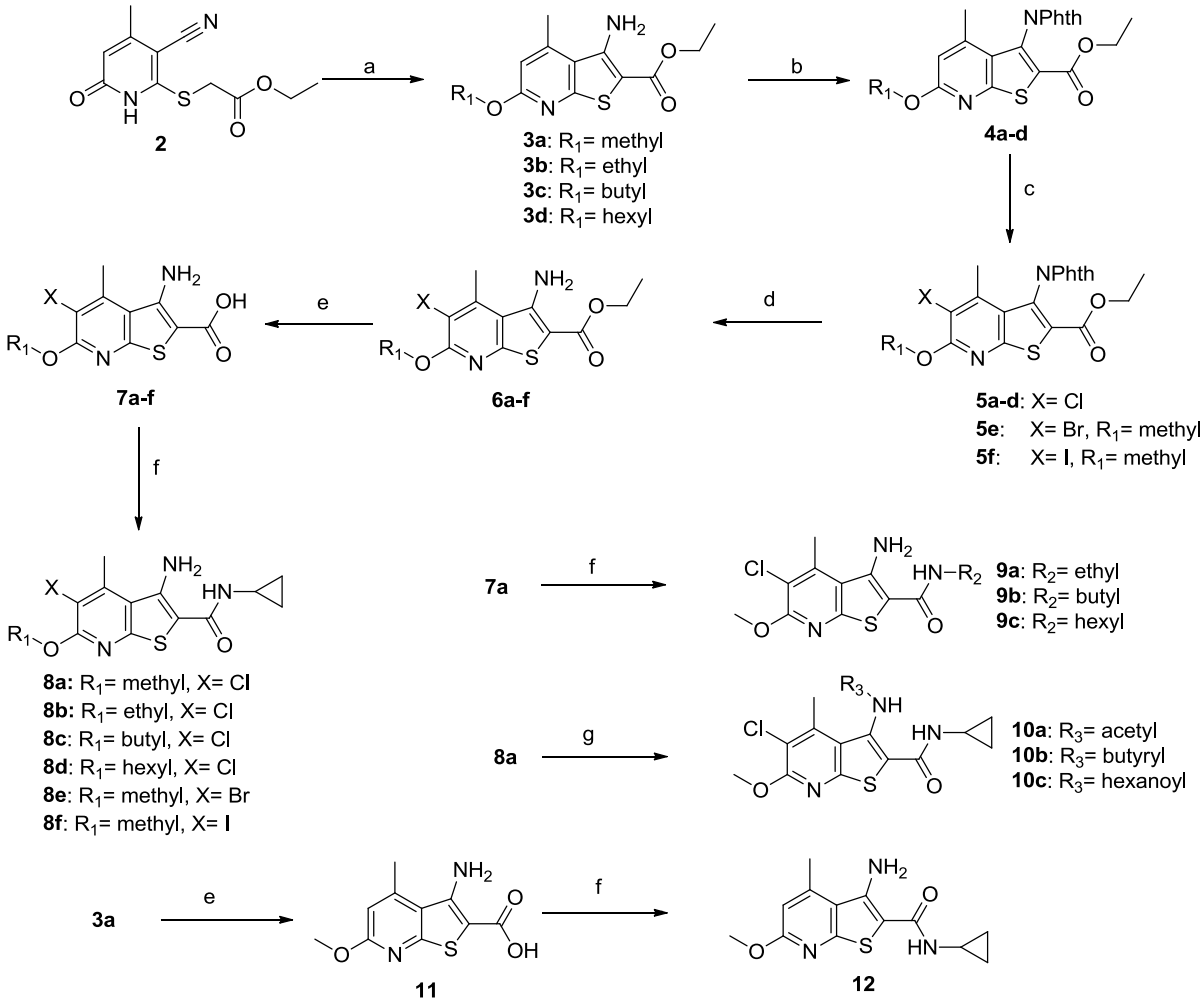

[a]Reagents and conditions: (a) (i) Alkyl-I, K_2CO_3, DMF, 4 h, RT; (ii) 1 M KOH, 15 min, 58-94%; (b) Phthalic anhydride, AcOH, reflux, 20 h, 48-86%; (c) *N*-halosuccinimide, conc. HCl, EtOH, reflux, 1.5 h, 80-99%; (d) $(NH_2)_2.H_2O$, EtOH, reflux, 3 h, 46-89%;(e) 2 M NaOH, EtOH, reflux, 1.5 h, 49-96%; (f) Alkanamine, BOP reagent, DIPEA, DMF, RT., 1-12 h, 15-72%; (g) Acid chloride, Et_3N, DCM, N_2, reflux, 2 days, 45-48%.

We envisaged the synthesis of the LY2033298/VU hybrid analogue (**18**) commencing from the pyridinone precursor (**13**) as illustrated in Scheme 2. The first chlorine atom was successfully installed at the 5′ position of the substituted pyridinone core using sulfuryl chloride to give intermediate **14**. Subsequent chlorination to furnish the dichloro substituted pyridine (**15**) was effected using phosphoryl chloride. Treatment of **15** with thiourea in ethanol at reflux smoothly afforded the versatile pyridinethione (**16**) in very good yield. Reaction of **16** with pre-synthesised

2-chloro-*N*-cyclopropylacetamide (**17**) under basic conditions produced the target thienopyridine (**18**) with the 5-chloro-4,6-dimethyl substitution pattern. Synthesis of the thienopyrimidine analogue (**21**) was successfully achieved by firstly reacting 3-aminocrotononitrile (**19**), acetyl chloride and ammonium thiocyanate to generate the substituted pyrimidine core (**20**), followed by treatment with chloroacetamide **17** and sodium metal in ethanol at reflux to give the product in very good yield.

Scheme 2. Synthesis of LY2033298/VU hybrid and thienopyrimidine analogues

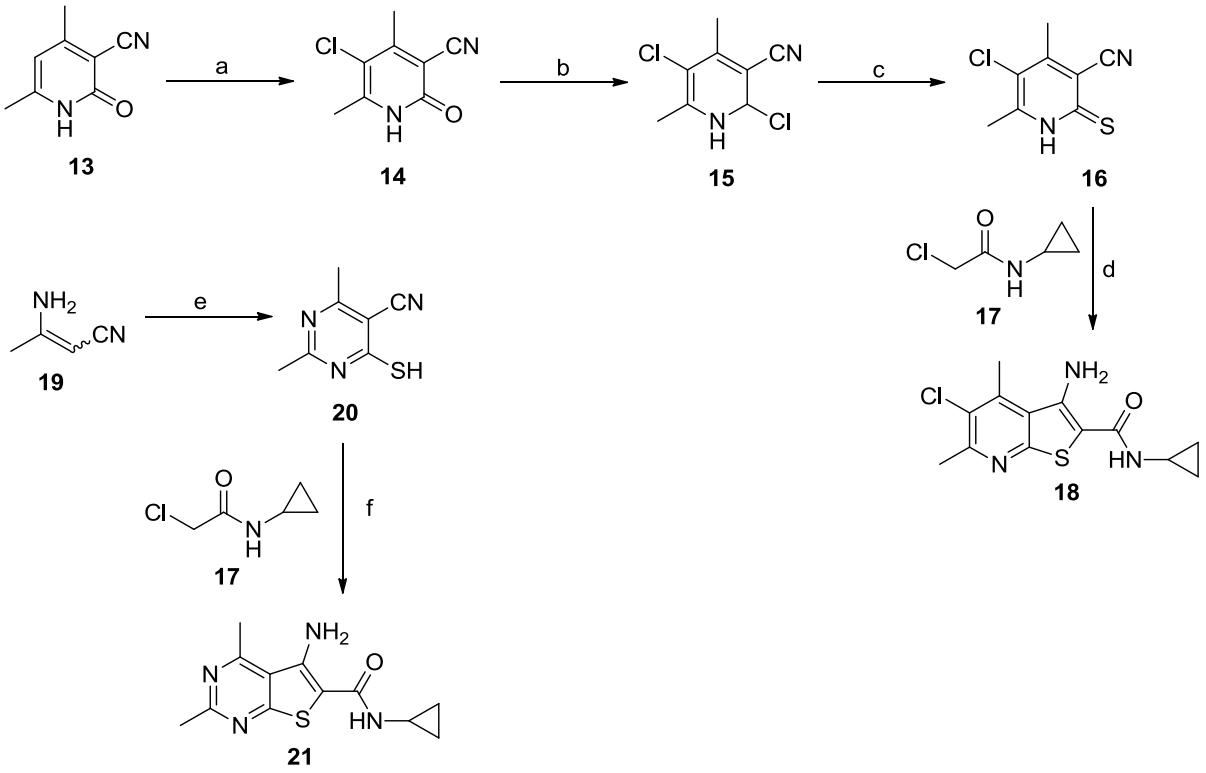

[a]Reagents and conditions: (a) SO_2Cl_2, DCE, reflux 6 h, 42%; (b) $POCl_3$, MW, 100 °C, 1h, 88%; (c) Thiourea, EtOH, relux, 24 h, 29%; (d) NaOMe, MeOH, relux, overnight, 30%; (e) Acetyl chloride, NH_4SCN, dioxane, 23%; (f) Na metal, EtOH, reflux 4 h,75%.

Pharmacology. To characterize the biological activity of the synthesized compounds incorporating *O*-alkyl (**8b-d**) and *N*-alkyl chains (**9a-c**) of the LY2033298 scaffold, halogen replacements (**8e-f**) and modification to the aromatic amine functionality (**10a-c**), we tested all analogues in a functional pERK1/2 assay using intact FlpIn-CHO cells stably transfected with the human M_4 mAChR. Compounds were initially tested in time-course assays (data not shown)

to determine the optimal incubation time for maximum ERK1/2 phosphorylation for each compound. As the response to all compounds peaked at a similar time to ACh, interaction studies were performed using varying concentrations of ACh (10 μM to 10 nM) at a stimulation time of 6 minutes. The results of these interaction studies are summarised in Table 1. By applying the operational model of allosterism, we derived values of functional affinity (pK_B), intrinsic efficacy (τ_B) and overall cooperativity ($\alpha\beta$) of the allosteric ligand's effect on ACh.

All ligands displayed no notable enhancement in functional affinity when compared across their respective groups, i.e. *O*-alkyl, *N*-alkyl or halogen derivatives. For the *O*-alkyl analogues, there was a significant loss in intrinsic efficacy when going from the methyl (**8a**) and ethyl (**8b**) to the butyl (**8c**) and hexyl (**8d**) derivatives. The intrinsic efficacy was maintained between **8a** and **8b** confirming that the addition of the extra carbon atom has little effect and that anything larger is detrimental to the compounds' agonism. The cooperativity of the *O*-alkyl derivatives with ACh was also maintained with **8a**, however again the larger butyl (**8c**) and hexyl (**8d**) substituents resulted in a substantial loss in the cooperativity (96- and 120-fold, respectively) when compared with **8a**. For the replacement of the chlorine at the 5′ position with bromine (**8e**) or iodine (**8f**), we observed no significant gain or loss in the intrinsic efficacy and the cooperativity of the ligands compared with the parent compound **8a**. As such, the thienopyridine scaffold tolerates larger halogen atoms with less electronegative properties. For the *N*-alkyl analogues, only the *N*-hexyl derivative (**9c**) showed a significant drop in intrinsic agonism (22-fold) and cooperativity (185-fold) when compared to the *N*-cyclopropyl compound (**8a**). There were no significant differences between the *N*-butyl compound **9b** compared to **8a**, confirming that a butyl linker is tolerated but the additional two carbon atoms significantly affect the agonistic and PAM properties of the ligand. The *N*-ethyl compound **9a** maintained similar allosteric properties to **8a**, as the ethyl occupies a similar chemical space to a cyclopropyl.

The general trend observed between the *O*-alkyl and *N*-alkyl analogues was that as we sequentially increased the alkyl chain length, we observed a decrease in both the intrinsic efficacy and the cooperativity of the compounds with ACh. This is illustrated in Figure 2 with *N*-alkyl analogues **9a-c** exhibiting a smaller decrease in activity as a function of chain length. As such the allosteric pocket on the M_4 mAChR appears to have more space to accommodate larger groups on this side (**9a-c**), which is in agreement with some of the VU compounds that incorporate larger alkyl and substituted benzyl groups at this position.[9] However, recent evidence on the binding mechanism of allosteric ligands to the M_2 mAChR showed that upon receptor activation and binding of an allosteric ligand, the allosteric site encloses the modulator, creating a tight fitting binding pocket.[15] Therefore major structural changes to PAMs may affect how they can fit in the allosteric site, and may result in a loss of their ability to exert effects upon the ligand in the orthosteric site.

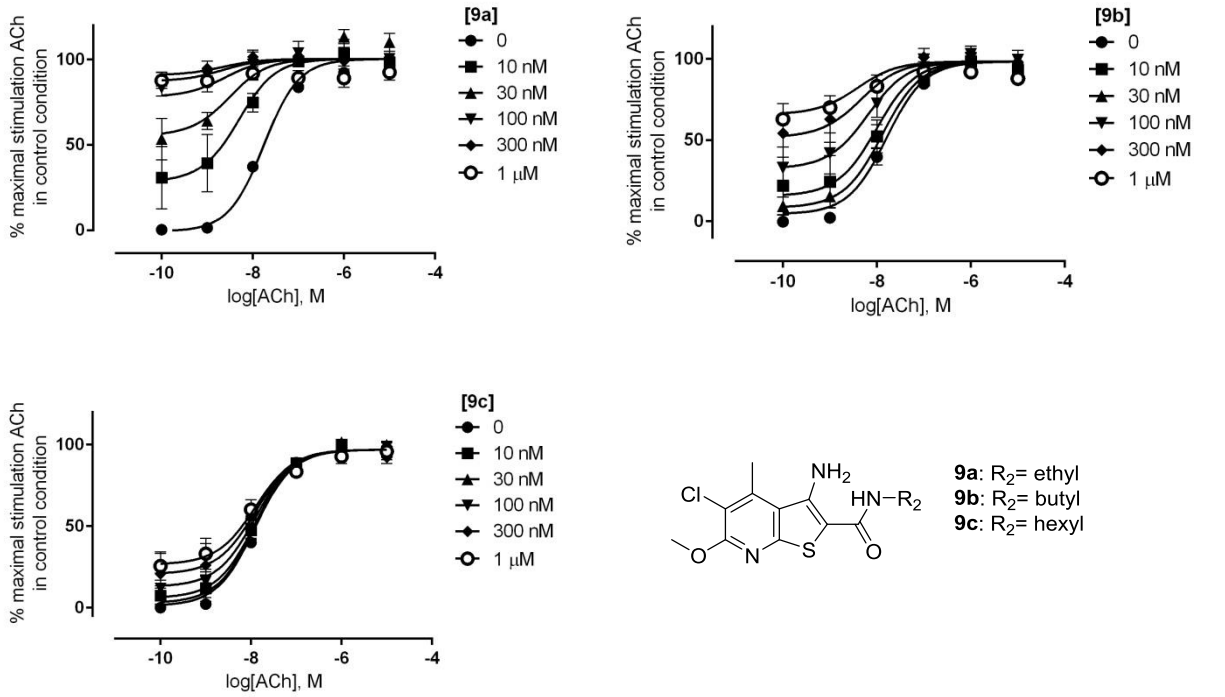

Figure 2. Effect of increasing alkyl chain length on the ability of *N*-alkyl analogues **9a-c** to allosterically modulate the activity of ACh in M_4 mAChR-mediated pERK1/2 assays. Data points represent the mean of three experiments performed in duplicate.

Due to many analogues showing very similar functional affinity, allosteric modulation and/or intrinsic efficacy to **8a**, we performed radioligand binding assays to gain greater insight into any subtle differences between the compounds, especially since the pERK1/2 experiments could not differentiate the individual contributions of affinity modulation versus efficacy modulation on the overall estimated cooperativity parameter ($\alpha\beta$). An advantage of performing binding assays is that they can provide a more direct estimate of affinity modulation of the compounds (α). Therefore we can then use this information to deduce the contribution of both parameters that the PAM has upon ACh.

All compounds in Table 1 were tested, excluding **8d** and **9c** as both were very weak PAMs in the pERK1/2 signalling pathway. Compared to **8a**, there was a significant loss in affinity modulation for *O*-alkyl analogues **8b** and **8c** (18- and 77-fold, respectively). The halogen substituted analogues **8e** and **8f** also had a small but significant loss in affinity modulation (5- and 6-fold, respectively) to that of **8a**. The *N*-alkyl analogues showed that **9a** was able to maintain a similar affinity modulation to **8a**, whereas extending to the butyl analogue (**9b**) resulted in a 14-fold loss. This suggests that increasing the size of *O*-alkyl substituents at the 6′ position on the thienopyridine affects affinity modulation. In comparison, substitution of alkyl groups at the amide nitrogen bearing the cyclopropyl group is more tolerated, but diminishes with greater than two carbon length alkyl chains compared to **8a**. No significant changes in the modulation of ACh efficacy (β) was observed for any compounds as compared to **8a** confirming that the differences between compounds are largely due to a combination of affinity modulation (α) and the intrinsic agonism of the compounds in their own right (τ_B). Additionally, much of the superior allosteric properties of **8a**, originate from its ability to modulate the affinity of ACh rather than the efficacy. Table 1 highlights that changes to the thienopyridine scaffold of **8a** can be tolerated, however larger structural changes such as hexyl alkyl chains on both the *O*-alkyl and *N*-alkyl analogues are detrimental to the allosteric modulatory properties of the ligand. There are

examples of ligands in the literature whereby substitutions at the 6′ position of the thienopyridine scaffold with pyridinylmethyl or morpholine derivatives show activity, however groups longer and more lipophilic tend to decrease the efficacy of the compounds.[8]

While it has been previously reported that the combination of the VU scaffold (4,6-dimethyl thienopyridine) and substitution at the primary aromatic amine is mostly tolerated but results in a loss of activity,[9] we found that the scaffold of **8a** (5-chloro-4-methyl-6-methoxy thienopyridine) in combination with acylation of the primary aromatic amine (**10a-c**) abolished activity completely.

Table 1. Functional ERK1/2 phosphorylation and binding data for LY2033298 (**8a**), *O*-alkyl analogues (**8b-d**), halogen replacement analogues (**8e-f**) and *N*-alkyl analogues (**9a-c**) at the M_4 mAChR[a]

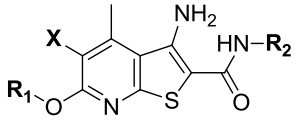

Compd	R_1	R_2	X	pK_i (K_i, μM)[b]	pK_B (K_B, μM)[c]	log τ_B (τ_B)[c]	log $\alpha\beta$ ($\alpha\beta$)[c]	*log α (α)[b]	log β (β)[d]
8a	Me		Cl	6.41 ± 0.11 (0.4)	-	0.93 ± 0.14 (8.5)	2.38 ± 0.23 (240)	3.24 ± 0.14 (1738)	-0.86 ± 0.09 (0.14)
8b	Et		Cl	6.71 ± 0.16 (0.2)	6.10 ± 0.37 (0.8)	0.97 ± 0.32 (9.3)	1.79 ± 0.44 (61.7)	1.98 ± 0.12 (95.5)	-0.19 ± 0.32 (0.65)
8c	Bu		Cl	5.57 ± 0.40 (2.7)	6.81 ± 0.40 (0.2)	-0.51 ± 0.20 (0.3)	0.40 ± 0.16 (2.5)	1.35 ± 0.16 (22.4)	-0.95 ± 0.0 (0.11)
8d	Hex		Cl	nt	7.42 ± 0.32 (0.04)	-0.75 ± 0.18 (0.2)	0.30 ± 0.11 (2.0)	nt	nt
8e	Me		Br	6.28 ± 0.07 (0.52)	6.52 ± 0.44 (0.3)	1.25 ± 0.40 (17.8)	1.91 ± 0.52 (81.3)	2.54 ± 0.11 (347)	-0.63 ± 0.41 (0.23)
8f	Me		I	5.78 ± 0.09 (1.7)	6.66 ± 0.33 (0.2)	0.37 ± 0.18 (2.3)	0.97 ± 0.44 (9.3)	2.43 ± 0.12 (269)	-1.46 ± 0.32 (0.03)
9a	Me	Et	Cl	5.37 ± 0.32 (4.3)	6.73 ± 0.39 (0.2)	0.94 ± 0.33 (8.7)	1.84 ± 0.53 (69.2)	2.75 ± 0.36 (562)	-0.91 ± 0.17 (0.12)
9b	Me	Bu	Cl	5.50 ± 0.14 (3.2)	6.29 ± 0.46 (0.5)	0.44 ± 0.30 (2.8)	1.19 ± 0.51 (15.5)	2.09 ± 0.18 (123)	-0.90 ± 0.33 (0.13)
9c	Me	Hex	Cl	nt	6.70 ± 0.32 (0.2)	-0.35 ± 0.12 (0.4)	0.13 ± 0.15 (1.3)	nt	nt

[a]Data represent the mean ± SEM of three-four separate experiments performed in duplicate. [b]Values are obtained via radioligand ([^{3}H]NMS) binding assays through interaction with varying concentrations of ACh. [c]Values are obtained from pERK1/2 assays via interaction with varying concentrations of ACh.*Log α' is calculated by fixing log α to -100.[d]Values of β are determined by subtracting log α' from log $\alpha\beta$. nt= Not tested in binding assays as cooperativity ($\alpha\beta$) in pERK1/2 assays was very low.

Table 2. LY2033298 core variants (**12**, **18** and **21**) in functional ERK1/2 phosphorylation assays at the M_4 mAChR[ab]

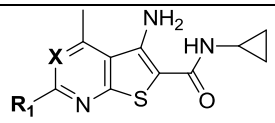

Compd	R_1	X	pK_B (K_B, μM)	log τ_B (τ_B)	log $\alpha\beta$ ($\alpha\beta$)
12	OMe	CH	5.55 ± 0.38 (2.8)	0.66 ± 0.30 (4.6)	1.46 ± 0.39 (28.8)
18	Me	C-Cl	6.45 ± 0.28 (0.4)	1.11 ± 0.26 (12.9)	1.89 ± 0.36 (77.6)
21	Me	N	4.90 ± 0.26 (12.5)	0.49 ± 0.16 (3.1)	1.15 ± 0.27 (14.1)
VU10004*[9]	Me	CH	5.37 ± 0.14 (4.3)	0.77 ± 0.11 (5.9)	1.72 ± 0.17 (52.5)

[a]Data represent the mean ± SEM of three separate experiments performed in duplicate. [b]Values are obtained via interaction with varying concentrations of ACh.*Values are from in-house data; currently unpublished.

The next part of our study was to elucidate if structural changes to the pyridine ring of the thienopyridine scaffold of **8a** had any major influences on its allosteric properties and to pinpoint what substitutions are crucial for its activity. The results of compounds **12**, **18**, **21** and **VU10004** are summarised in Table 2. The pyrimidine derivative (**21**), which was used to mimic the electronegativity and ring deactivating effects of the chlorine at that position whilst also reducing the chemical space, had no significant advantages as compared to the chlorine at that same position. There was no statistical significance for compounds **12**, **18**, **21** and **VU10004** as compared to **8a** and compared to each other for the functional affinity, intrinsic agonism and cooperativity of the compounds. As such these results highlight that the thienopyridine is able to tolerate small structural changes to its pyridine ring, however it is not clear what substitutions are essential for its activity and allosteric properties. Combined with the results from Table 1, the thienopyridine scaffold seems to be more affected when substituted with longer and more lipophilic groups. Changes to the scaffold itself, neither enhance nor diminish the pharmacological profile. The results do however reveal that a simple change from a butyl to a hexyl chain can alter the pharmacological profile. It is possible also that the *O*- and *N*-alkyl

chains may be too flexible and therefore more rigid functional groups should be employed from these relative positions of **8a**.

Conclusion

We performed a comprehensive SAR study of the PAM **8a** by substituting progressively longer *O*- or *N*-alkyl chains from the scaffold through the ether linkage (**8b-d**), halogen replacement (**8e-f**), the amide (**9a-c**) and different substitution combinations around the pyridine ring (**12**, **18** and **21**). The allosteric properties of the ligands progressively decreased when substituting alkyl chains greater than two carbon atoms from either side of **8a** (Table 1 and Figure 2). Additionally, halogen replacements were tolerated, but significantly decreased the ability of the compounds to positively modulate agonist affinity as compared to **8a**, confirming that compound **8a** largely modulates the affinity of ACh in the orthosteric pocket of the M_4 mAChR rather than modulating the efficacy. Acylation of the primary aromatic amine (**10a-c**) completely abolished activity. Due to the small molecule nature of PAMs at the M_4 mAChR and the recent advances into the understanding of mechanisms of how they bind to muscarinic receptors[15], the possibility of tethering larger functional groups for a dual acting or bitopic mode of action based on the scaffold of **8a** is likely to prove challenging. Furthermore whilst we can identify subtle differences between PAMs by utilising the operational model of allosterism, it is difficult to determine exactly what functional groups on the thienopyridine scaffold of **8a** were important for its PAM mode of action (Table 2). Nonetheless, these results show the benefits of profiling ligands using operational models of allosterism to gain a more comprehensive look into the contribution of each of the parameters for a PAM. Additionally the results represent useful SAR into understanding the thienopyridine scaffold of PAMs targeting the M_4 mAChR.

Experimental

Chemistry. All solvents and chemicals were purchased from standard suppliers and were used without any further purification. ^{1}H NMR and ^{13}C NMR spectra were acquired at 400.13 and 100.62 MHz respectively, on a Bruker Advance III 400 MHz UltrashieldPlus NMR spectrometer using TOPSPIN 2.1 software. Chemical shifts (δ) for all ^{1}H spectra are reported in parts per million (ppm) using tetramethylsilane (TMS, 0 ppm) as the reference. The data for all spectra are reported in the following format: chemical shift (δ), (multiplicity, coupling constants *J* (Hz), integral), where the multiplicity is defined as: s = singlet, d= doublet, t= triplet, q=quartet, p = pentet and m = multiplet. For ^{13}C NMR spectra C= quaternary carbon, CH= methine carbon, CH_2= methylene carbon, and CH_3= methyl carbon.

The purity and retention time of final products was determined on an analytical reverse-phase HPLC system fitted with a Luna C8 (2) 100 Å column (50 × 4.60 mm, 5 μm) using a binary solvent system; solvent A: 0.1% TFA/H_2O; solvent B: 0.1% TFA/80%MeOH/20%H_2O. Gradient elution was achieved using 100% A for 10 minutes, 20% A and 80% B over 2 minutes and 100% A over 10 minutes at a flow rate of 1 mL/min monitored at 214 nm using a Waters 996 Photodiode Array detector.

Thin layer chromatography (TLC) was carried out routinely on silica gel $60F_{254}$ pre-coated plates (0.25 mm, Merck).Flash column chromatography was carried out using Merck Silica gel 60, 230-400 mesh ASTM. Melting points were determined using an electronic MP50 Melting Point System by Mettler Toledo analytical 2009 and are uncorrected.

General procedure for formation of the thienopyridine bicycle: To a solution of **2** (1 equiv.) in *N*,*N*-dimethylformamide (15 mL) was added potassium carbonate (1.5 equiv.) and the required alkyl iodide (1.1 equiv). After stirring at room temperature for 1-2 h, 1 M aqueous potassium hydroxide (1 equiv.) was added dropwise. Following an additional 15 mins, 10-15 mL of water was added to cause precipitation and the product filtered and dried over high vacuum.

Ethyl 3-amino-6-methoxy-4-methylthieno[2,3-*b*]pyridine-2-carboxylate (3a).[14]

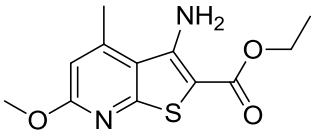

White solid (63 mg, 79%). ^{1}H NMR ($CDCl_3$): δ 1.38 (t, *J* 7.1 Hz, 3H), 2.68 (d, *J* 0.9 Hz, 3H), 3.98 (s, 3H), 4.33 (q, *J* 7.1 Hz, 2H), 6.11 (br s, 2H, NH_2), 6.43 (m, 1H). ^{13}C NMR ($CDCl_3$): δ 14.7 (CH_3), 20.4 (CH_3), 54.0 (CH_3), 60.4 (CH_2), 95.2 (C), 110.0 (CH), 119.4 (C), 145.9 (C), 149.5 (C), 160.6 (C),164.6 (C), 165.9 (C).

Ethyl 3-amino-6-ethoxy-4-methylthieno[2,3-*b*]pyridine-2-carboxylate (3b).

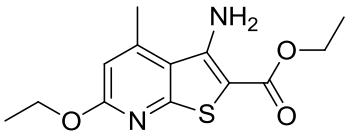

Fluffy white solid (521 mg, 94%). ^{1}H NMR ($CDCl_3$): δ 1.36-1.41 (q, *J* 7.1 Hz, 6H), 2.68 (d, *J* 0.9 Hz, 3H), 4.33 (q, *J* 7.1 Hz, 2H), 4.22 (q, *J* 7.1 Hz, 2H), 6.12 (br s, 2H, NH_2), 6.42 (m, 1H). ^{13}C NMR ($CDCl_3$): δ 14.7 (CH_3), 14.7 (CH_3), 20.4 (CH_3), 60.4 (CH_2), 62.6 (CH_2), 95.1 (C), 110.2 (CH), 119.3 (C), 146.0 (C), 149.5 (C), 160.4 (C), 164.2 (C), 165.9 (C).

Ethyl 3-amino-6-butoxy-4-methylthieno[2,3-*b*]pyridine-2-carboxylate (3c).

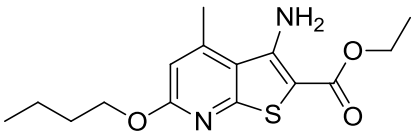

White solid (535 mg, 88%). ^{1}H NMR ($CDCl_3$): δ 0.98 (t, *J* 7.4 Hz, 3H), 1.37 (t, *J* 7.1 Hz, 3H) 1.47 (m, 2H), 1.76 (m, 2H), 2.68 (s, 3H), 4.30-4.37 (m, 4H), 6.12 (br s, 2H, NH_2), 6.43 (m, 1H). ^{13}C NMR ($CDCl_3$): δ 14.0 (CH_3), 14.7 (CH_3), 19.4 (CH_2), 20.4 (CH_3), 31.1 (CH_2), 60.3 (CH_2), 66.6 (CH_2), 95.1 (C), 110.2 (CH), 119.3 (C), 145.9 (C), 149.5 (C), 160.4 (C), 164.2 (C), 165.9 (C).

Ethyl 3-amino-6-(hexyloxy)-4-methylthieno[2,3-*b*]pyridine-2-carboxylate (3d).

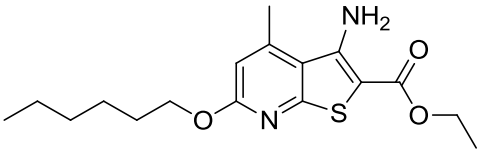

White solid (462 mg, 71%). ^{1}H NMR ($CDCl_3$): δ 0.90 (t, *J* 7.0 Hz, 3H), 1.32-1.36 (m, 4H), 1.37 (t, *J* 7.0 Hz, 3H), 1.41-1.48 (m, 2H), 1.76 (m, 2H), 2.67 (d, *J* 0.7 Hz, 3H), 4.30-4.36 (m, 4H), 6.11 (br s, 2H, NH_2), 6.42 (m, 1H). ^{13}C NMR ($CDCl_3$): δ 14.2 (CH_3), 14.7 (CH_3), 20.4 (CH_3), 22.7 (CH_2), 25.9 (CH_2), 29.1 (CH_2), 31.7 (CH_2), 60.3 (CH_2), 66.8 (CH_2), 95.1 (C), 110.2 (CH), 119.3 (C), 145.8 (C), 149.6 (C), 160.7 (C), 164.6 (C), 165.9 (C).

General procedure for phthalimide protection: To a solution of **3a-d** (1 equiv.) in acetic acid (15 mL), was added phthalic anhydride (2 equiv.), and the mixture was heated at reflux for 1.5 days. The reaction was cooled to room temperature, then placed in an ice bath to initiate precipitation of the final product as a white solid.

Ethyl 3-(1,3-dioxoisoindolin-2-yl)-6-methoxy-4-methylthieno[2,3-*b*]pyridine-2-carboxylate (4a).[14]

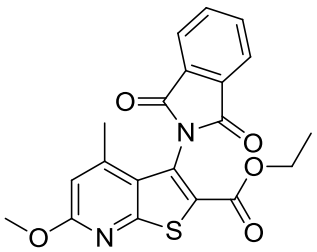

White solid (53 mg, 55%). ^{1}H NMR ($CDCl_3$): δ 1.11 (t, *J* 7.1 Hz, 3H), 2.37 (s, 3H), 4.02 (s, 3H), 4.20 (q, *J* 7.1 Hz, 2H), 6.59 (s, 1H), 7.83 (m, 2H), 8.00 (m, 2H). ^{13}C NMR ($CDCl_3$): δ 13.9 (CH_3), 18.5 (CH_3), 54.2 (CH_3), 61.7 (CH_2), 112.2 (CH), 124.2 (CH), 124.7 (C), 125.4 (C), 127.6 (C), 132.4 (C), 134.7 (CH), 145.9 (C), 159.1 (C), 161.1 (C), 164.5 (C), 167.6 (C).

Ethyl 3-(1,3-dioxoisoindolin-2-yl)-6-ethoxy-4-methylthieno[2,3-*b*]pyridine-2-carboxylate (4b).

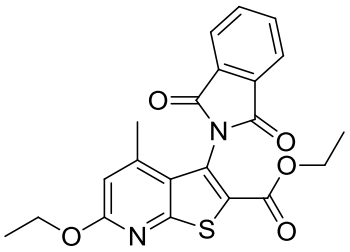

White solid (477 mg, 65%). ^{1}H NMR ($CDCl_3$): δ 1.11 (t, *J* 7.1 Hz, 3H), 1.42 (t, *J* 7.1 Hz, 3H), 2.36 (d, *J* 0.8 Hz, 3H), 4.20 (q, *J* 7.1 Hz, 2H), 4.47 (q, *J* 7.1 Hz, 2H), 6.57 (d, *J* 0.9 Hz, 1H), 7.84 (m, 2H), 8.00 (m, 2H). ^{13}C NMR ($CDCl_3$): δ 13.9 (CH_3), 14.6 (CH_3), 18.5 (CH_3), 61.7 (CH_2), 62.7 (CH_2), 112.4 (CH), 124.2 (CH), 124.6 (C), 125.2 (C), 127.7 (C), 132.5 (C), 134.7 (CH), 145.8 (C), 159.3 (C), 161.2 (C), 164.2 (C), 167.6 (C).

Ethyl 6-butoxy-3-(1,3-dioxoisoindolin-2-yl)-4-methylthieno[2,3-*b*]pyridine-2-carboxylate (4c).

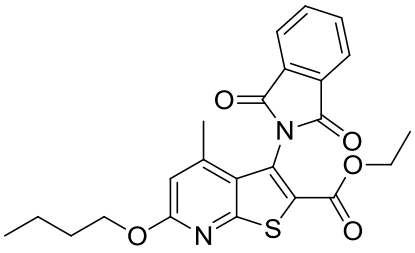

White solid (613 mg, 86%). ^{1}H NMR ($CDCl_3$): δ 0.99 (t, *J* 7.4 Hz, 3H), 1.11 (t, *J* 7.1 Hz, 3H), 1.49 (m, 2H), 1.78 (m, 2H), 2.36 (d, *J* 0.9 Hz, 3H), 4.20 (q, *J* 7.1 Hz, 2H), 4.41 (t, *J* 6.6 Hz, 2H), 6.57 (m, 1H), 7.84 (m, 2H), 8.00 (m, 2H). ^{13}C NMR (DMSO- d_6): δ 13.5 (CH_3), 13.7 (CH_3), 17.6 (CH_3), 18.7 (CH_2), 30.4 (CH_2), 61.8 (CH_2), 66.3 (CH_2), 112.4 (CH), 124.0 (C), 124.1 (C), 124.2 (CH), 127.9 (C), 131.4 (C), 135.6 (CH), 146.5 (C), 157.7 (C), 160.3 (C), 164.0 (C), 167.1 (C).

Ethyl 3-(1,3-dioxoisoindolin-2-yl)-6-(hexyloxy)-4-methylthieno[2,3-*b*]pyridine-2-carboxylate (4d).

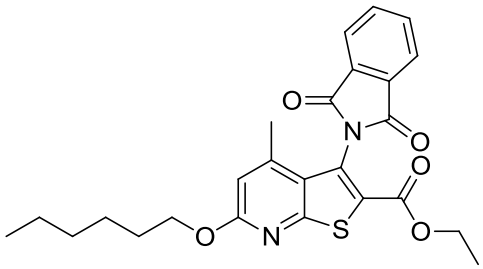

White solid (266 mg, 48%). ^{1}H NMR ($CDCl_3$): δ 0.91 (m, 3H), 1.11 (t, *J* 7.1 Hz, 3H), 1.36 (m, 4H), 1.46 (m, 2H), 1.79 (m, 2H), 2.36 (d, *J* 0.9 Hz, 3H), 4.20 (q, *J* 7.1 Hz, 2H), 4.40 (t, *J* 6.7 Hz, 2H), 6.57 (m, 1H), 7.83 (m, 2H), 8.00 (m, 2H). ^{13}C NMR ($CDCl_3$): δ 13.9 (CH_3), 14.2 (CH_3), 18.5 (CH_3), 22.8 (CH_2), 25.8 (CH_2), 29.0 (CH_2), 31.7 (CH_2), 61.7 (CH_2), 67 (CH_2), 112.4 (CH), 124.2 (CH), 124.6 (C), 125.2 (C), 127.7 (C), 132.5 (C), 134.7 (CH), 145.8 (C), 159.3 (C), 161.2 (C), 164.4 (C), 167.6 (C).

General procedure for halogenation at the 5′ position. Intermediate **4a-d** (1equiv.) was added to acetonitrile (15-25 mL) and warmed until completely dissolved. The required *N*-halogensuccinimide (2 equiv.) and 2-3 drops of concentrated HCl were added and the reaction mixture heated at reflux for 1.5–4 h under N_2. The reaction mixture was then diluted with chloroform (50 mL) and washed with water (3 × 20 mL), dried over anhydrous sodium sulfate, filtered and evaporated to dryness.

Ethyl-5-chloro-3-(1,3-dioxoisoindolin-2-yl)-6-methoxy-4-methylthieno[2,3-*b*]pyridine-2-carboxylate (5a).[14]

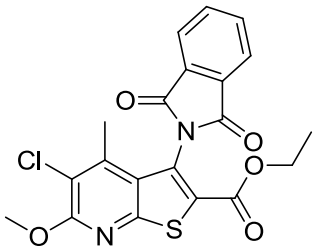

White solid (4.28 g, 86%). ^{1}H NMR ($CDCl_3$): δ 1.12 (t, *J* 7.1 Hz, 3H), 2.49 (s, 3H), 4.13 (s, 3H), 4.21 (q, *J* 7.1 Hz, 2H), 7.85 (m, 2H), 8.01 (m, 2H). ^{13}C NMR ($CDCl_3$): δ 13.9 (CH_3), 14.7 (CH_3), 55.4 (CH_3), 61.9 (CH_2), 118.8 (C), 124.3 (CH), 125.1 (C), 127.0 (C), 127.4 (C), 132.4 (C), 134.9 (CH), 143.0 (C), 155.9 (C), 159.5 (C), 160.9 (C), 167.6 (C).

Ethyl 5-chloro-3-(1,3-dioxoisoindolin-2-yl)-6-ethoxy-4-methylthieno[2,3-*b*]pyridine-2-carboxylate (5b).

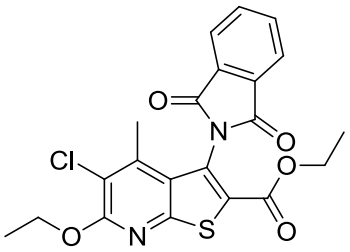

White solid (386 mg, 83%). ^{1}H NMR ($CDCl_3$): δ 1.12 (t, *J* 7.1 Hz, 3H), 1.49 (t, *J* 7.1 Hz, 3H), 2.48 (s, 3H), 4.21 (q, *J* 7.1 Hz, 2H), 4.57 (q, *J* 7.1 Hz, 2H), 7.85 (m, 2H), 8.01 (m, 2H). ^{13}C NMR ($CDCl_3$): δ 13.9 (CH_3), 14.6 (CH_3), 14.8 (CH_3), 61.9 (CH_2), 64.2 (CH_2), 118.9 (C), 124.3 (CH), 124.9 (C), 126.7 (C), 127.4 (C), 132.4 (C), 134.9 (CH), 142.8 (C), 156.0 (C), 159.2 (C), 160.9 (C), 167.6 (C).

Ethyl 6-butoxy-5-chloro-3-(1,3-dioxoisoindolin-2-yl)-4-methylthieno[2,3-*b*]pyridine-2-carboxylate (5c).

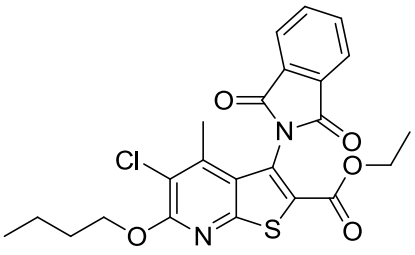

Yellow foam (650 mg, 99%). ^{1}H NMR ($CDCl_3$): δ 1.01 (t, *J* 7.4 Hz, 3H), 1.12 (t, *J* 7.1 Hz, 3H), 1.53 (m, 2H), 1.85 (m, 2H), 2.48 (s, 3H), 4.21 (q, *J* 7.1 Hz, 2H), 4.50 (t, *J* 6.6 Hz, 2H), 7.85 (m, 2H), 8.01 (m, 2H). ^{13}C NMR ($CDCl_3$): δ 13.9 (CH_3), 14.0 (CH_3), 14.7 (CH_3), 19.4 (CH_2), 30.9 (CH_2), 61.9 (CH_2), 68.1 (CH_2), 119.0 (C), 124.3 (CH), 124.8 (C), 126.7 (C), 127.4 (C), 132.4 (C), 134.9 (CH), 142.8 (C), 156.0 (C), 159.3 (C), 160.9 (C), 167.6 (C).

Ethyl 5-chloro-3-(1,3-dioxoisoindolin-2-yl)-6-(hexyloxy)-4-methylthieno[2,3-*b*]pyridine-2-carboxylate (5d).

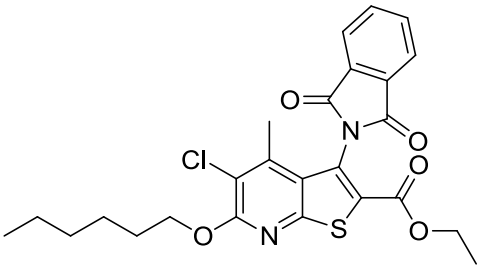

Colourless oil (274 mg, 99%). ^{1}H NMR ($CDCl_3$): δ 0.91 (m, 3H), 1.12 (t, *J* 7.1 Hz, 3H), 1.37 (m, 4H), 1.50 (m, 2H), 1.86 (m, 2H), 2.49 (s, 3H), 4.21 (q, *J* 7.1 Hz, 2H), 4.49 (t, *J* 6.7 Hz, 2H), 7.85 (m, 2H), 8.01 (m, 2H). ^{13}C NMR ($CDCl_3$): δ 13.9 (CH_3), 14.1 (CH_3), 14.7 (CH_3), 22.7 (CH_2), 25.8 (CH_2), 28.8 (CH_2), 31.6 (CH_2), 61.9 (CH_2), 68.3 (CH_2), 119.0 (C), 124.3 (CH), 124.8 (C), 126.7 (C), 127.4 (C), 132.4 (C), 134.8 (CH), 142.8 (C), 156.0 (C), 159.3 (C), 160.9 (C), 167.5 (C).

Ethyl 5-bromo-3-(1,3-dioxoisoindolin-2-yl)-6-methoxy-4-methylthieno[2,3-*b*]pyridine-2-carboxylate (5e).

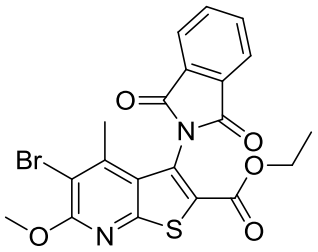

White solid (289 mg, 80%). ^{1}H NMR ($CDCl_3$): δ 1.12 (t, *J* 7.1 Hz, 3H), 2.53 (s, 3H), 4.12 (s, 3H), 4.21 (q, *J* 7.1 Hz, 2H), 7.85 (m, 2H), 8.01 (m, 2H). ^{13}C NMR ($CDCl_3$): δ 13.9 (CH_3), 17.9 (CH_3), 55.6 (CH_2), 61.9 (CH_3), 110.5 (C), 124.3 (CH), 125.3 (C), 126.9 (C), 127.3 (C), 132.4 (C), 134.9 (CH), 145.3 (C), 156.9 (C), 160.1 (C), 160.9 (C), 167.5 (C).

Ethyl 3-(1,3-dioxoisoindolin-2-yl)-5-iodo-6-methoxy-4-methylthieno[2,3-*b*]pyridine-2-carboxylate (5f).

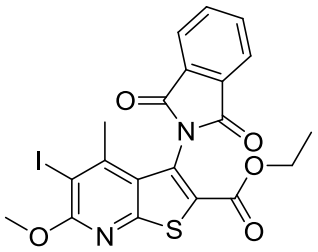

Pale yellow solid (1.11 g, 84%). ^{1}H NMR ($CDCl_3$): δ 1.12 (t, *J* 7.1 Hz, 3H), 2.59 (s, 3H), 4.10 (s, 3H), 4.21 (q, *J* 7.1 Hz, 2H), 7.85 (m, 2H), 8.01 (m, 2H). ^{13}C NMR ($CDCl_3$): δ 14.0 (CH_3), 24.0 (CH_3), 55.9 (CH_3), 61.9 (CH_2), 88.9 (C), 124.3 (CH), 125.1 (C), 126.5 (C), 127.1 (C), 132.4 (C), 134.9 (CH), 149.5 (C), 158.4 (C), 160.9 (C), 161.7 (C), 167.5 (C).

General procedure for phthalamide deprotection. To a solution of intermediate **5a-f** (1equiv.) in ethanol (15-20 mL) was added dropwise hydrazine monohydrate (4 equiv.), and the mixture was heated at reflux for 1h. After this time, the reaction mixture was cooled to room temperature and the white precipitate filtered and washed with chloroform (10 mL). The filtrate was collected

and diluted with a further 20 mL of chloroform and washed with water (3 × 20 mL), dried over anhydrous sodium sulfate, filtered and evaporated to dryness.

Ethyl 3-amino-5-chloro-6-methoxy-4-methylthieno[2,3-*b*]pyridine-2-carboxylate (6a).[14]

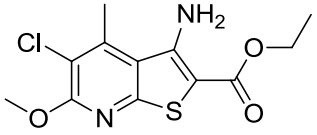

Pale yellow solid (85 mg, 84%). ^{1}H NMR ($CDCl_3$): δ 1.38 (t, *J* 7.1 Hz, 3H), 2.83 (s, 3H), 4.08 (s, 3H), 4.33 (q, *J* 7.1 Hz, 2H), 6.14 (br s, 2H, NH_2). ^{13}C NMR ($CDCl_3$): δ 14.6 (CH_3), 16.4 (CH_3), 55.2 (CH_3), 60.6 (CH_2), 116.3 (C), 120.1 (C), 142.9 (C), 149.1 (C), 157.3 (C), 159.5 (C), 165.7 (C), 168.4 (C).

Ethyl 3-amino-5-chloro-6-ethoxy-4-methylthieno[2,3-*b*]pyridine-2-carboxylate (6b).

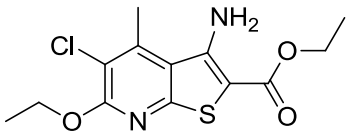

Yellow solid (234 mg, 89%). ^{1}H NMR ($CDCl_3$): δ 1.38 (t, *J* 7.1 Hz, 3H), 1.46 (2.83 t, *J* 7.1 Hz, 3H), 2.82 (s, 3H), 4.33 (q, *J* 7.1 Hz, 2H), 4.51 (q, *J* 7.1 Hz, 2H), 6.14 (br s, 2H, NH_2). ^{13}C NMR ($CDCl_3$): δ 14.6 (2 × CH_3), 16.4 (CH_3), 60.5 (CH_2), 63.9 (CH_2), 96.6 (C), 116.4 (C), 119.9 (C), 142.8 (C), 149.1 (C), 157.3 (C), 159.2 (C), 165.7 (C).

Ethyl 3-amino-6-butoxy-5-chloro-4-methylthieno[2,3-*b*]pyridine-2-carboxylate (6c).

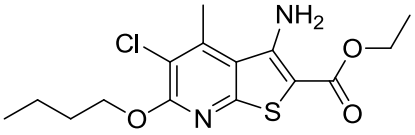

Yellow solid (215 mg, 46%). ^{1}H NMR ($CDCl_3$): δ 0.99 (t, *J* 7.4 Hz, 3H), 1.37 (2.83 t, *J* 7.1 Hz, 3H), 1.51 (m, 2H), 1.81 (m, 2H), 2.82 (s, 3H), 4.33 (q, *J* 7.1 Hz, 2H), 4.44 (t, *J* 6.6 Hz, 2H), 6.13 (br s, 2H, NH_2). ^{13}C NMR ($CDCl_3$): δ 14.0 (CH_3), 14.6 (CH_3), 16.4 (CH_3), 19.4 (CH_2), 31.0 (CH_2), 60.5 (CH_2), 67.8 (CH_2), 96.6 (C), 116.5 (C), 119.9 (C), 142.7 (C), 149.1 (C), 157.4 (C), 159.4 (C), 165.7 (C).

Ethyl 3-amino-5-chloro-6-(hexyloxy)-4-methylthieno[2,3-*b*]pyridine-2-carboxylate (6d).

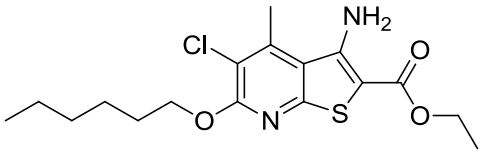

Yellow solid (173 mg, 80%). ^{1}H NMR ($CDCl_3$): δ 0.91 (m, 3H), 1.35 (m, 4H), 1.37 (t, *J* 7.1 Hz, 3H), 1.48 (m, 2H), 1.83 (m, 2H), 2.81 (s, 3H), 4.33 (q, *J* 7.1 Hz, 2H), 4.43 (t, *J* 6.7 Hz, 2H), 6.13 (br s, 2H, NH_2). ^{13}C NMR ($CDCl_3$): δ 14.2 (CH_3), 14.6 (CH_3), 16.4 (CH_3), 22.7 (CH_2), 25.8 (CH_2), 28.9 (CH_2), 31.7 (CH_2), 60.5 (CH_2), 68.1 (CH_2), 96.6 (C), 116.5 (C), 119.9 (C), 142.7 (C), 149.1 (C), 157.4 (C), 159.4 (C), 165.7 (C).

Ethyl 3-amino-5-bromo-6-methoxy-4-methylthieno[2,3-*b*]pyridine-2-carboxylate (6e).

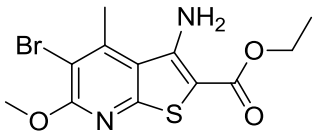

Fluffy beige solid (123 mg, 83%). ^{1}H NMR ($CDCl_3$): δ 1.38 (t, *J* 7.1 Hz, 3H), 2.87 (s, 3H), 4.74 (s, 3H), 4.33 (q, *J* 7.1 Hz, 2H), 6.07 (br s, 2H, NH_2). ^{13}C NMR ($CDCl_3$): δ 14.6 (CH_3), 19.8 (CH_3), 55.4 (CH_3), 60.6 (CH_2), 96.7 (C), 107.8 (C), 120.5 (C), 145.2 (C), 149.0 (C), 158.3 (C), 160.1 (C), 165.7 (C).

Ethyl 3-amino-5-iodo-6-methoxy-4-methylthieno[2,3-*b*]pyridine-2-carboxylate (6f).

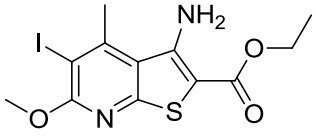

Pale yellow solid (336 mg, 89%). ^{1}H NMR ($CDCl_3$): δ 1.38 (t, *J* 7.1 Hz, 3H), 2.92 (s, 3H), 4.04 (s, 3H), 4.33 (q, *J* 7.1 Hz, 2H), 5.93 (br s, 2H, NH_2). ^{13}C NMR ($CDCl_3$): δ 14.6 (CH_3), 25.9 (CH_3), 55.7 (CH_3), 60.6 (CH_2), 85.8 (C), 96.3 (C), 120.4 (C), 148.8 (C), 149.4 (C), 159.8 (C), 161.9 (C), 165.7 (C).

General procedure for ester hydrolysis. Compounds **6a-f** (1 equiv) was added to ethanol (10 mL) and 2 M NaOH (10 mL) and heated at reflux for 1.5 h. The reaction mixture was then

cooled to room temperature and an excess of 2 M HCl was added causing precipitation of the product. The product was then filtered and washed with a small amount of cold water.

3-Amino-5-chloro-6-methoxy-4-methylthieno[2,3-*b*]pyridine-2-carboxylic acid (7a).[14]

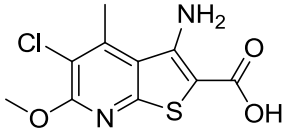

Beige-yellow solid (179 mg, 84%). ^{1}H NMR (DMSO- d_6): δ 2.77 (s, 3H), 3.96 (s, 3H), 6.41 (br s, 2H, NH_2). LCMS (ESI) *m/z*: 273.0 $[M+H]^+$ (90%), 275.0 (30%).

3-Amino-5-chloro-6-ethoxy-4-methylthieno[2,3-*b*]pyridine-2-carboxylic acid (7b).

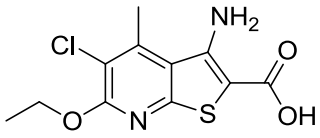

Beige-yellow solid (193 mg, 91%). ^{1}H NMR (DMSO- d_6): δ 1.37 (t, *J* 7.1 Hz, 3H), 2.79 (s, 3H), 4.43 (q, *J* 7.0 Hz, 2H), 6.76 (br s, 2H, NH_2). ^{13}C NMR (DMSO- d_6): δ 14.3 (CH_3), 16.3 (CH_3), 63.4 (CH_2), 94.9 (C), 114.9 (C), 120.1 (C), 144.4 (C), 149.6 (C), 156.0 (C), 158.3 (C), 166.2 (C).

3-Amino-6-butoxy-5-chloro-4-methylthieno[2,3-*b*]pyridine-2-carboxylic acid (7c).

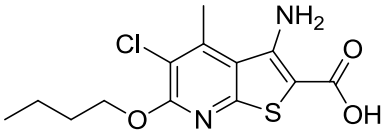

Yellow solid (91 mg, 49%). ^{1}H NMR (DMSO- d_6): δ 0.94 (t, *J* 7.4 Hz, 3H), 1.45 (m, 2H), 1.73 (m, 2H) 2.79 (s, 3H), 4.38 (t, *J* 6.5 Hz, 2H), 6.75 (br s, 2H, NH_2). ^{13}C NMR (DMSO- d_6): δ 13.7 (CH_3), 16.3 (CH_3), 18.7 (CH_2), 30.3 (CH_2), 67.2 (CH_2), 94.9 (C), 115.0 (C), 120.1 (C), 144.4 (C), 149.6 (C), 156.0 (C), 158.5 (C), 166.2 (C).

3-Amino-5-chloro-6-(hexyloxy)-4-methylthieno[2,3-*b*]pyridine-2-carboxylic acid (7d).

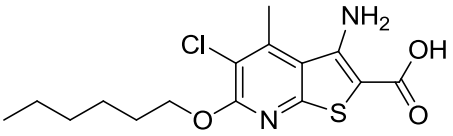

Beige solid (113 mg, 81%). ^{1}H NMR (DMSO- d_6): δ 0.87 (m, 3H), 1.32 (m, 4H), 1.43 (m, 2H), 1.74 (m, 2H) 2.79 (s, 3H), 4.36 (t, *J* 6.5 Hz, 2H), 6.75 (br s, 2H, NH_2). ^{13}C NMR (DMSO- d_6): δ 13.9 (CH_3), 16.3 (CH_3), 22.0 (CH_2), 25.1 (CH_2), 28.2 (CH_2), 30.7 (CH_2), 67.4 (CH_2), 95.1 (C), 115.0 (C), 120.2 (C), 144.4 (C), 149.5 (C), 155.9 (C), 158.4 (C), 166.3 (C).

3-Amino-5-bromo-6-methoxy-4-methylthieno[2,3-*b*]pyridine-2-carboxylic acid (7e).

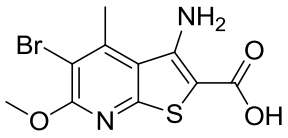

Beige solid (91 mg, 96%). ^{1}H NMR (DMSO- d_6): δ 2.82 (s, 3H), 3.95 (s, 3H), 6.41 (br s, 2H, NH_2). ^{13}C NMR (DMSO- d_6): δ 19.0 (CH_3), 54.6 (CH_3), 96.4 (C), 105.5 (C), 123.1 (C), 140.4 (C), 145.4 (C), 154.9 (C), 157.5 (C), 168.1 (C).

3-Amino-5-iodo-6-methoxy-4-methylthieno[2,3-*b*]pyridine-2-carboxylic acid (7f).

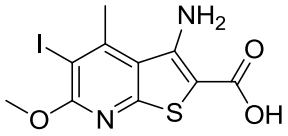

White solid (290 mg, 95%). ^{1}H NMR (DMSO- d_6): δ 2.88 (s, 3H), 3.93 (s, 3H), 6.48 (br s, 2H, NH_2). ^{13}C NMR (DMSO- d_6): δ 25.1 (CH_3), 55.1 (CH_3), 55.2 (C), 55.7 (C), 85.3 (C), 96.1 (C), 122.3 (C), 140.3 (C), 148.9 (C), 149.7 (C).

General procedure for BOP coupling. Carboxylic acids **7a-f** (1 equiv) were added to *N*,*N*-dimethylformamide (10 mL), followed by *N*,*N*-diisopropylethylamine (1.05 equiv.) and BOP (1.05 equiv.) under N_2 at room temperature and stirred for 5-10 mins. Cyclopropylamine or the required *N*-alkylamine (1.1 equiv.) was subsequently added and the reaction mixture stirred at room temperature for 2-3 h. The solvent was then removed in vacuo and the resulting residue

partitioned between dichloromethane (30 mL) and saturated sodium bicarbonate (50 mL). The organic layer was removed and the aqueous phase was further extracted with 3 × 20 mL portions of dichloromethane. The organic fractions were combined, washed with water (50 mL), brine (50 mL), dried over anhydrous sodium sulfate, filtered and concentrated to yield the crude product as an oily residue. To remove excess HMPA, crude products are dissolved in ethyl acetate and washed with 3 × 50 mL portions of 2 M brine. Purification of the product was performed by column chromatography and /or recrystalisation.

3-Amino-5-chloro-*N*-cyclopropyl-6-methoxy-4-methylthieno[2,3-*b*]pyridine-2-carboxamide (8a).[16]

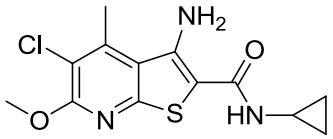

White crystalline solid (117 mg, 57%). mp: 175.5-176.7 °C (DCM/hexane). ^{1}H NMR ($CDCl_3$): δ 0.63 (m, 2H), 0.86 (m, 2H), 2.82 (m, 1H), 2.83 (s, 3H), 4.07 (s, 3H), 5.55 (br s, 1H, NH), 6.36 (br s, 2H , NH_2). ^{13}C NMR ($CDCl_3$): δ 7.1 (CH_2), 16.4 (CH_3), 23.0 (CH), 55.2 (CH_3), 97.6 (C), 116.6 (C), 121.1 (C), 143.1 (C), 147.7 (C), 154.5 (C), 159.3 (C), 167.3 (C). HPLC purity (λ= 214 nm): 98% t_R 9.95 min. HRMS (ESI)-TOF (*m/z)*: $[M+H]^+$ 312.0574 calcd for $C_{13}H_{14}ClN_3O_2S$; found $[M+H]^+$ 312.0569.

3-Amino-5-chloro-*N*-cyclopropyl-6-ethoxy-4-methylthieno[2,3-*b*]pyridine-2-carboxamide (8b).

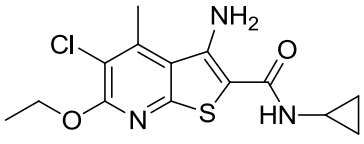

Yellow solid (21 mg, 15%). mp: 211.2- 212.7 °C. ^{1}H NMR ($CDCl_3$): δ 0.63 (m, 2H), 0.85 (m, 2H), 1.45 (t, *J* 7.1 Hz, 3H), 2.82 (m, 1H), 2.82 (s, 3H), 4.49 (q, *J* 7.1 Hz, 2H), 5.54 (br s, 1H, NH), 6.35 (br s, 2H, NH_2). ^{13}C NMR ($CDCl_3$): δ 7.0 (CH_2), 14.8 (CH_3), 16.4 (CH_3), 23.0 (CH), 63.8 (CH_2), 97.5 (C), 116.7 (C), 120.9 (C), 143.0 (C), 147.8 (C), 154.6 (C), 159.1 (C), 167.4 (C).

HPLC purity (λ= 214 nm): 98% t_R 10.38 min. HRMS (ESI)-TOF (*m/z)*: $[M+H]^+$ 326.0730 calcd for $C_{14}H_{16}ClN_3O_2S$; found $[M+H]^+$ 326.0738.

3-Amino-6-butoxy-5-chloro-*N*-cyclopropyl-4-methylthieno[2,3-*b*]pyridine-2-carboxamide (8c).

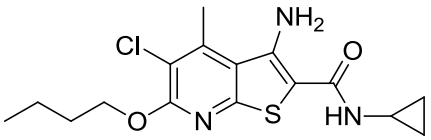

Yellow solid (61 mg, 65%). mp: 131.9- 134.2 °C. ^{1}H NMR ($CDCl_3$): δ 0.63 (m, 2H), 0.85 (m, 2H), 0.99 (t, *J* 7.4 Hz, 3H), 1.51 (m, 2H), 1.81 (m, 2H), 2.82 (m, 1H), 2.82 (s, 3H), 4.41 (t, *J* 6.6 Hz, 2H), 5.64 (br s, 1H, NH), 6.45 (br s, 2H, NH_2). ^{13}C NMR ($CDCl_3$): δ 7.0 (CH_2), 14.0 (CH_3), 16.4 (CH_3), 19.4 (CH_2), 23.0 (CH), 31.0 (CH_2), 67.7 (CH_2), 97.4 (C), 116.8 (C), 120.8 (C), 142.9 (C), 147.8 (C), 154.6 (C), 159.2 (C), 167.4 (C). HPLC purity (λ= 214 nm): 95% t_R 11.63 min. HRMS (ESI)-TOF (*m/z)*: $[M+H]^+$ 354.1043 calcd for $C_{16}H_{20}ClN_3O_2S$; found $[M+H]^+$ 354.1029.

3-Amino-5-chloro-*N*-cyclopropyl-6-(hexyloxy)-4-methylthieno[2,3-*b*]pyridine-2-carboxamide (8d).

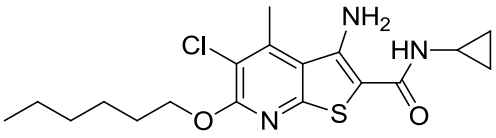

Yellow solid (47 mg, 42%). mp: 126.8- 128.3 °C. ^{1}H NMR ($CDCl_3$): δ 0.63 (m, 2H), 0.84 (m, 2H), 0.89-0.94 (m, 3H), 1.33-1.37 (m, 4H), 1.46 (m, 2H), 1.82 (m, 2H), 2.80 (s, 3H), 2.81 (m, 1H), 4.39 (t, *J* 6.7 Hz, 2H), 5.56 (br s, 1H, NH), 6.43 (br s, 2H, NH_2). ^{13}C NMR ($CDCl_3$): δ 7.0 (CH_2), 14.1 (CH_3), 16.3 (CH_3), 22.7 (CH_2), 23.0 (CH), 25.8 (CH_2), 28.8 (CH_2), 31.6 (CH_2), 68.0 (CH_2), 97.4 (C), 116.8 (C), 120.7 (C), 142.9 (C), 147.8 (C), 154.5 (C), 159.2 (C), 167.4 (C). HPLC purity (λ= 214 nm): 96% t_R 12.72 min. HRMS (ESI)-TOF (*m/z)*: $[M+H]^+$ 382.1356 calcd for $C_{18}H_{24}ClN_3O_2S$; found $[M+H]^+$ 382.1359.

3-Amino-5-bromo-*N*-cyclopropyl-6-methoxy-4-methylthieno[2,3-*b*]pyridine-2-carboxamide (8e).

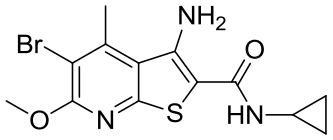

Yellow solid (67 mg, 70%). mp: 199.1- 201.5 °C. ^{1}H NMR ($CDCl_3$): 0.64 (m, 2H), 0.85 (m, 2H), 2.82 (m, 1H), 2.88 (s, 3H), 3.71 (br s, 2H, NH_2), 4.06 (s, 3H), 5.57 (br s, 1H, NH). ^{13}C NMR ($CDCl_3$): δ 7.1 (CH_2), 19.7 (CH_3), 23.0 (CH), 55.7 (CH_3), 97.5 (C), 108.3 (C), 121.4 (C), 145.4 (C), 147.7 (C), 155.6 (C), 160.0 (C), 167.4 (C). HPLC purity (λ= 214 nm): 98% t_R 11.23 min. HRMS (ESI)-TOF (*m/z)*: $[M+H]^+$ 356.0068 calcd for $C_{13}H_{14}BrN_3O_2S$; found $[M+H]^+$ 356.0057.

3-Amino-*N*-cyclopropyl-5-iodo-6-methoxy-4-methylthieno[2,3-*b*]pyridine-2-carboxamide (8f).

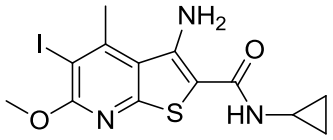

Beige solid (158 mg, 72%). mp: 226.1- 227.6 °C. ^{1}H NMR ($CDCl_3$): 0.64 (m, 2H), 0.86 (m, 2H), 2.28 (br s, 2H, NH_2), 2.82 (m, 1H), 2.94 (s, 3H), 4.04 (s, 3H), 5.56 (br s, 1H, NH). ^{13}C NMR ($CDCl_3$): δ 7.1 (CH_2), 23.0 (CH), 25.9 (CH_3), 55.7 (CH_3), 86.3 (C), 97.2 (C), 121.2 (C), 147.4 (C), 149.5 (C), 157.1 (C), 161.7 (C), 167.3 (C). HPLC purity (λ= 214 nm): 98% t_R 9.76 min. HRMS (ESI)-TOF (*m/z)*: $[M+H]^+$ 403.9930 calcd for $C_{13}H_{14}IN_3O_2S$; found $[M+H]^+$ 403.9923.

3-Amino-5-chloro-*N*-ethyl-6-methoxy-4-methylthieno[2,3-*b*]pyridine-2-carboxamide (9a).

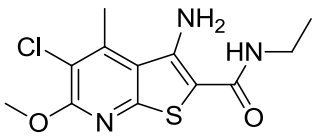

Yellow solid (52 mg, 56%). mp: 180.9- 182.4 °C. ^{1}H NMR ($CDCl_3$): δ 1.25 (t, *J* 7.2 Hz, 3H), 2.80 (s, 3H), 3.45 (m, 2H), 4.06 (s, 3H), 5.40 (t, *J* 5.7 Hz, 1H, NH), 6.28 (br s, 2H, NH_2). ^{13}C NMR ($CDCl_3$): δ 15.2 (CH_3), 16.3 (CH_3), 34.7 (CH_2), 55.1 (CH_3), 98.3 (C), 116.5 (C), 121.2 (C),

143.0 (C), 147.3 (C), 154.4 (C), 159.2 (C), 165.7 (C). HPLC purity (λ= 214 nm): 99% t_R 9.67 min. HRMS (ESI)-TOF (*m/z)*: $[M+H]^+$ 300.0574 calcd for $C_{12}H_{14}ClN_3O_2S$; found $[M+H]^+$ 300.0572.

3-Amino-*N*-butyl-5-chloro-6-methoxy-4-methylthieno[2,3-*b*]pyridine-2-carboxamide (9b).

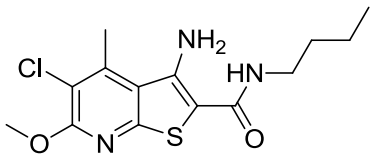

Beige solid (51 mg, 66%). mp: 138.7- 139.9 °C. ^{1}H NMR ($CDCl_3$): δ 0.96 (t, *J* 7.3 Hz, 3H), 1.42 (m, 2H), 1.59 (m, 2H) 2.80 (s, 3H), 3.41 (m, 2H), 4.06 (s, 3H), 5.41 (t, *J* 5.7 Hz, 1H, NH), 6.28 (br s, 2H, NH_2). ^{13}C NMR ($CDCl_3$): δ 13.9 (CH_3), 16.3 (CH_3), 20.7 (CH_2), 32.0 (CH_2), 39.6 (CH_2), 55.1 (CH_3), 98.3 (C), 116.5 (C), 121.2 (C), 143.0 (C), 147.3 (C), 154.4 (C), 159.1 (C), 165.7 (C). HPLC purity (λ= 214 nm): 99% t_R 10.73 min. HRMS (ESI)-TOF (*m/z)*: $[M+H]^+$ 328.0887 calcd for $C_{14}H_{18}ClN_3O_2S$; found $[M+H]^+$ 328.0889.

3-Amino-5-chloro-*N*-hexyl-6-methoxy-4-methylthieno[2,3-*b*]pyridine-2-carboxamide (9c).

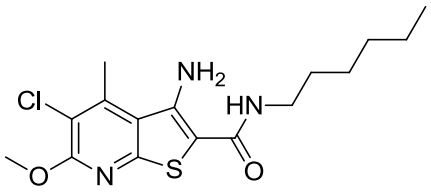

Yellow solid (54 mg, 64%). mp: 109.5- 110.8 °C. ^{1}H NMR ($CDCl_3$): δ 0.90 (t, *J* 7.3 Hz, 3H), 1.29- 1.39 (m, 6H), 1.60 (m, 2H) 2.80 (s, 3H), 3.38 (m, 2H), 4.05 (s, 3H), 5.43 (t, *J* 5.7 Hz, 1H, NH), 6.26 (br s, 2H, NH_2). ^{13}C NMR ($CDCl_3$): δ 14.1 (CH_3), 16.3 (CH_3), 22.7 (CH_2), 26.8 (CH_2), 29.9 (CH_2), 31.6 (CH_2), 39.8 (CH_2), 55.1 (CH_3), 98.3 (C), 116.5 (C), 121.1 (C), 143.0 (C), 147.2 (C), 154.3 (C), 159.1 (C), 165.7 (C). HPLC purity (λ= 214 nm): 98% t_R 11.77 min. HRMS (ESI)-TOF (*m/z)*: $[M+H]^+$ 356.1200 calcd for $C_{16}H_{22}ClN_3O_2S$; found $[M+H]^+$ 356.1205.

General procedure for amine substituted derivatives. Compound **8a** (1 equiv) was dissolved in dry DCM (3 mL) under N_2. Triethylamine (2 equiv) was added and the reaction mixture

cooled to 0 ^{0}C. The required acyl chloride (1.05 equiv) was added dropwise and the reaction heated at reflux for 2 d during which an additional (1-2 equiv) of the acyl chloride was added. Upon cooling to room temperature formed a white precipitate that was filtered and washed with a small amount of DCM.

3-Acetamido-5-chloro-*N*-cyclopropyl-6-methoxy-4-methylthieno[2,3-*b*]pyridine-2-carboxamide (10a).

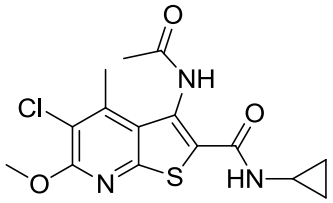

White solid (29 mg, 48%). mp: 289.9- 291.2 °C ^{1}H NMR (d_6-DMSO): δ 0.54 (m, 2H), 0.73 (m, 2H), 2.08 (s, 3H), 2.61 (s, 3H), 2.81 (m, 1H), 4.02 (s, 3H), 8.02 (d, *J* 3.7 Hz, 1H, NH), 9.78 (s, 1H, NH). ^{13}C NMR (d_6-DMSO): δ 6.09 (CH_2), 14.6 (CH_3), 22.8 (CH_3), 23.0 (CH), 54.9 (CH_3), 116.6 (C), 124.4 (C), 128.6 (C), 129.4 (C), 143.6 (C), 153.1 (C), 157.7 (C), 161.8 (C), 170.5 (C). HPLC purity (λ= 214 nm): 96% t_R 8.32 min. HRMS (ESI)-TOF (*m/z)*: $[M+H]^+$ 354.0679 calcd for $C_{15}H_{16}ClN_3O_3S$; found $[M+H]^+$ 354.0672.

3-Butyramido-5-chloro-*N*-cyclopropyl-6-methoxy-4-methylthieno[2,3-*b*]pyridine-2-carboxamide (10b).

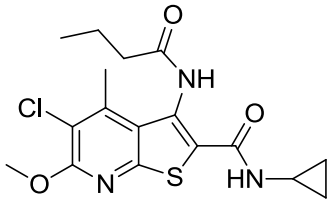

White solid (31 mg, 48%). mp: 282.0- 283.5 °C. ^{1}H NMR (d_6-DMSO): δ 0.54 (m, 2H), 0.73 (m, 2H), 0.95 (t, *J* 7.4 Hz, 3H), 1.63 (m, 2H), 2.34 (t, *J* 7.3 Hz, 2H), 2.60 (s, 3H), 2.81 (m, 1H), 4.02 (s, 3H), 8.04 (d, *J* 3.7 Hz, 1H, NH), 9.74 (s, 1H, NH). ^{13}C NMR (d_6-DMSO): δ 6.01 (CH_2), 13.8 (CH_3), 14.7 (CH_3), 18.2 (CH_2), 23.0 (CH), 37.4 (CH_2), 55.0 (CH_3), 116.6 (C), 124.5 (C), 128.5 (C), 129.6 (C), 134.9 (C), 143.6 (C), 153.1 (C), 157.8 (C), 173.2 (C). HPLC purity (λ= 214 nm):

96% t_R 7.27 min. HRMS (ESI)-TOF (*m/z)*: $[M+H]^+$ 382.0992 calcd for $C_{17}H_{20}ClN_3O_3S$; found $[M+H]^+$ 382.0996.

5-Chloro-*N*-cyclopropyl-3-hexanamido-6-methoxy-4-methylthieno[2,3-*b*]pyridine-2-carboxamide (10c).

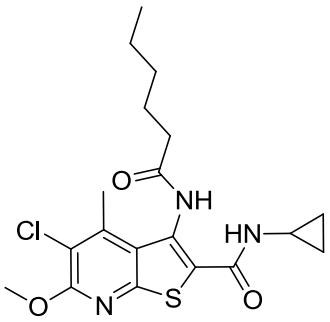

White solid (29 mg, 45%). mp: 256.4- 257.9 °C ^{1}H NMR (d_6-DMSO): δ 0.52 (m, 2H), 0.73 (m, 2H), 0.90 (m, 3H), 1.30-1.33 (m, 4H), 1.60 (m, 2H), 2.36 (t, *J* 7.3 Hz, 2H), 2.60 (s, 3H), 2.79 (m, 1H), 4.02 (s, 3H), 8.01 (d, *J* 3.7 Hz, 1H, NH), 9.73 (s, 1H, NH). ^{13}C NMR (d_6-DMSO): δ 6.00 (CH_2), 13.8 (CH_3), 14.7 (CH_3), 21.9 (CH_2), 23.0 (CH), 24.3 (CH_2), 30.9 (CH_2), 35.4 (CH_2), 55.0 (CH_3), 116.6 (C), 124.5 (C), 128.5 (C), 129.6 (C), 143.6 (C), 153.1 (C), 157.7 (C), 161.9 (C), 173.4 (C). HPLC purity (λ= 214 nm): 96% t_R 10.73 min. HRMS (ESI)-TOF (*m/z)*: $[M+H]^+$ 410.1305 calcd for $C_{19}H_{24}ClN_3O_3S$; found $[M+H]^+$ 410.1299.

Synthesis of compound 12.

3-Amino-6-methoxy-4-methylthieno[2,3-*b*]pyridine-2-carboxylic acid (11).

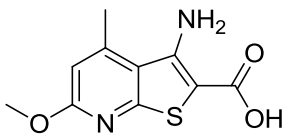

3a was dissolved in ethanol (30 mL) followed by the addition of 1 M sodium hydroxide solution (2.08 mL) where a white precipitate formed. The reaction mixture was refluxed for 2 h. The reaction mixture was cooled to room temperature where a white precipitate formed. The solid was filtered and dissolved in a minimum amount of water. 1 M Aqueous hydrogen chloride was

added dropwise where a white precipitate formed. The solid was filtered, washed with water and dried under vacuum to give the title compound (515 mg, 58%). ^{1}H NMR (d_6-DMSO) δ 2.69 (s, 3H), 3.90 (s, 3H), 6.62 (d, *J* 0.9, 1H), 6.69 (br s, 2H), 11.50 (br s, 1H). ^{13}C NMR (d_6-DMSO) δ 19.8 (CH_3), 53.6 (CH_3), 109.3 (CH), 119.5 (C), 147.6 (C), 149.9 (C), 159.0 (C), 161.6 (C), 163.9 (C), 166.4 (C).

3-Amino-*N*-cyclopropyl-6-methoxy-4-methylthieno[2,3-*b*]pyridine-2-carboxamide hydrochloride (12).

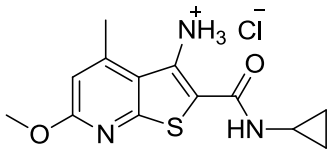

Compound **11** (362 mg, 1.52 mmol) was dissolved in dry DMF (5 mL) under N_2 atmosphere. Diisopropylethylamine (520 μL, 3.04 mmol) was added to the solution followed by BOP (605 mg, 1.60 mmol). The mixture was stirred for 10 mins until completely dissolved. Cyclopropylamine (116 μL, 1.67 mmol) dissolved in dry DMF (1 mL) was slowly added to the mixture. The reaction mixture was stirred at RT under N_2 for 3 h. Note: Additional amine may be required to consume starting material. The reaction mixture was partitioned between ethyl acetate (30 mL) and water (30 mL). The aqueous layer was extracted with ethyl acetate (2 × 20 mL). The combined ethyl acetate layers were washed with brine (20 mL), dried over anhydrous Na_2SO_4, filtered and concentrated in vacuo. ^{1}H NMR ($CDCl_3$) δ 0.61-0.65 (m, 2H), 0.82-0.87 (m, 2H), 2.69 (d, *J* 0.9 Hz, 3H), 2.80-2.84 (m, 1H), 3.97 (s, 3H), 5.54 (br s, 1H), 6.34 (br s, 2H), 6.44 (d, *J* 0.9 Hz, 1H). ^{13}C NMR ($CDCl_3$) δ 6.9 (CH_3), 20.2 (CH_2), 22.8 (CH), 53.9 (CH_3), 110.2 (CH), 120.3 (C), 145.9 (C), 148.0 (C), 157.7 (C), 162.1 (C), 164.3 (C), 167.4 (C). The product was dissolved in ethyl acetate and converted to the HCl salt using ethereal hydrogen chloride to give the product as a white solid (185 mg, 39%). mp: 180- 181 °C. HPLC purity (λ= 254 nm): 99.7% t_R 8.26 min. HRMS (ESI)-TOF (*m/z)*: $[M+H]^+$ 278.0963 calcd for $C_{13}H_{15}N_3O_2S$; found $[M+H]^+$ 278.0958.

Synthesis of compound 18.

5-Chloro-4,6-dimethyl-2-oxo-1,2-dihydropyridine-3-carbonitrile (14).[17]

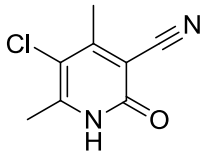

A mixture of cyanopyridone (**13,** 500 mg, 3.37 mmol) and sulfuryl chloride (1.09 mL, 13.5 mmol) in dry dichloroethane (10 mL) was refluxed for 6 h. The reaction mixture was cooled to RT and the precipitate was filtered and washed with DCM (50 mL) to give the desired product without requiring further purification (257 mg, 42%). ^{1}H NMR (d_6-DMSO) δ 2.35 (s, 3H), 2.41 (s, 3H), 12.8 (br s, 1H). ^{13}C NMR (d_6-DMSO) δ 18.2 (CH_3), 20.0 (CH_3), 100.8 (C), 115.4 (C), 115.5 (C), 121.6 (C), 159.2 (C), 159.3 (C).

2,5-Dichloro-4,6-dimethylnicotinonitrile (15).[17]

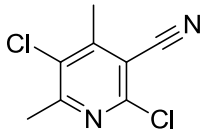

Compound **14** (502 mg, 2.80 mmol) and $POCl_3$ (2 mL) were combined in a microwave vessel. The mixture was heated to 100 °C for 1 h in a microwave. The resulting green solution was poured into ice (10 g). Following this, gas evolution occurred and a white precipitate formed. The solid was filtered and washed with ice water (3 × 15 mL). The solid was dried under vacuum, and the resulting white solid was used in subsequent reactions without further purification (487 mg, 88%). ^{1}H NMR (d_6-DMSO) δ 2.57 (s, 3H), 2.61 (s, 3H). ^{13}C NMR (d_6-DMSO) δ 19.7 (CH_3), 23.2 (CH_3), 109.3 (C), 114.0 (C), 130.3 (C), 148.2 (C), 152.3 (C), 160.1 (C).

5-Chloro-4,6-dimethyl-2-thioxo-1,2-dihydropyridine-3-carbonitrile (16).[17]

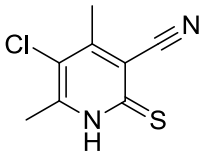

Thiourea (318 mg, 4.17 mmol) was added to a stirred solution of **15** (419 mg, 2.09 mmol) in absolute ethanol (25 mL). The mixture was refluxed for 24 h. The mixture was cooled to RT following which the product recrystallised from solution to form yellow needles. The product was then filtered and washed with cold ethanol and dried under vacuum (121 mg, 29%). ^{1}H NMR (*d*$_6$-DMSO) δ 2.45 (s, 3H), 2.46 (s, 3H), 13.1 (br s, 1H). ^{13}C NMR (*d*$_6$-DMSO) δ 18.1 (CH_3), 20.0 (CH_3), 114.9 (C), 116.0 (C), 119.3 (C), 151.0 (C), 154.0 (C), 175.6 (C).

2-Chloro-*N*-cyclopropylacetamide (17).[18]

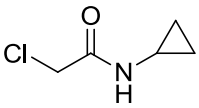

N-Cyclopropylamine (8.25 mmol) and triethylamine (1.26 mL, 9.08 mmol) was dissolved in dichloromethane (5-10 mL) under nitrogen and cooled to -2 to -5 °C in an ice/acetone bath. Chloroacetyl chloride (656 µL, 8.25 mmol) dissolved in dichloromethane (3 mL) was added dropwise to the mixture and a vigorous reaction occurred with a precipitate forming. The mixture was allowed to stir for 30 min at 0 °C and was then returned to RT and stirred for a further 30 min. The precipitate was then filtered and washed with dichloromethane. The filtrate was washed with 2 M aqueous hydrochloric acid (2 × 5 mL) and brine (2 × 15 mL). The organic layer was then dried over anhydrous sodium sulfate, filtered and concentrated in vacuo which was then recrystallised from dichloromethane/hexane to afford the desired compound (1.52 g, 65%). mp: 83- 84 °C. ^{1}H NMR ($CDCl_3$) δ 0.56-0.60 (m, 2H), 0.81-0.86 (m, 2H), 2.72-2.79 (m, 1H), 4.03 (s, 2H), 6.67 (br s, 1H). ^{13}C NMR ($CDCl_3$) δ 6.5 (CH_2), 22.8 (CH), 42.5 (CH_2), 167.3 (C).

3-Amino-5-chloro-*N*-cyclopropyl-4,6-dimethylthieno[2,3-*b*]pyridine-2-carboxamide hydrochloride (18).[13]

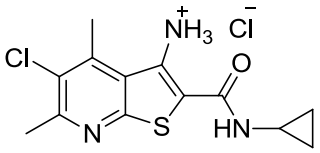

Sodium metal (40 mg, 1.55 mmol), was dissolved in methanol (15 mL) and stirred for 5 minutes. **16** (100 mg, 503 μmol) and **17** (74 mg, 554 μmol) were added to the sodium methoxide solution. The mixture was refluxed for 3 h, then cooled to RT. The solvent was removed by rotary evaporation and the product was purified by silica gel flash column chromatography eluting with a ratio of 2:1 ethyl acetate and hexane to afford the compound as the free base. ^{1}H NMR (d_6-DMSO) δ 0.56-0.62 (m, 2H), 0.62-0.69 (m, 2H), 2.62 (s, 3H), 2.74-2.81 (m, 1H), 2.82 (s, 3H), 6.86 (br s, 2H), 7.83 (d, *J* 3.7 Hz, 1H). ^{13}C NMR (d_6-DMSO) δ 5.7 (CH_2), 16.2 (CH_3), 22.8 (CH), 23.7 (CH_3), 99.6 (C), 124.4 (C), 127.5 (C), 141.8 (C), 147.1 (C), 155.4 (C), 155.8 (C), 166.3 (C). The compound was then converted to the HCl salt using ethereal hydrogen chloride to give the title compound as a bright yellow solid; (50 mg, 30%). mp: 214.5-215.8 °C. HPLC purity (λ= 254 nm): 98% t_R 9.21 min. HRMS (ESI)-TOF (*m/z*): $[M+H]^+$ 296.0624 calcd for $C_{13}H_{14}ClN_3OS$; found $[M+H]^+$ 296.0616.

Synthesis of compound 21.

4-Mercapto-2,6-dimethylpyrimidine-5-carbonitrile (20).[19]

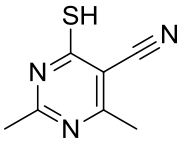

Acetyl chloride (4.34 mL, 61.0 mmol) and ammonium thiocyanate (**19**, 5.08 g, 66.7 mmol) were suspended in dioxane (100 mL) and refluxed for 15 mins. 3-Aminocrotonotrile (10.0g, 122 mmol) was added to the mixture and refluxed for 4 h. The reaction mixture was poured into an ice water mixture (300 mL). No precipitate had formed and the aqueous layer was washed with

ethyl acetate (200 mL). 6 M aqueous HCl solution was added to the aqueous layer to attain a pH of 2-3 and extracted with ethyl acetate (3 × 200 mL). The organic layer was washed with brine (200 mL), dried over anhydrous Na_2SO_4 , filtered and concentrated in vacuo to give the title compound without any further purification (2.29 g, 23%). ^{1}H NMR (d_6-DMSO) δ 2.44 (s, 6H), 3.34 (br s, 1H). ^{13}C NMR (d_6-DMSO) δ 21.5 (CH_3), 23.4 (CH_3), 110.4 (C), 115.7 (C), 136.4 (C), 161.4 (C), 169.1 (C).

5-Amino-*N*-cyclopropyl-2,4-dimethylthieno[2,3-*d*]pyrimidine-6-carboxamide (21).

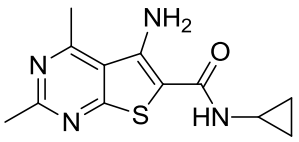

Sodium metal (140 mg, 6.05 mmol) was dissolved in absolute ethanol (25 mL) and stirred for 5 mins. Compound **20** (207 mg, 1.21 mmol) was added to the solution followed by **17** (178 mg, 1.33 mmol). The mixture was refluxed for 4 h. The reaction mixture was cooled to RT and the solvent was removed by rotary evaporation. The product was purified by silica gel flash column chromatography eluted with a gradient of ethyl acetate and petroleum benzene to give the product as a pale yellow solid as the free base (237 mg, 75%). mp: 194.9- 196.6 °C. ^{1}H NMR (d_6-DMSO) δ 0.55-0.60 (m, 2H), 0.62-0.69 (m, 2H), 2.62 (s, 3H), 2.74-2.81 (m, 1H), 2.84 (s, 3H), 6.98 (br s, 2H), 7.87 (d, *J* 3.5 Hz, 1H). ^{13}C NMR (d_6-DMSO) δ 5.8 (CH_2), 22.9 (CH), 23.3 (CH_3), 25.3 (CH_3), 96.8 (C), 120.7 (C), 145.5 (C), 163.1 (C), 164.4 (C), 165.7 (C), 166.1 (C). HPLC purity (λ= 254 nm): 99.5% t_R 5.93 min. HRMS (ESI)-TOF (*m/z*): $[M+H]^+$ 263.0967 calcd for $C_{12}H_{14}N_4OS$; found $[M+H]^+$ 263.0960.

Pharmacology.

ERK1/2 Phosphorylation Assay. FlpIn CHO cells stably expressing the M_4 receptor were seeded into 96-well plates at a density of 30 000 cells/ well. After 5h, cells were washed with phosphate-buffered saline (PBS) and incubated in serum-free DMEM overnight before assaying. Initially, time-course experiments were conducted at least twice for each ligand to determine the time

required to maximally promote ERK1/2 phosphorylation via the dopamine $D_{2L}R$. Interaction studies were performed using varying concentrations of test ligand and increasing concentrations ACh at 37 °C with a stimulation time of 6 minutes. Stimulation of the cells was terminated by removing the media followed by the addition of 100 μL of SureFire lysis buffer (PerkinElmer) to each well. The plate was shaken for 5 min at rt before transferring 5 μL of the lysates to a white 384-well Proxiplate (PerkinElmer). Then, 8 μL of a 240:1440:7:7 mixture of Surefire activation buffer:Surefire reaction buffer:Alphascreen acceptor beads:Alphascreen donor beads was added to the samples and incubated in the dark at 37 °C for 1.5 h. Plates were read using a Fusion-TM plate reader.

[^{3}H]NMS binding assay. FlpIn CHO cells stably expressing the human M_4 receptor were grown and maintained in DMEM containing 10% fetal bovine serum (FBS), and 200 μg/mL of Hygromycin-B. Cells were maintained at 37 °C in a humidified incubator containing 5% CO_2 and 95% O_2.Radioligand binding experiments were performed on whole cells, seeded at 25,000 cells/well and grown overnight at 37 °C. Cells were washed twice with 100 μL of binding buffer (10 mM HEPES, 100 mM NaCl, 10 mM $MgCl_2$, pH 7.4). Assays were performed in a total volume of 100 μl with a 1/10 dilution of drug, for a duration of 4 hours at 4 °C. Assays were terminated by buffer removal followed by rapid washing, twice, with ice-cold 0.9% NaCl (100 μl). OptiPhaseSupermix scintillation cocktail (100 μl) was added, plates were sealed (TopSeal^{TM}), and radioactivity was measured in a MicroBeta^{2}LumiJETmicroplate counter. All inhibition binding experiments were performed with 0.3 nM [^{3}H]NMS (K_D concentration) in presence of increasing concentrations of ACh with required analogues.

Data analysis

Computerized nonlinear regression was performed using Prism 6 (GraphPad Software, San Diego, CA).

Functional experiments measuring the interactions between ACh and allosteric modulators were fitted to an operational model of allosterism and agonism (equation 1) to derive functional estimates of modulator affinity, cooperativity and efficacy. Note that this model assumes the orthosteric agonist is a full agonist both in the presence and absence of allosteric modulators (which was the case in our studies).

$$\text{Response} = \text{Basal} + \frac{(E_m - \text{Basal})([\text{A}](K_B + \alpha\beta[\text{B}]) + (\tau_b[\text{B}][\text{EC}_{50}])}{[\text{EC}_{50}](K_B + [\text{B}]) + ([\text{A}](K_B + \alpha\beta[\text{B}]) + \tau_b[\text{B}][\text{EC}_{50}])} \quad (1)$$

where E_m is the maximum attainable system response for the pathway under investigation; [A] and [B] are the concentrations of orthosteric agonist and allosteric modulator/agonist, respectively; K_B is the dissociation constant of the allosteric modulator; EC_{50} is the concentration of orthosteric (full) agonist yielding 50% of the response between minimal and maximal receptor activation in the absence of allosteric ligand; n is a transducer slope factor linking occupancy to response; α and β are the cooperativity factors governing allosteric effects of the modulator on orthosteric agonist binding affinity and signalling efficacy, respectively; and τ_A and τ_B are operational measures of the ligands' respective signaling efficacies that incorporate receptor expression levels and efficiency of stimulus-response coupling. Statistical comparisons were performed with Prism using a one-way ANOVA followed by Newman-Keuls post test.

Competition binding curves between [^{3}H]NMS and ACh in the absence or presence of allosteric ligands, were fitted to the allosteric ternary complex model (equation 2):

$$Y = \frac{[\text{A}]}{[\text{A}] + \left(\frac{K_A K_B}{\alpha'[\text{B}] + K_B}\right)\left(1 + \frac{[\text{I}]}{K_I} + \frac{[\text{B}]}{K_B} + \frac{\alpha[\text{I}][\text{B}]}{K_I K_B}\right)} \quad (2)$$

where Y is percentage (vehicle control) binding, [A], [B], and [I] are the concentrations of [^{3}H]NMS, modulator and ACh, respectively, K_A and K_B are the equilibrium dissociation constants of [^{3}H]NMS and modulator, respectively, K_B is the equilibrium dissociation constant of the modulator and $\alpha'$and α are the cooperativities (or analogues) between modulator and [^{3}H]NMS or ACh, respectively. Values of α (or α') > 1 denote positive cooperativity; values < 1 (but > 0) denote negative cooperativity, and values =1 denote neutral cooperativity.

References

1. Langmead, C. J.; Watson, J.; Reavill, C. Muscarinic acetylcholine receptors as CNS drug targets. *Pharmacol. Ther.* **2008,** *117*, 232-243.

2. Money, T. T.; Scarr, E.; Udawela, M.; Gibbons, A. S.; Jeon, W. J.; Seo, M. S.; Dean, B. Treating schizophrenia: Novel targets for the cholinergic system. *CNS Neurol. Disord.-Drug Targets* **2010,** *9*, 241-256.

3. Raedler, T. J. The muscarinic hypothesis of schizophrenia: Implications for pharmacological treatment. *Psychiat. Times* **2008,** *25*, 14-15+16.

4. May, L. T.; Leach, K.; Sexton, P. M.; Christopoulos, A. Allosteric modulation of G protein-coupled receptors. *Annu. Rev. Pharmacol. Toxicol.* **2007,** *47*, 1-51.

5. Gregory, K. J.; Sexton, P. M.; Christopoulos, A. Allosteric modulation of muscarinic acetylcholine receptors. *Curr. Neuropharmacol.* **2007,** *5*, 157-167.

6. Keov, P.; Sexton, P. M.; Christopoulos, A. Allosteric modulation of G protein-coupled receptors: A pharmacological perspective. *Neuropharmacology* **2011,** *60*, 24-35.

7. Brady, A. E.; Jones, C. K.; Bridges, T. M.; Kennedy, J. P.; Thompson, A. D.; Heiman, J. U.; Breininger, M. L.; Gentry, P. R.; Yin, H.; Jadhav, S. B.; Shirey, J. K.; Conn, P. J.; Lindsley, C. W. Centrally active allosteric potentiators of the M_4 muscarinic acetylcholine receptor reverse amphetamine-induced hyperlocomotor activity in rats. *J. Pharmacol. Exp. Ther.* **2008,** *327*, 941-953.

8. Kennedy, J. P.; Bridges, T. M.; Gentry, P. R.; Brogan, J. T.; Kane, A. S.; Jones, C. K.; Brady, A. E.; Shirey, J. K.; Conn, P. J.; Lindsley, C. W. Synthesis and structure-activity relationships of allosteric potentiators of the M_4 muscarinic acetylcholine receptor. *ChemMedChem* **2009,** *4*, 1600-1607.

9. Shirey, J. K.; Xiang, Z.; Orton, D.; Brady, A. E.; Johnson, K. A.; Williams, R.; Ayala, J. E.; Rodriguez, A. L.; Wess, J.; Weaver, D.; Niswender, C. M.; Conn, P. J. An allosteric potentiator of M_4 mAChR modulates hippocampal synaptic transmission. *Nat. Chem. Biol.* **2008,** *4*, 42-50.

10. Huynh, T.; Valant, C.; Crosby, I. T.; Sexton, P. M.; Christopoulos, A.; Capuano, B. Probing structural requirements of positive allosteric modulators of the M_4 muscarinic receptor. *J. Med. Chem.* **2013,** *56*, 8196-8200.

11. Lane, J. R.; Sexton, P. M.; Christopoulos, A. Bridging the gap: Bitopic ligands of G-protein-coupled receptors. *Trends Pharmacol. Sci.* **2013,** *34*, 59-66.

12. Mohr, K.; Tränkle, C.; Kostenis, E.; Barocelli, E.; De Amici, M.; Holzgrabe, U. Rational design of dualsteric GPCR ligands: Quests and promise. *Brit. J. Pharmacol.* **2010,** *159*, 997-1008.

13. Le, U.; Melancon, B. J.; Bridges, T. M.; Vinson, P. N.; Utley, T. J.; Lamsal, A.; Rodriguez, A. L.; Venable, D.; Sheffler, D. J.; Jones, C. K.; Blobaum, A. L.; Wood, M. R.; Daniels, J. S.; Conn, P. J.; Niswender, C. M.; Lindsley, C. W.; Hopkins, C. R. Discovery of a selective M_4 positive allosteric modulator based on the 3-amino-

thieno[2,3-*b*]pyridine-2-carboxamide scaffold: Development of ML253, a potent and brain penetrant compound that is active in a preclinical model of schizophrenia. *Bioorg. Med. Chem. Lett.* **2013,** *23*, 346-350.

14. Szabo, M.; Klein Herenbrink, C.; Christopoulos, A.; Lane, J. R.; Capuano, B. Structure–activity relationships of privileged structures lead to the discovery of novel biased ligands at the dopamine D_2 receptor. *J. Med. Chem.* **2014,** *57*, 4924-4939.

15. Kruse, A. C.; Ring, A. M.; Manglik, A.; Hu, J.; Hu, K.; Eitel, K.; Hubner, H.; Pardon, E.; Valant, C.; Sexton, P. M.; Christopoulos, A.; Felder, C. C.; Gmeiner, P.; Steyaert, J.; Weis, W. I.; Garcia, K. C.; Wess, J.; Kobilka, B. K. Activation and allosteric modulation of a muscarinic acetylcholine receptor. *Nature* **2013,** *504*, 101-106.

16. Almudena Rubio Esteban, W. D. H. Thienopyridines as allosteric potentiators of the M_4 muscarinic receptor. WO 2006/047124 A1, May 4th, **2005**.

17. Dyadyuchenko, L. V.; Strelkov, V. D.; Mikhailichenko, S. N.; Zaplishny, V. N., Synthesis of some halogen- and nitro-substituted nicotinic acids and their fragmentation under electron impact. *Chem. Heterocycl. Compd.* **2004,** *40* (3), 308-314.

18. Musso, D. L.; Cochran, F. R.; Kelley, J. L.; McLean, E. W.; Selph, J. L.; Rigdon, G. C.; Orr, G. F.; Davis, R. G.; Cooper, B. R.; Styles, V. L.; Thompson, J. B.; Hall, W. R., Indanylidenes. 1. Design and synthesis of (*E*)-2-(4,6-difluoro-1-indanylidene)acetamide, a potent, centrally acting muscle relaxant with antiinflammatory and analgesic activity. *J. Med. Chem.* **2002,** *46* (3), 399-408.

19. Dagish, M.; Schulze, A.; Claudia, R.; Ludwig, A.; Leistner, S.; Heinicke, J.; Kroedel, A. Substituted carboxamides method for production and use thereof as TNF-alpha release inhibitors. WO2006/100095 24th March, **2006**.

Chapter 3- Structure-Activity Relationships of Privileged Structures Lead to the Discovery of Novel Biased Ligands at the Dopamine D_2 Receptor

Declaration for Thesis Chapter 3

The data presented in Chapter 3 was published as the following paper:

Szabo, M.; Klein Herenbrink, C.; Christopoulos, A.; Lane, J. R.; Capuano, B., Structure–activity relationships of privileged structures lead to the discovery of novel biased ligands at the dopamine D_2 receptor. *J. Med. Chem.* **2014,** *57* (11), 4924-4939.

Declaration by candidate

In the case of Chapter 3, the nature and extent of my contribution to the work was the following:

Nature of contribution	**Contribution (%)**
Design, synthesis, purification, characterisation and pharmacological testing of all analogues. Bias calculations. Main author of manuscript.	85

The following co-authors contributed to the work. Co-authors who are students at Monash University must also indicate the extent of their contribution in percentage terms:

Name	**Nature of contribution**	**Contribution (%)***
Carmen Klein Herenbrink	Testing of aripiprazole in cAMP and pERK1/2 assays. Bias calculations	5
Arthur Christopoulos	Co-author of manuscript	
J. Robert Lane	Co-author of manuscript	
Ben Capuano	Co-author of manuscript	

*Percentage contribution only shown for co-authors who were students at Monash University at the time of their contribution to this work.

Candidate's Signature: [redacted] 01/12/2014

Monika Szabo

Declaration by co-authors

The undersigned hereby certify that:

1. The above declaration correctly reflects the nature and extent of the candidate's contribution to this work, and the nature of the contribution of each of the co-authors.
2. They meet the criteria for authorship in that they have participated in the conception, execution, or interpretation, of at least that part of the publication in their field of expertise;
3. They take public responsibility for their part of the publication, except for the responsible author who accepts overall responsibility for the publication;
4. There are no other authors of the publication according to these criteria;
5. Potential conflicts of interest have been disclosed to (a) granting bodies, (b) the editor or publisher of journals or other publications, and (c) the head of the responsible academic unit; and
6. The original data are stored at the following location(s) and will be held for at least five years from the date indicated below:

   Department of Medicinal Chemistry, Monash Institute of Pharmaceutical Sciences, 381 Royal Parade, Parkville, Victoria, 3052, Australia

Co-author signatures:

Carmen Klein Herenbrink:  01/12/2014

J. Robert Lane: 01/12/2014

Arthur Christopoulos:  01/12/2014

Ben Capuano:  01/12/2014

Journal of Medicinal Chemistry

Article

pubs.acs.org/jmc

Structure–Activity Relationships of Privileged Structures Lead to the Discovery of Novel Biased Ligands at the Dopamine D_2 Receptor

Monika Szabo,[†,‡] Carmen Klein Herenbrink,[‡] Arthur Christopoulos,[‡] J. Robert Lane,*[,‡] and Ben Capuano*[,†]

[†]Medicinal Chemistry and [‡]Drug Discovery Biology, Monash Institute of Pharmaceutical Sciences, Monash University, Parkville 3052, Victoria, Australia

Supporting Information

ABSTRACT: Biased agonism at GPCRs highlights the potential for the discovery and design of pathway-selective ligands and may confer therapeutic advantages to ligands targeting the dopamine D_2 receptor (D_2R). We investigated the determinants of efficacy, affinity, and bias for three privileged structures for the D_2R, exploring changes to linker length and incorporation of a heterocyclic unit. Profiling the compounds in two signaling assays (cAMP and pERK1/2) allowed us to identify and quantify determinants of biased agonism at the D_2R. Substitution on the phenylpiperazine privileged structures (2-methoxy vs 2,3-dichloro) influenced bias when the thienopyridine heterocycle was absent. Upon inclusion of the thienopyridine unit, the substitution pattern (4,6-dimethyl vs 5-chloro-6-methoxy-4-methyl) had a significant effect on bias that overruled the effect of the phenylpiperazine substitution pattern. This latter observation could be reconciled with an extended binding mode for these compounds, whereby the interaction of the heterocycle with a secondary binding pocket may engender bias.

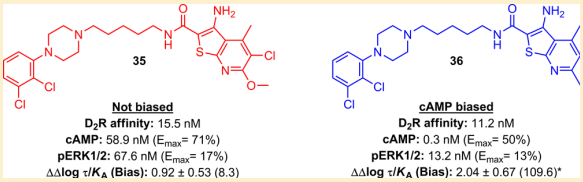

INTRODUCTION

Dopamine receptors (DRs) belong to the G-protein-coupled receptor (GPCR) superfamily that is characterized by seven transmembrane (TM) domains. There are five receptor subtypes (D_1–D_5) expressed both in the central nervous system (CNS) and in the periphery.[1] In the CNS the dopamine D_2 receptor (D_2R) is a primary target for the treatment of disease including Parkinson's and schizophrenia.[2] Antipsychotics have evolved from first generation antipsychotics (FGAs), which act as D_2 antagonists, to second generation antipsychotics (SGAs), which display robust polypharmacology with high affinities for GPCRs in addition to the D_2R.[3−5] Aripiprazole (**1**, Figure 1) is classified as a third generation antipsychotic (TGA). This comes from its unique pharmacological profile, as it is a potent partial agonist at both presynaptic and postsynaptic D_2 receptors while also displaying partial agonist activity at the serotonin 5-HT_{1A} receptor.[6−8] The exploration of D_2R partial agonists for treating schizophrenia was driven by the hypothesis that they would stabilize levels of dopamine in the CNS but avoid the extrapyramidal side effects associated with complete D_2R blockade (for a detailed review of the use of partial agonists in the treatment of schizophrenia and other related psychoactive disorders, see Tamminga et al.[9]). Since the discovery of aripiprazole, other partial agonists have emerged, such as cariprazine (**2**), brexpiprazole (**3**), and bifeprunox (**4**) (Figure 1), with **2** currently awaiting FDA approval and **3** in phase III clinical trials for the treatment of schizophrenia.

Biased agonism (sometimes termed "functional selectivity" or "stimulus bias") refers to the phenomenon by which different agonists acting at the same receptor can stabilize distinct receptor conformations linked to different functional responses.[10−12] Of interest, aripiprazole has been identified as a ligand that displays biased agonism, and evidence has been provided that this bias may contribute to its antipsychotic efficacy.[13] Previous SAR studies, focused on aripiprazole, revealed that small structural changes to the phenylpiperazine core, the linker region, and the bicyclic heterocycle resulted in changes in biased agonism. These studies identified novel D_2R ligands that displayed bias toward the recruitment of β-arrestin.[14,15] Further examples of biased agonists targeting the D_2R have been provided by a number of groups, including Mailman et al. with dihydrexidine,[16,17] Tschammer et al. with 1,4-disubstituted phenylpiperazines,[18] and Shonberg et al. with tetrahydroisoquinoline derivatives.[19]

Privileged structures are often versatile scaffolds that can be functionalized to produce ligands that may be selective for a class of receptors and, more ideally, a single receptor target.[20−23] Privileged structures can be "built in" to a molecule by replacing certain functional groups or can be used as the starting scaffold, where one can "build out" to create an optimized ligand. The aim of the current study was to investigate the structure–activity relationships underlying affinity and efficacy of distinct privileged structures for the

Received: March 24, 2014
Published: May 14, 2014

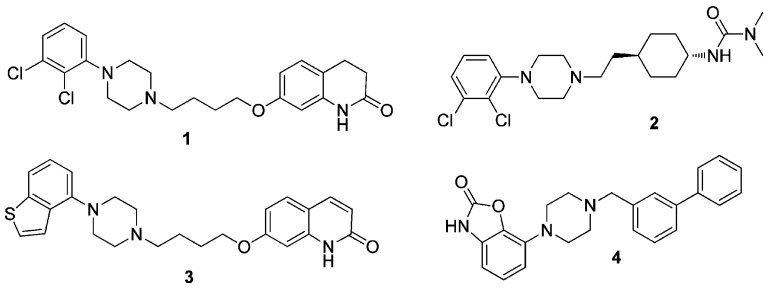

Figure 1. Partial agonists: aripiprazole (**1**), cariprazine (**2**), brexpiprazole (**3**), and bifeprunox (**4**).

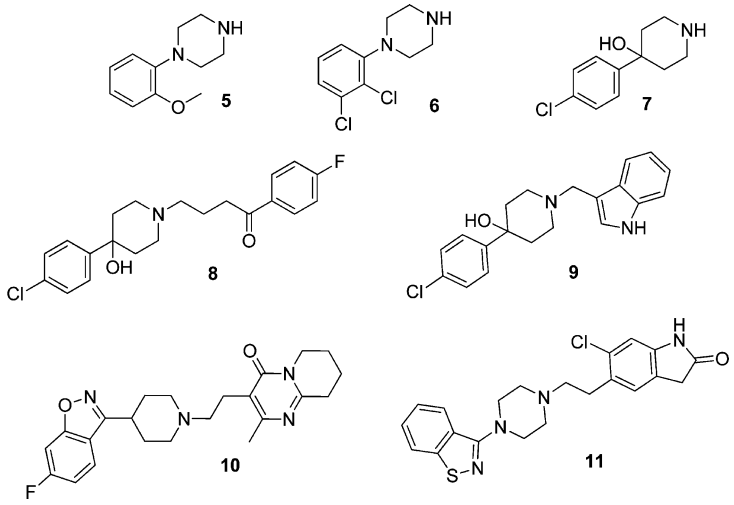

Figure 2. Privileged structures: 2-methoxyphenylpiperazine (**5**), 2,3-dichlorophenylpiperazine (**6**), and 4,4-chlorophenyl-4-hydroxypiperidine (**7**). Antipsychotics and/or potent D_2R antagonists: haloperidol (**8**), L-741,626 (**9**), risperidone (**10**), and ziprasidone (**11**).

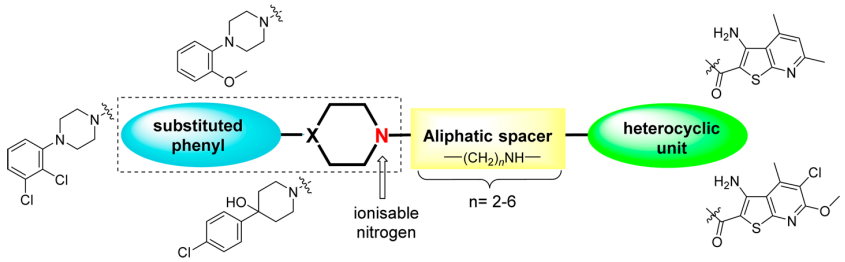

Figure 3. Model pharmacophore for the development of novel D_2R antagonists and/or partial agonists.

D_2R. Many ligands targeting the D_2R incorporate a substituted phenylpiperazine; therefore, we selected 2-methoxyphenylpiperazine (**5**) and 2,3-dichlorophenylpiperazine (**6**) to use as privileged structures in our study (Figure 2). We also investigated 4,4-chlorophenyl-4-hydroxypiperidine (**7**), as it represents a common structural feature of two very potent D_2 antagonists, haloperidol (**8**) and L-741,626 (**9**)[24] (Figure 2). Another structural attribute of many D_2R targeting antagonists and partial agonists is the incorporation of a linker to the ionizable nitrogen, usually from two to five atoms in length followed by a heterocyclic group. For example, the two antipsychotics risperidone (**10**) and ziprasidone (**11**), while devoid of a substituted phenylpiperazine moiety, retain either a piperazine or a piperidine system to bear the ionizable nitrogen, a spacer, and a heterobicyclic group (Figure 2). Such scaffolds have been shown to confer subtype selectivity across the D_2-like receptor subfamily.[25] However, of relevance to this study, Newman and co-workers revealed that the presence of a heterocyclic group, or even the linker alone, could modulate the efficacy of compounds based on **6** in an assay measuring activation of a $G\alpha_{o1}$ G protein. In contrast, an equivalent compound based on **5** displayed no agonism at this assay end point.[26] These observations beg the question whether such structural determinants of efficacy are consistent across different signaling end points or whether they differ and thus engender biased agonism.

In our study, we have synthesized and characterized a focused library of novel D_2R antagonists and partial agonists based on a previously described structural model[27] (Figure 3) incorporating the aforementioned three privileged structures,

dx.doi.org/10.1021/jm500457x | J. Med. Chem. 2014, 57, 4924−4939

Scheme 1. Synthesis of Various Linker Lengths Incorporating Privileged Structures[a]

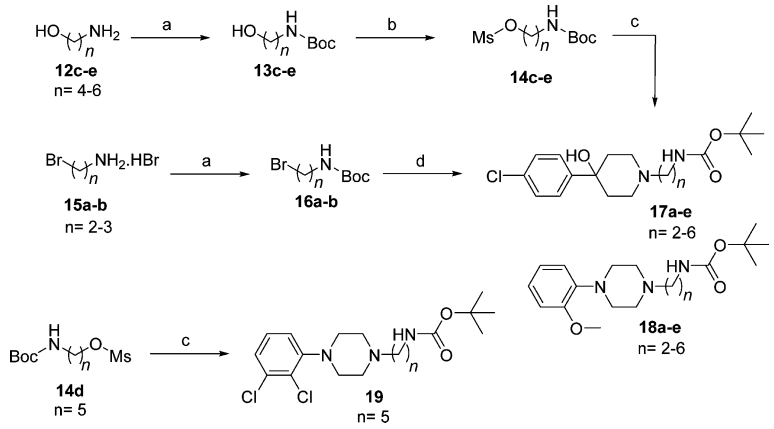

[a]Reagents and conditions: (a) Boc anhydride, Et_3N, DCM, rt, 1−1.5 h, 28−96%; (b) methanesulfonyl chloride, Et_3N, DCM, 0 °C → rt; (c) **5**, **6**, or **7**, CH_3CN, reflux, 24 h, 28−64%; (d) **5** or **7**, NaI, DIPEA, CH_3CN, reflux, 24 h, 34−93%.

Scheme 2. Synthesis of Key Thienopyridine Scaffolds[a]

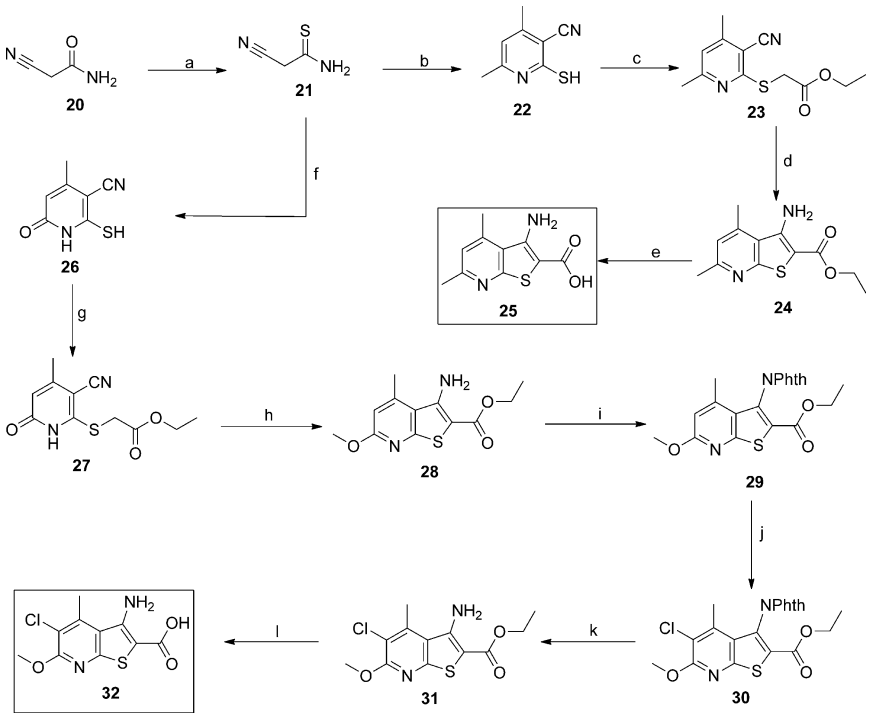

[a]Reagents and conditions: (a) P_4S_{10}, EtOAc, reflux 1.5−4 h, 30%; (b) acetylacetone, KOH, MeOH, reflux, 4 h, 67%; (c) ethyl 2-chloroacetate, Et_3N, 0 °C → rt, 3.5 h, 86%; (d) 1 M KOH, DMF, rt, 15 min, 93%; (e) 2 M NaOH, EtOH, reflux, 4 h, 83%; (f) methyl acetoacetate, morpholine, EtOH, reflux 8 h, 51%; (g) ethyl 2-chloroacetate, Et_3N, DMF, 0 °C → rt, 5 h, 81%; (h) (i) MeI, K_2CO_3, DMF, 4 h, rt; (ii) 1 M KOH, 15 min, 58%; (i) phthalic anhydride, AcOH, reflux, 20 h, 55%; (j) *N*-chlorosuccinimide, conc HCl, EtOH, reflux, 1.5 h, 93%; (k) $(NH_2)_2{\cdot}H_2O$, EtOH, reflux, 3 h, 84%; (l) 2 M NaOH, EtOH, reflux, 1.5 h, 84%.

different spacer lengths (ranging from two to six carbon atoms), and novel heterocyclic units identified from our in-house muscarinic GPCR drug discovery program. These versatile heterocyclic motifs were selected, as they exhibit structural similarities to that of the tetrahydroquinolinone moiety of aripiprazole. Additionally, the use of a thiophene has previously been shown to be advantageous in increasing the affinity for D_2-like receptor subtypes, relating to its electron-rich system and its ability to form hydrophobic interactions within a binding pocket, essentially acting as an isostere of benzene.[28] As such, we envisioned that our thienopyridine scaffolds may also exhibit these properties. The ligands generated were evaluated using in vitro assays to measure their ability to displace [^{3}H]spiperone binding at the D_2R and to stimulate ERK1/2 phosphorylation

dx.doi.org/10.1021/jm500457x | J. Med. Chem. 2014, 57, 4924−4939

through activation of the D_2R. For selected compounds, we extended our characterization to a second functional assay, inhibition of forskolin-induced cAMP production, to allow identification and quantification of biased agonism.[29]

RESULTS AND DISCUSSION

Chemistry. Derivatives of the previously described privileged structures (**5**–**7**) were synthesized utilizing a single linkage point, namely, the aliphatic nitrogen of the piperazine or piperidine, and included chain lengths of two to six carbon atoms (Scheme 1). To furnish derivatives with linker lengths of two to three carbon atoms, we commenced with bromoalkanamines (**15a**,**b**) and subsequently Boc-protected the amines to afford the intermediates **16a**,**b**. These compounds were then reacted with **5** or **7** to give products **17a**,**b** and **18a**,**b** in yields ranging from 34% to 93%. We utilized a modified pathway for generating the required analogues **17c**–**e** and **18c**–**e**, since linker lengths greater than four carbon atoms were not directly available as the bromoalkanamines. Aminoalkanols (**12c**–**e**) with carbon atom spacers of four to six were Boc-protected to give intermediates **13c**–**e** in excellent yields (83–96%). The primary alcohol functionality was activated with methanesulfonyl chloride to generate the mesylated intermediates **14c**–**e**. Because of the reactivity and/or stability of the mesylated compounds, the formation of products was confirmed by the disappearance of starting material via TLC and then reacted immediately without further purification in the next reaction. Subsequent reaction of **5** or **7** with the mesylates **14c**–**e** produced analogues **17c**–**e** and **18c**–**e**. To furnish the five carbon atom spaced Boc protected 2,3-dichlorophenylpiperazine (**19**), the mesylate **14d** was reacted with **6** under the same conditions as described above.

Synthesis of the thienopyridine scaffold is represented in Scheme 2 and commences with reacting 2-cyanoacetamide (**20**) with phosphorus pentasulfide (P_4S_{10}) to afford 2-cyanothioacetamide (**21**) in approximately 30% after recrystallization. To synthesize the 4,6-dimethylthienopyridine compound, **21** was reacted with acetylacetone under basic conditions to form the 4,6-dimethyl substituted pyridine core (**22**) in 67% yield. Subsequent reaction of **22** with ethyl 2-chloroacetate under basic conditions gave the monocyclic ethyl ester (**23**). The monocyclic structure was successfully converted to the bicyclic form (**24**) in rapid time (15 min) in the presence of 1 M aqueous potassium hydroxide. Ester hydrolysis of **24** using 2 M sodium hydroxide in ethanol, followed by acidic workup, gave the first key thienopyridine core carboxylic acid (**25**). To furnish the 5-chloro-6-methoxy-4-methylthienopyridine scaffold, compound **21** was reacted with methyl acetoacetate and morpholine which initially afforded the product as the morpholinium salt. The desired thiol (**26**) was isolated in the free form by acidification with 1 M aqueous hydrochloric acid. Further reaction with ethyl chloroacetate gave the monocyclic ethyl ester (**27**) in good yield (81%). In order to convert the pyridinone into the corresponding pyridine alkyl ether, **27** was reacted with iodomethane under basic conditions. One equivalent of a stronger base, such as 1 M aqueous potassium hydroxide, was necessary to ensure complete conversion to the thienopyridine scaffold (**28**). It was imperative to protect the free amine of the bicycle prior to chlorination at the 5′ position to avoid N-halogenation. Phthalic anhydride was employed under acidic conditions which resulted in the phthalimide-protected product (**29**) in good yield. *N*-Chlorosuccinimide (NCS) was used to install the chlorine atom at the 5′ position to give **30** in excellent yield. Subsequent removal of the phthalimide protecting group using hydrazine monohydrate afforded **31** in excellent yield. Finally, the base-catalyzed ester hydrolysis conditions mentioned earlier were commissioned that, following acidic workup, afforded the key carboxylic acid intermediate compound, **32**.

The syntheses of the target compounds incorporating privileged structures **5**, **6**, and **7** and the thienopyridine scaffolds are summarized in Scheme 3. We initially combined

Scheme 3. Synthesis of Full Length Structures Including Privileged Structures, Linker, and Thienopyridine Scaffold[a]

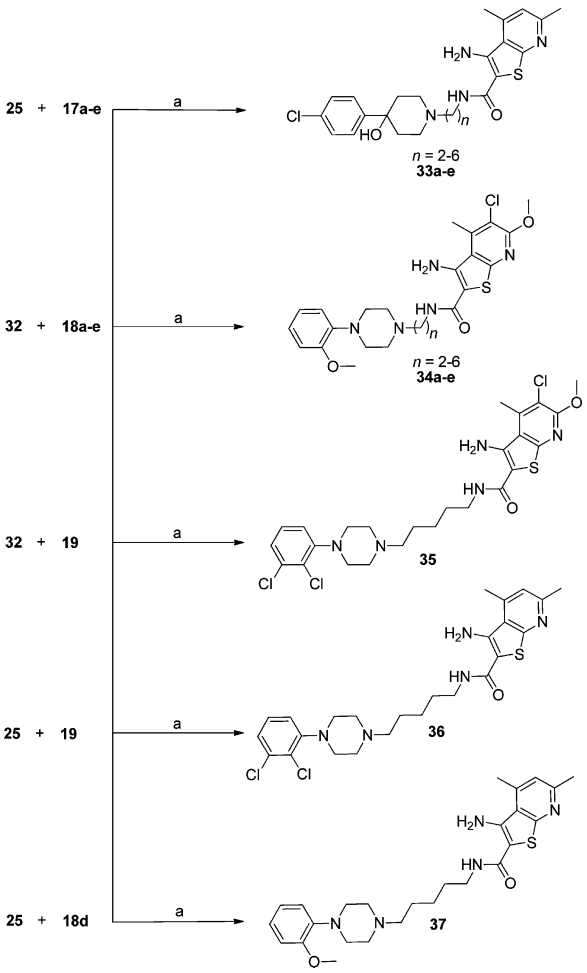

[a]Reagents and conditions: Compounds **17a**–**e**, **18a**–**e**, and **19** were all deprotected prior to performing the coupling reaction. (a) BOP reagent, DIPEA, DMF, rt, 1–12 h, 29–70%.

the 4,4-chlorophenyl-4-hydroxypiperidine analogues (**17a**–**e**), which were deprotected prior to use, with the 4,6-dimethylthienopyridinecarboxylic acid (**25**). This was carried out using a BOP-mediated coupling reaction to give analogues **33a**–**e** in 31–56% yield. Similarly the 2-methoxyphenylpiperazine analogues **18a**–**e** following Boc deprotection were coupled to the carboxylic acid **32** to furnish the target compounds **34a**–**e** in respectable yield. Compound **19**, following removal of the protecting group, was then

dx.doi.org/10.1021/jm500457x | J. Med. Chem. 2014, 57, 4924–4939

immediately reacted with **32** to yield the analogue **35**, while compound **25** furnished analogue **36**. Reaction of the carboxylic acid precursor **25** with **18d** (Boc deprotected) in the presence of BOP also afforded compound **37** in respectable yield.

Pharmacology. *Binding Characterization of Privileged Structures and Linkers.* Both **5** and **6** privileged structures have been evaluated in terms of their ability to bind the D_2R in a previous study.[26] We therefore evaluated the binding affinities of **7**, incorporating linker lengths of two to six carbon atoms and conserving the Boc group for stability purposes and to add lipophilicity to the end of the linker, with equivalent **5** structures as comparators. As expected, both privileged structures (**5** and **7**) demonstrated poor binding affinity (~10 μM, Table 1), most likely because of their small fragment-like size that confers minimal points for contact with residues in the D_2R orthosteric pocket. Modest increases in affinity were observed upon addition of the linkers to 7 (**17a–e**) with the six carbon atom linker (**17e**) conferring a 10-fold increase in affinity. Comparatively, a more pronounced increase in binding affinity was evident for the 2-methoxyphenylpiperazine derivatives (Table 1). Analogues containing a three, four, or five carbon atom linker (**18b–d**) demonstrated enhanced affinity compared to the two carbon atom linker (**18a**), with these analogues displaying a 200-fold increase in affinity compared to **5** alone. However, there seems to be no clear linker length dependence for affinity within this set of compounds **18b–e** (n = 3–6).

Table 1. Binding Data at the Dopamine D_2R for 2-Methoxyphenylpiperazine and 4,4-Chlorophenyl-4-hydroxypiperidine Linker Derivatives[a]

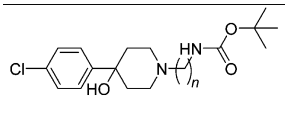

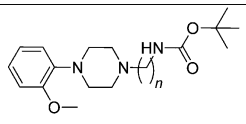

Compound	n	pK_i ± SEM (K_i, nM)	Compound	n	pK_i ± SEM (K_i, nM)
7	-	5.04 ± 0.13 (9090)	**5**	-	5.39 ± 0.08 (4110)
17a	2	5.56 ± 0.08 (2750)	**18a**	2	6.77 ± 0.17 (171)
17b	3	5.87 ± 0.07 (1350)	**18b**	3	7.80 ± 0.27 (16.1)
17c	4	5.68 ± 0.06 (2110)	**18c**	4	7.72 ± 0.17 (18.9)
17d	5	5.69 ± 0.05 (2050)	**18d**	5	7.92 ± 0.24 (12.1)
17e	6	6.05 ± 0.06 (902)	**18e**	6	7.13 ± 0.05 (74.8)

[a]Compounds were tested against [^{3}H]spiperone through competition binding studies using D_{2L} CHO cell membranes. Data represent the mean ± SEM of three separate experiments performed in duplicate.

Binding Characterization of Full-Length Structures. We then investigated the effect of the addition of a heterocyclic group to each of the linkers as indicated in our model pharmacophore (Figure 3). While the substitution pattern on each of the heterocycles listed in Table 2 is different (4,6-dimethyl vs 5-chloro-6-methoxy-4-methyl), the general core of the heterocycle (thienopyridine) is the same. The subtle differences in these substitutions and their consequences on pharmacology at the D_2R will be explored at a later stage in our SAR study. The results in Table 2 showed that analogues based on privileged structure 7 (**33a–e**) bind the D_2R with only moderate affinity (micromolar range) with no significant increase compared to the equivalent linker precursors (Table 1). A similar analogue using privileged structure 7 in combination with the heterocycle present in aripiprazole (dihydroquinolinone) showed poor binding affinity at the D_2R;[30] therefore, this is consistent with our results. Structures incorporating **5** retained their affinity, and in the cases of the two and six carbon atom spacers (**34a** and **34e**), their binding affinities were improved in comparison to their linker precursors (**18a** and **18e**). On this occasion, a definite trend of increasing binding affinity with carbon linker length was evident, with the six carbon atom linker derivative (**34e**) as the standout displaying subnanomolar affinity (K_i = 0.6 nM). This notable enhancement in affinity is supported by literature that describes a secondary hydrophobic pocket in the D_2R that is only reached via longer chain lengths. Interaction with this secondary pocket has been demonstrated to confer both increases in affinity and subtype selectivity.[18,26,31] While we acknowledge that the heterocycles added to these two distinct privileged structures are subtly different, the lack of affinity gain observed for the 4,6-dimethyl substituted thienopyridine derivatives (**33a–e**) is unlikely to be attributed to this difference.

Table 2. Binding Data at the Dopamine D_2R for 2-Methoxyphenylpiperazine and 4,4-Chlorophenyl-4-hydroxypiperidine Full Length Derivatives[a]

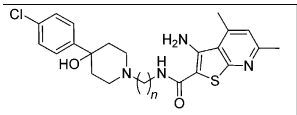

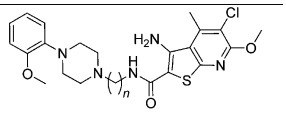

Compound	n	pK_i ± SEM (K_i, nM)	Compound	n	pK_i ± SEM (K_i, nM)
33a	2	6.04 ± 0.10 (910)	**34a**	2	7.32 ± 0.07 (48.3)
33b	3	5.77 ± 0.12 (1700)	**34b**	3	7.71 ± 0.18 (19.5)
33c	4	5.65 ± 0.08 (2250)	**34c**	4	8.20 ± 0.15 (6.3)
33d	5	5.70 ± 0.07 (1980)	**34d**	5	8.45 ± 0.06 (3.5)
33e	6	6.01 ± 0.04 (975)	**34e**	6	9.21 ± 0.03 (0.6)

[a]Compounds are tested against [^{3}H]spiperone through competition binding studies using D_{2L} CHO cell membranes. Data represent the mean ± SEM of three separate experiments performed in duplicate.

SAR of 2-Methoxyphenylpiperazine Linkers and Full Structures: ERK1/2 Phosphorylation Assays. To expand on our initial results with the **5** and **7** series linkers and full structures (Tables 1 and 2), we tested these compounds in functional ERK1/2 phosphorylation (pERK1/2) assays. Analogues **5**, **7**, **17a–e**, **18a–e**, **33a–c**, and **34a–e** at 10 μM were initially tested in time-course assays to identify potential agonists and determine the appropriate peak stimulation time for subsequent construction of concentration–response curves. Compounds derived from 7 displayed no agonism (data not shown). As such, while also considering their poor binding affinities, we did not pursue these compounds for further characterization. Ligands **5**, **18a**, and **18e** were determined to be antagonists (based on time-course data and binding data). They were further analyzed in a pERK1/2 assay for their ability to antagonize a 10 nM concentration of dopamine, to obtain values of inhibitory potency (pIC_{50}) for both compounds. We observed a striking increase in inhibitory potency from the parent molecule **5** (>1000 nM) to compounds containing a linker (**18a**, 93.3 nM; **18e**, 3.98 nM). The remainder of compounds displayed agonism in our time-course experiments (**18b–d**). These analogues exhibited partial agonism, consistent with the observations of Newman et al. using similar linked

Table 3. Functional ERK1/2 Phosphorylation Assays at the Dopamine D_2 Receptor for 2-Methoxyphenylpiperazine Linker Derivatives[a]

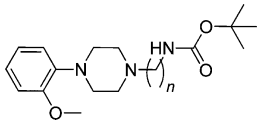

compd	*n*	pIC_{50} ± SEM (IC_{50}, nM)[b]	pEC_{50} ± SEM (EC_{50}, nM)[c]	E_{max} ± SEM (% DA)[d]
5	na	<6 (>1000)		
18a	2	7.03 ± 0.54 (93.3)		
18b	3		9.41 ± 0.15 (0.39)	31 ± 1
18c	4		9.22 ± 0.25 (0.60)	13 ± 1
18d	5		8.84 ± 0.16 (1.43)	19 ± 1
18e	6	8.40 ± 0.29 (3.98)		

[a]Data represent the mean ± SEM of three to four separate experiments performed in duplicate. [b]Values are obtained via interacting ligands with a 10 nM concentration of dopamine. [c]Values are obtained via concentration−response assays at the appropriate stimulation time. [d]E_{max} data are represented as a % of the maximal effect of dopamine (DA).

Table 4. Functional ERK1/2 Phosphorylation Assays at the Dopamine D_2R for Compounds Containing the 2-Methoxyphenylpiperazine Privileged Structure[a]

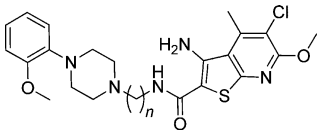

compd	*n*	pK_B ± SEM (K_B, nM)[b]	pEC_{50} ± SEM (EC_{50}, nM)[c]	E_{max} ± SEM (% DA)[d]
5	na	6.32 ± 0.18 (479)		
34a	2	6.45 ± 0.17 (355)		
34b	3	6.13 ± 0.16 (741)		
34c	4	6.31 ± 0.14 (490)		
34d	5		8.57 ± 0.66 (2.69)	17 ± 4
34e	6		8.26 ± 0.31 (5.49)	14 ± 2

[a]Data are the mean of four to five experiments ± SEM. [b]Data are based on interaction studies with varying concentrations of dopamine. Data are fit to the Gaddum−Schild model of competitive antagonism using Graph Pad Prism (version 6) with Schild slopes constrained to 1. [c]Values are attained from concentration−response curves at the appropriate concentration and stimulation time. [d]E_{max} data are represented as a % of the maximal effect of dopamine (DA).

derivatives of **5**[26] (Table 3). The four-carbon atom spacer **18c** has a lower E_{max} (the maximum stimulation achieved as a percentage of the maximal effect of dopamine, E_{max} = 13 ± 1) compared to the five-carbon atom spacer **18d** (E_{max} = 19 ± 1). The three-carbon atom spacer analogue (**18b**) displayed a significantly higher E_{max} of 31 ± 1 ($P < 0.05$). An enhancement of affinity at the D_2R was observed for a similar series of compounds upon addition of alkyl linkers to **5**.[26] We also observed an enhancement of affinity (Table 1) consistent with the hypothesis of Newman et al. whereby this increase in affinity is conferred by additional hydrophobic interactions between residues within the orthosteric pocket of the D_2R and the linker. However, we also observe a gain in agonist efficacy that is dependent on linker length (Table 3). This pattern is distinct from the lack of effect of the addition of a linker to the scaffold of **5** observed by Newman et al. This discrepancy could be due to the subtle differences between the two sets of compounds, the different cell backgrounds used in these experiments, or the different assay end point used to measure agonism (pERK1/2 of our study vs $G\alpha_{o1}$ G protein coupling of Newman et al).

Next we investigated if such linker length dependencies in efficacy are also observed for those compounds with a heterocyclic group attached to the linker. Table 4 represents the functional data for compounds **34a−e** at the D_2R. We identified compounds **34a−c** (linker lengths from two to four carbon atoms) as antagonists and compounds **34d−e** (with linker lengths of five and six carbon atoms, respectively) as partial agonists. This pattern is distinct from the linker only compounds (**18a−e**) in which a linker length of three carbon atoms was optimal in terms of the maximal effect of the agonist. The partial agonists **34d** and **34e** displayed the same maximum response at the D_2R (E_{max}= 17 ± 4 and 14 ± 2, respectively). Moreover, the partial agonism observed in the five carbon atom 2-methoxyphenylpiperazine linker (**18d**, E_{max} = 19 ± 1) was maintained upon incorporation of the heterocyclic group to the linker (**34d**, E_{max} = 17 ± 4). Compounds **34a−c** displayed no gain in functional affinity (pK_B) compared to the parent molecule **5**.

In combination, these data highlight that subtle changes to the linker length appear to be important in switching between antagonism and partial agonism. Of note, the pattern is different for linker analogues as opposed to the extended structures with a heterocycle group suggesting a different binding mode at the D_2R.

Biased Agonism at the D_2R. The partial agonists **34d** and **34e** displayed similar binding affinity (Table 2) and functional activity (Table 4). The 2,3-dichlorophenylpiperazine moiety

Table 5. Binding Data for Compounds at the D_2R That Incorporate 2,3-Dichlorophenylpiperazine and Have Variations to the Thienopyridine Unit[a]

Compound	Structure	$pK_i \pm SEM$ (K_i, nM)[b]
6	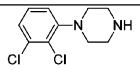	5.94 ± 0.05 (1160)
19	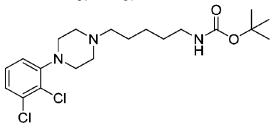	7.37 ± 0.08 (42.6)
35	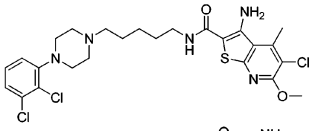	7.81 ± 0.11 (15.5)
36	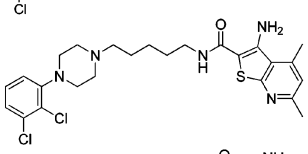	7.95 ± 0.06 (11.2)
37	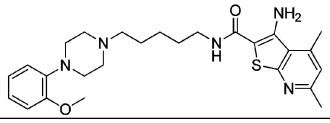	8.04 ± 0.03 (9.1)

[a]Compounds are tested using [^{3}H]spiperone through competition binding studies using D_{2L} CHO cell membranes. [b]Data represent the mean ± SEM of three separate experiments performed in duplicate.

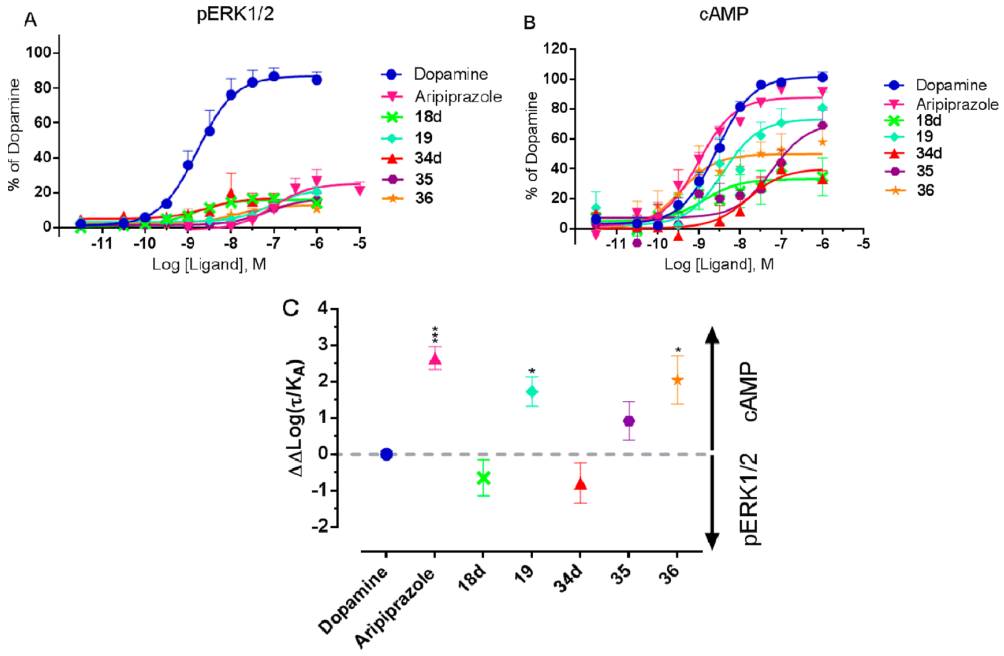

Figure 4. (A) ERK1/2 phosphorylation concentration−response assays. (B) Inhibition of FSK-induced cAMP production. (C) Bias plot representing the bias factor ($\Delta\Delta\log(\tau/K_A)$) of ligands between pERK1/2 and cAMP signaling pathways. Values are represented in Table 6

and the aromatic bicycle of aripiprazole are separated by a five-atom spacer. This is analogous to the five carbon atom spacer separating the substituted thienopyridine and the 2-methoxyphenylpiperazine motif of compound **34d**. Therefore, we decided to further investigate **34d** based upon its linker length and structural similarity to aripiprazole. In particular, given that a number of studies have described aripiprazole as a biased agonist,[8,13] we extended our characterization of a limited number of compounds to activity at two assay end points, ERK1/2 phosphorylation and inhibition of forskolin stimulated cAMP production. In order to gain some preliminary SAR around this compound, we synthesized a small number of compounds related to **34d**. We retained the five-carbon atom linker for all derivatives and instead focused on subtle structural

Table 6. Calculated Bias Factors and Functional Affinities for Selected Full Agonists and Partial Agonists at the Dopamine D_{2L} Receptor

		Inhibition of FSK-induced cAMP production[a]				ERK1/2 phosphorylation[a]				
Agonist	Structure	pK_A	logτ	Log τ/K_A	Δlog τ/K_A	pK_A	logτ	Log τ/K_A	Δlog τ/K_A	$\Delta\Delta$log τ/K_A (Bias)[b]
Dopamine	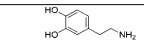	-	-	8.56 ± 0.07	0.00 ± 0.10	7.98 ± 0.18	0.79 ± 0.15	8.72 ± 0.05	0.00 ± 0.05	0.00 ± 0.09
Aripiprazole	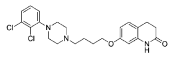	8.05 ± 0.29	0.82 ± 0.25	8.88 ± 0.13	0.32 ± 0.15	6.84 ± 0.33	-0.43 ± 0.10	6.39 ± 0.29	-2.33 ± 0.29	2.65 ± 0.33 (446.7)***
18d	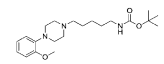	7.06 ± 0.27	0.19 ± 0.13	7.26± 0.21	-1.30 ± 0.22	8.77 ± 0.47	-0.67 ± 0.12	8.07 ± 0.45	-0.65 ± 0.45	-0.65 ± 0.50 (0.2)
19	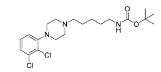	7.73 ± 0.26	0.43 ± 0.16	8.17 ± 0.16	-0.39 ± 0.17	7.14 ± 0.43	-0.51 ± 0.15	6.60 ± 0.37	-2.12 ± 0.37	1.73 ± 0.40 (53.7)*
34d	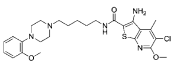	7.47 ± 0.43	-0.26 ± 0.18	7.23 ± 0.33	-1.33 ± 0.34	8.86 ± 0.48	-0.65 ± 0.13	8.18 ± 0.45	-0.54 ± 0.45	-0.79 ± 0.56 (0.2)
35	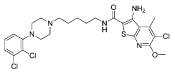	6.89 ± 0.32	0.28 ± 0.20	7.18 ± 0.18	-1.38 ± 0.19	7.10 ± 0.59	-0.65 ± 0.20	6.42± 0.50	-2.30 ± 0.50	0.92 ± 0.53 (8.3)
36	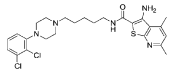	9.00 ± 0.29	-0.06 ± 0.11	8.96 ± 0.26	0.40 ± 0.27	7.90 ± 0.69	-0.78 ± 0.18	7.08 ± 0.62	-1.64 ± 0.62	2.04 ± 0.68 (109.6)*
37	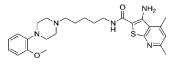	8.84 ± 0.39	-0.42 ± 0.13	8.45 ± 0.36	-0.11 ± 0.37	ND	ND	ND	ND	-

[a]Data are the mean of $n = 4$ experiments ± SEM. ND: no agonist activity detected. [b]Bias is defined as the fold bias relative to the reference agonist dopamine: (*) $P < 0.05$, (***) $P < 0.001$, significantly different from the reference agonist dopamine determined by a one-way ANOVA, Tukey post hoc test.

changes to the phenylpiperazine scaffold and the aromatic heterocyclic unit (thienopyridine scaffold). We utilized the 2,3-dichlorophenylpiperazine moiety present in aripiprazole and attached a five carbon atom spacer with the Boc appendage to generate ligand **19**. This compound was used as a comparator to compound **18d** which contains the same spacer but with the 2-methoxyphenylpiperazine moiety. We subsequently replaced the 2-methoxyphenylpiperazine moiety of **34d** with the 2,3-dichlorophenylpiperazine moiety to generate the target compound **35**. We also synthesized a further two analogues incorporating the simplified 4,6-dimethylthienopyridine to explore whether substitution around the thienopyridine core engendered an influence on bias. These structural motifs were combined with **6** and **5** to give **36** and **37**, respectively.

The new structures (**19** and **35**−**37**) were first tested in a binding assay to measure their biochemical affinity for the D_2R (Table 5). Compound **6** displayed a micromolar binding affinity for the D_2R similar to that of the other two privileged structures (**5** and **7**). A small but significant (3-fold) increase in affinity was observed upon addition of a heterocyclic unit (compounds **35** and **36**) to the linker derivative of **6**, compound **19** ($P < 0.05$). There is, however, no difference in the binding affinities of compounds **35**−**37**.

Given that the new set of analogues all exhibited noteworthy binding affinities (42.6−9.1 nM) for the D_2R, we extended our characterization to functional assays. Compounds **18d**, **19**, **34d**, **35**−**37**, the reference agonist dopamine, and control ligand aripiprazole were tested in pERK1/2 and cAMP (inhibition of forskolin-induced cAMP production) signaling pathways (Figure 4A and Figure 4B). We utilized a derivation of the operational model of agonism[32] to quantify bias by determining a transduction coefficient, log(τ/K_A), for all ligands at both pathways.[11] This transduction coefficient is a descriptor of the agonist effect of a single pathway that takes into account the intrinsic efficacy (τ) of the compound and its affinity (K_A) for the receptor coupled to that signaling pathway. The results from performing these analyses are summarized in Table 6 and displayed in Figure 4C. For values of potency (pEC_{50}) and maximal stimulation (E_{max}) for all compounds, see Supporting Information Table 1. We confirmed the biased action of aripiprazole, which displayed a 400-fold bias toward cAMP ($\Delta\Delta\log(\tau/K_A) = 2.65 \pm 0.32$) when compared to our reference agonist dopamine. Ligands **34d** and **35** both displayed no significant bias to either pathway; however, the linker derivative of **6** (**19**) showed a significant bias toward cAMP ($\Delta\Delta\log(\tau/K_A) = 1.73 \pm 0.40$). Conversely, the linker derivative of **5** (**18d**) did not display significantly different bias compared to dopamine. Compound **36** displayed biased agonism toward cAMP ($\Delta\Delta\log(\tau/K_A) = 2.04 \pm 0.67$), a bias profile that is statistically indistinguishable from that of aripiprazole and equates to a 100-fold bias toward the cAMP pathway. Compound **37** did not produce a response in pERK1/2 signaling assays but acted as a partial agonist in the cAMP assay. As such, we were unable to quantify the bias of this compound compared to dopamine. If we compare the transduction coefficient determined in the cAMP assay for **37** ($\log(\tau/K_A) = 8.45 \pm 0.36$) with those determined for **36** (changes in the phenyl substitution), **34d** (changes in the thienopyridine substitution pattern), and **18d** (no heterocyclic group), then compound **37** has a higher $\log(\tau/K_A)$ value in comparison to **34d** and **18d** and is similar to **36**. This means that compound **37** is at least as efficacious in the cAMP assay as compounds **34d**, **18d**, and **36** and suggests that compound **37** may also be a biased ligand. However, it is important to note that of all the

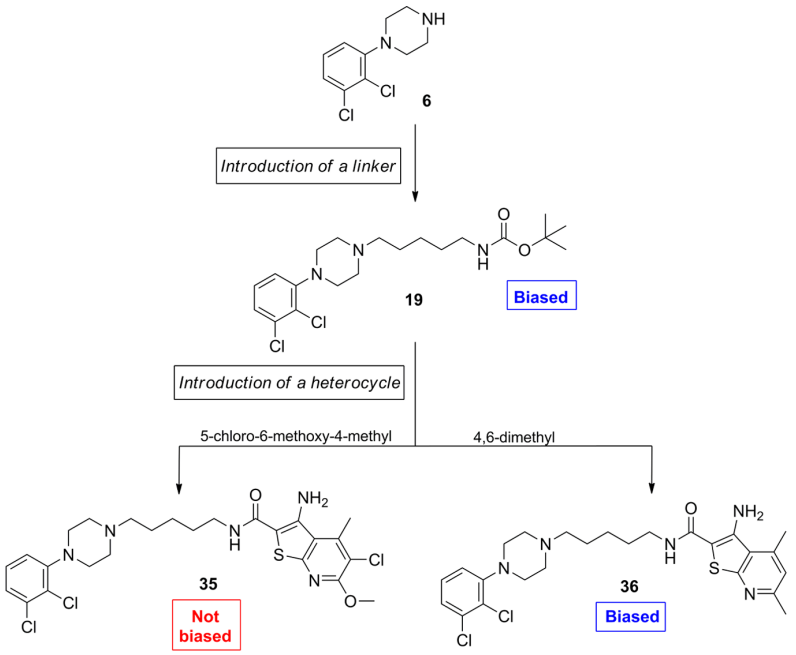

Figure 5. Progression of functionalizing privileged structure **6** with a linker (**19**) and substituted thienopyridine heterocycles (**35**, **36**).

compounds, **37** displays the lowest maximal effect (E_{max} = 33 ± 5) in the cAMP assay (Supporting Information Table 1). It is therefore possible that compound **37** is not a biased ligand relative to dopamine but that its action in the pERK1/2 assay was too weak to be detected.

Table 6 illustrates that the 2,3-dichlorophenylpiperazine derivative containing the *tert*-butylcarbamate five-carbon linker (**19**) is biased toward the cAMP pathway. Altering the substitution pattern on the phenyl ring from 2,3-dichloro to 2-methoxy gives compound **18d** that exhibits no bias for either the cAMP or pERK1/2 end points, thus highlighting that the substitution pattern on the phenylpiperazine moiety can itself confer differences in bias. Substitution around the phenyl ring on the phenylpiperazine moieties also seems to be important for bias for compounds that incorporate a tail heterocycle (**34d** versus **36**). Differences between 2-methoxyphenylpiperazine- and 2,3-dichlorophenylpiperazine-substituted analogues could be attributed to the electronic effects of these substituents, i.e., weakly inductively electron-withdrawing (-Cl) compared to moderately electron-donating (-OCH_3). Tschammer et al. also provided evidence that differential substitution of the phenyl moiety of phenylpiperazine ligands can modulate biased agonism at the D_2R.[18] Such observations are an extension of those made by Newman et al. whereby measuring G protein activation by the D_2R revealed that addition of linkers of different length and/or tail heterocyclic groups modulated agonist efficacy for derivatives of **6** whereas derivatives of **5** displayed no agonism.[26] However, replacing the 2-methoxyphenylpiperazine moiety on **34d** with **6** to give **35** does not produce significant biased agonism when compared to the reference agonist dopamine. If we simplify the thienopyridine core by altering the 5-chloro-6-methoxy-4-methyl substitution pattern with that of the 4,6-dimethyl substitution to give compound **36**, the biased agonism profile is recapitulated. This suggests that (1) the signaling pathway bias does not simply arise from the 2,3-dichlorophenylpiperazine moiety and (2) the substitution of the thienopyridine core has an important role in determining the bias profile of such compounds. The influence of the addition of a heterocycle upon both ligand affinity and efficacy suggests that this heterocycle makes an interaction with the D_2R. Newman et al. provided evidence of a secondary binding pocket that was exploited by extended phenylpiperazine ligands to gain subtype selectivity and modulate ligand efficacy.[26] It is tempting to speculate that our novel extended phenylpiperazine derivatives interact with an analogous secondary binding pocket and the nature of this interaction influences biased agonism.

Taking advantage of the partial agonism displayed by the compounds in this study, we were able to determine values of functional affinity (K_A) and efficacy (τ) as separate parameters rather than the composite transduction coefficient (log τ/K_A) (Table 6). By doing this, we can observe which of these parameters might be important drivers for signal bias at the D_2R. First, if we compare our partial agonists in Table 6, there are no significant differences between the ligands in terms of functional affinity (pK_A) in the pERK1/2 signaling pathway or efficacy (τ) at both pathways. However, in the cAMP signaling pathway, compound **36** exhibits a functional affinity that is significantly different from analogues **18d**, **34d**, and **35** (P < 0.05). As such, the distinct bias profile displayed by compound **36** is largely driven through a change in functional affinity at the cAMP assay. This is consistent with the findings of an SAR exploration of biased agonsim at the D_2R focused on cariprazine.[19] It is also of interest to compare the different parameters of compound **36** with that of aripiprazole. Both have very similar scaffolds and display a bias profile that is not statistically different. Although both have a similar transduction coefficient in the cAMP assay, compound **36** has a 10-fold higher functional affinity but a 10-fold lower efficacy at this pathway compared to aripiprazole. Similarly, in the pERK1/2 end point, compound **36** displays a 10-fold higher functional affinity than aripirazole but a smaller value of efficacy (τ).

As previously mentioned in the Introduction, aripiprazole has a high affinity at serotonin receptors, particularly 5-HT_{1A}.[7] Therefore, in light of the structural similarities of aripiprazole with some of our analogues, particularly the biased analogue (**36**), it is worth mentioning that these ligands may also have high affinities at serotonin receptors. As such, the action of these ligands may have an unprecedented complexity of action that should be considered in the characterization of bias not only at the D_2R but also at serotonin receptors as potential dual dopamine−serotonin biased ligands.

We have revealed that the SAR of biased agonism at the D_2R is complex and, depending on the functional scaffold explored, cannot be defined by a single functional group or transformation.[19] The differential bias observed for compounds **18d** and **19** is governed only by the nature of the privileged structure, i.e., **5** or **6**, with the latter conferring bias toward the cAMP assay. For the extended structures, it appears that the 4-methyl-5-chloro-6-methoxy substitution pattern on the thienopyridine scaffold (**34d** and **35**) engenders no bias irrespective of the privileged structure used. However, the 4,6-dimethyl substitution pattern on the thienopyridine motif appears to confer bias regardless of the privileged structure implemented (**36**) (Figure 5). Therefore, for these compounds, this suggests that the bias is driven primarily by the thienopyridine heterocycle and more specifically the substitution pattern upon this heterocycle whereby the influence of the privileged structure is overridden.

■ CONCLUSION

We explored the determinants of efficacy and affinity for three distinct privileged structures for the D_2R. The privileged structure **7** showed little gain in affinity in both the precursors containing the linkers (**17a−e**) and also the extended structures incorporating an additional thienopyridine heterocycle (**33a−e**). Focusing on the privileged structure **5**, we confirm that the addition of linker groups resulted in a gain in affinity (**18a−e**, Table 1) and in efficacy (Table 3). In particular, we observed a linker length relationship with efficacy with three to five carbon atoms engendering partial agonism (**18b−d**). Inclusion of a heterocyclic structure (**34a−e**) resulted in a different pattern of linker length dependent efficacy, as only extended compounds containing linker lengths of five and six carbon atoms (**34d−e**) exhibited partial agonism. It is therefore likely that compounds that possess only the linker component bind the D_2R in a different orientation to the extended structures incorporating a thienopyridine motif. Extending our studies around the novel partial agonist **34d**, we generated a focused set of compounds that explored the SAR around the two privileged structures **5** and **6**. Of note is that not only can the type of substitution on the phenylpiperazine influence bias, the substitution on the thienopyridine scaffold can have dramatic effects on bias to the point whereby the type of privileged structure used is no longer the principal driver of bias. This observation is consistent with the interaction of the thienopyridine scaffold with a secondary pocket previously identified to interact with other extended D_2R ligands. Our findings suggest that the nature of this interaction confers bias at the D_2R receptor. Our novel D_2R partial agonists **35** and **36** display a similar affinity for the D_2R as aripiprazole but exhibit distinct bias profiles. As such, they may represent useful tools to explore the contribution of biased agonism to antipsychotic efficacy.

■ EXPERIMENTAL SECTION

Chemistry. All solvents and chemicals were purchased from standard suppliers and were used without any further purification. ^{1}H NMR and ^{13}C NMR spectra were acquired at 400.13 and 100.62 MHz, respectively, on a Bruker Advance III 400 MHz Ultrashield Plus NMR spectrometer using TOPSPIN 2.1 software. Chemical shifts (δ) for all ^{1}H spectra are reported in parts per million (ppm) using tetramethylsilane (TMS, 0 ppm) as the reference. The data for all spectra are reported in the following format: chemical shift (δ), (multiplicity, coupling constants J (Hz), integral), where the multiplicity is defined as s = singlet, d = doublet, t = triplet, q = quartet, p = pentet, and m = multiplet. For ^{13}C NMR spectra C = quaternary carbon, CH = methine carbon, CH_2 = methylene carbon, and CH_3 = methyl carbon.

The purity and retention time of final products were determined on an analytical reverse-phase HPLC system fitted with a Luna C8 (2) 100 Å column (50 mm × 4.60 mm, 5 μm) using a binary solvent system: solvent A of 0.1% TFA/H_2O; solvent B of 0.1% TFA/80% MeOH/20% H_2O. Gradient elution was achieved using 100% A for 10 min, 20% A and 80% B over 2 min, and 100% A over 10 min at a flow rate of 1 mL/min monitored at 214 nm using a Waters 996 photodiode array detector.

Thin layer chromatography (TLC) was carried out routinely on silica gel $60F_{254}$ precoated plates (0.25 mm, Merck). Flash column chromatography was carried out using Merck silica gel 60, 230−400 mesh ASTM. Melting points were determined using an electronic MP50 melting point system by Mettler Toledo analytical 2009 and are uncorrected.

Synthesis of Linkers. General Procedure A. The required aminoalkanol **12c−e** (1 equiv) was added to 10−30 mL of dichloromethane. Di-*tert*-butyl dicarbonate (1 equiv) was then added followed by dropwise addition of triethylamine (1.1 equiv) at room temperature. The reaction mixture was stirred for 1 h. After this time, the solvent was removed in vacuo and the resulting oil purified via column chromatography (ethyl acetate).

***tert*-Butyl (4-Hydroxybutyl)carbamate (13c).** **12c** (0.41 mL, 4.49 mmol) and di-*tert*-butyl dicarbonate (979 mg, 4.49 mmol) were added to dichloromethane (10 mL). Triethylamine (0.69 mL, 4.94 mmol) was added dropwise and the mixture stirred for 1 h at room temperature and worked up according to general procedure A. Purification gave the product as a pale yellow oil (809 mg, 95%). ^{1}H NMR ($CDCl_3$): δ 1.44 (s, 9H), 1.53−1.62 (m, 4H), 2.52 (br s, 1H, OH), 3.14 (m, 2H), 3.65 (m, 2H), 4.78 (br s, 1H, NH). ^{13}C NMR ($CDCl_3$): δ 26.7 (CH_2), 28.5 (CH_3), 29.8 (CH_2), 40.4 (CH_2), 62.3 (CH_2), 79.2 (C), 156.3 (C).

General Procedure B. The required bromoalkanamine **15a,b** (1.1 equiv) was added to 20−30 mL of dichloromethane. Di-*tert*-butyl dicarbonate (1 equiv) was then added followed by dropwise addition of triethylamine (1.1 equiv) at room temperature. The reaction mixture was stirred for 1−1.5 h. After this time, an additional 20 mL of dichloromethane was added and the reaction mixture was washed with 3 × 50 mL portions of saturated potassium hydrogen sulfate solution. The organic layer was then dried over anhydrous sodium sulfate, filtered and the solvent removed to afford the crude product. Further purification of the product was achieved via column chromatography (9:1 petroleum spirits/ethyl acetate).

***tert*-Butyl (2-Bromoethyl)carbamate (16a).** **15a** (1.50 g, 7.32 mmol) and di-*tert*-butyl dicarbonate (1.45 g, 6.66 mmol) were added to dichloromethane (20 mL). Triethylamine (1.02 mL, 7.32 mmol) was added dropwise and the mixture stirred for 1.5 h at room temperature and worked up according to general procedure B to give the product as a colorless oil (413 mg, 28%). ^{1}H NMR ($CDCl_3$): δ 1.45 (s, 9H), 3.45 (m, 2H), 3.53 (m, 2H), 5.01 (br s, 1H, NH). ^{13}C NMR ($CDCl_3$): δ 28.5 (CH_3), 32.9 (CH_2), 42.5 (CH_2), 80.0 (C), 155.7 (C).

Coupling of Linkers with Privileged Structures 5, 6, and 7. General Procedure C. To a solution of **5** or **7** (1 equiv) in acetonitrile (30 mL) at room temperature under N_2 were added sodium iodide (1 equiv) and *N*,*N*-diisopropylethylamine (2 equiv).

The required Boc protected amines **16a,b** (1.1−1.5 equiv) were dissolved in 1−2 mL of acetonitrile and added slowly to the reaction mixture which was then heated at reflux for 24 h. The reaction was then concentrated in vacuo and the resulting residue partitioned between ethyl acetate (50 mL) and 1 M potassium carbonate (50 mL). The organic layer was removed, and the aqueous layer was further extracted with 2 × 50 mL portions of ethyl acetate. The organic fractions were pooled, washed with water (50 mL), brine (50 mL), dried over anhydrous sodium sulfate, and filtered and the solvent was removed to afford the crude product. Purification is achieved by column chromatography as indicated.

General Procedure D. The Boc protected aminoalkanol **13c−e** (1 equiv) was added to dichloromethane (5 mL). Triethylamine (3 equiv) was added and the reaction mixture cooled to 0 °C via an ice bath. Methanesulfonyl chloride (2 equiv) was then added slowly, and stirring continued for 30 min at 0 °C. After this time the temperature was warmed to room temperature and stirring continued for 1−12 h. The reaction mixture is then diluted with dichloromethane (10 mL), washed with water (3 × 15 mL), dried over anhydrous sodium sulfate, filtered and the solvent removed in vacuo. The mesylates were then reacted immediately with **5**, **6**, or **7** (2−2.5 equiv) in acetonitrile (5 mL) and heated at reflux for 8−24 h. The solvent was then removed in vacuo and the resulting residue redissolved in dichloromethane and washed with saturated sodium bicarbonate (3 × 20 mL). The organic layer was then dried over anhydrous sodium sulfate, filtered, and evaporated to dryness to give the crude product. Further purification was achieved by column chromatography as indicated.

***tert*-Butyl (2-(4-(4-Chlorophenyl)-4-hydroxypiperidin-1-yl)-ethyl)carbamate (17a).** **7** (300 mg, 1.21 mmol), sodium iodide (181 mg, 1.21 mmol), and *N*,*N*-diisopropylethylamine (0.21 mL, 1.21 mmol) were added to acetonitrile (30 mL) at room temperature under N_2. **16a** (350 mg, 1.56 mmol) was then combined with acetonitrile (2 mL) and added slowly to the reaction mixture (full amount added after 1.5 h). After 6 h of reflux, the reaction mixture was worked up as described in general procedure C to give the product as a white foam (348 mg, 81%). Mp: 129.8−131.1 °C. ^{1}H NMR ($CDCl_3$): δ 1.46 (s, 9H), 1.71−1.75 (m, 2H), 2.11 (td, *J* 13.2, 4.3 Hz, 2H), 2.46−2.55 (m, 4H), 2.79 (m, 2H), 3.26 (m, 2H), 5.02 (br s, 1H, NH), 7.31 (m, 2H), 7.44 (m, 2H). ^{13}C NMR ($CDCl_3$): δ 28.6 (CH_3), 38.5 (CH_2), 40.7 (CH_2), 49.4 (CH_2), 57.4 (CH_2), 71.1 (C), 79.4 (C), 126.3 (CH), 128.6 (CH), 133.0 (C), 147.0 (C), 156.1 (C). HPLC purity (λ = 214 nm): 97%, t_R = 7.68 min. HRMS (ESI) TOF (*m*/*z*): $[M + H]^+$ 355.1788 calcd for $C_{18}H_{27}ClN_2O_3$; found $[M + H]^+$ 355.1796.

***tert*-Butyl (6-(4-(4-Chlorophenyl)-4-hydroxypiperidin-1-yl)-hexyl)carbamate (17e).** **7** (292 mg, 1.38 mmol) was added to acetonitrile (5 mL) followed by dropwise addition of **14e** (204 mg, 0.691 mmol). Reflux occurred overnight, and then the reaction mixture was worked up as described in general procedure D to give the product as a white foam (183 mg, 64%). Mp: 64.4−65.7 °C. ^{1}H NMR ($CDCl_3$): δ 1.32−1.35 (m, 4H), 1.44 (s, 9H), 1.48 (m, 2H), 1.54 (m, 2H), 1.73 (m, 2H), 2.15 (m, 2H), 2.39−2.45 (m, 4H), 2.84 (m, 2H), 3.1 (m, 2H), 4.53 (br s, 1H, NH), 7.31 (m, 2H), 7.45 (m, 2H). ^{13}C NMR ($CDCl_3$): δ 26.8 (CH_2), 27.0 (CH_2), 27.4 (CH_2), 28.6 (CH_3), 30.2 (CH_2), 38.5 (CH_2), 40.7 (CH_2), 49.6 (CH_2), 58.9 (CH_2), 71.2 (C), 79.2 (C), 126.3 (CH), 128.6 (CH), 132.9 (C), 147 (C), 156.2 (C). HPLC purity (λ = 214 nm): 95%, t_R = 8.77 min. HRMS (ESI) TOF (*m*/*z*): $[M + H]^+$ 411.2414 calcd for $C_{22}H_{35}ClN_2O_3$; found $[M + H]^+$ 411.2429.

***tert*-Butyl (3-(4-(2-Methoxyphenyl)piperazin-1-yl)propyl)-carbamate (18b).** **5** (200 mg, 0.87 mmol) and *N*,*N*-diisopropylethylamine (0.15 mL, 1.87 mmol) were added to acetonitrile (5 mL) and stirred at room temperature under N_2 for 2 min to generate the free amine. Sodium iodide (131 mg, 0.87 mmol) and additional *N*,*N*-diisopropylethylamine (0.15 mL, 1.87 mmol) were then also added. **16b** (280 mg, 1.18 mmol) was then combined with acetonitrile (2 mL) and added slowly to the reaction mixture. After heating at reflux for 24 h, the reaction mixture was worked up as described in general procedure C and purified via a silica plug (ethanol) to give the product as a colorless oil (286 mg, 93%). ^{1}H NMR ($CDCl_3$): δ 1.44 (s, 9H), 1.70 (p, *J* 6.6 Hz, 2H), 2.49 (t, *J* 6.8 Hz, 2H), 2.65 (m, 4H), 3.10 (m, 4H), 3.22 (m, 2H), 3.86 (s, 3H), 5.49 (br s, 1H, NH), 6.85−7.02 (m, 4H). ^{13}C NMR ($CDCl_3$): δ 26.5 (CH_2), 28.6 (CH_3), 40.2 (CH_2), 50.8 (CH_2), 53.6 (CH_2), 55.5 (CH_3), 57.1 (CH_2), 78.9 (C), 111.3 (CH), 118.3 (CH), 121.1 (CH), 123.0 (CH), 141.4 (C), 152.4 (C), 156.2 (C). HPLC purity (λ = 214 nm): 99%, t_R = 7.74 min. HRMS (ESI) TOF (*m*/*z*): $[M + H]^+$ 350.2444 calcd for $C_{19}H_{31}N_3O_3$; found $[M + H]^+$ 350.2455.

***tert*-Butyl (5-(4-(2-Methoxyphenyl)piperazin-1-yl)pentyl)-carbamate (18d).** **5** (683 mg, 2.99 mmol) was dissolved in acetonitrile (10 mL) and triethylamine (0.21 mL, 1.49 mmol) and stirred for 5 min. **14d** (420 mg, 1.49 mmol) was then added dropwise to the reaction mixture which was refluxed for 24 h. Workup proceeded as described in general procedure D and the crude product was purified by column chromatography (10% chloroform/methanol−100% acetonitrile) to give a yellow/orange oil (334 mg, 59%). ^{1}H NMR ($CDCl_3$): δ 1.36 (m, 2H), 1.44 (s, 9H), 1.47−1.59 (m, 4H), 2.43 (m, 2H), 2.68 (m, 4H), 3.09−3.15 (m, 6H), 3.86 (s, 3H), 4.63 (br s, 1H, NH), 6.84−7.01 (m, 4H). ^{13}C NMR ($CDCl_3$): δ 24.8 (CH_2), 26.4 (CH_2), 28.5 (CH_3), 40.6 (CH_2), 50.5 (CH_2), 53.4 (CH_2), 55.4 (CH_3), 58.6 (CH_2), 79.1 (C), 111.2 (CH), 118.3 (CH), 121.1 (CH), 123.0 (CH), 141.3 (C), 152.3 (C), 156.1 (C). HPLC purity (λ = 214 nm): 98%, t_R = 8.18 min. HRMS (ESI) TOF (*m*/*z*): $[M + H]^+$ 378.2757 calcd for $C_{21}H_{35}N_3O_3$; found $[M + H]^+$ 378.2768.

***tert*-Butyl (5-(4-(2,3-Dichlorophenyl)piperazin-1-yl)pentyl)-carbamate (19). 6** (1.09 g, 4.07 mmol) was added to acetonitrile (15 mL) followed by **14d** (572 mg, 2.03 mmol) and triethylamine (0.57 mL, 4.07 mmol) and the mixture refluxed for 19 h. Workup proceeded as described in general procedure D and the crude product was purified by column chromatography (chloroform/methanol 99:1) to give a yellow oil (431 mg, 51%). ^{1}H NMR ($CDCl_3$): δ 1.36 (m, 2H), 1.44 (s, 9H), 1.47−1.59 (m, 4H), 2.41 (m, 2H), 2.63 (m, 4H), 3.07 (m, 4H), 3.12 (m, 2H), 4.62 (br s, 1H, NH), 6.96 (m, 1H), 7.12−7.17 (m, 2H). ^{13}C NMR ($CDCl_3$): δ 24.8 (CH_2), 26.6 (CH_2), 28.5 (CH_3), 30.1 (CH_2), 40.6 (CH_2), 51.4 (CH_2), 53.4 (CH_2), 58.6 (CH_2), 79.1 (C), 118.7 (CH), 124.6 (CH), 127.5 (CH), 127.6 (C), 134.1 (C), 151.4 (C), 156.1 (C). HPLC purity (λ = 214 nm): 98%, t_R = 10.43 min. HRMS (ESI) TOF (*m*/*z*): $[M + H]^+$ 416.1872 calcd for $C_{20}H_{31}Cl_2N_3O_2$; found $[M + H]^+$ 416.1870.

Synthesis of Substituted Thienopyridine Scaffolds. 2-Cyanothioacetamide (21). P_4S_{10} (1.00 g, 4.52 mmol) and 2-cyanoacetamide (**20**, 1.00 g, 11.89 mmol) were dissolved in ethyl acetate (12 mL). The mixture was heated at reflux for 1.5−4 h. The reaction mixture was then cooled to room temperature and the orange solid filtered off and washed with ethyl acetate (100 mL). The solid was recrystallized from toluene to give sharp yellow needles (389 mg, ∼30%). ^{1}H NMR (DMSO-d_6): δ 3.98 (s, 2H), 9.48 (s, 1H, NHa), 9.83 (s, 1H, NHb). ^{13}C NMR (DMSO-d_6): δ 33.9 (CH_2), 116.5 (C), 194.5 (C).

4,6-Dimethyl-2-thioxo-1,2-dihydropyridine-3-carbonitrile (22). 2-Cyanothioacetamide (**21**, 1.02 g, 10.2 mmol) and acetylacetone (1.04 mL, 10.2 mmol) were suspended in methanol (10 mL) and warmed until dissolved. Potassium hydroxide (0.75 g) dissolved in methanol (50 mL) was added to the solution, which was stirred for 2 h and then heated at reflux for a further 2 h. The mixture was cooled to room temperature and acidified with 6 M aqueous hydrochloric acid to pH 2−3, and a precipitate resulted. The precipitous mixture was then cooled overnight, filtered, and washed with water. The product was recrystallized from methanol to afford the title compound as yellow needles (1.13 g, 67%). Mp: 266.9−270 °C. ^{1}H NMR (DMSO-d_6): δ 2.34 (s, 3H), 2.35 (s, 3H), 6.69 (s, 1H), 13.83 (br s, 1H). ^{13}C NMR (DMSO-d_6): δ 18.8 (CH_3), 20.8 (CH_3), 113.4 (C), 114.9 (CH), 116.3 (C), 152.6 (C), 156.9 (C), 177.5 (C). HPLC purity (λ = 214 nm): 99%, t_R = 5.56 min.

Ethyl 2-((3-Cyano-4,6-dimethylpyridin-2-yl)thio)acetate (23). Compound **22** (1.00 g, 6.09 mmol) and triethylamine (0.93 mL, 6.70 mmol) were added to *N*,*N*-dimethylformamide (15 mL) and cooled to 0 °C. Ethyl-2-chloroacetate (0.65 mL, 6.09 mmol) was added to 1 mL of *N*,*N*-dimethylformamide and then added dropwise to the reaction mixture. The mixture was then warmed to room temperature for 3.5 h, and a yellow precipitate resulted. The solvent

was then removed and the resulting residue partitioned between dichloromethane (50 mL) and water (50 mL). The organic layer was removed, and the aqueous layer was then washed with further 3 × 50 mL portions of dichloromethane. The organic fractions were combined, dried over anhydrous sodium sulfate, and filtered, and the solvent was removed to leave a yellow solid. Further purification using a silica plug afforded the final compound as a white solid (1.30 g, 86%). ^{1}H NMR (DMSO-d_6): δ 1.17−1.21 (t, J 7.1 Hz, 3H), 2.41 (s, 3H), 2.43 (s, 3H), 4.07 (s, 2H), 4.09- 4.14 (q, J 7.1 Hz, 2H), 7.12 (s, 1H). ^{13}C NMR (DMSO-d_6): δ 14.1 (CH_3), 19.6 (CH_3), 24.2 (CH_3), 32.2 (CH_2), 61.0 (CH_2), 103.6 (C), 114.6 (C), 120.6 (CH), 152.6 (C), 159.7 (C), 161.4 (C), 168.5 (C).

Ethyl 3-Amino-4,6-dimethylthieno[2,3-*b*]pyridine-2-carboxylate (24). **23** (1.29 g, 5.15 mmol) was dissolved in 4−5 mL of *N*,*N*-dimethylformamide followed by 1 M potassium hydroxide (5.15 mL, 5.15 mmol). The reaction mixture was stirred for 15 min at room temperature. Quenching with water (15 mL) caused precipitation of the product that was then filtered to leave a yellow crystalline solid (1.20 g, 93%). Mp: 154.7−155.6 °C. ^{1}H NMR ($CDCl_3$): δ 1.39 (t, J 7.1 Hz, 3H), 2.58 (s, 3H), 2.72 (s, 3H), 4.34 (q, J 7.1 Hz, 2H), 6.14 (br s, 2H, NH_2), 6.84 (s, 1H). ^{13}C NMR ($CDCl_3$): 14.6 (CH_3), 20.3 (CH_3), 24.5 (CH_3), 60.6 (CH_2), 91.2 (C), 121.9 (CH), 122.5 (C), 143.7 (C), 149.1 (C), 159.8 (C), 161.5 (C), 165.9 (C). HPLC purity (λ = 214 nm): 99%, t_R = 8.38 min.

3-Amino-4,6-dimethylthieno[2,3-*b*]pyridine-2-carboxylic Acid (25). To a solution of **24** (1.16 g, 4.62 mmol) in ethanol (15 mL) was added an aqueous solution of sodium hydroxide (2 M, 8 mL), and the mixture was refluxed for 4 h. The solvent was removed in vacuo and the resulting residue dissolved in water (20 mL). Excess aqueous hydrochloric acid (1 M, 10 mL) was added which caused precipitation of the desired compound. Filtration of the precipitate gave the title compound as a yellow solid (856 mg, 83%). Mp: 151.9−152.9 °C. ^{1}H NMR (DMSO-d_6): δ 2.50 (s, 3H), 2.72 (s, 3H), 7.05 (s, 1H). ^{13}C NMR (DMSO-d_6): δ 19.9 (CH_3), 23.4 (CH_3), 95.2 (C), 121.9 (CH), 122.9 (C), 145.8 (C), 149.3 (C), 158.8 (C), 159.0 (C), 166.5 (C).

2-Mercapto-4-methyl-6-oxo-1,6-dihydropyridine-3-carbonitrile (26). A mixture of **21** (8.00 g, 79.89 mmol) and morpholine (6.99 mL, 79.9 mmol) in ethanol (50 mL) was warmed until all components dissolved. Methyl acetoacetate (8.59 mL, 79.9 mmol) was then added and the mixture heated at reflux for 8 h. After cooling to room temperature, the mixture was filtered and the residue washed with cold dichloromethane to give morpholinium 3-cyano-4-methyl-6-oxo-1,6-dihydropyridine-2-thiolate. The desired thiol was isolated by dissolving the thiolate in a minimum amount of water and then acidifying with excess 1 M aqueous hydrochloric acid, which caused precipitation of the molecule. The mixture was refrigerated overnight and then filtered to give the title compound as a pale yellow powder (6.83 g, 51%). Mp: 267−268.9 °C. LRMS (ESI) m/z: 165.1 $[M - H]^+$ (100%).

Ethyl 2-((3-Cyano-4-methyl-6-oxo-1,6-dihydropyridin-2-yl)thio)acetate (27). Compound **26** (200 mg, 1.2 mmol) and triethylamine (0.18 mL, 1.32 mmol) were added to *N*,*N*-dimethylformamide (8 mL) and cooled to 0 °C. Ethyl 2-chloroacetate (0.13 mL, 1.2 mmol) was added to 1 mL of *N*,*N*-dimethylformamide and then added dropwise to the reaction mixture. The mixture was then warmed to room temperature and stirred for 5 h. The solvent was then removed and the resulting residue dissolved in dichloromethane (50 mL) and partitioned between water (50 mL). The aqueous layer was then washed with further 3 × 50 mL portions of dichloromethane, and the organic layers were combined, dried over anhydrous sodium sulfate, and filtered. The solvent was removed to leave a yellow solid. Further purification by column chromatography afforded the final compound as a white solid (247 mg, 81%). Mp: 102.7−103.5 °C. ^{1}H NMR ($CDCl_3$): δ 1.28 (t, J 7.1 Hz, 3H), 2.38 (d, J 0.9 Hz, 3H), 3.93 (s, 2H), 4.23 (q, J 7.1 Hz, 2H), 6.33−6.35 (m, 1H), 11.03 (br s, 1H, NH). ^{13}C NMR ($CDCl_3$): δ 14.1 (CH_3), 20.9 (CH_3), 34.1 (CH_2), 62.8 (CH_2), 98.2 (C), 113.9 (CH), 114.9 (C), 153.4 (C), 154.3 (C), 163.6 (C), 169.6 (C).

Ethyl 3-Amino-6-methoxy-4-methylthieno[2,3-*b*]pyridine-2-carboxylate (28). Compound **27** (1.52 g, 6.02 mmol) was added to *N*,*N*-dimethylformamide (20 mL) followed by potassium carbonate (1.25 g, 9.04 mmol) and methyl iodide (0.41 mL, 6.63 mmol). The reaction mixture was then stirred at room temperature for 2 h before another 0.5−1 equiv of the methyl iodide was added. After 4 h, 1 M aqueous potassium hydroxide is added and the reaction mixture stirred for 15 min. Water (15 mL) is then added and the resulting white precipitate is filtered and dried overnight over high vacuum (0.91 g, 58%). Mp: 149.5−150.2 °C. ^{1}H NMR ($CDCl_3$): δ 1.38 (t, J 7.1 Hz, 3H), 2.68 (d, J 0.9 Hz, 3H), 3.98 (s, 3H), 4.33 (q, J 7.1 Hz, 2H), 6.11 (br s, 2H, NH_2), 6.43 (m, 1H). ^{13}C NMR ($CDCl_3$): δ 14.7 (CH_3), 20.4 (CH_3), 54.0 (CH_3), 60.4 (CH_2), 95.2 (C), 110.0 (CH), 119.4 (C), 145.9 (C), 149.5 (C), 160.6 (C),164.6 (C), 165.9 (C).

Ethyl 3-(1,3-Dioxoisoindolin-2-yl)-6-methoxy-4-methylthieno[2,3-*b*]pyridine-2-carboxylate (29). To a solution of **28** (65 mg, 0.244 mmol) in acetic acid (5 mL), a total of 4 equiv of phthalic anhydride (150 mg, 1.01 mmol) was added over the 20 h period. The reaction was stopped by cooling the mixture to room temperature and then over an ice bath to initiate precipitation of the final product as a white solid (53 mg, 55%). ^{1}H NMR ($CDCl_3$): δ 1.11 (t, J 7.1 Hz, 3H), 2.37 (s, 3H), 4.02 (s, 3H), 4.20 (q, J 7.1 Hz, 2H), 6.59 (s, 1H), 7.83 (m, 2H), 8.00 (m, 2H). ^{13}C NMR ($CDCl_3$): δ 13.9 (CH_3), 18.5 (CH_3), 54.2 (CH_3), 61.7 (CH_2), 112.2 (CH), 124.2 (CH), 124.7 (C), 125.4 (C), 127.6 (C), 132.4 (C), 134.7 (CH), 145.9 (C), 159.1 (C), 161.1 (C), 164.5 (C), 167.6 (C).

Ethyl 5-Chloro-3-(1,3-dioxoisoindolin-2-yl)-6-methoxy-4-methylthieno[2,3-*b*]pyridine-2-carboxylate (30). Compound **29** (500 mg, 1.26 mmol), *N*-chlorosuccinimide (337 mg, 2.52 mmol), and 3 drops of concentrated HCl were refluxed in acetonitrile (10 mL) for 1.5 h. The solvent was then removed in vacuo and the resulting residue redissolved in chloroform (50 mL) and washed with water (3 × 20 mL) and brine (50 mL). The organic layer was then dried over anhydrous sodium sulfate, filtered, and evaporated to dryness to give the compound as a white solid (506 mg, 93%). ^{1}H NMR ($CDCl_3$): δ 1.12 (t, J 7.1 Hz, 3H), 2.49 (s, 3H), 4.13 (s, 3H), 4.21 (q, J 7.1 Hz, 2H), 7.85 (m, 2H), 8.01 (m, 2H). ^{13}C NMR ($CDCl_3$): δ 13.9 (CH_3), 14.7 (CH_3), 55.4 (CH_3), 61.9 (CH_2), 118.8 (C), 124.3 (CH), 125.1 (C), 127.0 (C), 127.4 (C), 132.4 (C), 134.9 (CH), 143.0 (C), 155.9 (C), 159.5 (C), 160.9 (C), 167.6 (C).

Ethyl 3-Amino-5-chloro-6-methoxy-4-methylthieno[2,3-*b*]pyridine-2-carboxylate (31). A mixture of **30** (144 mg, 0.33 mmol) and hydrazine monohydrate (65 μL, 1.34 mmol) in ethanol (10 mL) was refluxed for 3 h. Upon cooling to room temperature, the white precipitate was filtered off and washed with cold chloroform (5 mL). The filtrate was then collected and diluted with a further 20 mL of chloroform and washed with water (3 × 20 mL), dried over anhydrous sodium sulfate, and filtered and the solvent removed in vacuo to give the product as a pale yellow solid (85 mg, 84%). ^{1}H NMR ($CDCl_3$): δ 1.38 (t, J 7.1 Hz, 3H), 2.83 (s, 3H), 4.08 (s, 3H), 4.33 (q, J 7.1 Hz, 2H), 6.14 (br s, 2H, NH_2). ^{13}C NMR ($CDCl_3$): δ 14.6 (CH_3), 16.4 (CH_3), 55.2 (CH_3), 60.6 (CH_2), 116.3 (C), 120.1 (C), 142.9 (C), 149.1 (C), 157.3 (C), 159.5 (C), 165.7 (C), 168.4 (C).

3-Amino-5-chloro-6-methoxy-4-methylthieno[2,3-*b*]pyridine-2-carboxylic Acid (32). Compound **31** (236 mg, 0.783 mmol) was was added to a 50:50 mix of ethanol and 2 M sodium hydroxide. Reflux occurs for 1.5 h before the mixture was cooled to room temperature. An excess of 2 M HCl is added to cause precipitation of the product which is then filtered and washed with a small amount of cold water, giving the product as a beige-yellow solid (179 mg, 84%). ^{1}H NMR (DMSO-d_6): δ 2.77 (s, 3H), 3.96 (s, 3H), 6.41 (br s, 2H, NH_2). LCMS (ESI) m/z: 273.0 $[M + H]^+$ (90%), 275.0 (30%).

General Procedure E for Amide Coupling Reactions Using BOP Reagent. The required carboxylic acids (1 equiv) were added to *N*,*N*-dimethylformamide (10 mL), followed by *N*,*N*-diisopropylethylamine (1.05 equiv) and BOP (1.05 equiv) under N_2 at room temperature and stirred for 5−10 min. The amine (1 equiv) was subsequently added and the reaction mixture stirred at room

temperature for 2−3 h. The solvent was then removed in vacuo and the resulting residue partitioned between dichloromethane (30 mL) and sodium bicarbonate (50 mL). The organic layer was removed, and the aqueous phase was further extracted with 3 × 20 mL portions of dichloromethane. The organic fractions were combined, washed with water (50 mL), brine (50 mL), dried over anhydrous sodium sulfate, filtered, and concentrated to yield the crude product as an oily residue. To remove excess HMPA, crude products are dissolved in ethyl acetate and washed with 3 × 50 mL portions of 2 M brine. Purification of the product was performed by column chromatography and/or recrystalisation as indicated.

3-Amino-*N*-(2-(4-(4-chlorophenyl)-4-hydroxypiperidin-1-yl)-ethyl)-4,6-dimethylthieno[2,3-*b*]pyridine-2-carboxamide (33a). Carboxylic acid **25** (50 mg, 0.225 mmol), *N*,*N*-diisopropylethylamine (0.041 mL, 0.24 mmol), and BOP (104 mg 0.24 mmol) were added to *N*,*N*-dimethylformamide (2 mL). **17a** (92 mg, 0.28 mmol) was dissolved in 2 mL of *N*,*N*-dimethylformamide and *N*,*N*-diisopropylethylamine (0.078 mL, 0.450 mmol) and then added to the reaction mixture. After the mixture was stirred for 16 h at room temperature, the crude product was worked up as per general procedure E to give an amber solid (32 mg, 31%). Mp: 159−163 °C. ^{1}H NMR (DMSO-d_6): δ 1.58 (d, J 12.1 Hz, 2H), 1.91 (td, J 12.9, 4.1 Hz, 2H), 2.44−2.53 (m, 7H), 2.71−2.72 (m, 5H), 3.36 (m, 2H), 4.9 (s, 1H, OH), 6.78 (s, 2H, NH_2), 7.02 (s, 1H), 7.36 (m, 2H), 7.50 (m, 2H), 7.55 (t, J 5.5 Hz, 1H, NH). ^{13}C NMR (DMSO-d_6): δ 19.7 (CH_3), 23.8 (CH_3), 36.7 (CH_2), 37.9 (CH_2), 49.1 (CH_2), 57.2 (CH_2), 69.4 (C), 97.6 (C), 121.8 (CH), 123.2 (C), 126.8 (CH), 127.7 (CH), 130.8 (C), 144.5 (C), 147.5 (C), 149.1 (C), 158.4 (C), 158.5 (C), 165.2 (C). HPLC purity (λ = 214 nm): 98%, t_R = 8.06 min. HRMS (ESI) TOF (m/z): [M + H]$^+$ 459.1621 calcd for $C_{23}H_{27}ClN_4O_2S$; found [M + H]$^+$ 459.1634.

3-Amino-*N*-(6-(4-(4-chlorophenyl)-4-hydroxypiperidin-1-yl)-hexyl)-4,6-dimethylthieno[2,3-*b*]pyridine-2-carboxamide (33e). Carboxylic acid **25** (61 mg, 0.274 mmol), *N*,*N*-diisopropylethylamine (0.146 mL, 0.837 mmol), and BOP (128 mg, 0.288 mmol) were added to *N*,*N*-dimethylformamide (2 mL). **17e** (116 mg, 0.302 mmol) was dissolved in 2 mL of *N*,*N*-dimethylformamide and *N*,*N*-diisopropylethylamine (0.096 mL, 0.550 mmol) and then added to the reaction mixture. After the mixture was stirred for 5 h at room temperature, the crude product was worked up as per general procedure E to give the product as a pale yellow solid (49 mg, 35%). Mp: 137.2−140.3 °C. ^{1}H NMR ($CDCl_3$): δ 1.39−1.42 (m, 4H), 1.57−1.65 (m, 4H), 1.72−7.75 (m, 3H), 2.19 (m, 2H), 2.43−2.5 (m, 4H), 2.58 (s, 3H), 2.74 (s, 1H), 2.87 (m, 2H), 3.42 (dd, J 13.1, 7 Hz, 2H), 5.55 (t, J 5.3 Hz, 1H, NH), 6.3 (s, 2H, NH_2), 6.87 (s, 1H), 7.29 (m, 2H), 7.44 (m, 2H). ^{13}C NMR ($CDCl_3$): δ 20.2 (CH_3), 24.3 (CH_3), 26.8 (CH_2), 27.0 (CH_2), 27.4 (CH_2), 29.9 (CH_2), 38.4 (CH_2), 39.8 (CH_2), 49.5 (CH_2), 58.7 (CH_2), 71.1 (C), 98.7 (C), 122.3 (CH), 123.8 (C), 126.3 (CH), 128.5 (CH), 132.9 (C), 143.8 (C), 147.0 (C), 147.3 (C), 159.1 (C), 159.2 (C), 166 (C). HPLC purity (λ = 214 nm): 98%, t_R = 8.39 min. HRMS (ESI) TOF (m/z): [M + H]$^+$ 515.2247 calcd for $C_{27}H_{35}ClN_4O_2S$; found [M + H]$^+$ 515.2254.

3-Amino-5-chloro-6-methoxy-*N*-(4-(4-(2-methoxyphenyl)-piperazin-1-yl)butyl)-4-methylthieno[2,3-*b*]pyridine-2-carboxamide (34c). Carboxylic acid **32** (100 mg, 0.367 mmol), *N*,*N*-diisopropylethylamine (0.067 mL, 0.385 mmol), and BOP (176 mg, 0.398 mmol) were added to *N*,*N*-dimethylformamide (10 mL). **18c** (121 mg, 0.403 mmol) was dissolved in 2 mL of *N*,*N*-dimethylformamide, and *N*,*N*-diisopropylethylamine (0.077 mL, 0.403 mmol) was then added to convert to the free base, which was added dropwise to the reaction mixture. The reaction mixture was then worked up as described in general procedure E to give the product as a tan crystalline solid (55 mg, 29%). Mp: 99.1−101.6 °C (methanol/water). ^{1}H NMR ($CDCl_3$): δ 1.62−1.69 (m, 4H), 2.46 (m, 2H), 2.67 (m, 4H), 2.80 (s, 3H), 3.11 (m, 4H), 3.44 (q, J 6.5 Hz, 2H), 3.86 (s, 3H), 4.06 (s, 3H), 5.66 (t, J 5.6 Hz, 1H, NH), 6.28 (s, 2H, NH_2), 6.84−7.01 (m, 4H). ^{13}C NMR ($CDCl_3$): δ 16.4 (CH_3), 24.4 (CH_2), 27.0 (CH_2), 39.7 (CH_2), 50.8 (CH_2), 53.7 (CH_2), 55.2 (CH_3), 55.5 (CH_3), 58.3 (CH_2), 98.4 (C), 111.3 (CH), 116.6 (C), 118.4 (CH), 121.1 (CH), 121.3 (C), 123.1 (CH), 141.5 (C), 143.1 (C), 147.4 (C), 152.4 (C), 154.5 (C), 159.3 (C), 165.8 (C). HPLC purity (λ = 214 nm): 97%, t_R = 9.30 min. HRMS (ESI) TOF (m/z): [M + H]$^+$ 518.1993 calcd for $C_{25}H_{32}ClN_5O_3S$; found [M + H]$^+$ 518.2005.

3-Amino-5-chloro-6-methoxy-*N*-(5-(4-(2-methoxyphenyl)-piperazin-1-yl)pentyl)-4-methylthieno[2,3-*b*]pyridine-2-carboxamide (34d). Carboxylic acid **32** (100 mg, 0.367 mmol), *N*,*N*-diisopropylethylamine (0.067 mL, 0.385 mmol), and BOP (170 mg, 0.385 mmol) were added to *N*,*N*-dimethylformamide (10 mL). **18d** (127 mg, 0.403 mmol) was dissolved in 2 mL of *N*,*N*-dimethylformamide, and *N*,*N*-diisopropylethylamine (0.11 mL, 0.403 mmol) was then added to convert to the free base, which was added dropwise to the reaction mixture. The reaction mixture was then worked up as described in general procedure E to give the product as pale red microneedles (97 mg, 50%). Mp: 96−97.7 °C (methanol/water). ^{1}H NMR ($CDCl_3$): δ 1.43 (m, 2H), 1.56−1.69 (m, 4H), 2.43 (m, 2H), 2.66 (m, 4H), 2.83 (s, 3H), 3.10 (m, 4H), 3.42 (m, 2H), 3.86 (s, 3H), 4.07 (s, 3H), 5.44 (t, J 5.6 Hz, 1H, NH), 6.30 (br s, 2H, NH_2), 6.84−7.02 (m, 4H). ^{13}C NMR ($CDCl_3$): δ 16.4 (CH_3), 25.1 (CH_2), 26.7 (CH_2), 29.9 (CH_2), 39.7 (CH_2), 50.8 (CH_2), 53.6 (CH_2), 55.2 (CH_3), 55.5 (CH_3), 58.7 (CH_2), 98.3 (C), 111.3 (CH), 116.6 (C), 118.3 (CH), 121.1 (CH), 121.3 (C), 123.0 (CH), 141.5 (C), 143.1 (C), 147.4 (C), 152.4 (C), 154.4 (C), 159.3 (C), 165.8 (C). HPLC purity (λ = 214 nm): 99%, t_R = 9.84 min. HRMS (ESI) TOF (m/z): [M + H]$^+$ 532.2149 calcd for $C_{26}H_{34}ClN_5O_3S$; found [M + H]$^+$ 532.2166.

3-Amino-5-chloro-*N*-(5-(4-(2,3-dichlorophenyl)piperazin-1-yl)pentyl)-6-methoxy-4-methylthieno[2,3-*b*]pyridine-2-carboxamide (35). Carboxylic acid 32 (80 mg, 0.293 mmol), *N*,*N*-diisopropylethylamine (0.05 mL, 0.308 mmol), and BOP (136 mg, 0.308 mmol) were added together. Compound **19**, which was Boc deprotected and isolated as the HCl salt (114 mg, 0.298 mmol), was dissolved in 2 mL of *N*,*N*-dimethylformamide, and *N*,*N*-diisopropylethylamine (0.05 mL) was then added to convert to the free base, which was added dropwise to the reaction mixture. The reaction mixture was then worked up as described in general procedure E to give the product as a beige solid (106 mg, 63%). Mp: 114.5−116.5 °C. ^{1}H NMR ($CDCl_3$): δ 1.41 (m, 2H), 1.57−1.67 (m, 4H), 2.44 (m, 2H), 2.64 (m, 4H), 2.81 (s, 3H), 3.07 (m, 4H), 3.42 (m, 2H), 4.06 (s, 3H), 5.48 (t, J 5.7 Hz, 1H, NH), 6.30 (br s, 2H, NH_2), 6.94 (dd, J 7.2, 2.4, 1H), 7.10−7.16 (m, 2H). ^{13}C NMR ($CDCl_3$): δ 16.3 (CH_3), 24.9 (CH_2), 26.6 (CH_2), 29.9 (CH_2), 39.7 (CH_2), 51.3 (CH_2), 53.4 (CH_2), 55.1 (CH_3), 58.5 (CH_2), 98.2 (C), 116.5 (C), 118.7 (CH), 121.2 (C), 124.6 (CH), 127.5 (CH), 127.5 (C), 134.1 (C), 143.0 (C), 147.3 (C), 151.4 (C), 154.3 (C), 159.2 (C), 165.7 (C). HPLC purity (λ = 214 nm): 99%, t_R = 11.66 min. HRMS (ESI) TOF (m/z): [M + H]$^+$ 570.1264 calcd for $C_{25}H_{30}Cl_3N_5O_2S$; found [M + H]$^+$ 570.1265.

3-Amino-*N*-(5-(4-(2,3-dichlorophenyl)piperazin-1-yl)pentyl)-4,6-dimethylthieno[2,3-*b*]pyridine-2-carboxamide (36). Carboxylic acid **25** (73 mg, 0.32 mmol), *N*,*N*-diisopropylethylamine (0.059 mL, 0.34 mmol), and BOP (150 mg, 0.34 mmol) were added to *N*,*N*-dimethylformamide (2 mL). Compound **19**, which was Boc deprotected and isolated as the HCl salt (126 mg, 0.36 mmol), was dissolved in 2 mL of *N*,*N*-dimethylformamide and *N*,*N*-diisopropylethylamine (0.062 mL, 0.36 mmol) and then added to the reaction mixture. The reaction mixture was then worked up as described in general procedure E to give the product as a fluffy beige solid (119 mg, 70%). Mp: 142.9−143.8 °C. ^{1}H NMR ($CDCl_3$): δ 1.42 (m, 2H), 1.57−1.67 (m, 4H), 2.44 (m, 2H), 2.58 (s, 3H), 2.63 (m, 4H), 2.73 (s, 3H), 3.07 (m, 4H), 3.42 (m, 2H), 5.59 (t, J 5.6, 1H, NH), 6.31 (br s, 2H, NH_2), 6.86 (s, 1H), 6.94 (dd, J 7.0, 2.6 Hz, 1H), 7.10−7.15 (m, 2H). ^{13}C NMR ($CDCl_3$): δ 20.3 (CH_3), 24.4 (CH_3), 24.9 (CH_2), 26.6 (CH_2), 29.9 (CH_2), 39.7 (CH_2), 51.4 (CH_2), 53.4 (CH_2), 58.5 (CH_2), 98.6 (C), 118.7 (CH), 122.3 (CH), 123.7 (C), 124.6 (CH), 127.5 (CH), 127.6 (C), 134.1 (C), 143.7 (C), 147.3 (C),151.4 (C), 159.0 (C), 159.1 (C), 165.9 (C). HPLC purity (λ = 214 nm): 99%, t_R = 10.13 min. HRMS (ESI) TOF (m/z): [M + H]$^+$ 520.1705 calcd for $C_{25}H_{31}Cl_2N_5OS$; found [M + H]$^+$ 520.1703.

3-Amino-*N*-(5-(4-(2-methoxyphenyl)piperazin-1-yl)pentyl)-4,6-dimethylthieno[2,3-*b*]pyridine-2-carboxamide (37). Carboxylic acid **25** (80 mg, 0.36 mmol), *N*,*N*-diisopropylethylamine

(0.066 mL, 0.38 mmol), and BOP (167 mg, 0.38 mmol) were added to *N*,*N*-dimethylformamide (2 mL). **18d** (124 mg, 0.40 mmol) was dissolved in 2 mL of *N*,*N*-dimethylformamide and *N*,*N*-diisopropylethylamine (0.069 mL, 0.40 mmol) and then added to the reaction mixture. The reaction mixture was then worked up as described in general procedure E to give the product as a yellow-orange solid (66 mg, 38%). Mp: 127.6−128.2 °C. ^{1}H NMR ($CDCl_3$): δ 1.42 (m, 2H), 1.57−1.67 (m, 4H), 2.53 (m, 2H), 2.58 (s, 3H), 2.72 (s, 3H), 2.77 (m, 4H), 3.14 (m, 4H), 3.40 (m, 2H), 3.85 (s, 3H), 5.64 (t, *J* 5.7, 1H, NH), 6.30 (br s, 2H, NH_2), 6.84−7.02 (m, 5H). ^{13}C NMR ($CDCl_3$): δ 20.2 (CH_3), 24.4 (CH_3), 24.8 (CH_2), 26.1 (CH_2), 29.8 (CH_2), 39.6 (CH_2), 50.2 (CH_2), 53.5 (CH_2), 55.5 (CH_3), 58.5 (CH_2), 98.7 (C), 111.3 (CH), 118.4 (CH), 121.1 (CH), 122.3 (CH), 123.2 (CH), 123.7 (C), 141.0 (C), 143.7 (C), 147.3 (C), 152.3 (C), 159.0 (C), 159.1 (C), 166.0 (C). HPLC purity (λ = 214 nm): 97%, t_R = 8.89 min. HRMS (ESI) TOF (m/z): $[M + H]^+$ 482.2590 calcd for $C_{26}H_{35}N_5O_2S$; found $[M + H]^+$ 482.2590.

Pharmacology. Cell Lines and Transfection. FlpIn CHO cells (Invitrogen) were grown in Dulbecco's modified Eagle medium (DMEM) supplemented with 10% fetal bovine serum and maintained at 37 °C in a humidified incubator containing 5% CO_2. The FlpIn CHO cells were transfected with the pOG44 vector encoding Flp recombinase and the pDEST vector encoding the wild-type long isoform of the human D_2 receptor ($D_{2L}R$) at a ratio of 9:1 using polyethylenimine as the transfection reagent. At 24 h after transfection, the cells were subcultured, and the medium was supplemented with 700 μg/mL HygroGold as a selection agent. Cells were grown and maintained in DMEM containing 20 mM HEPES, 5% fetal bovine serum, and 200 μg/mL hygromycin B. Cells were maintained at 37 °C in a humidified incubator containing 5% CO_2 and 95% O_2.

Preparation of FlpIN CHO Cell Membranes. When cells were approximately 90% confluent, they were harvested and centrifuged (300*g*, 3 min). The resulting pellet was resuspended in assay buffer (20 mM HEPES, 100 mM NaCl, 6 mM $MgCl_2$, 1 mM EGTA, and 1 mM EDTA, pH 7.4), and the centrifugation procedure was repeated. The intact cell pellet was then resuspended in assay buffer and homogenized using a Polytron homogenizer for three 10 s intervals on the maximum setting, with 30 s periods on ice between each burst. The homogenate volume was brought up to 30 mL. The sample was centrifuged (1000*g*, 10 min, 25 °C). The pellet was discarded, and the supernatant was recentrifuged at 30 000*g* for 1 h at 4 °C. The resulting pellet was resuspended in 5 mL of assay buffer, and the protein content was determined using the method of Bradford. The homogenate was then separated into 0.5 mL aliquots and stored frozen at −80 °C until it was required for binding assays.

[^{3}H]Spiperone Binding Assay. Cell membranes (D_{2L}-FlpIn CHO, 3 μg) were incubated with varying concentrations of test compound in binding buffer (20 mM HEPES, 100 mM NaCl, 6 mM $MgCl_2$, 1 mM EGTA, and 1 mM EDTA, pH 7.4) containing 0.05 nM of [^{3}H]spiperone and 100 μM GppNHp to a final volume of 1 mL and were incubated at 37 °C for 3 h. Binding was terminated by fast-flow filtration over GF/B membranes using a Brandel harvester followed by three washes with ice-cold 0.9% NaCl. Bound radioactivity was measured in a Tri-Carb 2900TR liquid scintillation counter (PerkinElmer).

ERK1/2 Phosphorylation Assay. FlpIn CHO cells stably expressing the $D_{2L}R$ were seeded into 96-well plates at a density of 50 000 cells/well. After 5 h, cells were washed with phosphate buffered saline (PBS) and incubated in serum-free DMEM overnight before assaying. Initially, time-course experiments were conducted at least twice for each ligand to determine the time required to maximally promote ERK1/2 phosphorylation via the dopamine $D_{2L}R$. Dose−response experiments were performed in the absence and presence of increasing concentrations of each ligand at 37 °C. Stimulation of the cells was terminated by removing the media followed by the addition of 100 μL of SureFire lysis buffer (PerkinElmer) to each well. The plate was shaken for 5 min at room temperature before transferring 5 μL of the lysates to a white 384-well Proxiplate (PerkinElmer). Then 8 μL of a 240:1440:7:7 mixture of Surefire activation buffer/Surefire reaction buffer/Alphascreen acceptor beads/Alphascreen donor beads was added to the samples and incubated in the dark at 37 °C for 1.5 h. Plates were read using a Fusion plate reader.

cAMP Accumulation Assays. The cells were grown and incubated overnight and then preincubated for 45 min in 80 μL of stimulation buffer (Hank's buffered salt solution: 0.14 M NaCl, 5.4 mM KCl, 0.8 μM $MgSO_4$, 1.3 mM $CaCl_2$, 0.2 mM Na_2HPO_4, 0.44 mM KH_2PO_4, 5.6 mM D-glucose, 1 mg/mL BSA, 0.5 mM 3-isobutyl-1-methylxanthine, and 5 mM HEPES, pH 7.4). The agonists (10 μL) and 300 nM forskolin (10 μL) were added simultaneously to the cells and incubated for 30 min at 37 °C. Stimulation was terminated via the removal of the stimulation buffer and addition of 50 μL of ice cold 100% ethanol. The plates were then incubated at 37 °C to allow evaporation of the ethanol. Then 50 μL of detection buffer (1 mg/mL BSA, 0.3% Tween-20, and 5 mM HEPES, pH 7.4) was added and 5 μL of each well transferred to a 384-well Optiplate (PerkinElmer, Waltham, MA, U.S.). Anti-cAMP acceptor beads (0.2 units/μL) diluted in stimulation buffer was added under green light for 30 min before the addition of 15 μL of the donor beads/biotinylated cAMP (0.07 units/μL) diluted in detection buffer. The plates were incubated for 1 h at room temperature and read using a Fusion-α plate reader using AlphaScreen presettings.

Inhibition Assays for Analogues 5, 18a, and 18e. The required analogues were added to the cells at the appropriate dilutions and incubated at 37 °C for 30 min before the addition of 10 nM dopamine. After an additional 5 min stimulation time, termination of the ERK1/2 phosphorylation was as stated above.

Concentration−Response Assays for Analogues 18b−d, 19, 34d, 35, and 36. The required analogues were added to the cells at the appropriate dilutions and incubated at 37 °C for 5−10 min as predetermined for each compound in the time-course assays. Termination of the ERK1/2 phosphorylation was as stated above.

Interaction Studies with Dopamine for Compounds 34a−e. The required analogues and dopamine were added to the cells simulataneously at the appropriate dilutions and incubated at 37 °C for 5 min. Termination of the ERK1/2 phosphorylation was as stated above.

Data Analysis. Computerized nonlinear regression was performed using Prism 6.0 (GraphPad Software, San Diego, CA).

Agonist concentration−response curves were fitted via nonlinear regression to the three-parameter logistic function (eq 1):

$$E = \text{basal} + \frac{E_{max} - \text{basal}}{1 + 10^{(-pEC_{50} - \log[A])}} \quad (1)$$

where E is response, E_{max} and basal are the top and bottom asymptotes of the curve, respectively, log[A] is the logarithm of the agonist concentration, and pEC_{50} is the negative logarithm of the agonist concentration that gives a response halfway between E_{max} and basal.

To compare agonist profiles and quantify stimulus bias, agonist concentration−response curves were fitted to the following form of the operational model of agonism (eq 2):

$$Y = \text{basal} + \frac{(E_m - \text{basal})\left(\frac{\tau}{K_A}\right)^n [A]^n}{[A]^n\left(\frac{\tau}{K_A}\right)^n + \left(1 + \frac{[A]}{K_A}\right)^n} \quad (2)$$

where E_m is the maximal possible response of the system; basal is the basal level of response; K_A denotes the equilibrium dissociation constant of the agonist (A); τ is an index of the signaling efficacy of the agonist and is defined as R_T/K_E, where R_T is the total number of receptors and K_E is the coupling efficiency of each agonist-occupied receptor; and n is the slope of the transducer function that links occupancy to response. The analysis assumes that the maximal system responsiveness (E_m) and the transduction machinery utilized for a given cellular pathway are the same for all agonists such that the E_m and transducer slope (n) are shared between agonists. The ratio τ/K_A (determined as a logarithm, i.e., $\log(\tau/K_A)$) is referred to herein as the "transduction coefficient", as this composite parameter is sufficient to describe agonism and bias for a given pathway; i.e., stimulus-biased agonism can result from either a selective affinity ($K_{A\text{-}1}$) of an agonist

for a given receptor state(s) and/or a differential coupling efficacy (τ) toward certain pathways. To cancel the impact of cell-dependent effects on the observed agonism at each pathway, the $\log(\tau/K_A)$ values were then normalized to that determined for the endogenous agonist dopamine at each pathway to yield a "normalized transduction coefficient", $\Delta\log(\tau/K_A)$, i.e., $\Delta\log(\tau/K_A) = \log(\tau/K_A)_{test} - \log(\tau/K_A)_{dopamine}$.

To determine the actual bias of each agonist for different signaling pathways, the $\Delta\log(\tau/K_A)$ values were evaluated statistically between the pathways. The ligand bias of an agonist for one pathway, j1, over another, j2 is given as (eq 3)

$$\Delta\Delta\log\left(\frac{\tau}{K_A}\right)_{j1-j2} = \Delta\log\left(\frac{\tau}{K_A}\right)_{j1} - \Delta\log\left(\frac{\tau}{K_A}\right)_{j2} \quad (3)$$

A lack of stimulus bias compared to a reference agonist (in this case dopamine) will result in values of $\Delta\Delta\log(\tau/K_A)$ not significantly different from 0 between pathways. To account for the propagation of error associated with the determination of composite parameters, eq 5 was used:

$$\text{SEM} = \frac{\sigma}{\sqrt{n}} \quad (4)$$

where σ is the standard deviation and n is the number of experiments,

$$\text{pooled SEM} = \sqrt{(\text{SEM1})^2 + (\text{SEM2})^2} \quad (5)$$

All affinity, potency, and transduction ratio parameters were estimated as logarithms. All results are expressed as the mean ± SEM. Statistical analyses were performed where appropriate using one-way ANOVA with the Tukey's post hoc test. Statistical significance was taken as $p < 0.05$. For a more detailed explanation and analysis of using bias calculations see van der Westhuizen et al.[33]

■ ASSOCIATED CONTENT

Supporting Information

Values of potency (pEC_{50}) and maximal stimulation (E_{max}) for dopamine, aripiprazole, **18d**, **19**, **34d**, and **35**–**37** for cAMP and pERK1/2 signaling assays; full experimental and characterization of compounds **13d**–**e**, **16b**, **17b**–**d**, **18a**,**c**,**e**, **33b**–**d**, **34a**,**b**,**e**. This material is available free of charge via the Internet at http://pubs.acs.org.

■ AUTHOR INFORMATION

Corresponding Authors

*J.R.L.: phone, +613 9903 9095; fax, +613 9903 9581; e-mail, rob.lane@monash.edu.

*B.C.: phone, +61 3 9903 9556; fax, +61 3 9903 9581; e-mail, ben.capuano@monash.edu.

Notes

The authors declare no competing financial interest.

■ ACKNOWLEDGMENTS

This research was supported by Project Grants 1049564 and 1011920 of the National Health and Medical Research Council (NHMRC). A.C. is a Principle Research Fellow (NHMRC). J.R.L. is a R. D. Wright Biomedical Career Development Fellow (Grant 1052304, NHMRC) and a Larkin's Fellow (Monash University, Australia). M.S. acknowledges an Australian postgraduate award. C.K.H. acknowledges a Monash graduate scholarship. Special thanks are given to Dr. Jason Dang for running HRMS on final compounds.

■ ABBREVIATIONS USED

GPCR, G-protein-coupled receptor; CNS, central nervous system; TLC, thin layer chromatography; ERK, extracellular signal-regulated kinase; cAMP, cyclic adenosine monophosphate; FSK, forskolin; Boc, *tert*-butyloxycarbonyl; NMR, nuclear magnetic resonance; BOP, (benzotriazol-1-yloxy)tris-(dimethylamino)phosphonium hexafluorophosphate

■ REFERENCES

(1) Missale, C.; Nash, S. R.; Robinson, S. W.; Jaber, M.; Caron, M. G. Dopamine receptors: from structure to function. *Physiol. Rev.* **1998**, *78*, 189–225.

(2) Seeman, P. Targeting the dopamine D2 receptor in schizophrenia. *Expert Opin. Ther. Targets* **2006**, *10*, 515–531.

(3) Shin, J. K.; Malone, D. T.; Crosby, I. T.; Capuano, B. Schizophrenia: a systematic review of the disease state, current therapeutics and their molecular mechanisms of action. *Curr. Med. Chem.* **2011**, *18*, 1380–1404.

(4) Tandon, R. Pharmacologic treatment of schizophrenia: current status and future trends. *Curr. Psychosis Ther. Rep.* **2006**, *4*, 40–49.

(5) Rosen, W. G.; Mohs, R. C.; Johns, C. A.; Small, N. S.; Kendler, K. S.; Horvath, T. B.; Davis, K. L. Positive and negative symptoms in schizophrenia. *Psychiatry Res.* **1984**, *13*, 277–284.

(6) Inoue, T.; Domae, M.; Yamada, K.; Furukawa, T. Effects of the novel antipsychotic agent 7-(4-[4-(2,3-dichlorophenyl)-1-piperazinyl]-butyloxy)-3,4-dihydro-2(1*H*)-quinolinone (OPC-14597) on prolactin release from the rat anterior pituitary gland. *J. Pharmacol. Exp. Ther.* **1996**, *277*, 137–143.

(7) Jordan, S.; Koprivica, V.; Chen, R.; Tottori, K.; Kikuchi, T.; Altar, C. A. The antipsychotic aripiprazole is a potent, partial agonist at the human 5-HT1A receptor. *Eur. J. Pharmacol.* **2002**, *441*, 137–140.

(8) Shapiro, D. A.; Renock, S.; Arrington, E.; Chiodo, L. A.; Liu, L.-X.; Sibley, D. R.; Roth, B. L.; Mailman, R. Aripiprazole, a novel atypical antipsychotic drug with a unique and robust pharmacology. *Neuropsychopharmacology* **2003**, *28*, 1400–1411.

(9) Tamminga, C. A. Partial dopamine agonists in the treatment of psychosis. *J. Neural Transm.* **2002**, *109*, 411–420.

(10) Kenakin, T. Functional selectivity and biased receptor signaling. *J. Pharmacol. Exp. Ther.* **2011**, *336*, 296–302.

(11) Kenakin, T.; Christopoulos, A. Signalling bias in new drug discovery: detection, quantification and therapeutic impact. *Nat. Rev. Drug Discovery* **2013**, *12*, 205–216.

(12) Stallaert, W.; Christopoulos, A.; Bouvier, M. Ligand functional selectivity and quantitative pharmacology at G protein-coupled receptors. *Expert Opin. Drug Discovery* **2011**, *6*, 811–825.

(13) Urban, J. D.; Vargas, G. A.; von Zastrow, M.; Mailman, R. B. Aripiprazole has functionally selective actions at dopamine D2 receptor-mediated signaling pathways. *Neuropsychopharmacology* **2006**, *32*, 67–77.

(14) Allen, J. A.; Yost, J. M.; Setola, V.; Chen, X.; Sassano, M. F.; Chen, M.; Peterson, S.; Yadav, P. N.; Huang, X.-p.; Feng, B.; Jensen, N. H.; Che, X.; Bai, X.; Frye, S. V.; Wetsel, W. C.; Caron, M. G.; Javitch, J. A.; Roth, B. L.; Jin, J. Discovery of β-arrestin-biased dopamine D2 ligands for probing signal transduction pathways essential for antipsychotic efficacy. *Proc. Natl. Acad. Sci. U.S.A.* **2011**, *108*, 18488–18493.

(15) Chen, X.; Sassano, M. F.; Zheng, L.; Setola, V.; Chen, M.; Bai, X.; Frye, S. V.; Wetsel, W. C.; Roth, B. L.; Jin, J. Structure–functional selectivity relationship studies of β-arrestin-biased dopamine D2 receptor agonists. *J. Med. Chem.* **2012**, *55*, 7141–7153.

(16) Gay, E. A.; Urban, J. D.; Nichols, D. E.; Oxford, G. S.; Mailman, R. B. Functional selectivity of D2 receptor ligands in a Chinese hamster ovary hD2L cell line: evidence for induction of ligand-specific receptor states. *Mol. Pharmacol.* **2004**, *66*, 97–105.

(17) Mottola, D. M.; Kilts, J. D.; Lewis, M. M.; Connery, H. S.; Walker, Q. D.; Jones, S. R.; Booth, R. G.; Hyslop, D. K.; Piercey, M.; Wightman, R. M.; Lawler, C. P.; Nichols, D. E.; Mailman, R. B. Functional selectivity of dopamine receptor agonists. I. Selective activation of postsynaptic dopamine D2 receptors linked to adenylate cyclase. *J. Pharmacol. Exp. Ther.* **2002**, *301*, 1166–1178.

(18) Tschammer, N.; Bollinger, S.; Kenakin, T.; Gmeiner, P. Histidine 6.55 is a major determinant of ligand-biased signaling in dopamine D2L receptor. *Mol. Pharmacol.* **2011**, *79*, 575−585.
(19) Shonberg, J.; Herenbrink, C. K.; López, L.; Christopoulos, A.; Scammells, P. J.; Capuano, B.; Lane, J. R. A structure−activity analysis of biased agonism at the dopamine D2 receptor. *J. Med. Chem.* **2013**, *56*, 9199−9221.
(20) DeSimone, R. W.; Currie, K. S.; Mitchell, S. A.; Darrow, J. W.; Pippin, D. A. Privileged structures: applications in drug discovery. *Comb. Chem. High Throughput Screening* **2004**, *7*, 473−493.
(21) Costantino, L.; Barlocco, D. Privileged structures as leads in medicinal chemistry. *Curr. Med. Chem.* **2010**, *5*, 381−422.
(22) Duarte, C. D.; Barreiro, E. J.; Fraga, C. A. M. Privileged structures: a useful concept for the rational design of new lead drug candidates. *Mini-Rev. Med. Chem.* **2007**, *7*, 1108−1119.
(23) Bondensgaard, K.; Ankersen, M.; Thøgersen, H.; Hansen, B. S.; Wulff, B. S.; Bywater, R. P. Recognition of privileged structures by G-protein coupled receptors. *J. Med. Chem.* **2004**, *47*, 888−899.
(24) Kulagowski, J. J.; Broughton, H. B.; Curtis, N. R.; Mawer, I. M.; Ridgill, M. P.; Baker, R.; Emms, F.; Freedman, S. B.; Marwood, R.; Patel, S.; Patel, S.; Ragan, C. I.; Leeson, P. D. 3-[[4-(4-Chlorophenyl)-piperazin-1-yl]methyl]-1*H*-pyrrolo[2,3-*b*]pyridine: an antagonist with high affinity and selectivity for the human dopamine D4 receptor. *J. Med. Chem.* **1996**, *39*, 1941−1942.
(25) Löber, S.; Hübner, H.; Tschammer, N.; Gmeiner, P. Recent advances in the search for D3- and D4-selective drugs: probes, models and candidates. *Trends Pharmacol. Sci.* **2011**, *32*, 148−157.
(26) Newman, A. H.; Beuming, T.; Banala, A. K.; Donthamsetti, P.; Pongetti, K.; LaBounty, A.; Levy, B.; Cao, J.; Michino, M.; Luedtke, R. R.; Javitch, J. A.; Shi, L. Molecular determinants of selectivity and efficacy at the dopamine D3 receptor. *J. Med. Chem.* **2012**, *55*, 6689−6699.
(27) Capuano, B.; Crosby, I. T.; Lloyd, E. J.; Podloucka, A.; Taylor, D. A. Synthesis and preliminary pharmacological evaluation of 4′-arylalkyl analogues of clozapine. IV. The effects of aromaticity and isosteric replacement. *Aust. J. Chem.* **2008**, *61*, 930−940.
(28) Abdel-Fattah, M. A. O.; Lehmann, J.; Abadi, A. H. An interactive SAR approach to discover novel hybrid thieno probes as ligands for D2-like receptors with affinities in the subnanomolar range. *Chem. Biodiversity* **2013**, *10*, 2247−2266.
(29) Kenakin, T.; Watson, C.; Muniz-Medina, V.; Christopoulos, A.; Novick, S. A simple method for quantifying functional selectivity and agonist bias. *ACS Chem. Neurosci.* **2011**, *3*, 193−203.
(30) Vangveravong, S.; Zhang, Z.; Taylor, M.; Bearden, M.; Xu, J.; Cui, J.; Wang, W.; Luedtke, R. R.; Mach, R. H. Synthesis and characterization of selective dopamine D2 receptor ligands using aripiprazole as the lead compound. *Bioorg. Med. Chem.* **2011**, *19*, 3502−3511.
(31) Tschammer, N.; Elsner, J.; Goetz, A.; Ehrlich, K.; Schuster, S.; Ruberg, M.; Kühhorn, J.; Thompson, D.; Whistler, J.; Hübner, H.; Gmeiner, P. Highly potent 5-aminotetrahydropyrazolopyridines: enantioselective dopamine D3 receptor binding, functional selectivity, and analysis of receptor−ligand interactions. *J. Med. Chem.* **2011**, *54*, 2477−2491.
(32) Black, J. W.; Leff, P. Operational models of pharmacological agonism. *Proc. R. Soc. London, Ser. B* **1983**, *220*, 141−162.
(33) van der Westhuizen, E. T.; Breton, B.; Christopoulos, A.; Bouvier, M. Quantification of ligand bias for clinically relevant *β*2-adrenergic receptor ligands: implications for drug taxonomy. *Mol. Pharmacol.* **2014**, *85*, 492−509.

Supporting Information- Chapter 3

Supporting Information Table 1. Calculated bias factors for selected full agonists and partial agonists at the dopamine D_{2L} receptor

	Inhibition of FSK-induced cAMP production [a]				ERK1/2 phosphorylation [a]			
Agonist	**pEC_{50} (EC_{50}, nM)**	**E_{max} (%DA)**	**Log τ/K_A**	**Δlog τ/K_A**	**pEC_{50} (EC_{50}, nM)**	**E_{max} (%DA)**	**Log τ/K_A**	**Δlog τ/K_A**	**$\Delta\Delta$log τ/K_A (Bias)[b]**
DA	8.57 ± 0.07 (2.7)	102 ± 3	8.56 ± 0.07	0 ± 0.07	8.79 ± 0.11 (1.6)	87 ± 4	8.72 ± 0.05	0 ± 0.05	0 ± 0.09
AP	9.01 ± 0.12 (0.9)	88 ± 3	8.88 ± 0.13	0.32 ± 0.13	7.03 ± 0.30 (93.3)	25 ± 3	6.39 ± 0.29	-2.33 ± 0.29	2.65 ± 0.32 (446.7)***
18d	7.47 ± 0.24 (33.9)	64 ± 5	7.26 ± 0.21	-1.30 ± 0.21	8.89 ± 0.15 (1.3)	16 ± 1	8.07 ± 0.45	-0.65 ± 0.45	-0.65 ± 0.50 (0.2)
19	8.42 ± 0.28 (3.8)	73 ± 8	8.17 ± 0.16	-0.39 ± 0.16	7.07 ± 0.23 (85.1)	22 ± 3	6.60 ± 0.37	-2.12 ± 0.37	1.73 ± 0.40 (53.7)*
34d	7.81 ± 0.29 (15.5)	40 ± 6	7.23 ± 0.33	-1.33 ± 0.33	8.57 ± 0.66 (2.7)	17 ± 4	8.18 ± 0.45	-0.54 ± 0.45	-0.79 ± 0.56 (0.2)
35	7.23 ± 0.26 (58.9)	71 ± 11	7.18 ± 0.18	-1.38 ± 0.18	7.17 ± 0.29 (67.6)	17 ± 3	6.42± 0.50	-2.30 ± 0.50	0.92 ± 0.53 (8.3)
36	9.46 ± 0.36 (0.3)	50 ± 5	8.96 ± 0.26	0.40 ± 0.26	7.88 ± 0.40 (13.2)	13 ± 2	7.08 ± 0.62	-1.64 ± 0.62	2.04 ± 0.67 (109.6)*
37	8.88 ± 0.55 (1.3)	33 ± 5	8.45 ± 0.36	-0.11 ± 0.36	ND	ND	ND	ND	-

*$P < 0.05$, ***$P < 0.001$, significantly different from the reference agonist dopamine determined by a one-way ANOVA, Tukey post-hoc test. ND- No agonist activity detected. [a]Data are the mean of n= 4 experiments ± SEM. [b]Bias is defined as the fold bias relative to the reference agonist dopamine. DA= Dopamine, AP= Aripiprazole.

Experimental

For general procedures A-E, refer to main manuscript.

***tert*-Butyl (5-hydroxypentyl)carbamate (13d).**

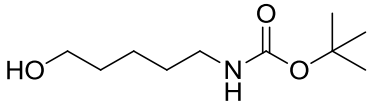

12d (500 mg, 4.85 mmol), di-*tert*-butyl dicarbonate (1.06 g, 4.85 mmol) was added to dichloromethane (30 mL). Triethylamine (0.74 mL, 5.33 mmol) was added dropwise and the reaction stirred for 1 h at room temperature and worked up according to procedure A. Purification gave the product as an orange oil (819 mg, 83%). ^{1}H NMR ($CDCl_3$): δ 1.39 (m, 2H), 1.44 (s, 9H), 1.47-1.62 (m, 4H), 1.94 (br s, 1H, OH), 3.12 (m, 2H), 3.64 (t, *J* 6.5 Hz, 2H), 4.63 (br s, 1H, NH). ^{13}C NMR ($CDCl_3$): δ 23.0 (CH_2), 28.5 (CH_3), 30.0 (CH_2), 32.4 (CH_2), 40.5 (CH_2), 62.7 (CH_2), 79.2 (C), 156.2 (C). LRMS (ESI) *m/z*: 204.2 $[M+H]^+$ (100%).

***tert*-Butyl (6-hydroxyhexyl)carbamate (13e).**

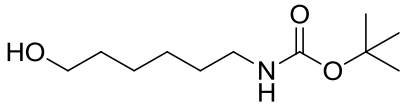

12e (400 mg, 3.41 mmol), di-*tert*-butyl dicarbonate (744.9 mg, 3.41 mmol) was added to dichloromethane (10 mL). Triethylamine (0.52 mL, 3.75 mmol) was added dropwise and the reaction stirred for 1 h at room temperature and worked up according to procedure A. Purification gave the product as a white solid (709 mg, 96%). mp: 39.8-41 °C. ^{1}H NMR ($CDCl_3$): δ 1.32-1.41 (m, 4H), 1.44 (s, 9H), 1.49 (m, 2H), 1.56 (m, 2H), 1.63 (br s, 1H, OH), 3.12 (m, 2H), 3.63 (m, 2H), 4.52 (br s, 1H, NH). ^{13}C NMR ($CDCl_3$): δ 25.4 (CH_2), 26.5 (CH_2), 28.5 (CH_3), 30.2 (CH_2), 32.7 (CH_2), 40.5 (CH_2), 62.8 (CH_2), 79.2 (C), 156.2 (C).

***tert*-Butyl (3-bromopropyl)carbamate (16b).**

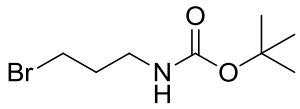

15b (2.00 g, 9.14 mmol), di-*tert*-butyl dicarbonate (1.81 g, 8.31 mmol) was added to dichloromethane (30 mL). Triethylamine (1.27 mL, 9.14 mmol) was added dropwise and the reaction stirred for 1 h at room temperature and worked up according to general procedure B. Purification gave the product as a colourless oil (1.66 g, 84%). ^{1}H NMR ($CDCl_3$): δ 1.44 (s, 9H), 2.05 (m, 2H), 3.27 (m, 2H), 3.43 (m, 2H), 4.73 (br s, 1H, NH). ^{13}C NMR ($CDCl_3$): δ 28.5 (CH_3), 30.9 (CH_2), 32.8 (CH_2), 39.1 (CH_2), 66.9 (C), 156.1 (C).

***tert*-Butyl (3-(4-(4-chlorophenyl)-4-hydroxypiperidin-1-yl)propyl)carbamate (17b).**

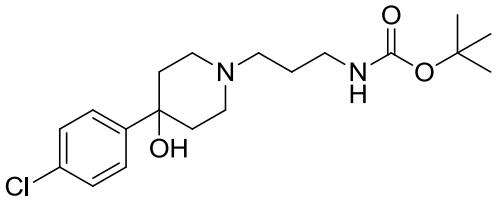

7 (1.00 g, 4.72 mmol), sodium iodide (708.1 mg, 4.72 mmol) and *N*,*N*-diisopropylethylamine (0.82 mL, 4.72 mmol) was added to acetonitrile (30 mL) at room temperature under N_2. **16b** (1.24 g, 5.20 mmol) then combined with acetonitrile (2 mL) and added slowly to the reaction mixture. Reflux occurred for 3 h before an additional 0.32 equiv. of **16b** was added and reflux continued for a further 2 h. The reaction mixture was worked up as described in general procedure C to give the product as a colourless foam (1.20 g, 69%). mp: 116.5-177.7 °C. ^{1}H NMR ($CDCl_3$): δ 1.44 (s, 9H), 1.69- 1.76 (m, 4H), 1.87 (s, 1H, OH), 2.13 (td, *J* 13.4, 4.4 Hz, 2H), 2.41-2.53 (m, 4H), 2.84 (m, 2H), 3.21 (m, 2H), 5.71 (s, 1H, NH), 7.31 (m, 2H), 7.44 (m, 2H). ^{13}C NMR ($CDCl_3$): δ 26.4 (CH_2), 28.6 (CH_3), 38.7 (CH_2), 40.2 (CH_2), 49.5 (CH_2), 57.1 (CH_2), 71.2 (C), 79.9 (C), 126.22 (CH), 128.5 (CH), 132.9 (C), 147 (C), 156.2 (C). HRMS (ESI)-TOF (*m/z)*: $[M+H]^+$ 369.1945 calcd for $C_{19}H_{29}ClN_2O_3$; found $[M+H]^+$ 369.1956.

***tert*-Butyl (4-(4-(4-chlorophenyl)-4-hydroxypiperidin-1-yl)butyl)carbamate (17c).**

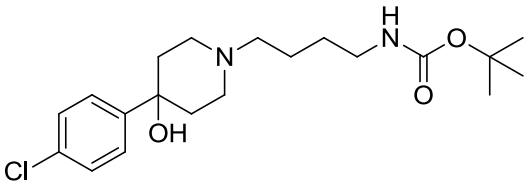

7 (200 mg, 0.94 mmol) was added to acetonitrile (30 mL) followed by dropwise addition of **14c** (210 mg, 0.79 mmol). Reflux occurred overnight before an additional 0.80 equiv. of **7** (133 mg, 0.63 mmol) was added and reflux continued (total reaction time 22 h). The reaction mixture was worked up as described in general procedure D to give the product as a white solid (154.5 mg, 51%). mp: 102.7-103.1 °C ^{1}H NMR ($CDCl_3$): δ 1.43 (s, 9H), 1.45-1.60 (m, 4H), 1.65 (br s, 1H, OH), 1.73 (m, 2H), 2.18 (m, 2H), 2.42-2.45 (m, 4H), 2.83 (m, 2H), 3.14 (m, 2H), 5.28 (br s, 1H, NH), 7.31 (m, 2H), 7.45 (m, 2H). ^{13}C NMR ($CDCl_3$): δ 26.7 (CH_2), 28.2 (CH_2), 28.6 (CH_3), 38.5 (CH_2), 40.6 (CH_2), 49.5 (CH_2), 58.2 (CH_2), 71.2 (C), 79.6 (C), 126.3 (CH), 128.6 (CH), 133.0 (C), 147.0 (C), 156.2 (C). HRMS (ESI)-TOF (*m/z*): $[M+H]^+$ 383.2101 calcd for $C_{20}H_{31}ClN_2O_3$; found $[M+H]^+$ 383.2108.

***tert*-Butyl (5-(4-(4-chlorophenyl)-4-hydroxypiperidin-1-yl)pentyl)carbamate (17d).**

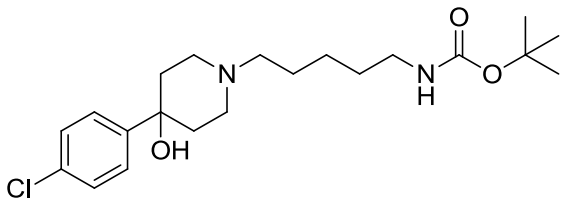

7 (100 mg, 0.43 mmol) were added to acetonitrile (5 mL) followed by dropwise addition of **14d** (100 mg, 0.36 mmol). Reflux occurred overnight before an additional 1.3 equiv. of **7** (114 mg, 0.46 mmol) was added and reflux continued (total reaction time 24 h). The reaction mixture was worked up as described in general procedure D to give the product as a white solid (154.5 mg, 51%). ^{1}H NMR ($CDCl_3$): δ 1.32 (m, 2H), 1.42 (s, 9H), 1.48 (m, 2H), 1.55 (m, 2H), 1.73 (m, 2H), 2.16 (m, 2H), 2.4-2.53 (m, 4H), 2.84 (m, 2H), 3.08 (m, 2H), 4.69 (br s, 1H, NH), 7.29 (m, 2H), 7.44 (m, 2H).^{13}C NMR ($CDCl_3$): δ 24.8 (CH_2), 26.3 (CH_2), 28.5 (CH_3), 30 (CH_2), 38.1 (CH_2),

40.5 (CH_2), 49.4 (CH_2), 58.6 (CH_2), 70.7 (C), 79.6 (C), 126.3 (CH), 128.4 (CH), 132.7 (C), 147.1 (C), 156.1 (C). HRMS (ESI)-TOF (*m/z*): $[M+H]^+$ 397.2258 calcd for $C_{21}H_{33}ClN_2O_3$; found $[M+H]^+$ 397.2251.

***tert*-Butyl (2-(4-(2-methoxyphenyl)piperazin-1-yl)ethyl)carbamate (18a).**

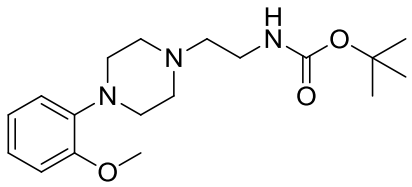

7 (230 mg, 1.01 mmol) and *N*,*N*-diisopropylethylamine (0.18 mL, 1.01 mmol) were added to acetonitrile (5 mL) and stirred at room temperature under N_2 for 2 mins to generate the free amine. Sodium iodide (151 mg, 1.01 mmol) and *N*,*N*-diisopropylethylamine (0.18 mL, 1.01 mmol) were then also added. **16a** (270 mg, 1.21 mmol) was then combined with acetonitrile (2 mL) and added slowly to the reaction mixture. After 24 h reflux, the reaction mixture was worked up as described in general procedure C and purified via column chromatography (1:1 petroleum spirits/ethyl acetate) to give the product as an orange oil (116.3 mg, 34%). ^{1}H NMR ($CDCl_3$): δ 1.46 (s, 9H), 2.52 (t, *J* 6 Hz, 2H), 2.65 (m, 4H), 3.08 (m, 4H), 3.26 (m, 2H), 3.85 (s, 3H), 5.12 (br s, 1H, NH), 6.84-7.01 (m, 4H). ^{13}C NMR ($CDCl_3$): δ 28.5 (CH_3), 37.1 (CH_2), 50.6 (CH_2), 53.2 (CH_2), 55.3 (CH_3), 57.3 (CH_2), 79.1 (C), 111.2 (CH), 118.2 (CH), 120.9 (CH), 122.9 (CH), 141.3 (C), 152.2 (C), 156.0 (C). HPLC purity (λ= 214 nm): 99% t_R 7.66 min (gradient). HRMS (ESI)-TOF (*m/z*): $[M+H]^+$ 336.2287 calcd for $C_{18}H_{29}N_3O_3$; found $[M+H]^+$ 336.2297.

***tert*-Butyl (4-(4-(2-methoxyphenyl)piperazin-1-yl)butyl)carbamate (18c).**

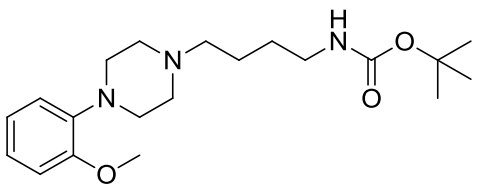

5 (424 mg, 1.59 mmol) was dissolved in acetonitrile (10 mL) and triethylamine (0.22 mL, 1.59 mmol) and stirred for 5. **14c** (424 mg, 1.59 mmol) was then added dropwise to the reaction

mixture which was refluxed for 24 h. Work up proceeded as described in general procedure D and the crude product purified by column chromatography (19:1 chloroform/methanol) to give a yellow/orange oil (282.5 mg, 49%). ^{1}H NMR ($CDCl_3$): δ 1.44 (s, 9H), 1.54-1.59 (m, 4H), 2.42 (t, *J* 7.0 Hz, 2H), 2.65 (m, 4H), 3.12-3.1 (m, 6H), 3.86 (s, 3H), 5.31 (br s, 1H, NH), 6.85-7.02 (m, 4H). ^{13}C NMR ($CDCl_3$): δ 24.5 (CH_2), 28.1 (CH_2), 28.6 (CH_3), 40.7 (CH_2), 50.7 (CH_2), 53.5 (CH_2), 55.5 (CH_3), 58.3 (CH_2), 79.0 (C), 111.3 (CH), 118.3 (CH), 121.1 (CH), 123.0 (CH), 141.4 (C), 152.4 (C), 156.2 (C). HPLC purity (λ= 214 nm): 99% t_R 7.88 min (gradient). HRMS (ESI)-TOF (*m/z*): $[M+H]^+$ 364.2600 calcd for $C_{20}H_{33}N_3O_3$; found $[M+H]^+$ 364.2603.

***tert*-Butyl (6-(4-(2-methoxyphenyl)piperazin-1-yl)hexyl)carbamate (18e).**

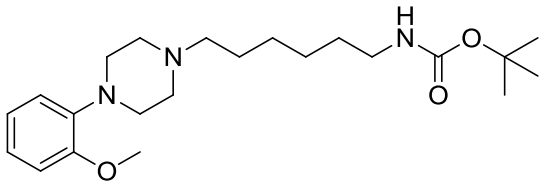

5 (541 mg, 2.36 mmol) was dissolved in acetonitrile (10 mL) and triethylamine (0.33 mL, 1.18 mmol) and stirred for 5 mins. **14e** (349 mg, 1.18 mmol) was then added dropwise to the reaction mixture which was refluxed for 8 h. Work up proceeded as described in general procedure D and the crude product purified by column chromatography (100% ethyl acetate) to give a yellow oil (131.5 mg, 28%). ^{1}H NMR ($CDCl_3$): δ 1.32-1.36 (m, 4H), 1.44 (s, 9H), 1.46-1.53 (m, 4H), 2.40 (m, 2H), 2.65 (m, 4H), 3.11 (m, 6H), 3.86 (s, 3H), 4.56 (br s, 1H, NH), 6.84-7.01 (m, 4H). ^{13}C NMR ($CDCl_3$): δ 26.8 (CH_2), 26.9 (CH_2), 27.4 (CH_2), 28.5 (CH_3), 30.1 (CH_2), 40.6 (CH_2), 50.7 (CH_2), 53.6 (CH_2), 55.4 (CH_3), 58.8 (CH_2), 79.1 (C), 111.2 (CH), 118.3 (CH), 121.1 (CH), 123.0 (CH), 141.5 (C), 152.4 (C), 156.1 (C). HPLC purity (λ= 214 nm): 98% t_R 8.61 min (gradient). HRMS (ESI)-TOF (*m/z*): $[M+H]^+$ 392.2913 calcd for $C_{22}H_{37}N_3O_3$; found $[M+H]^+$ 392.2919.

3-Amino-*N*-(3-(4-(4-chlorophenyl)-4-hydroxypiperidin-1-yl)propyl)-4,6-dimethylthieno[2,3-*b*]pyridine-2-carboxamide (33b).

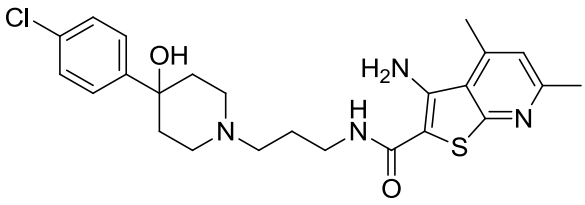

Carboxylic acid **25** (71.0 mg, 0.32 mmol), *N*,*N*-diisopropylethylamine (0.059 mL, 0.333 mmol) and BOP (148.4 mg, 0.34 mmol) was added to *N*,*N*-dimethylformamide (2 mL). **17b** (120.1 mg, 0.35 mmol) was dissolved in 2 mL of *N*,*N*-dimethylformamide and *N*,*N*-diisopropylethylamine (0.12 mL, 0.71 mmol) and then added to the reaction mixture. After 16 h stirring at room temperature, the crude product was worked up as per general procedure E to give white solid (59.4 mg, 39%). mp: 244.3-245.2 °C. ^{1}H NMR (d_6-DMSO): δ 1.57 (d, *J* 12.7 Hz, 2H), 1.70 (m, 2H), 2.05 (m, 2H), 2.35 (t, *J* 11.1 Hz, 2H), 2.46 (m, 2H), 2.55 (s, 3H), 2.72 (s, 3H), 2.77 (m, 2H), 3.34 (m, 2H), 4.94 (s, 1H, OH), 6.76 (s, 2H, NH_2), 7.05 (s, 1H), 7.38 (m, 2H), 7.55 (m, 2H), 8.04 (t, *J* 5.2 Hz, 1H, NH). ^{13}C NMR (d_6-DMSO): δ 19.7 (CH_3), 23.8 (CH_3), 25.2 (CH_2), 38 (CH_2), 39.1 (CH_2), 49.4 (CH_2), 57.4 (CH_2), 69.7 (C), 97.5 (C), 121.9 (CH), 123.4 (C), 126.9 (CH), 127.8 (CH), 130.7 (C), 144.5 (C), 147.3 (C), 149.2 (C), 158.3 (C), 158.4 (C), 165.1 (C). HPLC purity (λ= 214 nm): 99% t_R 8.08 min (gradient). HRMS (ESI)-TOF (*m/z*): $[M+H]^+$ 473.1778 calcd for $C_{24}H_{29}ClN_4O_2S$; found $[M+H]^+$ 473.1794.

3-Amino-*N*-(4-(4-(4-chlorophenyl)-4-hydroxypiperidin-1-yl)butyl)-4,6-dimethylthieno[2,3-*b*]pyridine-2-carboxamide (33c).

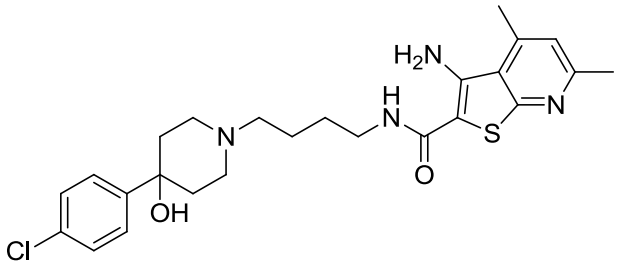

Carboxylic acid **25** (65 mg, 0.29 mmol), *N*,*N*-diisopropylethylamine (0.053 mL, 0.31 mmol) and BOP (135.8 mg, 0.31 mmol) was added to *N*,*N*-dimethylformamide (2 mL). **17c** (114.4 mg, 0.32 mmol) was dissolved in 2 mL of *N*,*N*-dimethylformamide and *N*,*N*-diisopropylethylamine (0.112 mL, 0.64 mmol) and then added to the reaction mixture. After stirring at room temperature for 1.5 h, the crude product was worked up as per general procedure E to give a pale yellow solid (79.7 mg, 56%). mp: 188.6-187.9 °C. ^{1}H NMR ($CDCl_3$): δ 1.63-1.75 (m, 6H), 1.79 (br s, 1H, OH), 2.13 (dt, *J* 12.9, 4.2 Hz, 2H),2.42-2.47 (m, 4H), 2.58 (s, 3H), 2.74 (s, 1H), 2.82 (m, 2H), 3.44 (dd, *J* 13, 6.6 Hz, 2H), 5.75 (t, *J* 5.5 Hz, 1H, NH), 6.28 (s, 2H, NH_2), 6.87 (s, 1H), 7.29 (m, 2H), 7.43 (m, 2H). ^{13}C NMR ($CDCl_3$): δ 20.3 (CH_3), 24.4 (CH_3), 24.7 (CH_2), 28 (CH_2), 38.6 (CH_2), 39.7 (CH_2), 49.6 (CH_2), 58.4 (CH_2), 71.2 (C), 98.7 (C), 122.3 (CH), 123.7 (C), 126.3 (CH), 128.5 (CH), 132.8 (C), 143.8 (C), 147.1 (C), 147.3 (C), 159.1 (C), 159.2 (C), 166 (C). HPLC purity (λ= 214 nm): 95% t_R 7.99 min (gradient). HRMS (ESI)-TOF (*m/z*): $[M+H]^+$ 487.1934 calcd for $C_{25}H_{31}ClN_4O_2S$; found $[M+H]^+$ 487.1942.

3-Amino-*N*-(5-(4-(4-chlorophenyl)-4-hydroxypiperidin-1-yl)pentyl)-4,6-dimethylthieno[2,3-*b*]pyridine-2-carboxamide (33d).

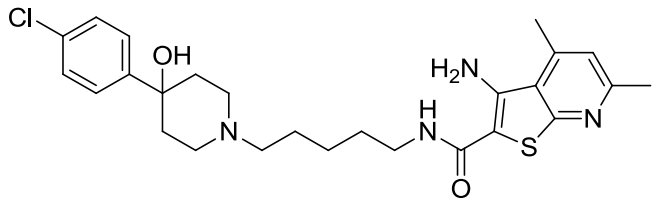

Carboxylic acid **25** (51 mg, 0.23 mmol) and *N*,*N*-diisopropylethylamine (0.042 mL, 0.24 mmol) and BOP (106.6 mg, 0.241 mmol) was added to *N*,*N*-dimethylformamide (2 mL). **17d**, 93.3 mg, 0.25 mmol) was dissolved in 2 mL of *N*,*N*-dimethylformamide and *N*,*N*-diisopropylethylamine (0.09 mL, 0.51 mmol) and then added to the reaction mixture. After 4 h stirring at room temperature, the crude product was worked up as per general procedure E to give a yellow solid (58.8 mg, 51%). mp: 159-162.2 °C. ^{1}H NMR ($CDCl_3$): δ 1.43 (m, 2H), 1.58-1.74 (m, 7H), 2.13 (dt, *J* 13.3, 4 Hz, 2H), 2.42-2.46 (m, 4H), 2.59 (s, 3H), 2.74 (s, 1H), 2.83 (m, 2H), 3.42 (dd, *J* 13, 7.1 Hz, 2H), 5.53 (t, *J* 5.5 Hz, 1H, NH), 6.30 (s, 2H, NH_2), 6.87 (s, 1H), 7.29 (m, 2H), 7.43 (m, 2H). ^{13}C NMR ($CDCl_3$): δ 20.3 (CH_3), 24.4 (CH_3), 25 (CH_2), 26.7(CH_2), 29.9 (CH_2), 38.5 (CH_2), 39.7 (CH_2), 49.7 (CH_2), 58.6 (CH_2), 71.2 (C), 98.7 (C), 122.3 (CH), 123.7 (C), 126.8 (CH), 128.5 (CH), 132.8 (C), 143.8 (C), 147.1 (C), 147.3 (C), 159.1 (C), 159.2 (C), 166 (C). HPLC purity (λ= 214 nm): 99% t_R 8.15 min (gradient). HRMS (ESI)-TOF (*m/z*): $[M+H]^+$ 501.2091 calcd for $C_{26}H_{33}ClN_4O_2S$; found $[M+H]^+$ 501.2104.

3-Amino-5-chloro-6-methoxy-*N*-(2-(4-(2-methoxyphenyl)piperazin-1-yl)ethyl)-4-methylthieno[2,3-*b*]pyridine-2-carboxamide (34a).

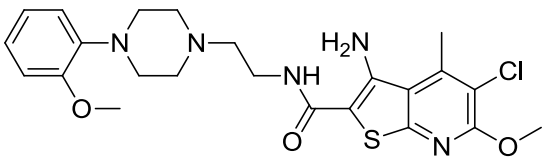

Carboxylic acid **32** (78 mg, 0.29 mmol), *N*,*N*-diisopropylethylamine (0.052 mL, 0.3 mmol) and BOP (134 mg, 0.30 mmol) were added to *N*,*N*-dimethylformamide (10 mL). **18a** (85.5 mg, 0.32

mmol) was dissolved in 2 mL of *N*,*N*-dimethylformamide and *N*,*N*-diisopropylethylamine (0.06 mL, 0.32 mmol) was then added to convert to the free base, which was added dropwise to the reaction mixture. The reaction mixture was then reacted and worked up as described in general procedure E to give the product as beige microneedles (57.2 mg, 41%). mp: 93.2-94.1 °C (Methanol/water). ^{1}H NMR ($CDCl_3$): δ 2.67 (t, *J* 6 Hz, 2H), 2.72 (m, 4H), 2.84 (s, 3H), 3.13 (m, 4H), 3.52 (m, 2H), 3.87 (s, 3H), 4.07 (s, 3H), 6.29 (br s, 2H, NH_2), 6.30 (t, *J* 4.5 Hz, 1H, NH), 6.86-7.02 (m, 4H). ^{13}C NMR ($CDCl_3$): δ 16.2 (CH_3), 35.9 (CH_2), 50.9 (CH_2), 53.0 (CH_2), 55.0 (CH_3), 55.4 (CH_3), 56.1 (CH_2), 98.6 (C), 111.3 (CH), 116.3 (C), 118.3 (CH), 121.0 (CH), 121.1 (C), 123.0 (CH), 141.2 (C), 142.9 (C), 147.1 (C), 152.3 (C), 154.5 (C), 159.0 (C), 165.6 (C). HPLC purity (λ= 214 nm): 96% t_R 9.28 min (gradient). HRMS (ESI)-TOF (*m/z*): $[M+H]^+$ 490.1680 calcd for $C_{23}H_{28}ClN_5O_3S$; found $[M+H]^+$ 490.1694.

3-Amino-5-chloro-6-methoxy-*N*-(3-(4-(2-methoxyphenyl)piperazin-1-yl)propyl)-4-methylthieno[2,3-*b*]pyridine-2-carboxamide (34b).

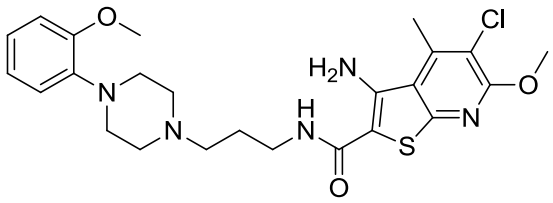

Carboxylic acid **32** (100 mg, 0.37 mmol), *N*,*N*-diisopropylethylamine (0.07 mL, 0.39 mmol) and BOP (176 mg, 0.40 mmol) were added to *N*,*N*-dimethylformamide (10 mL). **18b** (130.4 mg, 0.46 mmol) was dissolved in 2 mL of *N*,*N*-dimethylformamide and *N*,*N*-diisopropylethylamine (0.08 mL, 0.46 mmol) was then added to convert to the free base, which was added dropwise to the reaction mixture. The reaction mixture was then reacted and worked up as described in general procedure E to give the product as a white solid (83.6 mg, 45%). mp: 123.4-124.9 °C (Methanol/water). ^{1}H NMR ($CDCl_3$): δ 1.81 (m, 2H), 2.62 (m, 2H), 2.73 (m, 4H), 2.83 (s, 3H), 3.27 (m, 4H), 3.55 (dd, *J* 11.3 5.4 Hz, 2H), 3.87 (s, 3H), 4.04 (s, 3H), 6.28 (br s, 2H, NH_2), 6.86-7.06 (m, 4H), 7.51 (t, *J* 4.5 Hz, 1H, NH). ^{13}C NMR ($CDCl_3$): δ 16.4 (CH_3), 24.6 (CH_2), 40.8

(CH_2), 50.2 (CH_2), 54.0 (CH_2), 55.1 (CH_3), 55.5 (CH_3), 58.8 (CH_2), 99.9 (C), 111.3 (CH), 116.4 (C), 118.8 (CH), 121.1 (CH), 121.3 (C), 123.2 (CH), 141.5 (C), 142.9 (C), 147.0 (C), 152.6 (C), 154.5 (C), 159.1 (C), 165.9 (C). HPLC purity (λ= 214 nm): 98% t_R 9.46 min (gradient). HRMS (ESI)-TOF (*m/z*): $[M+H]^+$ 504.1836 calcd for $C_{24}H_{30}ClN_5O_3S$; found $[M+H]^+$ 504.1841.

3-Amino-5-chloro-6-methoxy-*N*-(6-(4-(2-methoxyphenyl)piperazin-1-yl)hexyl)-4-methylthieno[2,3-*b*]pyridine-2-carboxamide (34e).

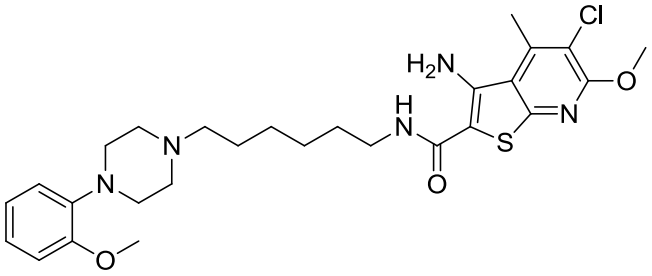

Carboxylic acid **32** (74.0 mg, 0.27 mmol), *N*,*N*-diisopropylethylamine (0.05 mL, 0.285 mmol) and BOP (126 mg, 0.285 mmol) were added to *N*,*N*-dimethylformamide (10 mL). **18e** (97.9 mg, 0.30 mmol) was dissolved in 2 mL of *N*,*N*-dimethylformamide and *N*,*N*-diisopropylethylamine (0.05 mL, 0.30 mmol) was then added to convert to the free base, which was added dropwise to the reaction mixture. The reaction mixture was then reacted and worked up as described in general procedure E to give the product as a yellow foam (86.1 mg, 58%). ^{1}H NMR ($CDCl_3$): δ 1.39 (m, 4H), 1.54-1.64 (m, 4H), 2.41 (m, 2H), 2.66 (m, 4H), 2.81 (s, 3H), 3.10 (m, 4H), 3.39 (m, 2H), 3.86 (s, 3H), 4.06 (s, 3H), 5.42 (t, *J* 5.6 Hz, 1H, NH), 6.28 (br s, 1H, NH_2), 6.84-7.01 (m, 4H). ^{13}C NMR ($CDCl_3$): δ 16.3 (CH_3), 26.9 (CH_2), 27.0 (CH_2), 27.4 (CH_2), 29.9 (CH_2), 39.7 (CH_2), 50.7 (CH_2), 53.6 (CH_2), 55.1 (CH_3), 55.4 (CH_3), 58.8 (CH_2), 98.3 (C), 111.3 (CH), 116.5 (C), 118.3 (CH), 121.1 (CH), 121.2 (C), 123.0 (CH), 141.5 (C), 143.0 (C), 147.3 (C), 152.4 (C), 154.4 (C), 159.2 (C), 165.7 (C). HPLC purity (λ= 214 nm): 98% t_R 9.80 min (gradient). HRMS (ESI)-TOF (*m/z*): $[M+H]^+$ 546.2306 calcd for $C_{27}H_{36}ClN_5O_3S$; found $[M+H]^+$ 546.2320.

Chapter 4- Designed Multiple Ligands Targeting the Dopamine D_2 and Muscarinic M_1 Receptors

Declaration for Thesis Chapter 4

The data presented in Chapter 4 was submitted to the *Journal of Medicinal Chemistry* as a brief article on the 29th of August 2014. The paper is currently pending approval and is presented in this thesis in the form of a manuscript.

Declaration by candidate

In the case of Chapter 4 the nature and extent of my contribution to the work was the following:

Nature of contribution	**Contribution (%)**
Design, synthesis, purification, characterisation and pharmacological testing of all analogues. Main author of manuscript.	80

The following co-authors contributed to the work. Co-authors who are students at Monash University must also indicate the extent of their contribution in percentage terms:

Name	**Nature of contribution**	**Contribution (%)***
Herman D. Lim	Conducting binding experiments at the M_1 mAChR	5
Carmen Klein Herenbrink	Testing of compound **11** in cAMP	
Arthur Christopoulos	Co-author of manuscript	
J. Robert Lane	Co-author of manuscript	
Ben Capuano	Co-author of manuscript	

*Percentage contribution only shown for co-authors who were students at Monash University at the time of their contribution to this work.

Candidate's Signature: [redacted] 01/12/2014

Monika Szabo

Declaration by co-authors

The undersigned hereby certify that:

1. The above declaration correctly reflects the nature and extent of the candidate's contribution to this work, and the nature of the contribution of each of the co-authors.
2. They meet the criteria for authorship in that they have participated in the conception, execution, or interpretation, of at least that part of the publication in their field of expertise;
3. They take public responsibility for their part of the publication, except for the responsible author who accepts overall responsibility for the publication;
4. There are no other authors of the publication according to these criteria;
5. Potential conflicts of interest have been disclosed to (a) granting bodies, (b) the editor or publisher of journals or other publications, and (c) the head of the responsible academic unit; and
6. The original data are stored at the following location(s) and will be held for at least five years from the date indicated below:

   Department of Medicinal Chemistry, Monash Institute of Pharmaceutical Sciences, 381 Royal Parade, Parkville, Victoria, 3052, Australia

Co-author signatures:

Herman D. Lim:	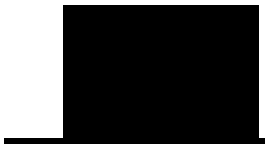	01/12/2014
Carmen Klein Herenbrink:	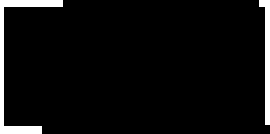	01/12/2014
J. Robert Lane:	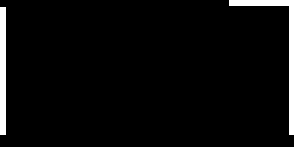	01/12/2014
Arthur Christopoulos:		01/12/2014
Ben Capuano:		01/12/2014

Designed Multiple Ligands Targeting the Dopamine D_2 and Muscarinic M_1 Receptors

Monika Szabo†‡, Herman D. Lim‡, Carmen Klein Herenbrink‡, Arthur Christopoulos‡, J. Robert Lane‡,, Ben Capuano†,**

†Medicinal Chemistry, ‡Drug Discovery Biology, Monash Institute of Pharmaceutical Sciences, Monash University, 381 Royal Parade, Parkville 3052, Victoria, Australia.

KEYWORDS: Dopamine receptor, D_2, muscarinic receptor, M_1, serotonin receptor, 5-HT_{2A}, designed multiple ligands, DML, merged, polypharmacology, privileged structures, antipsychotics, schizophrenia

Abstract

Herein we describe the hybridization of a benzoxazinone M_1 scaffold with D_2 privileged structures derived from putative and clinically relevant antipsychotics to develop designed multiple ligands. The M_1 mAChR is an attractive target for the cognitive deficits in key CNS disorders. Moreover, activity at D_2 and 5-HT_{2A} receptors has proven useful for antipsychotic efficacy. We identified **9** which retained functional activity at the target M_1 mAChR and D_2R and demonstrated high affinity for the 5-HT_{2A}R.

Introduction

All antipsychotic drugs currently on the market for the treatment of schizophrenia antagonize the dopamine D_2 receptor (D_2R), a member of the G Protein-Coupled Receptor (GPCR) family. They are effective in alleviating the positive symptoms of schizophrenia (hallucinations, delusions) which are postulated to arise from hyperdopaminergia in the mesolimibic pathway of the brain.[1] Antipsychotics such as ziprasidone (**1**) and risperidone (**2**, Figure 1) have also shown some improvements in the negative symptoms (social withdrawal, lack of motivation) due to their favourable polypharmacology, and in particular their action as high affinity antagonists at the serotonin 5-HT_{2A} receptor (5-HT_{2A}R).[2,3] Indeed the favourable polypharmacology that is observed with many atypical antipsychotics such as clozapine was achieved through serendipitous discovery rather than by a rational drug design process.[4] A newer class of clinically used antipsychotics are the D_2R partial agonists, of which aripiprazole (**3**, Figure 1), is the most commonly prescribed antipsychotic in the US for the treatment of schizophrenia and other CNS disorders.[5] Partial agonists act to stabilise dopaminergic signalling rather than exert the complete inhibition associated with D_2R antagonists.[6] Since the success of aripiprazole, other D_2R partial agonists have emerged such as cariprazine[7] and brexpiprazole,[8] which both have the 2,3-dichlorophenylpiperazine motif present in **3**. Another D_2R partial agonist bifeprunox (**4**) exhibits a structurally more diverse heterocycle attached to the piperazine and incorporates a hydrophobic

and unfunctionalized biphenyl substituent. There are also high affinity D_2R partial agonists such as **5** that contain a 2-methoxy substituted phenylpiperazine motif rather than 2,3-dichlorophenylpiperazine.[9] However, no current antipsychotic drug addresses the cognitive deficits associated with schizophrenia, which is an equally important component of the aetiology of schizophrenia.

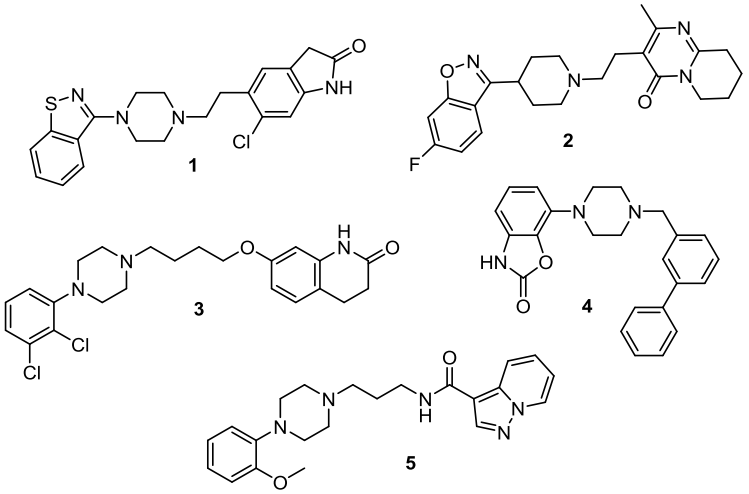

Figure 1. Antipsychotics: ziprasidone (**1**), risperidone (**2**), aripiprazole (**3**), bifeprunox (**4**) and a high affinity D_2 partial agonist (**5**).

There is evidence to support that targeting the M_1 muscarinic acetylcholine receptor (M_1 mAChR), also belonging to the GPCR family, improves the cognitive deficits of patients suffering from schizophrenia and other CNS disorders.[10,11] However, selective targeting of this receptor remains a challenge due to the high conservation of the orthosteric site across the mAChR receptor family and activity at other receptors in this family is associated with limiting side effects.[12] Of interest, M_1 allosteric agonists have particularly gained a great deal of research focus.[13] Ligands that act at an allosteric site (a topographically distinct site to the orthosteric site) offer the added benefit of possibly being subtype selective, as the residues are less conserved in an allosteric site versus an orthosteric site.[14] The putative M_1 allosteric agonist LuAE51090 (**6**, Figure 2) has a favourable M_1 profile (EC_{50}= 61 nM; intracellular Ca^{2+} mobilization assay) but exhibits poor binding affinity at both the D_2R and the 5-$HT_{2A}R$ (K_i~1 μM).[15] We found this

surprising, as **6** displays some common pharmacophoric features of many D_2R ligands, both antagonists and partial agonists as highlighted in Figure 2 and in an earlier publication.[16]

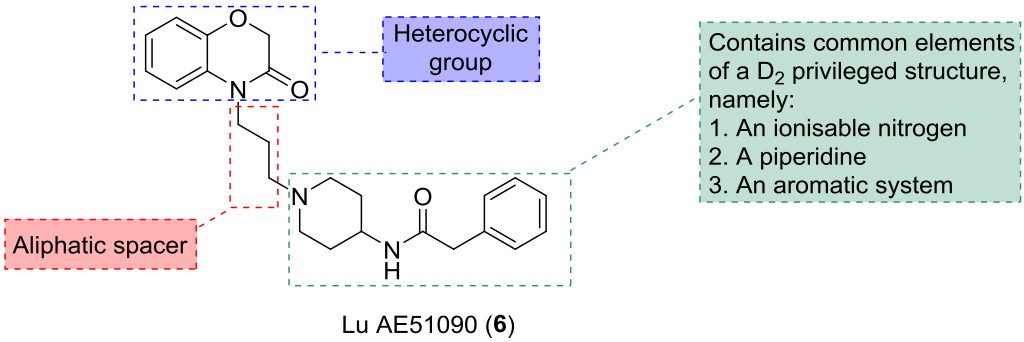

Figure 2. Structure of **6** highlighting common dopaminergic D_2 structural characteristics; a motif containing features of common privileged structures namely an aryl system and ionisable nitrogen atom, an aliphatic spacer/linker and a heterocyclic group.

Therefore, utilising compound **6** as our primary scaffold, we envisioned that we could design in an enhanced D_2R binding profile using the designed multiple ligand (DML) approach described by Morphy that takes two separate pharmacophores with distinct pharmacology and integrates them into one molecule that has the attributes of both parent molecules. In this approach the degree of integration is systematically increased until the structure becomes merged and essentially more drug-like.[17] We made use of privileged structures from known D_2R ligands that covered three distinct classes (Figure 3); 1) phenylpiperazines which are known to be important motifs for D_2R affinity and functional activity. Our previous work demonstrated that compounds incorporating the 2,3-dichlorophenylpiperazine and 2-methoxyphenylpiperazine scaffolds are useful in the design of antagonists and partial agonists for the D_2R.[16] 2) Using privileged structures from two distinct antipsychotics (ziprasidone and risperidone) that have a piperazine or piperidine moiety followed by similar structural heterocycles.[18] 3) Using a privileged structure from a partial agonist (bifeprunox) which is unique compared to the 2,3-dichloro- and 2-methoxyphenylpiperazine family.

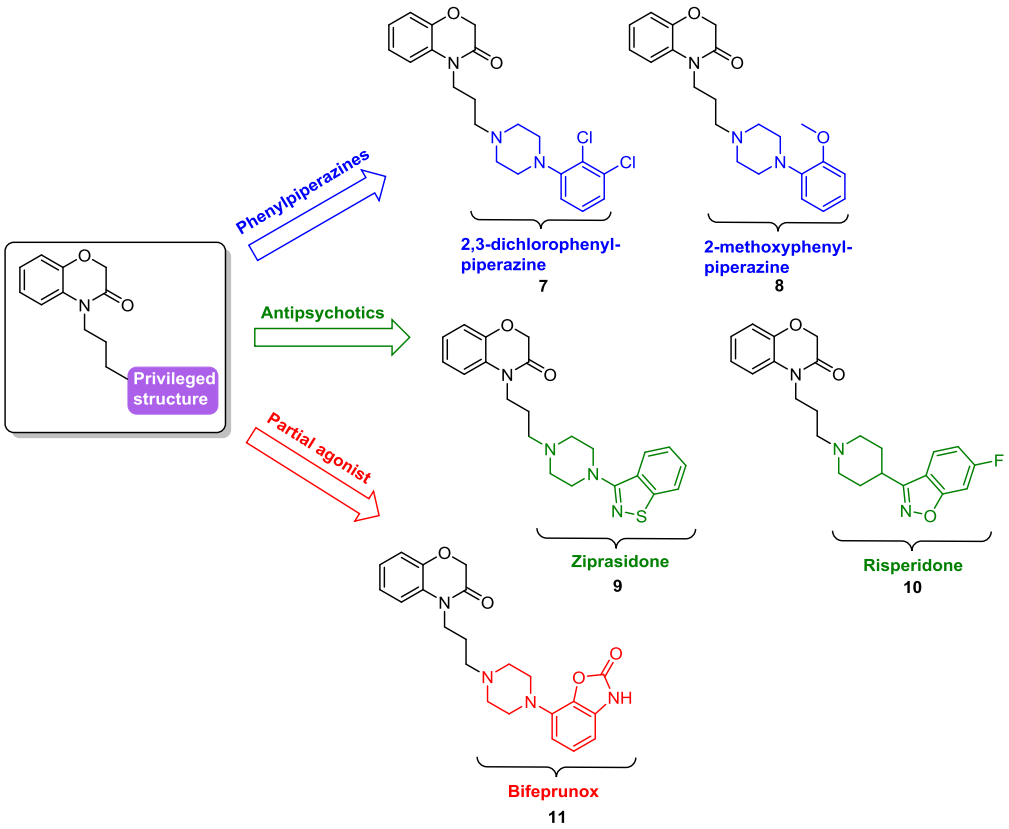

Figure 3. Merged DMLs (**7-11**) derived from combining the propyl benzoxazinone moiety from **6** with D_2 privileged structures (coloured segments) from parent ligands **1-5**.

As such, rather than embarking on a screening program to identify ligands that display the desired pharmacology for two or more receptors required for activity, we hoped to achieve this polypharmcology through the rational combination of distinct pharmacophores.[19] To characterise the ligands, we pharmacologically evaluated them in radioligand binding assays for all three receptors (D_2R, M_1 mAChR and 5-$HT_{2A}R$). To evaluate the ligands in functional assays we tested them in ERK1/2 phosphorylation assays for the D_2R, intracellular Ca^{2+} mobilisation assays for the M_1 mAChR and IP_1 accumulation assays for the 5-$HT_{2A}R$.

Results and discussion

Chemistry. The syntheses of all DMLs and the reference M_1 ligand (**6**) are outlined in Scheme 1. This initially required the installation of a 3-carbon atom spacer to the precursor benzoxazinone (**12**). This reaction was performed under alkaline conditions using 60% sodium

hydride and a large excess of dibromopropane to give the key intermediate **13**. Rapid diversification with compound **13** and the required privileged structures, as illustrated in Figure 3, furnished the target DMLs (**7-11**) in yields of 17-75%. The chemical synthesis of compound **6** (which is also commercially available) followed similar conditions to that previously published.[15] Compound **13** was refluxed under basic conditions with 4-*N*-Boc-aminopiperidine to afford compound **14** in respectable yield. The final step was achieved by removal of the Boc protecting group (**15**) and subsequent reaction with 2-phenylacetyl chloride to generate the target compound (**6**) in 82% yield.

Scheme 1. Synthesis of DMLs (**7-11**) and compound **6**[a]

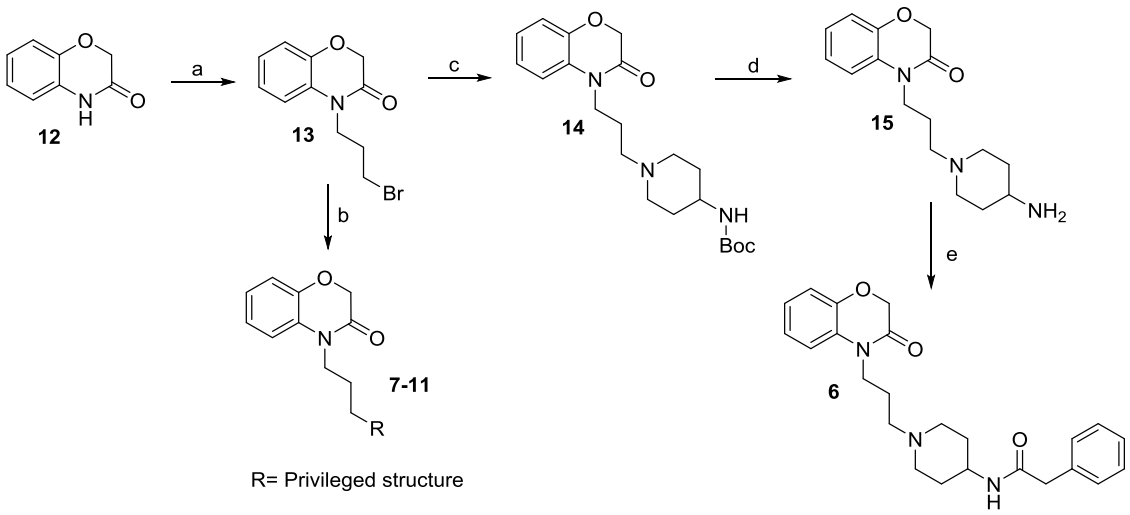

[a]Reagents and conditions: (a) Dibromopropane, NaH (60%), DMF, N_2, RT, 67%; (b) privileged structures, DIPEA, NaI, CH_3CN, reflux, 5 h or overnight, 17-75%; (c) 4-*N*-Boc-aminopiperidine, K_2CO_3, CH_3CN, 80 °C, 62%; (d) TFA, DCM, RT, overnight, 73%; (e) 2-phenylacetyl chloride, Et_3N, THF, N_2, 0 °C→RT, 1.5 h, 82%.

Pharmacology.

D_2R binding and functional characterization of DMLs. The synthesized DMLs were pharmacologically characterized in both radioligand binding and functional ERK1/2 phosphorylation (pERK1/2) assays for the D_2R. The pERK assay provides a robust readout for D_2R activation and is medium throughput thereby allowing efficient screening of a number of

compounds. The results of these studies are summarized in Table 1. Compound **6** demonstrated the weakest binding affinity (pK_i) consistent with previously published results.[15] Compounds **10** and **11** (consisting of the motifs from risperidone (**2**) and bifeprunox (**4**), respectively) exhibited the highest binding affinities (K_i = 3.2 nM and 1.7 nM, respectively) for the D_2R overall. This result is consistent with the high affinity of the parent compounds **2** and **4**.[20] Indeed the incorporation of D_2R privileged structures conferred a significant increase in D_2R affinity for all compounds as compared to **6** apart from the incorporation of the 2,3-dichlorophenylpiperazine moiety (**7**). The high binding affinity of **10** at the D_2R may be attributed to its bicyclic system of greater molecule size as opposed to compound **8** (phenylpiperazine), and its piperidine moiety compared to the piperazine of both **8** and **9**. Furthermore, the equally high binding affinity of **11** may result from being the only heterocyclic moiety that contains a H-bond donor capable of hydrogen bond interactions with residues such as serines present in transmembrane domain 5 in the orthosteric binding site. For functional pERK1/2 assays, all ligands were initially tested in time-course assays (data not shown), upon which we identified ligands **7-10** to be antagonists at the D_2R and compound **11** as an agonist. Importantly, this latter result is consistent with the partial agonist action of bifeprunox; the ligand from which the 7-(piperazin-1-yl)benzo[*d*]oxazol-2(3*H*)-one moiety was derived. To determine the functional affinity (pK_B) of each of the antagonists, we performed interaction studies using varying concentrations of dopamine. The functional affinities correlated well with the binding affinities obtained. Compound **11**, derived from merging the privileged structure of **4** with **6**, was a potent agonist at the D_2R in both pERK1/2 and cAMP signaling assays (Table 2; 0.64 nM and 96 pM, respectively). We calculated a bias factor for compound **11** relative to the full agonist ropinirole (Supporting Information Table 1 and Figure 1) and found that **11** displays a similar bias towards cAMP over pERK1/2 to that previously determined for aripiprazole (fold bias = 448 and 102, respectively).[16] The results from Table 1 show that the D_2 profile of the ligands are significantly enhanced with

the incorporation of the privileged structures and compounds from all three classes (phenylpiperazines, antipsychotics and partial agonists) with the benzoxazinone scaffold from **6** at the D_2R.

Table 1. Binding and functional data at the D_2R, M_1 mAChR and 5-$HT_{2A}R$ for all DMLs[a]

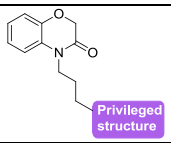

		D_2R		M_1 mAChR			5-$HT_{2A}R$	
Compd	**Privileged structure**	**Binding pK_i ± SEM (K_i, nM)[b]**	**pERK1/2 pK_B ± SEM (K_B, nM)[c]**	**Binding pIC_{50} ± SEM (IC_{50}, nM)[b]**	**Ca^{2+} pEC_{50} ± SEM (EC_{50}, nM)**	**Ca^{2+} E_{max} ± SEM[d]**	**Binding pK_i ± SEM (K_i, nM)[b]**	**IP_1 pK_B± SEM (K_B, nM)[e]**
6	-	6.08 ± 0.28 (834)	5.68 ± 0.34 (2091)	5.07 ± 0.11 (8525)	6.89 ± 0.14 (129)	101 ± 6	5.98 ± 0.29 (1042)	5.80 ± 0.06 (1574)
7	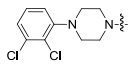	6.56 ± 0.10 (273)	7.00 ± 0.12 (99.0)	5.73 ± 0.09 (1872)	n/a	n/a	7.12 ± 0.21 (75.8)	5.73 ± 0.03 (1861)
8	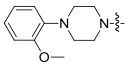	7.37 ± 0.10 (42.7)	8.11 ± 0.11 (7.8)	5.29 ± 0.08 (5180)	n/a	n/a	6.56 ± 0.31 (275)	6.24 ± 0.09 (578)
9	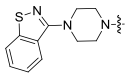	7.75 ± 0.10 (17.7)	8.16 ± 0.10 (7.0)	5.38 ± 0.13 (4191)	5.98 ± 0.25 (1042)	64 ± 10	8.24 ± 0.37 (5.8)	6.63 ± 0.05 (235)
10	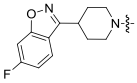	8.49 ± 0.12 (3.2)	8.91 ± 0.16 (1.2)	5.49 ± 0.07 (3253)	n/a	n/a	8.57 ± 0.16 (2.7)	7.67 ± 0.07 (21.2)
11	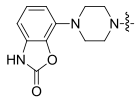	8.76 ± 0.14 (1.7)	-	5.37 ± 0.10 (4259)	n/a	n/a	6.25 ± 0.44 (568)	5.94 ± 0.10 (1138)

[a]Data are the mean of three-four experiments ± SEM performed in duplicate. [b]Binding affinity values are obtained using [^{3}H]raclopride (D_{2L} whole cells) or [^{3}H]NMS (M_1 mAChR whole cells) or [^{3}H]ketanserin (5-HT_{2A} membranes). [c]Interaction studies with varying concentrations of dopamine in an assay measuring levels of pERK1/2. Data are fit to the Gaddum/Schild analysis. [d]E_{max} is the percentage of maximal activity relative to the maximal activity of ACh in the intracellular calcium mobilization assay. [e]IP_1 accumulation assay through interaction with varying concentrations of serotonin. n/a= compound not active.

Table 2. Profiling of compound **11** in functional assays at the D_2R[ab]

	ERK1/2 phosphorylation		**cAMP**	
Compd	**pEC_{50} ± SEM (EC_{50}, nM)**	**E_{max}[c] ± SEM**	**pEC_{50} ± SEM (EC_{50}, nM)**	**E_{max}[c] ± SEM**
11	9.20 ± 0.29 (0.64)	26 ± 3	10.02 ± 0.13 (0.096)	97 ± 2

[a]Data are the mean of four-six experiments ± SEM performed in duplicate. [b]Data is generated via concentration-response curves. [c]E_{max} is the percentage of maximal activity relative to the maximal activity of FBS (pERK1/2) or ropinirole (cAMP).

M_1 mAChR binding and functional characterization of DMLs. As previously indicated, we tested compounds in both radioligand binding and functional assays at the M_1 mAChR (Table 1). All compounds displaced [^{3}H]NMS at the M_1 mAChR with relatively weak inhibitory potencies (IC_{50}), with compound **7** displaying the highest inhibitory potency (IC_{50}= 1.9 μM), as compared to **6** (IC_{50}= 8.5 μM, $p < 0.05$). As a functional assay for the M_1 mAChR we used an intracellular Ca^{2+} mobilization assay as a measure of coupling to G_q pathways. Only DML **9**, showed activity at the M_1 mAChR, displaying a diminished potency (EC_{50} =1.04 μM) as compared to **6** (EC_{50}= 129 nM) equating to an 8-fold loss in potency. The maximal stimulation (E_{max}) of **9** was also reduced to 64% compared to **6** which demonstrated an E_{max} of 101% (defined by the maximal effect of ACh) consistent with an action as a partial agonist. The subtle differences in the D_2R privileged structures used could account for their loss in M_1 mAChR activity. For example the M_1 mAChR may not accommodate the more linear orientation of the phenylpiperazine analogues **7** and **8** as compared to a more flexible structure present in **6**. For the antipsychotics, the ziprasidone and risperidone privileged structures reveal slightly different heterocycles (benzoisothiazole vs benzoisoxazole), in addition to the absence of a fluorine substituent on the aromatic ring, perhaps making **9** more favourable for the M_1 mAChR than **10**, as a fluorine atom is powerfully electron-withdrawing and subsequently deactivates an aromatic system. This makes it partially positive in nature and complementary to relatively electron rich and activated aryl systems of amino acids in a receptor such as tryptophan, tyrosine and phenylalanine. The results also suggest that it is unclear whether a piperazine or piperidine is more ideally suited for activity at the M_1 mAChR and perhaps the functionality before and after the six-membered ring containing ionisable nitrogen at physiological pH is more detrimental for activity. Compound **11**, as compared to similar structures **9** and **10**, was connected to the flexible piperazine through the phenyl ring as opposed to the five-membered ring being directly connected to the piperazine or

piperidine, which possibly affected the binding of the ligand at the M_1 mAChR and therefore attributed to its loss of activity.

5-HT_{2A}R binding and functional characterization of DMLs.

There is substantial literature evidence that the antagonism of serotonin 5-HT_{2A} receptors (5-HT_{2A}R) is important for the therapeutic efficacy of atypical antipyschotics such as clozapine.[21] In addition, compounds **9** and **10** stem from antipsychotics **1** and **2** respectively that display high affinity for the 5-HT_{2A}R. Therefore we deemed it prudent to investigate if this attribute was maintained upon integration of these privileged structures into the M_1 mAChR/D_2R DML and tested the ligands in a radioligand binding assay to determine their affinities for this receptor (Table 1). Consistent with the literature,[15] the M_1 mAChR agonist **6**, demonstrated poor binding to the 5-HT_{2A}R (K_i ~ 1 μM). Both phenylpiperazine analogues **7** and **8** showed no notable enhancements in affinity as compared to **6**. Of note, DMLs **9** and **10** show a strong binding affinity for the 5-HT_{2A}R (K_i values of 5.8 nM and 2.7 nM, respectively). Compound **11**, which as mentioned previously has a slightly different heterocycle following the piperazine, had a diminished binding affinity similar to its M_1 mAChR functional profile. As both **9** and **10** maintain their D_2/5-HT_{2A} binding profiles, it is evident that both privileged structures exhibit versatility for use in the design of ligands with favourable polypharmacology. The compounds were also tested in an IP_1 functional assay at the 5-HT_{2A}R. When tested in the absence of serotonin (Supporting Figure 2.) all compounds showed no activation of the receptor, except for compound **7**. As such compounds **8-11** are all antagonists at the serotonin receptor. In agreement with the binding data for the 5-HT_{2A}R, compound **6** demonstrated the weakest functional affinity. DMLs containing the ziprasidone and risperidone privileged structures both showed the highest functional affinities with compound **10** displaying an 11-fold increase over compound **9** ($p < 0.05$). As mentioned in the introduction, antagonism at the 5-HT_{2A}R is useful for

antipsychotics, therefore all DMLs, excluding compound **7**, are useful starting compounds for further SAR studies and optimization.

Compound **9** was our most promising candidate as it displayed activity at all three receptor targets. Despite showing strong affinities for both the D_2R and 5-$HT_{2A}R$ (Table 1; K_i values of 17.7 nM and 5.8 nM, respectively), there was a significant reduction in potency at the M_1 mAChR (EC_{50}= 1.04 μM, E_{max}= 64%). However, we have shown that we can use a merged DML approach utilizing D_2R privileged structures to confer a D_2R pharmacological profile to a putative M_1 mAChR allosteric agonist. In addition to this, privileged structures derived from parent structures with known D_2/5-HT_{2A} receptor binding profiles were maintained thus validating their usefulness in a DML approach. It should be noted that it was difficult to maintain activity at the M_1 mAChR as only one structure was able to show any noteworthy agonism. It is therefore possible that key elements in the structure of **6** that account for its M_1 mAChR allosteric agonist profile were lost as a result of the integration process. As such, new structural analogues may look at incorporating greater elements of the original structure. To expand on this work, it may also be useful to incorporate other benzoxazinones or heterocyclic compounds similar to this scaffold as a way to optimize and possibly enhance the M_1 mAChR profile. Additionally, other selective M_1 mAChR agonists[22,23] may be explored for optimization as a DML.

Conclusion

In terms of antipsychotic action, engaging multiple targets has become useful in the drug design process in order to address the numerous symptom domains of schizophrenia. The DML approach offers a way to selectively design in polypharmacology by using privileged structures that are known to be advantageous towards the targets of interest. Ligands in this study were designed to be D_2 antagonists or partial agonists for the positive symptoms, M_1 mAChR

allosteric agonists for the cognitive deficits and antagonists at the 5-HT_{2A}R to address the negative symptoms and reduce the occurrence of extrapyramidal side effects. The privileged structures covered phenylpiperazines in addition to mixed piperazine/piperidine heterocyclic compounds derived from antipsychotics or a clinically developed compound. The final DMLs (**7-11**) were generally well-tolerated at the D_2R and 5-HT_{2A}R, but are in need of further development at the M_1 mAChR. Despite this, we identified compound **9**, incorporating a privileged structure derived from the antipsychotic ziprasidone, that retained strong binding and functional activity at the D_2R and 5-HT_{2A}R and weak partial agonism at the M_1 mAChR. Compound **9** represents a useful starting point for further optimization to improve its M_1 mAChR profile.

References

1. Seeman, P. Antipsychotic drugs, dopamine receptors, and schizophrenia. *Clin. Neurosci. Res.* **2001,** *1*, 53-60.

2. Leysen, J. E.; Janssen, P. M. F.; Megens, A. A. H. P.; Schotte, A. Risperidone: A novel antipsychotic with balanced serotonin-dopamine antagonism, receptor occupancy profile, and pharmacologic activity. *J. Clin. Psychiatry* **1994,** *55*, 5-12.

3. Seeger, T. F.; Seymour, P. A.; Schmidt, A. W.; Zorn, S. H.; Schulz, D. W.; Lebel, L. A.; McLean, S.; Guanowsky, V.; Howard, H. R.; Lowe, J. A. Ziprasidone (CP-88,059): A new antipsychotic with combined dopamine and serotonin receptor antagonist activity. *J. Pharmacol. Exp. Ther.* **1995,** *275*, 101-113.

4. Roth, B. L.; Sheffler, D. J.; Kroeze, W. K. Magic shotguns versus magic bullets: Selectively non-selective drugs for mood disorders and schizophrenia. *Nat. Rev. Drug. Discov.* **2004,** *3*, 353-359.

5. Lindsley, C. W. The top prescription drugs of 2012 globally: Biologics dominate, but small molecule CNS drugs hold on to top spots. *ACS Chem. Neurosci.* **2013,** *4*, 905-907.

6. Kikuchi, T.; Tottori, K.; Uwahodo, Y.; Hirose, T.; Miwa, T.; Oshiro, Y.; Morita, S. 7-(4-[4-(2,3-dichlorophenyl)-1-piperazinyl]butyloxy)-3,4-dihydro-2(1H)-quinolinone (opc-14597), a new putative antipsychotic drug with both presynaptic dopamine autoreceptor agonistic activity and postsynaptic D_2 receptor antagonistic activity. *J. Pharmacol. Exp. Ther.* **1995,** *274*, 329-336.

7. Kiss, B.; Horváth, A.; Némethy, Z.; Schmidt, É.; Laszlovszky, I.; Bugovics, G.; Fazekas, K.; Hornok, K.; Orosz, S.; Gyertyán, I.; Ágai-Csongor, É.; Domány, G.; Tihanyi, K.; Adham, N.; Szombathelyi, Z. Cariprazine (RGH-188), a dopamine D_3 receptor-preferring, D_3/D_2 dopamine receptor antagonist–partial agonist antipsychotic candidate: In vitro and neurochemical profile. *J. Pharmacol. Exp. Ther.* **2010,** *333*, 328-340.

8. Citrome, L. A review of the pharmacology, efficacy and tolerability of recently approved and upcoming oral antipsychotics: An evidence-based medicine approach. *CNS Drugs* **2013,** *27*, 879-911.

9. Ehrlich, K.; Gotz, A.; Bollinger, S.; Tschammer, N.; Bettinetti, L.; Harterich, S.; Hubner, H.; Lanig, H.; Gmeiner, P. Dopamine D_2, D_3, and D_4 selective phenylpiperazines as molecular probes to explore the origins of subtype specific receptor binding. *J. Med. Chem.* **2009,** *52*, 4923-4935.

10. Anagnostaras, S. G.; Murphy, G. G.; Hamilton, S. E.; Mitchell, S. L.; Rahnama, N. P.; Nathanson, N. M.; Silva, A. J. Selective cognitive dysfunction in acetylcholine M_1 muscarinic receptor mutant mice. *Nat. Neurosci.* **2003,** *6*, 51-58.

11. Shekhar, A.; Potter, W. Z.; Lightfoot, J.; Lienemann, J.; Dube, S.; Mallinckrodt, C.; Bymaster, F. P.; McKinzie, D. L.; Felder, C. C. Selective muscarinic receptor agonist xanomeline as a novel treatment approach for schizophrenia. *Am. J. Psychiatry* **2008,** *165*, 1033-1039.

12. Conn, P. J.; Jones, C. K.; Lindsley, C. W. Subtype-selective allosteric modulators of muscarinic receptors for the treatment of CNS disorders. *Trends Pharmacol. Sci.* **2009,** *30*, 148-155.

13. Davie, B. J.; Christopoulos, A.; Scammells, P. J. Development of M_1 mAChR allosteric and bitopic ligands: Prospective therapeutics for the treatment of cognitive deficits. *ACS Chem. Neurosci.* **2013,** *4*, 1026-1048.

14. Jeffrey Conn, P.; Christopoulos, A.; Lindsley, C. W. Allosteric modulators of GPCRs: A novel approach for the treatment of CNS disorders. *Nat. Rev. Drug. Discov.* **2009,** *8*, 41-54.

15. Sams, A. G.; Hentzer, M.; Mikkelsen, G. K.; Larsen, K.; Bundgaard, C.; Plath, N.; Christoffersen, C. T.; Bang-Andersen, B. Discovery of *N*-{1-[3-(3-oxo-2,3-dihydrobenzo[1,4]oxazin-4-yl)propyl]piperidin-4-yl}-2-phenylacetamide (Lu AE51090): An allosteric muscarinic M_1 receptor agonist with unprecedented selectivity and procognitive potential. *J. Med. Chem.* **2010,** *53*, 6386-6397.

16. Szabo, M.; Klein Herenbrink, C.; Christopoulos, A.; Lane, J. R.; Capuano, B. Structure–activity relationships of privileged structures lead to the discovery of novel biased ligands at the dopamine D_2 receptor. *J. Med. Chem.* **2014,** *57*, 4924-4939.

17. Morphy, R.; Rankovic, Z. Designing multiple ligands - medicinal chemistry strategies and challenges. *Curr. Pharm. Design* **2009,** *15*, 587-600.

18. Chen, Y.; Wang, S.; Xu, X.; Liu, X.; Yu, M.; Zhao, S.; Liu, S.; Qiu, Y.; Zhang, T.; Liu, B.-F.; Zhang, G. Synthesis and biological investigation of coumarin piperazine (piperidine) derivatives as potential multireceptor atypical antipsychotics. *J. Med. Chem.* **2013,** *56*, 4671-4690.

19. Sams, A. G.; Larsen, K.; Mikkelsen, G. K.; Hentzer, M.; Christoffersen, C. T.; Jensen, K. G.; Frederiksen, K.; Bang-Andersen, B. Hit-to-lead investigation of a series of novel combined dopamine D_2 and muscarinic M_1 receptor ligands with putative antipsychotic and pro-cognitive potential. *Bioorg. Med. Chem. Lett.* **2012,** *22*, 5134-5140.

20. Feenstra, R. W.; de Moes, J.; Hofma, J. J.; Kling, H.; Kuipers, W.; Long, S. K.; Tulp, M. T. M.; van der Heyden, J. A. M.; Kruse, C. G. New 1-aryl-4-(biarylmethylene)piperazines as potential atypical antipsychotics sharing dopamine D_2-receptor and serotonin 5-HT_{1A}-receptor affinities. *Bioorg. Med. Chem. Lett.* **2001,** *11*, 2345-2349.

21. Meltzer, H. Y. The role of serotonin in antipsychotic drug action. *Neuropsychopharmacology* **1999,** *21*, 106S-115S.

22. Avlani, V. A.; Langmead, C. J.; Guida, E.; Wood, M. D.; Tehan, B. G.; Herdon, H. J.; Watson, J. M.; Sexton, P. M.; Christopoulos, A. Orthosteric and allosteric modes of interaction of novel selective agonists of the M_1 muscarinic acetylcholine receptor. *Mol. Pharmacol.* **2010,** *78*, 94-104.

23. Keov, P.; Valant, C.; Devine, S. M.; Lane, J. R.; Scammells, P. J.; Sexton, P. M.; Christopoulos, A. Reverse engineering of the selective agonist TBPB unveils both orthosteric and allosteric modes of action at the M_1 muscarinic acetylcholine receptor. *Mol. Pharmacol.* **2013,** *84*, 425-437.

Supporting Information- Chapter 4

Supporting Information Table 1. Calculated bias factors for compound **11** and the full agonist ropinirole at the D_2R. For full details of calculations, refer to previous publication.[1]

	pERK1/2		cAMP		
Compd	**Log τ/K_A**	**Δ Log τ/K_A**	**Log τ/K_A**	**Δ Log τ/K_A**	**ΔΔ Log τ/K_A (Bias)**
Ropinirole	8.82 ± 0.08	0 ± 0.08	8.07 ± 0.05	0 ± 0.05	0 ± 0.09
11	8.76 ± 0.32	-0.06 ± 0.33	10.02 ± 0.05	1.95 ± 0.05	2.01 ± 0.33** (102.3)

Data are the mean of four separate experiments ± SEM performed in duplicate. Bias is defined as the fold bias relative to the reference agonist ropinirole. Statistical significance is measured by a two-tailed t-test; (**) $p < 0.01$.

Supporting Information Figure 1. Bias plot representing the bias factor (ΔΔ Log τ/K_A) of ligands between pERK1/2 and cAMP signaling pathways. Value from aripiprazole is from a previous publication.[1]

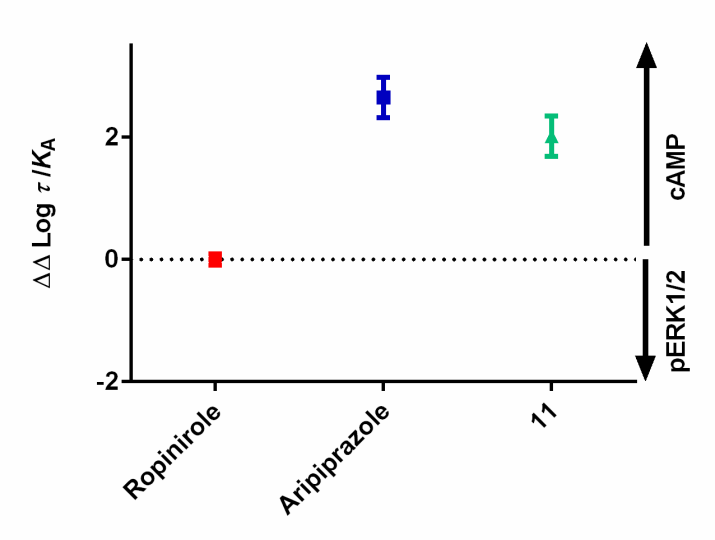

Supporting Information Figure 2. Compounds tested in the IP_1 accumulation assay at the 5-HT_{2A}R in the absence of serotonin. Compound **7** shows weak activation.

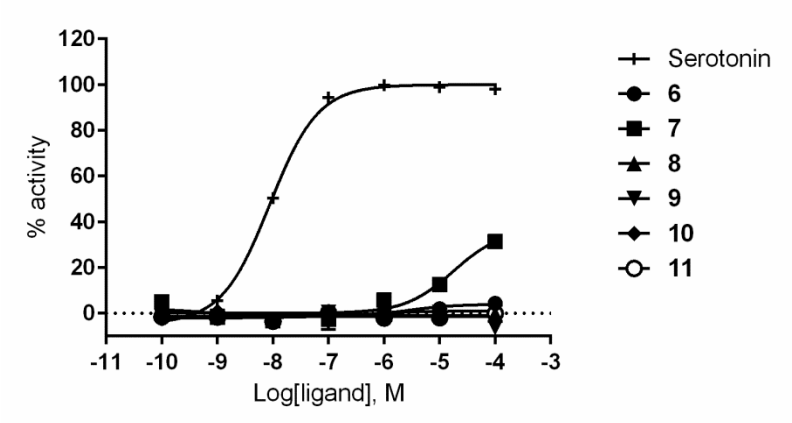

Experimental

Chemistry. All solvents and chemicals were purchased from standard suppliers and were used without any further purification. ^{1}H NMR and ^{13}C NMR spectra were acquired at 400.13 and 100.62 MHz respectively, on a Bruker Advance III 400 MHz UltrashieldPlus NMR spectrometer using TOPSPIN 2.1 software. Chemical shifts (δ) for all ^{1}H spectra are reported in parts per million (ppm) using tetramethylsilane (TMS, 0 ppm) as the reference. The data for all spectra are reported in the following format: chemical shift (δ), (multiplicity, coupling constants *J* (Hz), integral), where the multiplicity is defined as: s = singlet, d= doublet, t= triplet, q=quartet, p= pentet, st= sextet and m = multiplet. For ^{13}C NMR spectra C= quaternary carbon, CH= methine carbon, CH_2= methylene carbon, and CH_3= methyl carbon.

The purity and retention time of final products was determined on an Agilent 1260 Infinity analytical reverse-phase HPLC system fitted with a Poroshell 120 SB-C18 4.6X 100mm 2.7u column. The HPLC operates on Agilent OpenLAB CDS Rev C.01.04 software. Solvent A is water + 0.1% TFA and solvent B is acetonitrile + 0.1% TFA. Samples were run using a gradient method (5-100% solvent B over 10 minutes). The purity of all compounds are ≥ 95%.

Thin layer chromatography (TLC) was carried out routinely on silica gel $60F_{254}$ pre-coated plates (0.25 mm, Merck). Flash column chromatography was carried out using Merck Silica gel 60, 230-400 mesh ASTM.

Synthesis of key intermediate, 4-(3-bromopropyl)-2*H*-benzo[*b*][1,4]oxazin-3(4*H*)-one (13).[2]

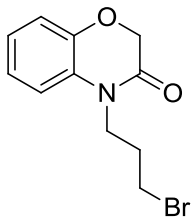

Compound **12** (5.06 g, 33.4 mmol) was dissolved in DMF (20 mL). Nitrogen gas was bubbled through the solution for 10 mins before the addition of 60% NaH (1.49 g, 37.3 mmol), which was added slowly to the reaction mixture. After stirring for 1.5 h at rt, the dibromopropane (17.2 mL, 170 mmol) was added dropwise. After overnight stirring, 20 mL of brine was added and once cooled back to rt, the product was extracted with ethyl acetate (2 × 20 mL). The organic layers were pooled, dried over anhydrous sodium sulfate, filtered and evaporated to dryness to give the crude product. Further purification by flash gradient column chromatography (petroleum spirits: ethyl acetate 5:1) gave the product as a colorless oil (6.16 g, 67%). ^{1}H NMR ($CDCl_3$): δ 2.21-2.28 (m, 2H), 3.48 (t, *J* 6.4 Hz, 2H), 4.07-4.11 (m, 2H), 4.60 (s, 2H), 7.00-7.04 (m, 2H), 7.05-7.07 (m, 2H). ^{13}C NMR ($CDCl_3$): δ 30.2 (CH_2), 30.5 (CH_2), 40.1 (CH_2), 67.7 (CH_2), 114.8 (CH), 117.4 (CH), 123.1 (CH), 124.2 (CH), 128.4 (C), 145.4 (C), 164.6 (C).

General procedure for the synthesis of merged DMLs.

Compound **13** (1 equiv.) was dissolved in CH_3CN (10 mL). NaI (1 equiv.), DIPEA (1-2 equiv.) and the required amine (1 equiv.) were added and heated at reflux for 5-6 h. After this time, the CH_3CN was removed in vacuo and the resulting residue dissolved in ethyl acetate (20 mL). Aqueous K_2CO_3 (1 M, 20 mL) was added and the product further extracted with ethyl acetate (2 × 20 mL). The organic layers were combined and washed with water (20 mL) and brine (20 mL),

dried over anhydrous Na_2SO_4, filtered and evaporated to dryness to give the crude product. Purification via column chromatography (petroleum spirits/ethyl acetate 1:1) gave the pure product.

4-(3-(4-(2,3-Dichlorophenyl)piperazin-1-yl)propyl)-2*H*-benzo[*b*][1,4]oxazin-3(4*H*)-one (7).

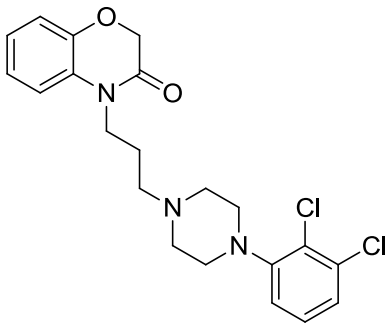

Yellow oil (225 mg, 72%). ^{1}H NMR ($CDCl_3$): δ 1.86-1.93 (m, 2H), 2.51 (t, *J* 7.0 Hz, 2H), 2.63 (m, 4H), 3.07 (m, 4H), 4.01-4.05 (m, 2H), 4.60 (s, 2H), 6.95-7.05 (m, 4H), 7.10-7.16 (m, 3H). ^{13}C NMR ($CDCl_3$): δ 24.5 (CH_2), 39.5 (CH_2), 51.4 (CH_2), 53.4 (CH_2), 55.6 (CH_2), 67.7 (CH_2), 115.1 (CH), 117.3 (CH), 118.7 (CH), 122.8 (CH), 123.9 (CH), 124.7 (CH), 127.5 (CH), 127.6 (C), 128.7 (C), 134.1 (C), 145.5 (C), 151.3 (C), 164.4 (C). HPLC purity (λ= 214 nm): 100%, t_R = 6.62 min. HRMS (ESI)-TOF (*m/z*): $[M+H]^+$ 420.1246 calcd for $C_{21}H_{23}Cl_2N_3O_2$; found $[M+H]^+$ 420.1249.

4-(3-(4-(2-Methoxyphenyl)piperazin-1-yl)propyl)-2*H*-benzo[*b*][1,4]oxazin-3(4*H*)-one (8).

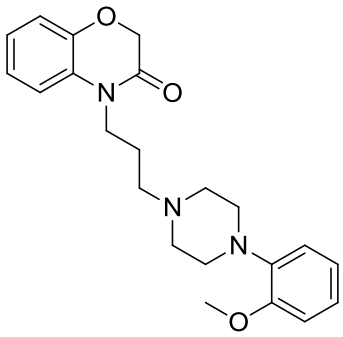

Orange oil (143 mg, 43%). ^{1}H NMR ($CDCl_3$): δ 1.86-1.93 (m, 2H), 2.49 (t, *J* 7.0 Hz, 2H), 2.64 (m, 4H), 3.10 (m, 4H), 3.85 (s, 3H), 4.00-4.04 (m, 2H), 4.59 (s, 2H), 6.84-7.04 (m, 7H), 7.11 (m, 1H). ^{13}C NMR ($CDCl_3$): δ 24.5 (CH_2), 39.5 (CH_2), 50.7 (CH_2), 53.5 (CH_2), 55.4 (CH_3), 55.6

(CH_2), 67.7 (CH_2), 111.2 (CH), 115.1 (CH), 117.1 (CH), 118.2 (CH), 121.0 (CH), 122.8 (CH), 123.0 (CH), 123.8 (CH), 128.7 (C), 141.4 (C), 145.4 (C), 152.3 (C), 164.4 (C). HPLC purity (λ= 214 nm): 98%, t_R = 5.83 min. HRMS (ESI)-TOF (*m/z*): $[M+H]^+$ 382.2131 calcd for $C_{22}H_{27}N_3O_3$; found $[M+H]^+$ 382.2129.

4-(3-(4-(Benzo[*d*]isothiazol-3-yl)piperazin-1-yl)propyl)-2*H*-benzo[*b*][1,4]oxazin-3(4*H*)-one (9).

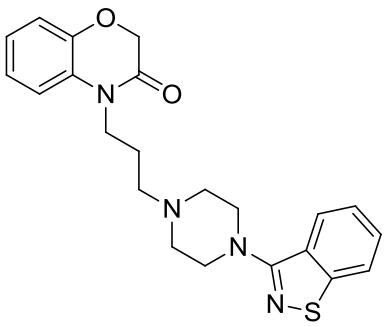

Pale Yellow oil (208 mg, 69%). ^{1}H NMR ($CDCl_3$): δ 1.91 (m, 2H), 2.51 (t, *J* 6.9 Hz, 2H), 2.65-2.68 (m, 4H), 3.55-3.57 (m, 4H), 4.04 (t, *J* 7.3 Hz, 2H), 4.60 (s, 2H), 6.98-7.05 (m, 3H), 7.13 (d, *J* 7.6 Hz, 1H), 7.35 (t, *J* 7.5 Hz, 1H) 7.45 (t, *J* 7.5 Hz, 1H), 7.80 (d, *J* 8.1 Hz, 1H), 7.90 (d, *J* 8.2 Hz, 1H). ^{13}C NMR ($CDCl_3$): δ 24.5 (CH_2), 39.5 (CH_2), 50.2 (CH_2), 53.1 (CH_2), 55.6 (CH_2), 67.7 (CH_2), 115.1 (CH), 117.2 (CH), 120.7 (CH), 122.9 (CH), 123.9 (CH),12.9 (CH), 124.0 (CH), 127.6 (CH), 128.1 (C), 128.7 (C), 145.4 (C), 152.8 (C), 164.0 (C), 164.4 (C). HPLC purity (λ= 214 nm): 100%, t_R = 6.19 min. HRMS (ESI)-TOF (*m/z*): $[M+H]^+$ 409.1698 calcd for $C_{22}H_{24}N_4O_2S$; found $[M+H]^+$ 409.1701.

4-(3-(4-(6-Fluorobenzo[*d*]isoxazol-3-yl)piperidin-1-yl)propyl)-2*H*-benzo[*b*][1,4]oxazin-3(4*H*)-one (10).

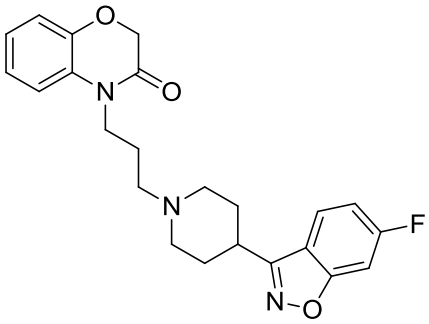

Yellow oil (226 mg, 75%). ^{1}H NMR ($CDCl_3$): δ 1.91 (m, 2H), 2.04-2.18 (m, 6H), 2.48 (t, *J* 6.9 Hz, 2H), 3.03-3.11 (m, 3H), 4.04 (t, *J* 7.3 Hz, 2H), 4.60 (s, 2H), 6.99-7.08 (m, 4H), 7.13 (d, *J* 7.7 Hz, 1H), 7.23 (dd, *J* 8.5, 1.9 Hz, 1H), 7.70 (dd, *J* 8.7, 5.1 Hz, 1H). ^{13}C NMR ($CDCl_3$): δ 24.6 (CH_2), 30.7 (CH_2), 34.6 (CH), 39.6 (CH_2), 53.7 (CH_2), 55.8 (CH_2), 67.7 (CH_2), 97.5 (CH, d, $^2J_{CF}$ 26.7 Hz)112.4 (CH, d, $^2J_{CF}$ 25.3 Hz), 115.1 (CH), 117.2 (CH), 117.4 (C), 122.7 (CH, d, $^3J_{CF}$11.1 Hz), 122.8 (CH), 123.9 (CH), 128.7 (C), 145.4 (C), 161.2 (C), 162.9 (C), 163.9 (C, d, $^3J_{CF}$ 13.6 Hz), 164.3 (C), 164.2 (C, d, $^1J_{CF}$ 250.6 Hz).HPLC purity (λ= 214 nm): 98%, t_R = 6.17min. HRMS (ESI)-TOF (*m/z*): $[M+H]^+$ 410.1880 calcd for $C_{23}H_{24}FN_3O_3$; found $[M+H]^+$ 410.1880.

4-(3-(4-(2-Oxo-2,3-dihydrobenzo[*d*]oxazol-7-yl)piperazin-1-yl)propyl)-2*H*-benzo[*b*][1,4]oxazin-3(4*H*)-one (11).

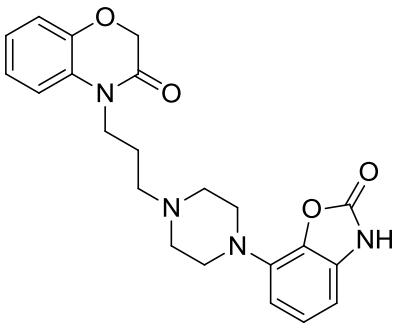

White solid (46 mg, 17%). ^{1}H NMR (DMSO-d_6): δ 1.72-1.79 (m, 2H), 2.39 (t, *J* 6.8 Hz, 2H), 2.52 (m, 4H), 3.18 (m, 4H), 3.96 (t, *J* 7.2 Hz, 2H), 4.63 (s, 2H), 6.60-6.64 (m, 2H), 7.00-7.02 (m, 3H) 7.08 (m, 1H), 7.28 (d, *J* 7.9 Hz, 1H). ^{13}C NMR (DMSO-d_6): δ 23.9 (CH_2), 38.7 (CH_2), 48.8 (CH_2), 52.6 (CH_2), 54.9 (CH_2), 67.1 (CH_2), 102.3 (CH), 109.8 (CH), 115.4 (CH), 116.6 (CH),

122.7 (CH), 123.4 (CH), 124.3 (CH), 128.5 (C), 131.1 (C), 133.3 (C), 135.3 (C), 145.0 (C), 154.0 (C), 163.9 (C). HPLC purity (λ= 214 nm): 98%, t_R = 5.17 min. HRMS (ESI)-TOF (*m/z*): $[M+H]^+$ 409.1876 calcd for $C_{22}H_{24}N_4O_4$; found $[M+H]^+$ 409.1882.

Synthesis of LuAE51090[2]

***tert*-Butyl (1-(3-(3-oxo-2*H*-benzo[*b*][1,4]oxazin-4(3*H*)-yl)propyl)piperidin-4-yl)carbamate (14).**

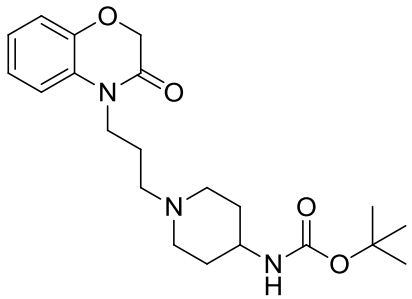

Compound **13** (717 mg, 2.7 mmol) and 4-*N*-Bocaminopiperidine (1.50 g, 7.5x mmol) were dissolved in CH_3CN (20 mL). K_2CO_3 (1.00 g, 7.2x mmol) was added and the reaction mixture stirred at 80 °C overnight. The reaction mixture was then cooled to room temperature and 20 mL of water was added. The aqueous layer was extracted with ethyl acetate (3 × 20 mL). The combined organic layers were then dried over anhydrous Na_2SO_4, filtered and evaporated to dryness to give the crude product. Purification via column chromatography (1:1 petroleum spirits/ ethylacetate to 100% ethyl acetate) yielded the desired product as a colourless oil (636 mg, 62%). ^{1}H NMR ($CDCl_3$): δ 1.37-1.47 (m, 2H), 1.44 (s, 9H), 1.84 (m, 2H), 1.94 (m, 2H), 2.06 (m, 2H), 2.40 (t, *J* 7.1 Hz, 2H), 2.81 (m, 2H), 3.46 (m, 1H), 3.98 (m, 2H), 4.44 (m, 1H), 4.58 (s, 2H), 6.98-7.09 (m, 4H). ^{13}C NMR ($CDCl_3$): δ 24.8 (CH_2), 28.5 (CH_3), 31.1 (CH), 32.7 (CH_2), 39.6 (CH_2), 52.6 (CH_2), 55.6 (CH_2), 67.8 (CH_2), 79.4 (C), 115.1 (CH), 117.2 (CH), 122.8 (CH), 123.9 (CH), 128.7 (C), 145.5 (C), 155.3 (C), 164.4 (C).

4-(3-(4-Aminopiperidin-1-yl)propyl)-2*H*-benzo[*b*][1,4]oxazin-3(4*H*)-one (15).

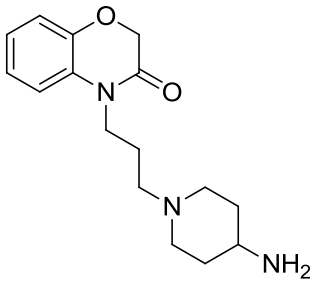

Compound **19** (350 mg, 0.9 mmol) was dissolved in DCM (5 mL) and TFA (0.5 mL) and stirred at room temperature overnight. The reaction mixture was then diluted with DCM (10 mL) and water (10 mL). 1 M aqueous NaOH was added until a pH of ~12. The aqueous layer was then extracted with 2 × 20 mL portions of DCM and the combined organic layers washed with water (20 mL), brine (20 mL), dried over anhydrous Na_2SO_4, filtered and evaporated to dryness to give the product as a colourless oil (191 mg, 73%). ^{1}H NMR ($CDCl_3$): δ 1.33-1.43 (m, 4H), 1.79-1.87 (m, 4H), 1.98 (m, 2H), 2.38 (m, 2H), 2.65 (m, 1H), 2.83 (m, 2H), 3.98 (m, 2H), 4.58 (s, 2H), 6.96-7.04 (m, 3H), 7.10-7.12 (m, 1H). ^{13}C NMR ($CDCl_3$): δ 24.7 (CH_2), 35.9 (CH_2), 39.4 (CH_2), 48.6 (CH), 52.5 (CH_2), 55.3 (CH_2), 67.5 (CH_2), 114.9 (CH), 116.9 (CH), 122.6 (CH), 123.6 (CH), 128.5 (C), 145.2 (C), 164.0 (C).

***N*-(1-(3-(3-Oxo-2*H*-benzo[*b*][1,4]oxazin-4(3*H*)-yl)propyl)piperidin-4-yl)-2-phenylacetamide (6).**

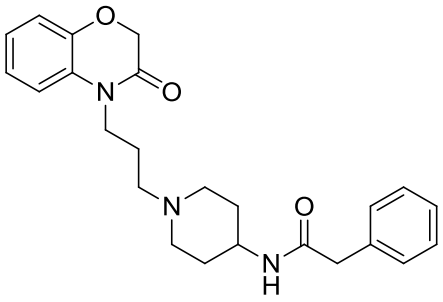

Compound **20** (188 mg, 0.65 mmol) and triethylamine (0.18 mL, 1.30 mmol) were dissolved in THF (8 mL) under N_2 and the reaction mixture cooled to 0 °C. Phenylacetyl chloride (201 mg, 1.30 mmol) was then added dropwise and after complete addition, the reaction mixture was

allowed to warm to room temperature and stirred for a further 1.5 h. The reaction mixture was partitioned between DCM (20 mL) and 1 M K_2CO_3 (20 mL) and the organic layer was removed. The aqueous phase was extracted with an additional 20 mL portion of DCM. The combined organic extracts were washed with water (30 mL), brine (30 mL), dried over anhydrous Na_2SO_4, filtered and the solvent removed in vacuo. The resulting crude product was purified via column chromatography (100% chloroform to 5% methanol) to give the title compound as a pale yellow solid (217 mg, 82%). ^{1}H NMR ($CDCl_3$): δ 1.35 (m, 2H), 1.78-1.88 (m, 4H), 2.07 (m, 2H), 2.38 (t, *J* 7.1 Hz, 2H), 2.72 (m, 2H), 3.55 (s, 2H), 3.80 (m, 1H), 3.95 (m, 2H), 4.57 (s, 2H), 5.24 (d, *J* 7.8 Hz, 1H), 6.96-7.05 (m, 4H), 7.24-7.38 (m, 5H). ^{13}C NMR ($CDCl_3$): δ 24.7 (CH_2), 32.0 (CH_2), 39.5 (CH_2), 44.1 (CH_2), 46.5 (CH), 52.3 (CH_2), 55.5 (CH_2), 67.8 (CH_2), 115.1 (CH), 117.3 (CH), 122.9 (CH), 123.9 (CH), 127.5 (CH), 128.7 (C), 129.2 (CH), 129.5 (CH), 135.1 (C), 145.5 (C), 164.4 (C), 170.4 (C). HPLC purity (λ= 214 nm): 97%, t_R = 5.40 min. HRMS (ESI)-TOF (*m/z*): $[M+H]^+$ 408.2287 calcd for $C_{24}H_{29}N_3O_3$; found $[M+H]^+$ 408.2291.

Pharmacology

[^{3}H]Raclopride and [^{3}H]NMS Binding Assays. FlpIn CHO cells stably expressing the human M_1 or D_{2L} receptor were grown and maintained in DMEM supplemented with 10% fetal bovine serum (FBS), and 200 μg/mL of Hygromycin-B, at 37°C in a humidified incubator containing 5% CO_2. Radioligand binding experiments were performed with receptors expressed on intact cells, which were seeded at 10,000 (M_1) or 40,000 (D_{2L}) cells/well and grown overnight at 37 °C. Assays were performed in a total volume of 200 μL in binding buffer (10 mM HEPES, 146 mM NaCl, 10 mM D-glucose, 5 mM KCl, 1 mM $MgSO_4.7H_2O$, 2 mM $CaCl_2$, 1.5 mM $NaHCO_3$, pH 7.4) containing 0.25 nM [^{3}H]Raclopride (for the dopamine D_2 receptor) or 0.3 nM [^{3}H]NMS (for the acetylcholine M_1 receptor), in the absence or presence of the competing compounds, and incubated for 1 hour at 37 °C. Assays were terminated by removal of the binding reaction mixture, followed by rapid washing, twice, with ice-cold 0.9% NaCl (100 μL/well). OptiPhase

Supermix scintillation cocktail (100 μL) was added, plates were sealed (TopSeal™), and radioactivity was measured in a MicroBeta^2 LumiJET microplate counter.

[^{3}H]Ketanserin Binding Assay.

Membrane preparation: FlpIn CHO cells stably expressing the human 5-HT_{2A} receptor were grown and maintained in DMEM/HAM's F12 media supplemented with 10% dialyzed fetal bovine serum (FBS), and 200 μg/mL of Hygromycin-B gold. Cells were maintained at 37 °C in a humidified incubator containing 5% CO_2. When cells were approximately 90-100% confluent, they were harvested and centrifuged (300g, 3 min). The resulting pellet was resuspended in wash buffer (50 mM TrisHCl, pH 7.4, cold), and the centrifugation procedure was repeated. The intact cell pellet was then resuspended in wash buffer and homogenized using a Polytron homogenizer for three 10 s intervals on the maximum setting, with 30 s periods on ice between each burst. The resulting sample was then recentrifuged at 40 000g for 30 min at 4 °C. The resulting pellet was resuspended in binding buffer (50 mM TrisHCl, 10 mM, $MgCl_2$, 0.1 EDTA, pH 7.4, RT) containing 250 mM sucrose and the protein content was determined using the method of Bradford. The membrane was stored at −80 °C until it was required for binding assays.

Binding assay: Cell membranes (5-HT_{2A}-FlpIn CHO, 25μg) were incubated with varying concentrations of test compound in binding buffer and 0.6-0.9 nM of [^{3}H]ketanserin to a final volume of 400 μL and incubated at 37 °C for 1 h. Non-specific binding was defined with 10 μM clozapine. Binding was terminated by fast-flow filtration over GF/B membranes pretreated with 0.5% polyethylenimine using a brandel harvester, followed by three washes with ice-cold wash buffer. Bound radioactivity was measured in a Tri-Carb 2900TR liquid scintillation counter (PerkinElmer).

ERK1/2 Phosphorylation Assay. FlpIn CHO cells stably expressing the $D_{2L}R$ were seeded into 96-well plates at a density of 50 000 cells/ well. After 5h, cells were washed with phosphate-buffered saline (PBS) and incubated in serum-free DMEM overnight before assaying. Initially,

time-course experiments were conducted at least twice for each ligand to determine the time required to maximally promote ERK1/2 phosphorylation via the dopamine $D_{2L}R$. Interaction studies were performed using varying concentrations of test ligand and increasing concentrations dopamine at 37 °C with a stimulation time of 5 minutes. Stimulation of the cells was terminated by removing the media followed by the addition of 100 µL of SureFirelysis buffer (PerkinElmer) to each well. The plate was shaken for 5 min at rt before transferring 5 µL of the lysates to a white 384-well Proxiplate (PerkinElmer). Then, 8 µL of a 240:1440:7:7 mixture of Surefire activation buffer:Surefire reaction buffer:Alphascreen acceptor beads:Alphascreen donor beads was added to the samples and incubated in the dark at 37 °C for 1.5 h. Plates were read using a Fusion-^{TM} plate reader.

cAMP Accumulation Assays. The cells were grown and incubated overnight and then pre-incubated for 45 min in 80 µL of stimulation buffer (Hank's buffered salt solution: 0.14 M NaCl, 5.4 mM KCl, 0.8 µM $MgSO_4$, 1.3 mM $CaCl_2$, 0.2 mM Na_2HPO_4, 0.44 mM KH_2PO_4, 5.6 mM D-glucose, 1 mg/mL BSA, 0.5 mM 3-isobutyl-1-methylxanthine and 5mM HEPES, pH 7.4). The agonist (10 µL) and 300 nM of forskolin (10 µL) were added simultaneously to the cells and incubated for 30 min at 37 °C. Stimulation was terminated via the removal of the stimulation buffer and adding 50 µL of ice cold 100% ethanol. The plates were then incubated at 37 °C to allow evaporation of the ethanol. 50 µL of detection buffer (1 mg/mL BSA, 0.3% Tween-20 and 5 mM HEPES, pH 7.4) was added and 5 µL of each well transferred to a 384-well Optiplate (PerkinElmer, Waltham, USA). Anti-cAMP acceptor beads (0.2 units/µL) diluted in stimulation buffer was added under green light for 30 mins before the addition of 15 µL of the donor beads/biotinylated cAMP (0.07 units/µL) diluted in detection buffer. The plates were incubated for 1 h at room temperature and read using a Fusion-α™ plate reader using AlphaScreen pre-settings.

Intracellular Ca^{2+} Mobilisation Assay. FlpIn CHO cells stably expressing the M_1R were seeded into 96-well plates at a density of 30 000 cells/ well and incubated overnight. Cells were washed twice with 200 µL of assay buffer (150 mM NaCl, 2.6 mM KCl, 1.2 mM $MgCl_2.H_2O$, 10 mM D-glucose, 10 mM HEPES, 2.2 mM $CaCl_2.2H_2O$, 0.05% (w/v) BSA, 4 mM Probenecid; pH 7.4). To the cells, 100 µL of Fluo4-AM diluted in assay buffer was added to each well and the plate incubated for 37 °C in the dark for 1 h. The cells were again washed twice with 200 µL of assay buffer and 180 µL of buffer added with drug solutions prepared as a × 10 concentrated solution. The assay is completed on a FLEXstation (SoftMax Pro) with a runtime of 60 seconds per well at an interval of 1.5 seconds. Excitation and emission filters were set to 485 nm and 520 nm, respectively. Ionomycin was used as the positive control at a final concentration of 0.2 µM.

IP_1 Accumulation Assay. The IP-One assay kit (Cisbio, France) was used for the direct quantitative measurement of myo-Inositol 1 phosphate (IP_1) in FlpIn CHO cells stably expressing the $5\text{-}HT_{2A}R$. The cells were detached and resuspended in IP_1 stimulation buffer (Hepes 10 mM, $CaCl_2$ 1 mM, $MgCl_2$ 0.5 mM, KCl 4.2 mM, NaCl 146 mM, glucose 5.5 mM, LiCl 50 mM, pH 7.4). The stimulations were performed in 384-well Proxy-plates (PerkinElmer) in a total volume of 14 µl, in the absence or presence of increasing concentrations of serotonin and compounds 6-11, at a cell density of 2-2.5 million cells/ml for 1h at 37°C, 5% CO_2. The reactions were terminated by addition of 6 µl lysis buffer containing HTRF reagents (the anti-IP1 Tb cyrptate conjugate and the IP1-D2 conjugate), followed by incubation for 1h at room temperature. The emission signals were measured at 590 and 665 nm after excitation at 340 nm using the Envision multi-label plate reader (PerkinElmer) and the signal was expressed as the HTRF ratio: $F = ((\text{fluorescence}_{665\ nm}/\text{fluorescence}_{590\ nm}) \times 10^4)$.

Data Analysis. Computerized nonlinear regression was performed using Prism 6.0 (GraphPad Software, San Diego, CA).

References

1. Szabo, M.; Klein Herenbrink, C.; Christopoulos, A.; Lane, J. R.; Capuano, B. Structure–activity relationships of privileged structures lead to the discovery of novel biased ligands at the dopamine D_2 receptor. *J. Med. Chem.* **2014,** *57*, 4924-4939.

2. Sams, A. G.; Hentzer, M.; Mikkelsen, G. K.; Larsen, K.; Bundgaard, C.; Plath, N.; Christoffersen, C. T.; Bang-Andersen, B. Discovery of N-{1-[3-(3-oxo-2,3-dihydrobenzo[1,4]oxazin-4-yl)propyl]piperidin-4-yl}-2-phenylacetamide (Lu AE51090): An allosteric muscarinic M_1 receptor agonist with unprecedented selectivity and procognitive potential. *J. Med. Chem.* **2010,** *53*, 6386-6397.

Chapter 5- Fluorescently Labelled Ligands for the Dopamine D_2 Receptor

Declaration for Thesis Chapter 5

The data presented in Chapter 5 contains research which is in manuscript format for submission to the *Journal of Medicinal Chemistry*.

Declaration by candidate

In the case of Chapter 5 the nature and extent of my contribution to the work was the following:

Nature of contribution	**Contribution (%)**
Design, synthesis, purification, characterisation and pharmacological testing of all analogues. Confocal microscopy. Main author of manuscript.	85

The following co-authors contributed to the work. Co-authors who are students at Monash University must also indicate the extent of their contribution in percentage terms:

Name	**Nature of contribution**	**Contribution (%)***
Cameron J. Nowell	Assistance with confocal microscopy. Co-author of manuscript	
Arthur Christopoulos	Co-author of manuscript	
J. Robert Lane	Co-author of manuscript	
Ben Capuano	Co-author of manuscript	

*Percentage contribution only shown for co-authors who were students at Monash University at the time of their contribution to this work.

Candidate's Signature: [redacted] 01/12/2014

Monika Szabo

Declaration by co-authors

The undersigned hereby certify that:

1. The above declaration correctly reflects the nature and extent of the candidate's contribution to this work, and the nature of the contribution of each of the co-authors.
2. They meet the criteria for authorship in that they have participated in the conception, execution, or interpretation, of at least that part of the publication in their field of expertise;
3. They take public responsibility for their part of the publication, except for the responsible author who accepts overall responsibility for the publication;
4. There are no other authors of the publication according to these criteria;
5. Potential conflicts of interest have been disclosed to (a) granting bodies, (b) the editor or publisher of journals or other publications, and (c) the head of the responsible academic unit; and
6. The original data are stored at the following location(s) and will be held for at least five years from the date indicated below:

   Department of Medicinal Chemistry, Monash Institute of Pharmaceutical Sciences, 381 Royal Parade, Parkville, Victoria, 3052, Australia

Co-author signatures:

Cameron J. Nowell: [redacted] 01/12/2014

J. Robert Lane: [redacted] 01/12/2014

Arthur Christopoulos: [redacted] 01/12/2014

Ben Capuano: [redacted] 01/12/2014

Fluorescently Labelled Ligands for the Dopamine D_2 Receptor

Monika Szabo[†‡], *Cameron J. Nowell*[‡], *Arthur Christopoulos*[‡], *J. Robert Lane*[‡,*], *Ben Capuano*[†,*]

[†]Medicinal Chemistry, [‡]Drug Discovery Biology, Monash Institute of Pharmaceutical Sciences, Monash University, 381 Royal Parade, Parkville 3052, Victoria, Australia.

KEYWORDS: Dopamine D_2 receptor, D_2R, fluorophore, fluorescently labelled ligands, confocal microscopy.

Abstract

Fluorescently labelled ligands are useful pharmacological tools for a range of applications, particularly for the development of competition-based ligand binding assays. The Dopamine D_2 Receptor (D_2R) is implicated in multiple CNS disorders, thus making it an important therapeutic target for drug discovery. However, there is a notable lack of available fluorescent ligand tools for the D_2R. We have developed a series of fluorescently labelled ligands based on two clinical compounds, clozapine (inverse agonist/antagonist) and ropinirole (agonist), in addition to a negative allosteric modulator SB269652 and its high-affinity variant 2-MPP-SB269652. All compounds were tethered to a spectrum of fluorophores (BODIPY 630/650-X, Cy5, Cy3, FITC and LRB). Three of the four chemical series maintained functionality at the D_2R, with the fluorescently labelled derivatives of 2-MPP-SB269652 maintaining binding affinities closest to the parent compound. We identified three novel fluorescent ligands (**35b-c** and **35e**) with high affinity for the D_2R that demonstrated rather specific cell membrane binding and very weak non-specific binding. These fluorescent ligands represent useful tools to be adapted towards multiple applications for the D_2R.

Introduction

The study of G protein-coupled receptors (GPCRs) and their implication in central nervous system (CNS) disorders such as schizophrenia and Parkinson's disease, is extensive.[1,2] As such, there is an ongoing need to develop techniques for not only the study of GPCRs but to identify new ligands and scaffolds that target these receptors. The development of fluorescently labelled small molecules has become a useful tool for investigating ligand receptor interactions. High affinity fluorescently labelled antagonists can be used to label the receptor of interest whilst fluorescently labelled agonists have utility to explore receptor internalization, compartmentalization and trafficking.[3] More significant to our study is that fluorescently labelled

ligands can be adapted towards competition-based binding assays that may be evolved into a potential high throughput screening (HTS) approach.[4-6] Fluorophores are small organic dyes that can be covalently attached to a ligand of interest. These conjugated molecules are excited at a specific wavelength and the light emitted can be detected and imaged. There are many commercially available fluorophores and each have been optimized to exhibit a variety of properties that make them versatile for an array of biological purposes.[7,8]

Considerable work has been done on developing fluorescently labelled ligands that target class A GPCRs implicated in CNS disorders, such as adenosine receptors,[9] muscarinic receptors[10] and serotonin receptors.[11] Our research focussed on developing fluorescently labelled ligands that target the dopamine D_2 receptor (D_2R). Fluorescent tools for this receptor are relatively limited, with the last derivatives developed some 15 years ago. Work on the D_2 antagonists spiperone (Figure 1, **1**) and *N*-(*p*-aminophenethyl)spiperone (NAPS) showed that they could be tethered to either a fluorophore or biotin and still retain high affinity for the D_2R and selectivity over the D_1 receptor subtype.[12-14] Furthermore, it has also been demonstrated that fluorophores can be coupled to a D_2R agonist, 2-(*N*-phenthyl-*N*-propyl)amino-5-hydroxytetralin, and still retain full agonist efficacy.[15]

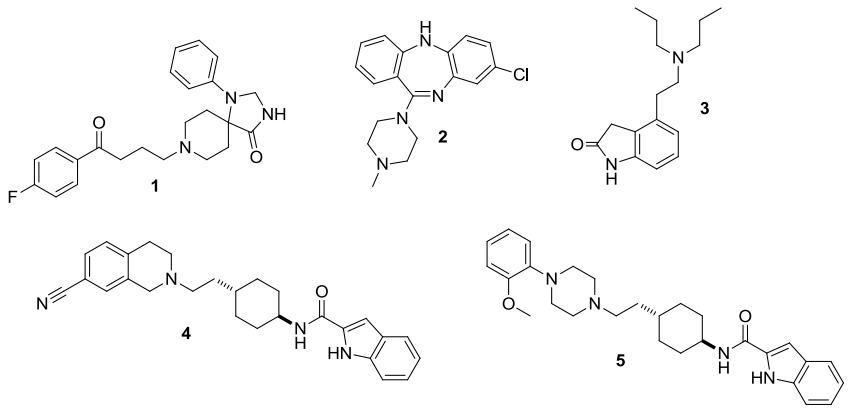

Figure 1. Ligands for the D_2R: spiperone (**1**), clozapine (**2**), ropinirole (**3**), SB269652 (**4**) and 2-MPP-SB269652 (**5**).

As the dopamine D_2 receptor (D_2R) is a key receptor in many CNS disorders, such as schizophrenia[16] and Parkinson's disease[2] we wanted to create a "toolbox" of fluorescently labelled derivatives that can be used to screen for novel compounds and scaffolds. The advantages of fluorescent derivatives include avoiding the use of radioactive materials, and intrinsically enhanced sensitivity, i.e. visualizing biochemical events down to sub-cellular localisation.[17] We chose four ligands (Figure 1) as part of our toolbox, each with their own unique pharmacology. Clozapine (**2**), a second generation clinical atypical antipsychotic, displays favourable polypharmacology, namely as an antagonist at both the D_2R and serotonin 5-HT_{2A} receptor, that is beneficial to both the positive symptoms (hallucinations, delusions) and the negative symptoms (lack of motivation, social withdrawal) of schizophrenia, respectively.[18,19] Ropinirole (**3**), also a clinical therapeutic, is a D_2 agonist effective against the progression of Parkinson's disease.[20] As a result of previously published work on both these ligands[21,22] in our group, we had insight into the SAR of these compounds and hence a suitable position for linking fluorophores. The third ligand we chose to explore was SB269652 (**4**) initially identified by Stemp et al.[23] and later characterized as a negative allosteric modulator (NAM) at D_2/D_3Rs.[24] Compound **4** has a distinct mode of action as it is thought to produce its allosteric mode of action across a D_2R dimer.[25] Therefore a fluorescent derivative of **4** could aid in confirming this mechanism of action and give more insight into the location of the allosteric pocket at the D_2R. The last derivative, **5**, is a high affinity antagonist for the D_2R developed in-house, which replaces the 1,2,3,4-tetrahydroisoquinoline-7-carbonitrile of **4**, with the D_2R privileged motif, 2-methoxyphenylpiperazine. Compared to ligands **2-4**, compound **5** is a novel antagonist for the D_2R and our group has generated SAR data around both **4** and **5** (unpublished work), which gave a good indication of where we could link fluorophores for the generation of our molecular probes.

To increase the probability of retaining inherent pharmacological profiles, we chose to functionalize the ligands with a variety of commercially available fluorophores (Figure 2) with pre-installed reactive functional groups, except for the tetrazine (which was activated in situ). The resulting fluorescently labelled ligands were characterized in a radioligand binding assay and select ligands were then utilized in confocal microscopy using D_{2L} CHO cells.

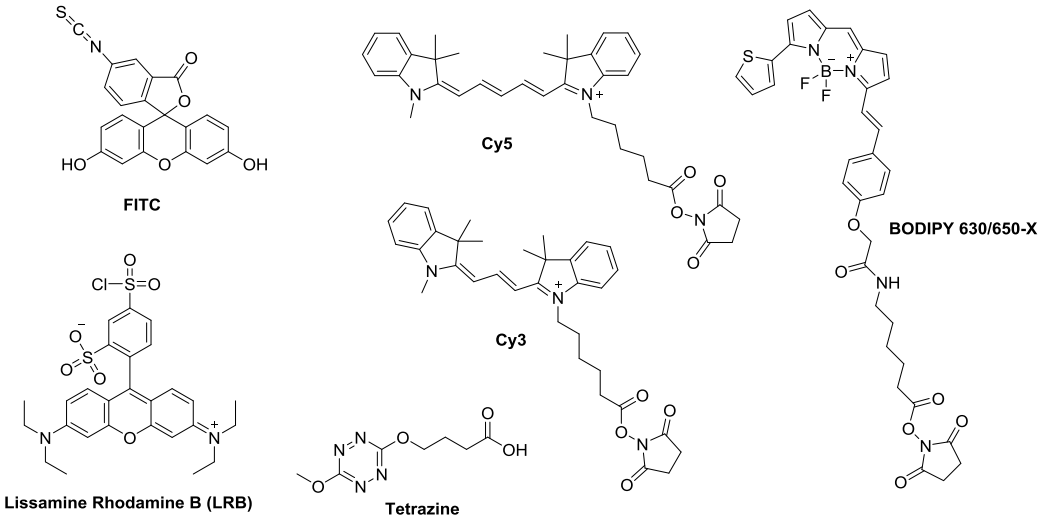

Figure 2. Commercially available activated fluorophores for the generation of fluorescently labelled ligands.

Results and Discussion

Chemistry. The synthesis of clozapine-based fluorescently labelled ligands (Scheme 1) commenced with the N-demethylation of clozapine (**2**) to give desmethylclozapine (**6**). The installation of the three carbon unit spacer was effected via the use of Boc protected 3-bromopropamine in good yield (80%). The Boc protecting group from compound **7** was then removed under standard acidic conditions, and following workup, furnished the free base (**8**) in excellent yield. Reaction of compound **8** with each of the activated fluorophores (BODIPY, Cy5 and Cy3) as their succinimidyl esters gave the final compounds **11a-c** in varying yields (12-25%)

after overnight reaction. All fluorescently labelled ligands were isolated as the TFA salts following purification via preparative HPLC. We noted that the fluorophores containing BODIPY, Cy5 or Cy3 all incorporated alkyl chains of 6 or more atoms that separated the fluorophore from the ligand. As a result, we wanted to ensure that this structural feature was conserved throughout all final compounds and therefore an additional 6 atom spacer was introduced for attachment to LRB and FITC fluorophores. We estimated that this inclusion would provide sufficient length for the fluorophores to reach into the extracellular space. Compound **8** was combined with 6-((*tert*-butoxycarbonyl)amino)hexanoic acid using COMU as an amide coupling reaction to generate **9** in a yield of 51%. Removal of the Boc group under standard conditions and workup gave the free base (**10**), which was subsequently reacted with LRB-sulfonyl chloride and fluoroscein-NCS to form the final compounds **11d-e**.

Scheme 1. Synthesis of clozapine fluorescently labelled ligands[a]

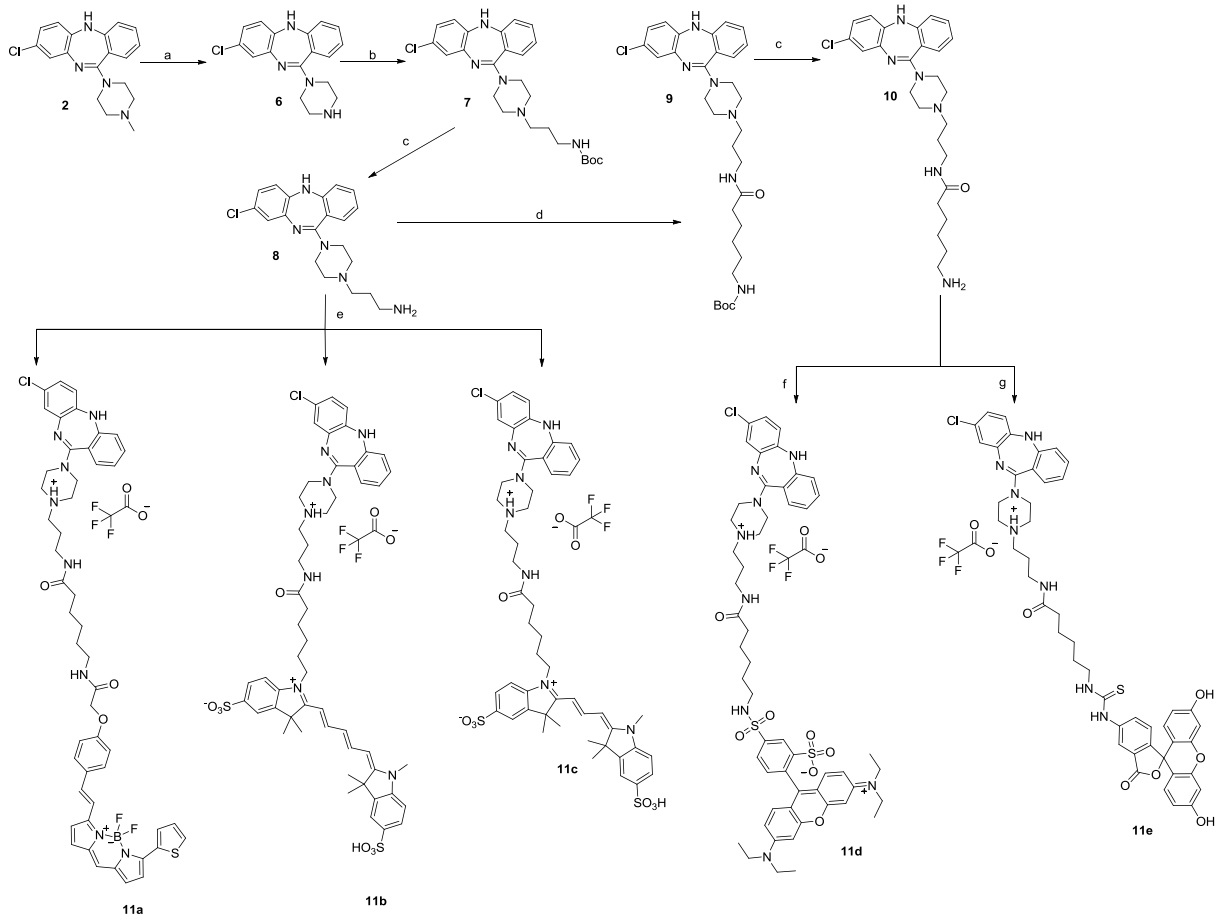

[a]Reagents and conditions: (a) 1-Chloroethyl chloroformate, MeOH, 1,2-DCE, N_2, 0 °C→reflux, 24 h 54%; (b) *tert*-Butyl (3-bromopropyl)carbamate, NaI, DIPEA, N_2, CH_3CN, reflux 24 h, 80%; (c) TFA/DCM, RT, 1-2 h 78-97%; (d) 6-((*tert*-butoxycarbonyl)amino)hexanoic acid, COMU, DIPEA, N_2, 0 °C→RT, 5 h 51%; (e) BODIPY-, Cy5- or Cy3-NHS ester, DMF, RT, 12 h, 12-25%; (f) LRB-sulfonyl chloride, DIPEA, $CHCl_3$, 12 h, 0 °C → RT, 26%; (g) Fluoroscein-NCS, DIPEA, DMF, RT, 4 h, 23%.

The synthesis of ropinirole-derived fluorescently labelled ligands (Scheme 2) commenced with the reaction of des-propyl ropinirole (**12**) with Boc protected 3-bromopropamine under basic conditions to give compound **13**. Removal of the Boc group was again performed under standard conditions and workup to generate the free base (**14**). Subsequent reaction with the activated fluorophores (BODIPY, Cy5 and Cy3) as the succinimidyl ester afforded the final compounds **17a-c** in modest yields ranging from 22-48%. As in the case of the clozapine-derived fluorescently labelled ligands **11d-e**, we required the installation of an additional 6 carbon atom linker for the LRB and FITC analogues. Therefore compound **14** was reacted with 6-((*tert*-

butoxycarbonyl)amino)hexanoic acid via a BOP-mediated coupling reaction to give compound **15** whereby the protecting group was subsequently removed under standard acidic conditions and workup to furnish the free base **16**. Following the above stipulated conditions, compound **16** was reacted with the activated LRB and FITC fluorophores to successfully yield derivatives **17d** and **17e**.

Scheme 2. Synthesis of ropinirole fluorescently labelled ligands[a]

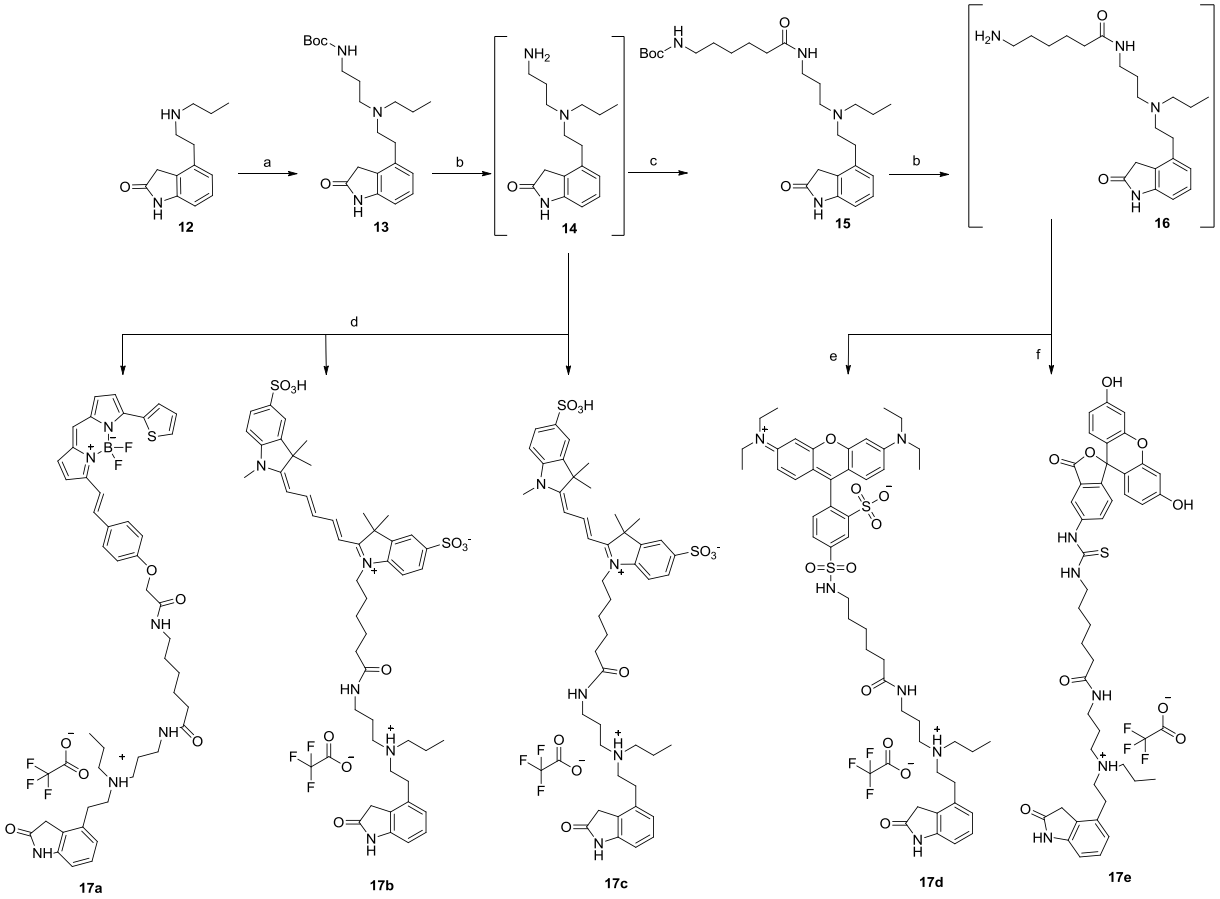

[a]Reagents and conditions: (a) *tert*-Butyl (3-bromopropyl)carbamate, K_2CO_3, CH_3CN, reflux 24 h, 43%; (b) TFA/DCM, RT, 1-2 h; (c) 6-((*tert*-butoxycarbonyl)amino)hexanoic acid, BOP, DIPEA, N_2, RT, 12 h, 20%; (d) BODIPY-, Cy5- or Cy3-NHS ester, DMF, RT, 12 h, 22-48%; (e) LRB-sulfonyl chloride, DIPEA, $CHCl_3$/DMF, 12 h, 0 °C → RT, 27%; (f) Fluoroscein-NCS, DIPEA, DMF, RT 6 h, 20%.

To synthesise both the SB269652 and 2-MPP-SB269652 fluorescently labelled ligands, we were firstly required to generate some key intermediates as indicated in Scheme 3. To furnish the functionalized indole, we commenced with 5-hydroxy-2-indole carboxylic acid (**18**) and formed the ethyl ester using Fischer esterification conditions which gave **19** in good yield (79%). The indololic NH was then Boc protected to give compound **20** in excellent yield (97%). To install the desired 3-carbon spacer, we employed sodium hydride to deprotonate the hydroxyl at the 5′ position and then reacted the indolol anion with 3-bromopropyl carbamate to generate compound **21**. The ethyl ester was subsequently hydrolysed to the corresponding carboxylic acid (**22**) in excellent yield using lithium hydroxide. To build up the other side of the ligand, we commenced with 2-((*trans*)-4-((*tert*-butoxycarbonyl)amino)cyclohexyl)acetic acid (**23**) which was activated with EDC and then converted to the ethyl ester **24**. Reduction of the ester functionality of **24** to the corresponding aldehyde (**25**) proceeded smoothly in modest yield following treatment with DIBAL-H. The versatile aldehyde was independently reacted with 1,2,3,4-tetrahydroisoquinoline-7-carbonitrile (**26**) and 2-methoxyphenylpiperazine (**27**) under reductive amination conditions to furnish **28** and **29**, which were subsequently de-protected under standard conditions and workup to afford **30** and **31**, respectively, as their free bases. Both compounds were then coupled with the key intermediate carboxylic acid **22** via a BOP-mediated amide bond formation reaction to give **32** and **33** in modest yields of 57% and 59%, respectively, after purification. The key intermediates **32** and **33** were treated with trifluoroacetic acid effecting removal of the Boc group, and the subsequent products used immediately in reactions with the various fluorophores under similar conditions as previously stated to give compounds **34a-e** and **35a-f**, respectively. Due to limited quantities of the tetrazine fluorophore and the relatively greater binding affinity of 2-MPP-SB269652, only the corresponding fluorescently labelled derivative of 2-MPP-SB269652 was synthesized.

Scheme 3. Synthesis of key SB269652 and 2-MPP-SB269652 intermediates[a]

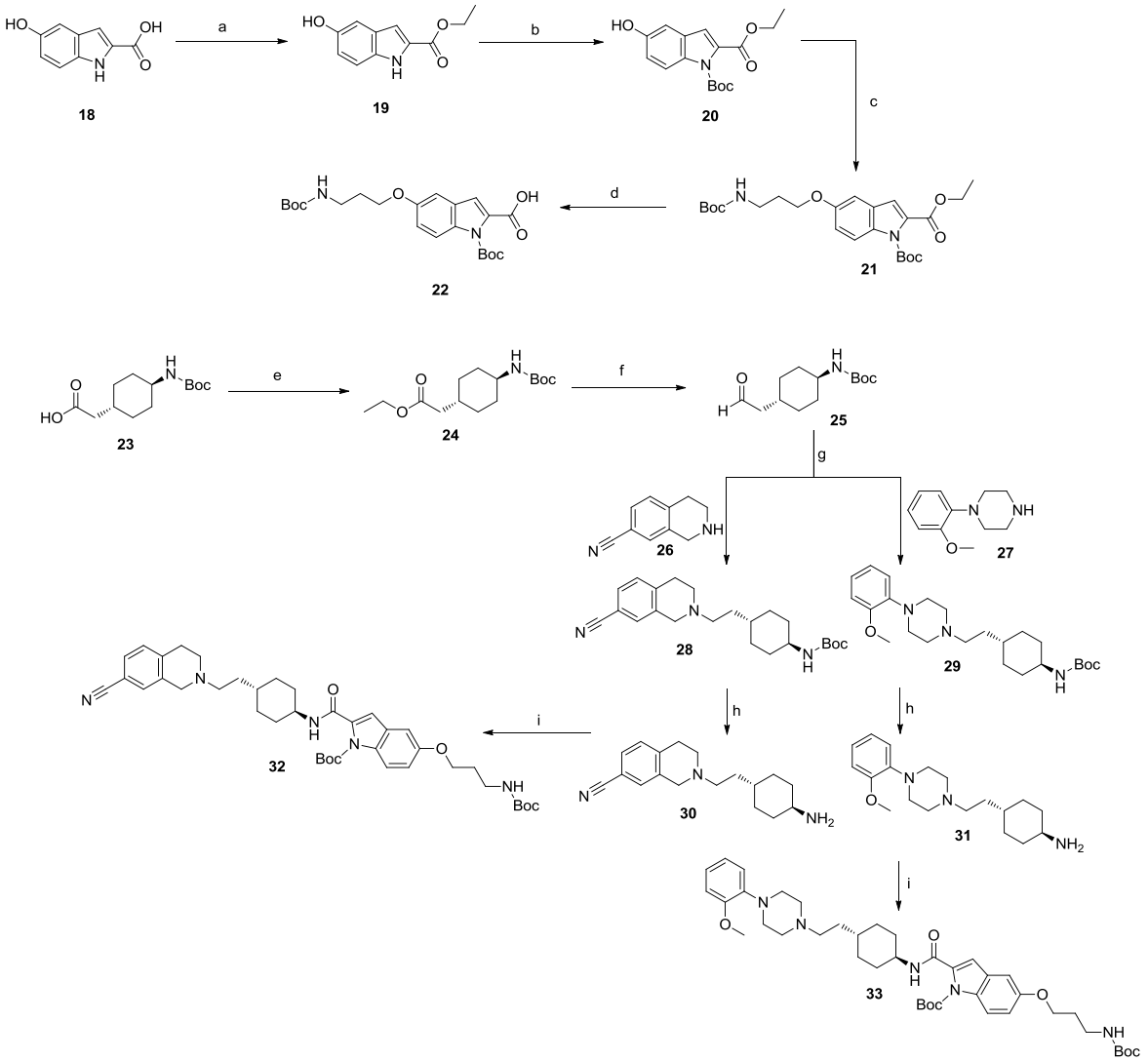

[a]Reagents and conditions: (a) H_2SO_4, EtOH, reflux 24 h, 79%; (b) Boc anhydride, Et_3N, 1,4-dioxane, reflux 3 h, 97%; (c) *tert*-Butyl (3-bromopropyl)carbamate, 60% NaH, DMF, N_2, RT, 12 h, 78%; (d) LiOH.H_2O, THF, RT, 12 h, 93%; (e) EDC, DMAP, EtOH, 24 h, RT, 59%; (f) DIBAL-H, 1,2-DCE, N_2, -78 °C, 1 h, 55%; (g) **26** or **27**, $NaBH(OAc)_3$, N_2, RT, 24 h, 55 and 97%; (h) TFA/DCM, RT, 1-2 h; (i) **28** or **29**, **22**, BOP, DIPEA, DMF, RT, 7-12 h, 57 and 59%.

Scheme 4. Synthesis of SB269652 and 2-MPP-SB269652 fluorescently labelled ligands.

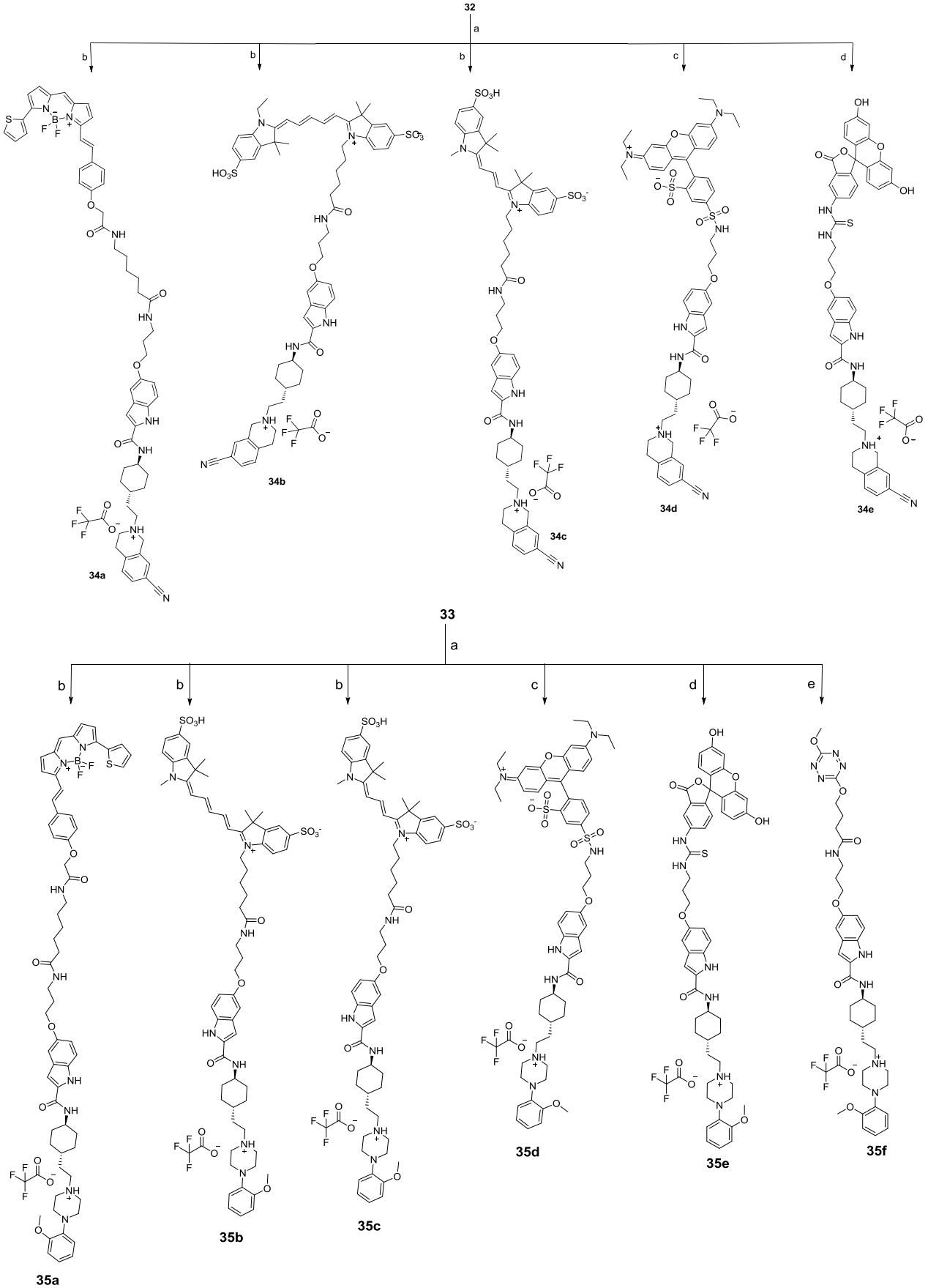

[a]Reagents and conditions: (a) TFA/DCM, RT, 1-2 h; (b) BODIPY-, Cy5- or Cy3-NHS ester, DMF, RT,

12 h, 22-48%; (c) LRB-sulfonyl chloride, DIPEA, $CHCl_3$/DMF, 12 h, 0 °C → RT, 29%; (d) Fluorescein-NCS, DIPEA, DMF, RT 6 h, 20%. (e) 4-((6-methoxy-1,2,4,5-tetrazin-3-yl)oxy)butanoic acid, BOP, DIPEA, N_2, RT, 12 h, 17%;

Pharmacology. To evaluate the pharmacology of our fluorescently labelled ligands, we screened them (n=1; Supporting Information Table 1) in ERK1/2 phosphorylation assays using CHO cells expressing the D_{2L} receptor to determine whether their functionality remained, i.e. agonist, antagonist or NAM. From our results we determined that the clozapine-based fluorescently labelled ligands (**11b-e**) remained as antagonists, the ropinirole-derived fluorescently labelled ligands (**17a-e**) remained as agonists and the fluorescently labelled derivatives of 2-MPP-SB269652 (**35a-f**) also remained as antagonists. No ligands from the SB269652 series (**34a-e**) exhibited properties of negative allosteric modulation following the attachment of fluorophores. Nevertheless, we tested all fluorescently labelled ligands in a radioligand binding assay to comprehensively determine their binding affinities for the D_2R with a view to elucidate potential SAR. These results are summarised in Table 1.

Compared to the parent compound, clozapine, the fluorescently labelled ligands (**11b-e**) all displayed a 4-8-fold loss in affinity. Additionally, the BODIPY analogue (**11a**) was completely inactive. Previous work by McRobb et al.[21] investigating homobivalent ligands of clozapine demonstrated that up to 18-atom spacers between the two clozapine units resulted in a K_i (D_{2L}) of 1.35 nM. The shortest spacer with 14-atoms displayed a K_i of 3.6 nM. Our fluorescently labelled ligands have, on average, a 10-atom spacer therefore it is possible that a longer spacer may be required to increase the binding affinity and to reach into the extracellular space.

Of the family of ropinirole fluorescently labelled ligands (**17a-e**), members incorporating the Cy3 (**17c**), LRB (**17d**) and FITC (**17e**) fluorophores all demonstrated binding affinities (K_i) of < 10 μM. The Cy5 analogue (**17b**) had no significant gain in affinity as compared to ropinirole.

The BODIPY analogue (**17a**) showed a 5-fold gain in affinity ($p < 0.05$) compared to ropinirole. This was a promising result as in the case of the other series of compounds, the BODIPY analogues were either inactive (**11a** and **34a**) or the weakest binders of the 2-MPP-269252 series (**35a**). Similar to the clozapine-derived fluorescently labelled ligands, compounds **17a-e** may require longer linkers in order for the fluorophore to reach up into the extraceullar space or bind at the top of the transmembrane helices. As this is a preliminary study, a 'second generation' series of compounds may focus on longer linker lengths between ropinirole and the fluorophore. Indeed work by Jorg et al.[22] showed that homobivalent ligands of ropinirole with linker lengths of up to 30 atoms between the ionisable nitrogen atoms are still able to maintain a potency (EC_{50}) of 14 nM ([^{35}S]GTPγS assay). This observation supports the notion that there is still space to explore longer linkers, in addition to variations in linkers such as polyethylene glycol (PEG) to ultimately decrease the lipophilicity and increase solubility.

Table 1. Binding affinities of all fluorescently labelled ligands and parent structures at the D_2R[a,b]

Parent compd	Fluorophore used	Compd	Binding pK_i ± SEM (K_i, nM)[b]
Clozapine	None	Clozapine (**2**)	6.97 ± 0.13 (107)
	BODIPY	**11a**	n/a
	Cy5	**11b**	6.07 ± 0.11 (861)
	Cy3	**11c**	6.35 ± 0.10 (446)
	LRB	**11d**	6.31 ± 0.11 (485)
	FITC	**11e**	6.21 ± 0.12 (617)
Ropinirole	None	Ropinirole (**3**)	6.06 ± 0.08 (872)
	BODIPY	**17a**	6.79 ± 0.11 (164)
	Cy5	**17b**	5.20 ± 0.43 (6264)
	Cy3	**17c**	< 10 μM
	LRB	**17d**	< 10 μM
	FITC	**17e**	< 10 μM
SB269652	BODIPY	**34a**	n/a
	Cy5	**34b**	6.64 ± 0.17 (228)
	Cy3	**34c**	6.32 ± 0.13 (470)
	LRB	**34d**	7.04 ± 0.12 (91.0)
	FITC	**34e**	6.72 ± 0.12 (190)
2-MPP-SB269652	None	2-MPP-SB269652 (**5**)	7.55 ± 0.07 (28.0)
	BODIPY	**35a**	6.40 ± 0.31 (394)
	Cy5	**35b**	7.35 ± 0.10 (45.2)
	Cy3	**35c**	7.13 ± 0.11 (73.9)
	LRB	**35d**	7.88 ± 0.20 (13.2)
	FITC	**35e**	7.27 ± 0.12 (53.3)
	Tetrazine	**35f**	7.58 ± 0.10 (26.2)

[a]Compounds are tested against [^{3}H]spiperone through competition binding studies using D_{2L} whole cells.[b]Data represent the mean ± SEM of three separate experiments performed in duplicate. n/a= compound not active.

As a consequence of the SB269652 fluorescently labelled ligands (**34a-e**) not retaining their NAM functionality at the D_2R, we did not characterize the parent compound (**4**) as part of this series. From Table 1, the only significant difference was the LRB analogue (**34d**) which showed a 5-fold gain in affinity ($p < 0.05$) compared to the weakest Cy3 derivative (**34c**). SB269652 concomitantly interacts with the orthosteric site of the D_2R and extends towards a secondary pocket, with the indole-2-caboxamide moiety closest to the extracellular space.[25] Therefore, with the added 3-carbon spacer following the fluorophores, we concluded that this would provide the necessary distance to ensure the fluorophores did not affect the intrinsic functionality of SB269652. However, the pharmacology of both positive and negative allosteric modulators can drastically be affected by small structural changes.[26-28] Therefore whilst the fluorophores may be

reaching out into the extracellular space, the substitution at the 5-position of the indole effects the NAM activity. The next generation of analogues may therefore look at substituting at other positions near the indole moiety of **4**, in addition to other commercially available fluorophores that may not drastically affect the final binding orientation.

The 2-MPP-SB269652 fluorescently labelled ligands (**35a-e**) maintained the best binding affinities as compared to the parent compound (**5**). The BODIPY analogue (**35a**) encountered a 7-30-fold loss compared to **5** and analogues **35b** and **35d-f**. The subtle change in binding affinity of the parent compound following the addition of a fluorophore suggests that the fluorophores are substituted at the correct position on the indole moiety and are also of the ideal length. As this series was least affected by the addition of the fluorophore, we chose to only pursue this series for our prospective confocal work. Due to the poor binding affinity of the BODIPY derivative compared to the other analogues, **35a** was subsequently dropped from future studies. Compounds **35b-f** were firstly analysed in a spectrometer to ensure they still fluoresced with 2-MPP-SB269652 attached. We were able to generate an excitation and emission profile for compounds (**35b-e**) in a variety of different aqueous buffers and in methanol (Supporting Information Figure 1).[29] Compound **35f** which had the tetrazine fluorophore attached was the only fluorescently labelled ligand for which we could not generate a fluorescence profile for. Therefore only ligands **35b-e** were used for further studies.

Confocal Imaging. The confocal images of the fluorescently labelled ligands **35b-c** and **35e** are represented in Figure 3. Each of the ligands were tested at two different concentrations, 1 μM and 300 nM and incubated for 30 mins at 37 ºC before imaging. The ligands show clear labelling of the cell membrane in CHO cells expressing the D_{2L} receptor in the control conditions. Additionally, there is little difference between the two different concentrations for **35b** and **35c** which represent the Cy5 and Cy3 derivatives, respectively. The FITC analogue **35e** did however

show a decrease in intensity when going from the 1 μM to 300 nM. The FITC fluorophore has less photo stability than the Cy5 and Cy3 fluorophores,[8] which therefore accounts for its loss in intensity. Nonetheless, when cells were pre-incubated with the non-fluorescent antagonist haloperidol (1 μM), all three fluorescently labelled ligands were displaced and therefore showed no weak non-specific binding at both concentrations. We conducted the same experiments for the LRB analogues **34d**. However, on this occasion the fluorescently labelled ligand could not be displaced following pre-incubation with haloperidol, indicating high non-specific binding of **34d** for the D_2R (Supporting Information Figure 2). Conversely, **35b-c** and **35e** show high specificity for the D_2R.

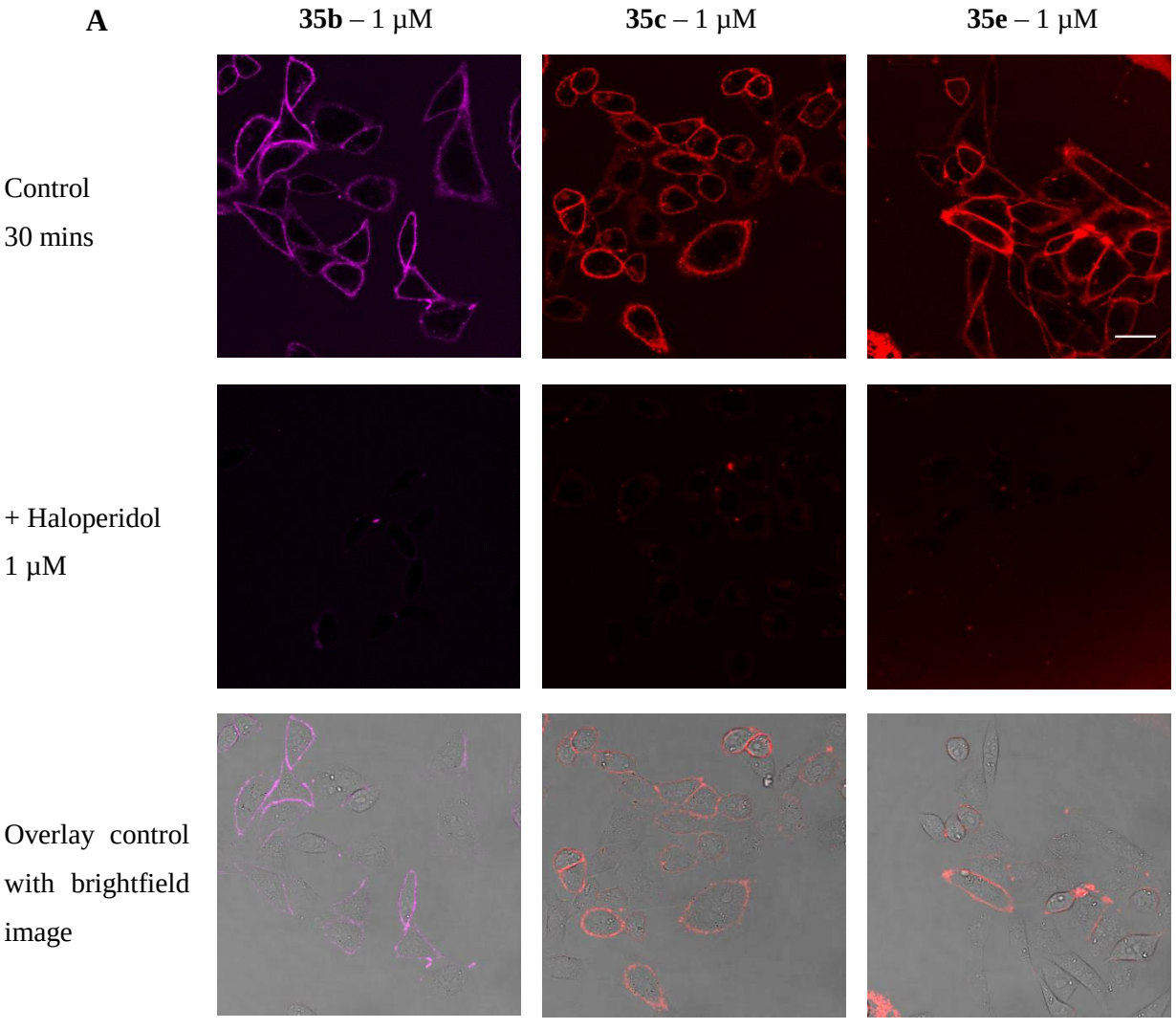

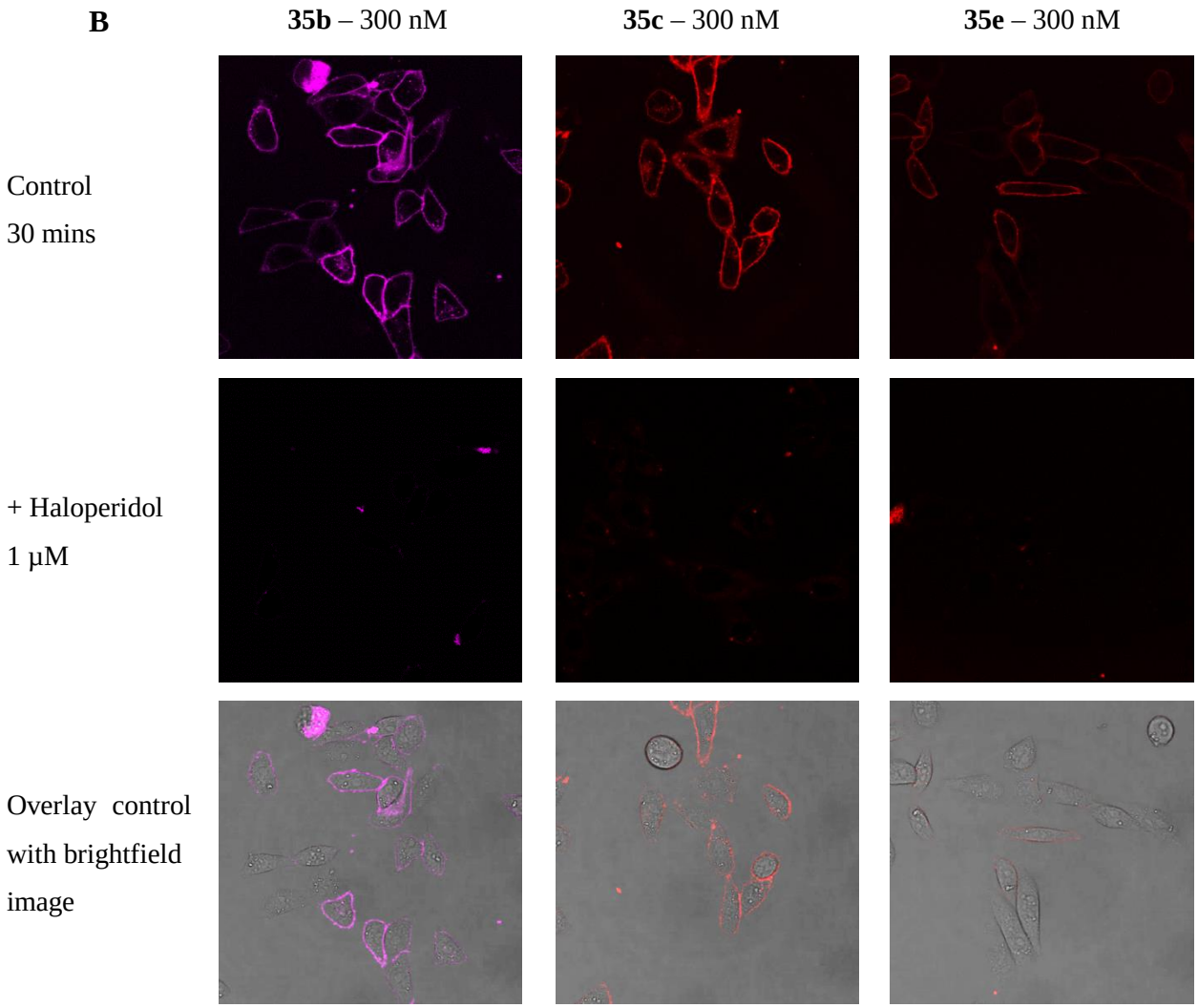

Figure 3. Confocal images of 2-MPP-SB269652 fluorescently labelled ligands **35b-c** and **35e** at 1 µM (A) and 300 nM (B). Scale bar= 25µm

This work highlights the advantage of using a variety of different fluorophores in the development of fluorescently labelled ligands. The 2-MPP-SB269652 series in particular showed that the BODIPY fluorophore for compound **35a** significantly weakened the binding affinity at the D_2R, whilst the remainder of analogues (**35b-e**) all had binding affinities in a similar range (13.2-73.9 nM). However, there were clear differences when we applied them to a confocal microscopy imaging technique. The cyanine dyes (Cy5 and Cy3; analogues **35b-c**) had a significantly greater intensity than the FITC fluorophore for compound **35e** at the lower concentration. Additionally, the non-specific binding of the LRB fluorophore (**35d**) made it obsolete for use as an imaging agent, irrespective of its noteworthy binding affinity. Whilst the

goal was to create a toolbox of fluorescently labelled ligands, there are a variety of other applications for the final fluorescently labelled ligands **35b-c** and **34e**. For instance they could be used as ligands in primary neurons to determine the location of D_2 cells on the membrane, for kinetics studies and the study of ligand-receptor complexes through techniques such as fluorescence correlation spectroscopy.[30]

Conclusion.

We synthesized and characterised four novel series of fluorescently labelled ligands each representing unique functional properties towards the D_2R. All fluorescently labelled ligands were able to maintain their functionality following the addition of linkers and the fluorophore unit itself apart from the series based on the NAM SB269652. Due to the limited number of fluorescently labelled ligands available for the D_2R, both commercially and in the literature, the compounds described herein provide valuable insight into structure activity relationships for this receptor and a useful starting point towards optimising new fluorescent probes. We were able to identify the fluorescently labelled antagonists **35b-c** and **35e** which displayed binding affinities ranging from 53.3-73.9 nM, specific cell membrane binding and weak non-specific binding for the D_{2L} receptor. These ligands may therefore be applied to a competitive binding assay that can facilitate the determination of affinities of prospective ligands and therefore potentially screen for new ligands for the D_2R as an alternative to using radioligand binding assays.

Experimental

Chemistry. All solvents and chemicals were purchased from standard suppliers and were used without any further purification. ^{1}H NMR and ^{13}C NMR spectra were acquired at 400.13 and 100.62 MHz respectively, on a Bruker Advance III 400 MHz UltrashieldPlus NMR spectrometer using TOPSPIN 2.1 software. Chemical shifts (δ) for all ^{1}H spectra are reported in parts per

million (ppm) using tetramethylsilane (TMS, 0 ppm) as the reference. The data for all spectra are reported in the following format: chemical shift (δ), (multiplicity, coupling constants *J* (Hz), integral), where the multiplicity is defined as: s = singlet, d= doublet, t= triplet, q=quartet, p= pentet, st= sextet and m = multiplet. For ^{13}C NMR spectra C= quaternary carbon, CH= methine carbon, CH_2= methylene carbon, and CH_3= methyl carbon. We were unable to observe the sulfonic acid proton of the cyanine fluorophores, therefore it is not quoted. The PREP HPLC is an Agilent 1260 infinity coupled with binary prep pump and Agilent 1260 FC-PS fraction collector. The column is a Alltima C8 5 u 22 mm × 250 mm. The purity and retention time of final products was determined on an Agilent 1260 Infinity analytical reverse-phase HPLC system fitted with a Poroshell 120 SB-C18 4.6 × 100 mm 2.7 u column. The HPLC and PREP HPLC both operate on Agilent OpenLAB CDS Rev C.01.04 software. Solvent A is water + 0.1% TFA and solvent B is acetonitrile + 0.1% TFA. Samples were run using a gradient method (5-100% solvent B over 10 minutes).

Thin layer chromatography (TLC) was carried out routinely on silica gel $60F_{254}$ pre-coated plates (0.25 mm, Merck). Flash column chromatography was carried out using Merck Silica gel 60, 230-400 mesh ASTM.

General procedures for coupling of fluorophores:

General procedure A for BODIPY 630/650-X, Cy5 and Cy3 coupling: The free amine (1 equiv.) followed by the required fluorophore as the NHS ester (1 equiv.) was added to DMF (0.5-1 mL) under a N_2 atmosphere. The reaction was stirred at room temperature for 12 h in the absence of light. The reaction mixture was then purified immediately via preparative-HPLC. The clean fractions were collected, pooled and the water removed via lyophilisation to obtain the product as the TFA salt.

General procedure B for Lissamine Rhodamine B (LRB) coupling: The free amine (1 equiv.) followed by LRB sulfonyl chloride (1.1 equiv.) and DIPEA (1.1 equiv.) was added to $CHCl_3$

(0.5-1 mL) under a N_2 atmosphere at 0 °C. In some circumstances 0.1 mL of DMF was required to assist with solubilisation. The reaction was stirred at 0 °C for 1 h before being warmed up to room temperature and stirring continued for 12 h without light. The reaction mixture was then purified immediately via preparative-HPLC. The clean fractions were collected, pooled and the water removed via lyophilisation to obtain the product as the TFA salt.

General procedure C for fluorescein coupling: The free amine (1 equiv.) followed by fluorescein-NCS (1.1 equiv.) and DIPEA (1.1 equiv.) was added to DMF (0.5-1 mL) under a N_2 atmosphere. The reaction was stirred at room temperature for 4-6 h without light. The reaction mixture was then purified immediately via preparative-HPLC. The clean fractions were collected, pooled and the water removed via lyophilisation to obtain the product as the TFA salt.

General procedure D for tetrazine coupling: The tetrazine carboxylic acid (1 equiv.) was added to DMF (1 mL) under a N_2 atmosphere. DIPEA (1.1 equiv) followed by BOP (1.05 equiv.) were also added. The required amine (1 equiv.) was then added and the reaction mixture left to stir overnight at room temperature in the absence of light. The reaction mixture was then purified immediately via preparative-HPLC. The clean fractions were collected, pooled and the water removed via lyophilisation to obtain the product as the TFA salt.

Synthesis of clozapine fluorescently labelled ligands.

***N*-Desmethylclozapine (6).[21]**

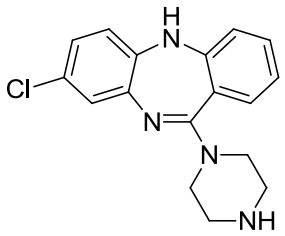

Clozapine (**2**, 2.50 g, 7.65 mmol) was dissolved in 1,2-dichloroethane (20 mL) under N_2 and cooled to 0 °C. 1-Chloroethyl chloroformate (3.30 mL, 30.6 mmol) was added dropwise to the reaction mixture. After 10 mins, the reaction mixture was warmed up to RT and subsequently

heated up to reflux for 24 h. The brown reaction mixture was concentrated in vacuo, and the residue was dissolved in methanol (30 mL) and heated at 50 ˚C for 2 h, cooled, and again concentrated in vacuo. The resulting residue was partitioned between ethyl acetate (50 mL) and 1 M aqueous hydrochloric acid (50 mL). The aqueous layer was collected and the pH adjusted to ~10 using concentrated sodium hydroxide then extracted with ethyl acetate (3 × 50 mL). The combined organic layers were washed with water (50 mL) and saturated brine (50 mL), dried over anhydrous Na_2SO_4, filtered and evaporated to dryness. Purified was achieved via column chromatography (chloroform/methanol, 10%) to give a yellow foam (1.30 g, 54% yield). ^{1}H NMR ($CDCl_3$) δ 2.57 (br s, 1H), 3.01 (m, 4H), 3.48 (m, 4H), 4.90 (s, 1H), 6.61 (d, *J* 8.3 Hz, 1H), 6.81-6.84 (m, 2H), 7.02 (td, *J* 7.6, 1.1 Hz, 1H), 7.06 (d, *J* 2.4 Hz, 1H), 7.25-7.32 (m, 2H). ^{13}C NMR ($CDCl_3$) δ 45.7 (CH_2), 48.2 (CH_2), 120.1 (CH), 120.2 (CH), 123.2 (CH), 123.2 (CH), 123.5 (C), 126.9 (CH), 129.2 (C), 130.4 (CH), 132.0 (CH), 140.5 (C), 141.9 (C), 152.8 (C), 163.1 (C).

***tert*-Butyl (3-(4-(8-chloro-5*H*-dibenzo[*b*,*e*][1,4]diazepin-11-yl)piperazin-1-yl)propyl)carbamate (7).[21]**

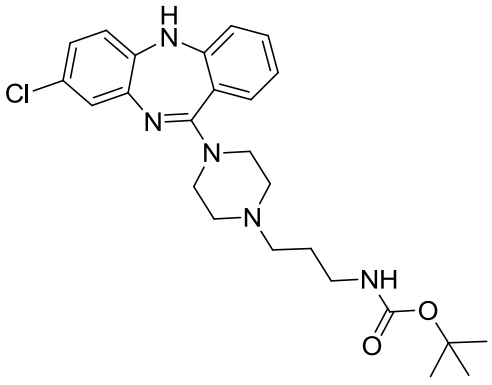

N-Desmethylclozapine (**6**, 500 mg, 1.60 mmol), sodium iodide (240 mg, 1.60 mmol) and *N*,*N*-diisopropylethylamine (0.31 mL, 1.76 mmol) were added to acetonitrile (30 mL) under N_2. *tert*-Butyl (3-bromopropyl)carbamate (419 mg, 1.76 mmol) was added and the reaction mixture was heated at reflux for 24 h. After cooling to room temperature the solvent was removed and the residue was partitioned between ethyl acetate (30 mL) and washed with water (2 × 30 mL)

followed by brine (50 mL), and dried over anhydrous Na_2SO_4, filtered and concentrated to give the crude product. Further purification via column chromatography (chloroform/methanol, 5%) gave the title compound as a yellow foam (602 mg, 80%). ^{1}H NMR ($CDCl_3$) δ 1.44 (s, 9H), 1.69 (m, 2H), 2.46 (t, *J* 6.8 Hz, 2H), 2.52 (m, 4H), 3.21 (m, 2H), 3.47 (m, 4H), 4.90 (s, 1H), 5.26 (br s, 1H), 6.61 (d, *J* 8.3 Hz, 1H), 6.80-6.83 (m, 2H), 7.01 (td, *J* 7.6, 1.1 Hz, 1H), 7.06 (d, *J* 2.4 Hz, 1H), 7.24-7.32 (m, 2H). ^{13}C NMR ($CDCl_3$) δ 26.6 (CH_2), 28.6 (CH_3), 39.9 (CH_2), 47.3 (CH_2), 53.3 (CH_2), 57.0 (CH_2), 79.0 (C), 120.1 (CH), 120.2 (CH), 123.2 (CH), 123.2 (CH), 123.5 (C), 126.9 (CH), 129.2 (C), 130.4 (CH), 132.0 (CH), 140.5 (C), 141.9 (C), 152.8 (C), 156.2 (C), 162.8 (C).

3-(4-(8-Chloro-5*H*-dibenzo[*b*,*e*][1,4]diazepin-11-yl)piperazin-1-yl)propan-1-amine (8).[21]

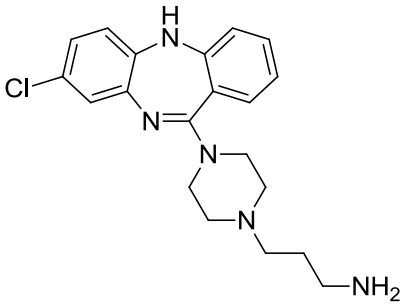

Compound **7** (328 mg, 0.70x mmol) was dissolved in DCM (10 mL) and TFA (2 mL) was added dropwise. Stirring at room temperature occurred for 1-2 h before the reaction mixture was diluted with a further 20 mL of DCM. Saturated K_2CO_3 (20 mL) was added slowly and further extracted with 3 × 20 mL portions of DCM. The combined organic layers were further washed with water (50 mL), brine (50 mL), dried over anhydrous Na_2SO_4, filtered and concentrated to give the product as a yellow foam which was not purified any further (249 mg, 97%). ^{1}H NMR ($CDCl_3$) δ 1.30 (br s, 2H), 1.67 (m, 2H), 2.46 (m, 2H), 2.53 (m, 4H), 2.77 (t, *J* 6.8 Hz, 2H) 3.47 (m, 4H), 4.90 (s, 1H), 6.61 (d, *J* 8.3 Hz, 1H), 6.80-6.83 (m, 2H), 7.01 (td, *J* 7.6, 1.1 Hz, 1H), 7.06 (d, *J* 2.4 Hz, 1H), 7.24-7.32 (m, 2H). ^{13}C NMR ($CDCl_3$) δ 30.7 (CH_2), 40.9 (CH_2), 47.4 (CH_2), 53.4 (CH_2), 56.6 (CH_2), 120.1 (CH), 120.2 (CH), 123.2 (CH), 123.2 (CH), 123.6 (C), 126.9 (CH), 129.2 (C), 130.4 (CH), 132.0 (CH), 140.5 (C), 141.9 (C), 152.8 (C), 162.9 (C).

***tert*-Butyl (6-((3-(4-(8-chloro-5*H*-dibenzo[*b*,*e*][1,4]diazepin-11-yl)piperazin-1-yl)propyl)amino)-6-oxohexyl)carbamate (9).**

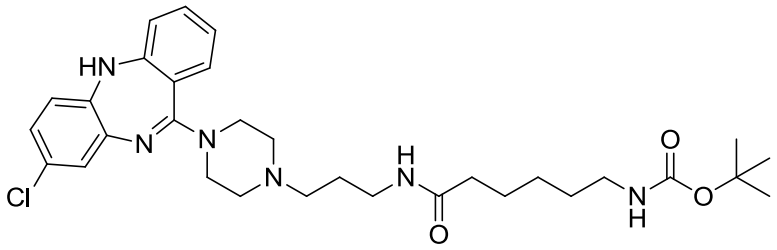

Compound **8** (240 mg, 0.65x mmol), 6-((tert-butoxycarbonyl)amino)hexanoic acid (150 mg, 0.65x mmol) and *N*,*N*-diisopropylethylamine (0.23 mL, 1.30 mmol) were combined in DMF (10 mL) and cooled down to 0 °C under N_2. COMU (277 mg, 0.65 mmol) was then added and stirring occurred for 1 h before being warmed up to room temperature and stirred for an additional 4 h. The solvent was removed in vacuo and the resulting residue dissolved in ethyl acetate (10 mL) and washed with 1 M HCl (2 × 5 mL), saturated $NaHCO_3$ (2 × 5 mL), brine (50 mL), dried over anhydrous Na_2SO_4, filtered and concentrated to give the crude product. Further purification via column chromatography (chloroform/methanol 5-10%) gave the final compound as a yellow oil (193 mg, 51%). ^{1}H NMR ($CDCl_3$) δ 1.34 (m, 2H), 1.44 (s, 9H), 1.47 (m, 2H), 1.63 (m, 2H), 1.71 (m, 2H), 2.14 (t, *J* 7.6 Hz, 2H), 2.54 (m, 2H), 2.58 (m, 4H), 3.09 (m, 2H), 3.34 (m, 2H), 3.45 (m, 4H), 4.65 (br s, 1H), 5.08 (s, 1H), 6.64 (d, *J* 8.3 Hz, 1H), 6.82-6.86 (m, 2H), 6.98 (br s, 1H), 7.02 (td, *J* 7.6, 1.0 Hz, 1H), 7.06 (d, *J* 2.4 Hz, 1H), 7.25-7.32 (m, 2H). ^{13}C NMR ($CDCl_3$) δ 25.2 (CH_2), 25.6 (CH_2), 26.6 (CH_2), 28.6 (CH_3), 29.9 (CH_2), 36.9 (CH_2), 39.5 (CH_2), 40.5 (CH_2), 47.5 (CH_2), 53.2 (CH_2), 57.7 (CH_2), 79.1 (C), 120.3 (CH), 120.3 (CH), 123.2 (CH), 123.4 (C), 123.5 (CH), 126.9 (CH), 129.1 (C), 130.3 (CH), 132.2 (CH), 140.7 (C), 141.7 (C), 153.0 (C), 156.1 (C), 163.1 (C) 172.9 (C). HPLC purity (λ= 214 nm): 100% t_R 5.90 min. HRMS (ESI)-TOF (*m/z*): $[M+H]^+$ 583.3163 calcd for $C_{31}H_{44}ClN_6O_3$; found $[M+H]^+$ 583.3162.

6-Amino-*N*-(3-(4-(8-chloro-5*H*-dibenzo[*b*,*e*][1,4]diazepin-11-yl)piperazin-1-yl)propyl)hexanamide (10).

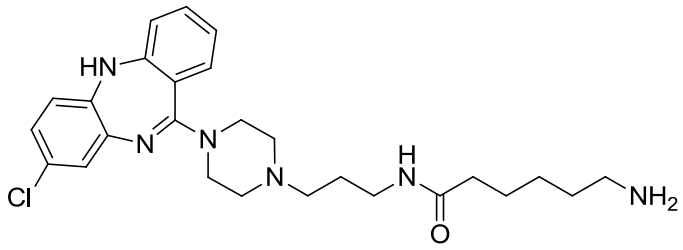

Compound **9** (193 mg, 0.33x mmol) was dissolved in DCM (5 mL) and TFA (2 mL) was added dropwise. Stirring at room temperature occurred for 1-2 h before the reaction mixture was diluted with a further 20 mL of DCM. Saturated K_2CO_3 (20 mL) was added slowly and further extracted with 3 × 20 mL portions of DCM. The combined organic layers were further washed with water (50 mL), brine (50 mL), dried over anhydrous Na_2SO_4, filtered and concentrated to give the product as a yellow oil which was not purified any further (123 mg, 78%). ^{1}H NMR ($CDCl_3$) δ 1.34 (m, 2H), 1.42-1.49 (m, 4H), 1.64 (m, 2H), 1.70 (m, 2H), 2.14 (t, *J* 7.5 Hz, 2H), 2.51 (t, *J* 6.3 Hz, 2H), 2.56 (m, 4H), 2.67 (t, *J* 6.8 Hz, 2H), 3.34 (m, 2H), 3.44 (m, 4H), 5.05 (s, 1H), 6.63 (d, *J* 8.3 Hz, 1H), 6.81-6.85 (m, 2H), 6.94 (t, *J* 4.5 Hz, 1H), 7.02 (td, *J* 7.6, 1.0 Hz, 1H), 7.06 (d, *J* 2.4 Hz, 1H), 7.25-7.32 (m, 2H). ^{13}C NMR ($CDCl_3$) δ 25.3 (CH_2), 25.8 (CH_2), 26.7 (CH_2), 33.6 (CH_2), 37.0 (CH_2), 39.6 (CH_2), 42.1 (CH_2), 47.6 (CH_2), 53.2 (CH_2), 57.8 (CH_2), 120.2 (CH), 120.3 (CH), 123.2 (CH), 123.4 (C), 123.4 (CH), 126.9 (CH), 129.2 (C), 130.3 (CH), 132.2 (CH), 140.6 (C), 141.8 (C), 153.0 (C), 163.0 (C) 172.9 (C).

(*E*)-3-(4-(2-((6-((3-(4-(8-Chloro-5*H*-dibenzo[*b*,*e*][1,4]diazepin-11-yl)piperazin-1-ium-1-yl)propyl)amino)-6-oxohexyl)amino)-2-oxoethoxy)styryl)-5,5-difluoro-7-(thiophen-2-yl)-5*H*-dipyrrolo[1,2-*c*:2',1'-*f*][1,3,2]diazaborinin-4-ium-5-uide 2,2,2-trifluoroacetate (11a).

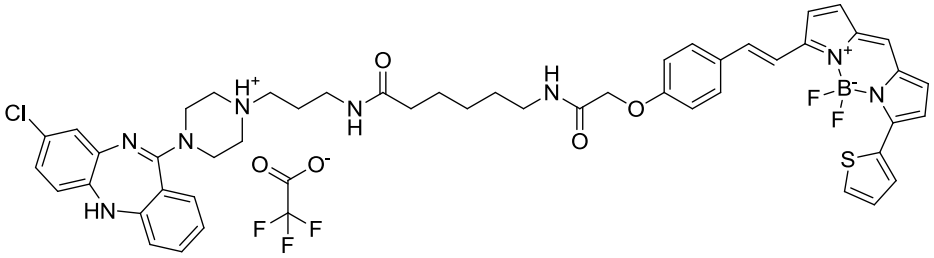

Blue solid (1 mg, 12%). ^{1}H NMR (d_6-DMSO) δ 1.20-1.27 (m, 3H), 1.42-1.52 (m, 4H), 1.79 (m, 2H), 2.07 (m, 2H), 3.10-3.14 (m, 8H), 3.51 (m, 3H), 3.95 (m, 2H), 4.54 (s, 2H), 6.87-6.96 (m, 4H), 7.00-7.09 (m, 4H), 7.26-7.30 (m, 4H), 7.35-7.42 (m, 4H), 7.61 (t, *J* 4.4 Hz, 3H), 7.74 (d, *J* 15.7 Hz, 1H), 7.83 (dd, *J* 5.1, 0.9 Hz, 1H), 7.95 (t, *J* 5.7 Hz, 1H), 8.04 (dd, *J* 3.8, 1.0 Hz, 1H), 8.15 (t, *J* 5.4 Hz, 1H), 9.52 (br s, 1H). HPLC purity (λ= 214 nm): 100%, t_R = 4.84 min. HRMS (ESI)-TOF (*m/z*): $[M+H]^+$ 915.3549 calcd for $C_{49}H_{50}BClF_2N_8O_3S$; found $[M+H]^+$ 915.3567.

1-(6-((3-(4-(8-Chloro-5*H*-dibenzo[*b*,*e*][1,4]diazepin-11-yl)piperazin-1-ium-1-yl)propyl)amino)-6-oxohexyl)-3,3-dimethyl-2-((1*E*,3*E*,5*E*)-5-(1,3,3-trimethyl-5-sulfoindolin-2-ylidene)penta-1,3-dien-1-yl)-3*H*-indol-1-ium-5-sulfonate 2,2,2-trifluoroacetate (11b).

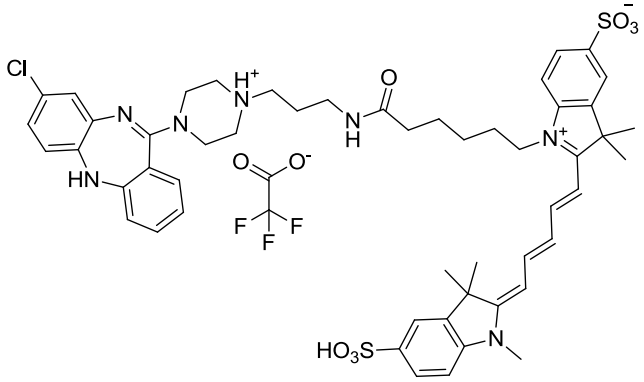

Blue solid (2 mg, 18%). ^{1}H NMR (d_6-DMSO) δ 0.83 (m, 2H), 1.15-1.29 (m, 5H), 1.51 (m, 2H), 1.69 (s, 12H), 2.02 (t, *J* 7.1 Hz, 2H), 2.97 (m, 2H), 2.97-3.40 (m, 7H, under water peak), 3.60 (s, 3H), 3.94 (m, 2H), 4.12 (m, 2H), 6.29 (m, 2H), 6.56 (t, *J* 12.6 Hz, 1H), 6.88-6.94 (m, 3H), 7.01-7.09 (m, 2H), 7.29-7.41 (m, 5H), 7.64-7.66 (m, 2H), 7.83-7.84 (m, 3H), 8.36 (m, 2H), 9.58 (br s,

1H). HPLC purity (λ= 214 nm): 95%, t_R = 4.89 min. HRMS (ESI)-TOF (*m/z)*: $[M+H]^+$ 994.3762 calcd for $C_{52}H_{60}ClN_7O_7S_2$; found $[M+H]^+$ 994.3765.

1-(6-((3-(4-(8-Chloro-5*H*-dibenzo[*b*,*e*][1,4]diazepin-11-yl)piperazin-1-ium-1-yl)propyl)amino)-6-oxohexyl)-3,3-dimethyl-2-((1*E*,3*E*)-3-(1,3,3-trimethyl-5-sulfoindolin-2-ylidene)prop-1-en-1-yl)-3*H*-indol-1-ium-5-sulfonate 2,2,2-trifluoroacetate (11c).

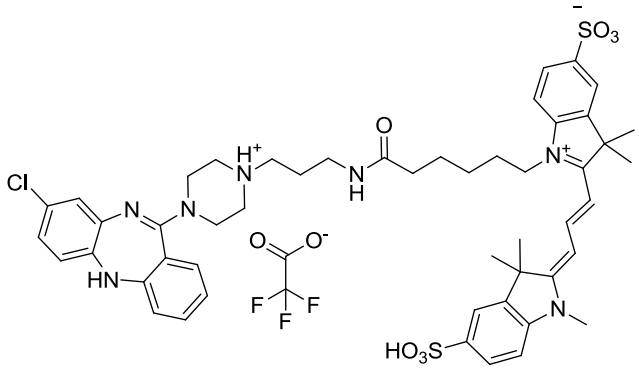

Pink solid (4 mg, 25%). ^{1}H NMR (d_6-DMSO) δ 1.29 (m, 2H), 1.54 (m, 2H), 1.62-1.79 (m, 15H), 2.04 (t, *J* 6.9 Hz, 2H), 2.98 (m, 2H), 3.09 (m, 2H), 3.18 (m, 4H), 3.503-3.80 (m, 6H, under water peak), 3.96 (m, 2H), 4.14 (m, 2H), 6.49 (dd, *J* 13.4, 4.3 Hz, 2H),6.91-6.98 (m, 3H), 7.03-7.08 (m, 2H), 7.33 (d, *J* 7.6 Hz, 1H), 7.38-7.48 (m, 4H), 7.69 (dt, *J* 8.3, 1.5 Hz, 2H), 7.83 (dd, *J* 3.7, 1.5 Hz, 2H), 7.86 (t, *J* 5.6 Hz, 1H), 8.34 (t, *J* 13.5 Hz, 1H), 9.58 (br s, 1H). HPLC purity (λ= 214 nm): 100%, t_R = 4.64 min. HRMS (ESI)-TOF (*m/z)*: $[M+H]^+$ 968.3606 calcd for $C_{50}H_{58}ClN_7O_7S_2$; found $[M+H]^+$ 994.3591.

5-(*N*-(6-((3-(4-(8-Chloro-5*H*-dibenzo[*b*,*e*][1,4]diazepin-11-yl)piperazin-1-ium-1-yl)propyl)amino)-6-oxohexyl)sulfamoyl)-2-(6-(diethylamino)-3-(diethyliminio)-3*H*-xanthen-9-yl)benzenesulfonate 2,2,2-trifluoroacetate (11d).

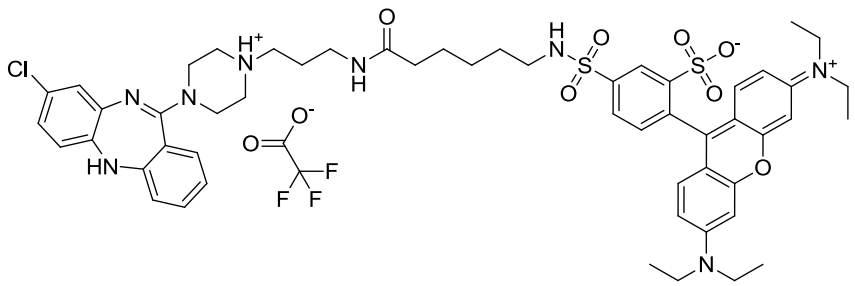

Pink solid (4 mg, 26%). ^{1}H NMR (d_6-DMSO) δ 1.20 (t, J 7.1 Hz, 12H), 1.18-1.28 (m, 4H), 1.38 (m, 2H), 1.47 (m, 2H), 1.78 (m, 2H), 2.07 (m, 2H), 2.88 (m, 2H), 3.07-3.14 (m, 6H), 3.30-3.50 (4H, under water peak), 3.61-3.64 (m, 8H), 6.87-7.06 (m, 11H), 7.25 (d, *J* 7.8 Hz, 1H), 7.35-7.39 (m, 2H), 7.48 (d, *J* 7.9 Hz, 1H), 7.92-7.95 (m, 3H), 8.42 (d, *J* 1.8 Hz, 1H), 9.55 (br s, 1H, NH). HPLC purity (λ= 214 nm): 100%, t_R = 6.59 min. HRMS (ESI)-TOF (*m/z)*: $[M+H]^+$ 1023.4028 calcd for $C_{53}H_{63}ClN_8O_7S_2$; found $[M+H]^+$ 1023.4050.

4-(8-Chloro-5*H*-dibenzo[*b*,*e*][1,4]diazepin-11-yl)-1-(3-(6-(3-(3',6'-dihydroxy-3-oxo-3*H*-spiro[isobenzofuran-1,9'-xanthen]-5-yl)thioureido)hexanamido)propyl)piperazin-1-ium 2,2,2-trifluoroacetate (11e).

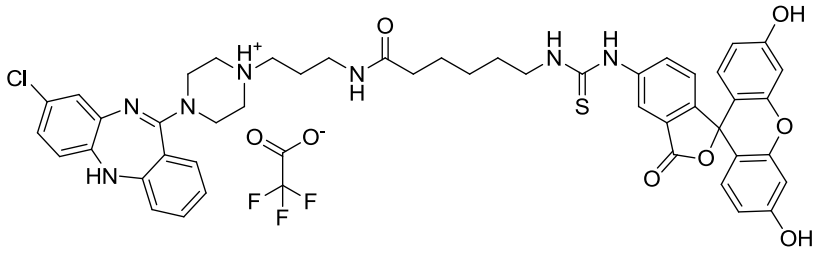

Yellow solid (4 mg, 23%). ^{1}H NMR (d_6-DMSO) δ 1.31 (m, 2H), 1.56 (m, 4H), 1.81 (m, 2H), 2.11 (t, *J* 7.4 Hz, 2H), 3.12-3.15 (m, 8H), 3.47-3.58 (m, 6H), 6.55-6.61 (m, 4H), 6.67-6.68 (m, 2H), 6.89-6.91 (m, 1H), 6.95-6.96 (m, 2H), 7.02-7.07 (m, 2H), 7.18 (d, *J* 8.3 Hz, 1H), 7.31 (dd, *J* 7.7, 1.1 Hz, 1H), 7.38-7.42 (m, 2H), 7.72 (d, *J* 7.3 Hz, 1H), 7.98 (t, *J* 5.8 Hz, 1H), 8.17 (br s, 1H), 8.23 (m, 1H), 9.64 (br s, 1H), 9.96 (br s, 1H), 10.14 (br s, 2H). HPLC purity (λ= 214 nm):

95%, t_R = 5.72 min. HRMS (ESI)-TOF (*m/z*): $[M+H]^+$ 872.2997 calcd for $C_{47}H_{46}ClN_7O_6S$; found $[M+H]^+$ 872.2994.

Synthesis of ropinirole fluorescently labelled ligands.

***tert*-Butyl (3-((2-(2-oxoindolin-4-yl)ethyl)(propyl)amino)propyl)carbamate (13).[22]** Des-propyl ropinirole (**12**, 382 mg, 1.75 mmol), K_2CO_3 (266 mg, 1.92 mmol) and *tert*-butyl (3-bromopropyl)carbamate (417 mg, 1.75 mmol) were combined in acetonitrile (20 mL). Reflux occurred for 24 h before the reaction mixture was cooled to room temperature and the solvent removed. The crude product is then purified by column chromatography (100% chloroform to 5% methanol) to give the title compound as a purple oil (285 mg, 43%). ^{1}H NMR ($CDCl_3$) δ 0.90 (t, *J* 7.3 Hz, 3H), 1.44 (s, 9H), 1.48 (m, 2H), 1.63 (m, 2H), 2.44 (m, 2H), 2.55 (t, *J* 6.6 Hz, 2H), 2.64-2.71 (m, 4H), 3.17 (m, 2H), 3.48 (s, 2H), 5.45 (s, 1H), 6.75 (d, *J* 7.6 Hz, 1H), 6.84 (d, *J* 7.8 Hz, 1H), 7.15 (t, *J* 7.8 Hz, 1H), 9.11 (br s, 1H). ^{13}C NMR ($CDCl_3$) δ 11.9 (CH_3), 20.2 (CH_2), 26.8 (CH_2), 28.5 (CH_3), 30.5 (CH_2), 35.2 (CH_2), 39.9 (CH_2), 52.6 (CH_2), 53.9 (CH_2), 55.9 (CH_2), 78.9 (C), 107.8 (CH), 122.7 (CH), 124.0 (C), 128.1 (CH), 136.7 (C), 142.8 (C), 156.2 (C), 177.9 (C). HRMS (ESI)-TOF (*m/z*): $[M+H]^+$ 376.2600 calcd for $C_{21}H_{33}N_3O_3$; found $[M+H]^+$ 376.2599.

***tert*-Butyl (6-oxo-6-((3-((2-(2-oxoindolin-4-yl)ethyl)(propyl)amino)propyl)amino)hexyl)carbamate (15).[22]**

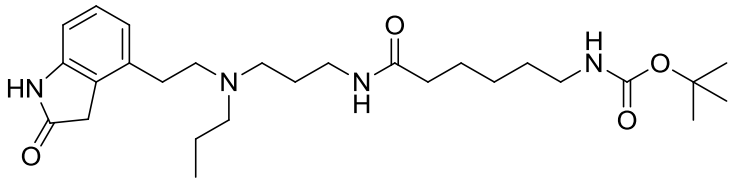

Compound **13** was Boc de-protected prior to use via standard conditions as previously mentioned for other analogues and confirmed by TLC and used immediately due to instability. 6-((tert-butoxycarbonyl)amino)hexanoic acid (50 mg, 0.22 mmol) and *N*,*N*-diisopropylethylamine (0.04 mL, 0.24 mmol) was added to dimethylformamide (5 mL) under N_2 at room temperature. BOP (100 mg, 0.23 mmol) was then added and the reaction left to stir for 5-10 mins. Compound **14**

(63 mg, 0.23 mmol) was then added slowly to the reaction mixture and stirred at room temperature overnight. The solvent was then removed in vacuo and the resulting residue dissolved in dichloromethane (20 mL) and partitioned between sodium bicarbonate (30 mL). The aqueous phase was further extracted with 3 × 10 mL portions of dichloromethane. The organic layers were then collected and washed with water (30 mL), brine (30 mL), dried over anhydrous Na_2SO_4, filtered and concentrated to give the crude product. To remove excess HMPA, the crude product was dissolved in ethyl acetate and washed with 3 × 20 mL portions of 2 M brine. Purification of the product was performed by column chromatography ($CHCl_3$/MeOH: 10-20%) to give the product as pale yellow oil that turns purple upon standing (21 mg, 20%). ^{1}H NMR (d_6-DMSO) δ 0.82 (t, *J* 7.3 Hz, 3H), 1.19 (m, 3H), 1.31-1.54 (m, 17H), 2.02 (m, 2H), 2.37 (m, 2H), 2.43 (m, 2H), 2.58 (m, 3H), 2.87 (m, 2H), 3.03 (m, 2H), 3.43 (s, 2H), 6.64 (d, *J* 7.3 Hz, 1H), 6.73-6.77 (m, 2H), 7.07 (t, *J* 7.7 Hz, 1H), 7.72 (t, *J* 5.4 Hz, 1H), 10.32 (br s, 1H). ^{13}C NMR (d_6-DMSO) δ 11.8 (CH_3), 20.1 (CH_2), 25.1 (CH_2), 26.0 (CH_2), 26.9 (CH_2), 28.3 (CH_3), 29.3 (CH_2), 29.9 (CH_2), 34.5 (CH_2), 35.5 (CH_2), 36.9 (CH_2), 39.8 (CH_2), 51.0 (CH_2), 53.7 (CH_2), 55.3 (CH_2), 77.3 (C), 106.8 (CH), 121.8 (CH), 124.4 (C), 127.5 (CH), 136.7 (C), 143.4 (C), 155.6 (C), 171.8 (C), 176.3 (C). HRMS (ESI)-TOF (*m/z)*: $[M+H]^+$ 489.3441 calcd for $C_{27}H_{44}N_4O_4$; found $[M+H]^+$ 489.3441.

6-Amino-*N*-(3-((2-(2-oxoindolin-4-yl)ethyl)(propyl)amino)propyl)hexanamide (16).

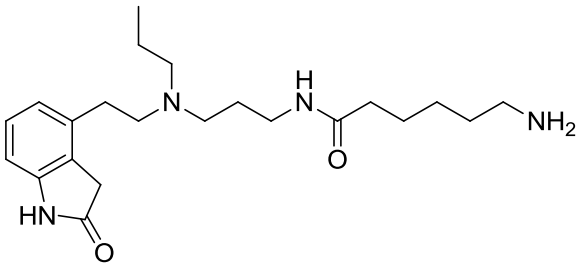

Compound **15** was Boc de-protected prior to use via standard conditions as previously mentioned for other analogues and confirmed by TLC and used immediately in general procedures B and C due to instability.

(*E*)-5,5-Difluoro-3-(4-(2-oxo-2-((6-oxo-6-((3-((2-(2-oxoindolin-4-yl)ethyl)(propyl)ammonio)propyl)amino)hexyl)amino)ethoxy)styryl)-7-(thiophen-2-yl)-5*H*-dipyrrolo[1,2-*c*:2',1'-*f*][1,3,2]diazaborinin-4-ium-5-uide 2,2,2-trifluoroacetate (17a).

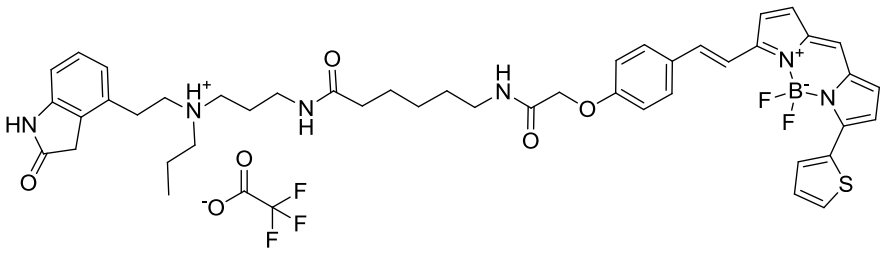

Blue solid (3 mg, 48%). ^{1}H NMR (d_6-DMSO) δ 0.93 (t, *J* 7.3 Hz, 3H), 1.21-1.27 (m, 4H), 1.40-1.54 (m, 4H), 1.64 (m, 2H), 1.79 (m, 2H), 2.08 (t, *J* 7.4 Hz, 2H), 2.87 (m, 2H), 3.11-3.12 (m, 8H), 3.24 (m, 2H), 4.53 (s, 2H), 6.73 (d, *J* 7.6 Hz, 1H), 6.85 (d, *J* 7.5 Hz, 1H), 6.96 (d, *J* 4.2 Hz, 1H), 7.07-7.09 (m, 2H), 7.15 (t, *J* 7.7 Hz, 1H), 7.27-7.31 (m, 3H), 7.38-7.42 (m, 2H), 7.61-7.63 (m, 3H), 7.75 (d, *J* 16.3 Hz, 1H), 7.84 (dd, *J* 5.1, 1.0 Hz, 1H), 7.97 (t, *J* 5.6 Hz, 1H), 8.05 (dd, *J* 3.8, 1.0 Hz, 1H), 8.15 (t, *J* 5.7 Hz, 1H), 9.34 (br s, 1H), 10.43 (s, 1H). HPLC purity (λ= 214 nm): 95%, t_R = 7.45 min. HRMS (ESI)-TOF (*m/z)*: $[M+H]^+$ 821.3832 calcd for $C_{45}H_{51}BF_2N_6O_4S$; found $[M+H]^+$ 821.3863.

3,3-Dimethyl-1-(6-oxo-6-((3-((2-(2-oxoindolin-4-yl)ethyl)(propyl)ammonio)propyl)amino)hexyl)-2-((1*E*,3*E*,5*E*)-5-(1,3,3-trimethyl-5-sulfoindolin-2-ylidene)penta-1,3-dien-1-yl)-3*H*-indol-1-ium-5-sulfonate 2,2,2-trifluoroacetate (17b).

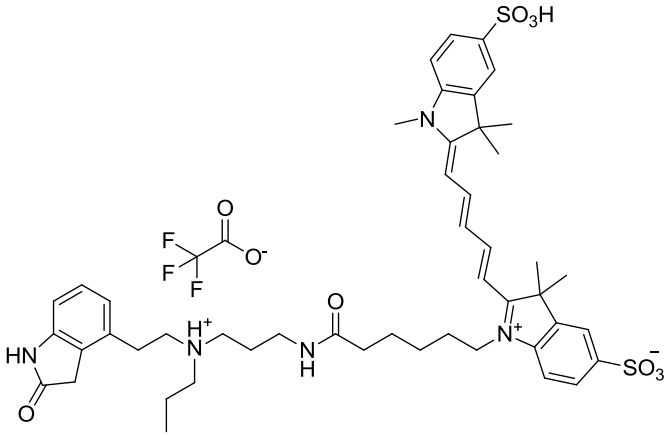

Blue solid (2 mg, 22%). ^{1}H NMR (d_6-DMSO) δ 0.92 (t, *J* 7.3 Hz, 3H), 1.27 (m, 2H), 1.53 (m, 3H), 1.63-1.70 (m, 17H), 2.04 (m, 2H), 2.88 (m, 2H), 3.01-3.09 (m, 6H), 3.23 (m, 2H), 3.55 (m, 2H), 3.61 (m, 3H), 4.11 (m, 2H), 6.29 (t, *J* 13.3 Hz, 2H), 6.56 (m, 1H), 6.72 (d, *J* 7.7 Hz, 1H), 6.86 (d, *J* 7.4 Hz, 1H), 7.14 (t, *J* 7.8 Hz, 1H), 7.29-7.35 (m, 2H), 7.62-7.67 (m, 2H), 7.82-7.87 (m, 3H), 8.33-8.40 (m, 2H), 9.30 (br s, 1H), 10.42 (s, 1H). HPLC purity (λ= 214 nm): 100%, t_R = 4.47 min. HRMS (ESI)-TOF (*m/z)*: $[M+H]^+$ 900.4040 calcd for $C_{48}H_{61}N_5O_8S_2$; found $[M+H]^+$ 900.4028.

3,3-Dimethyl-1-(6-oxo-6-((3-((2-(2-oxoindolin-4-yl)ethyl)(propyl)ammonio)propyl)amino)hexyl)-2-((1*E*,3*E*)-3-(1,3,3-trimethyl-5-sulfoindolin-2-ylidene)prop-1-en-1-yl)-3*H*-indol-1-ium-5-sulfonate 2,2,2-trifluoroacetate (17c).

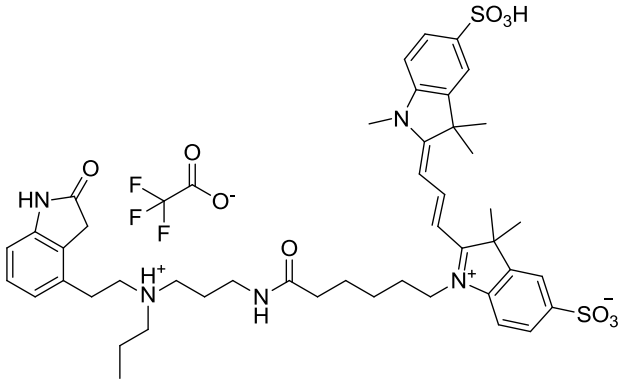

Pink solid (4 mg, 40%). ^{1}H NMR (d_6-DMSO) δ 0.93 (t, *J* 7.3 Hz, 3H), 1.31 (m, 2H), 1.55 (m, 2H), 1.63-1.74 (m, 18H), 2.06 (t, *J* 7.1 Hz, 2H), 2.88 (m, 2H), 3.02 (m, 2H), 3.07-3.12 (m, 4H), 3.23 (m, 2H), 3.55 (s, 2H), 3.66 (s, 3H), 4.13 (t, *J* 6.3 Hz, 2H), 6.48 (d, *J* 13.5 Hz, 1H), 6.49 (d, *J* 13.3 Hz, 1H), 6.72 (d, *J* 7.6 Hz, 1H), 6.86 (d, *J* 7.5 Hz, 1H), 7.15 (t, *J* 7.8 Hz, 1H), 7.39 (d, *J* 8.4 Hz, 1H), 7.41 (d, *J* 8.4 Hz, 1H), 7.68 (dd, *J* 3.6, 1.6 Hz, 1H), 7.70 (dd, *J* 3.6, 1.6 Hz, 1H), 7.82-7.83 (m, 2H), 7.89 (t, *J* 5.5 Hz, 1H), 8.34 (t, *J* 13.5 Hz, 1H), 9.29 (br s, 1H), 10.42 (s, 1H). HPLC purity (λ= 214 nm): 100%, t_R = 4.19 min. HRMS (ESI)-TOF (*m/z*): $[M+H]^+$ 874.3883 calcd for $C_{46}H_{59}N_5O_8S_2$; found $[M+H]^+$ 874.3875.

2-(6-(Diethylamino)-3-(diethyliminio)-3*H*-xanthen-9-yl)-5-(*N*-(6-oxo-6-((3-((2-(2-oxoindolin-4-yl)ethyl)(propyl)ammonio)propyl)amino)hexyl)sulfamoyl)benzenesulfonate 2,2,2-trifluoroacetate (17d).

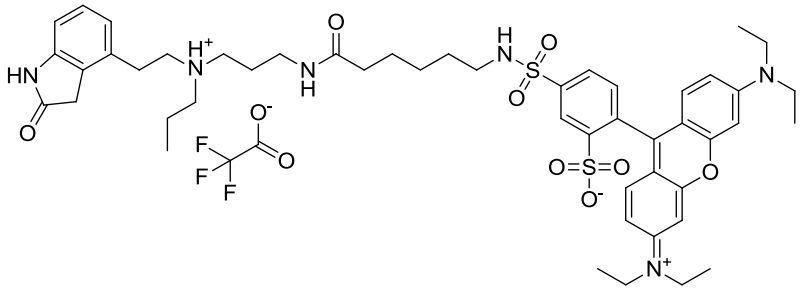

Purple solid (3 mg, 27%). ^{1}H NMR (d_6-DMSO) δ 0.92 (t, *J* 7.1 Hz, 3H), 1.19-1.23 (m, 12H), 1.39-1.49 (m, 4H), 1.64 (m, 2H), 1.79 (m, 2H), 2.07 (m, 2H), 2.86-2.88 (m, 4H), 3.11-3.13 (m, 4H), 3.23-3.51 (m, 6H, under H_2O peak), 3.55 (s, 2H), 3.64-3.65 (m, 8H), 6.73 (d, *J* 7.8 Hz, 1H), 6.85 (d, *J* 7.6 Hz, 1H), 6.94-6.98 (m, 4H), 7.05-7.07 (m, 2H), 7.15 (m, 1H), 7.49 (d, *J* 7.4 Hz, 1H), 7.92-7.97 (m, 3H), 8.42 (s, 1H), 9.40 (br s, 1H), 10.42 (s, 1H). HPLC purity (λ= 214 nm): 100%, t_R = 6.46 min. HRMS (ESI)-TOF (*m/z*): $[M+H]^+$ 929.4305 calcd for $C_{49}H_{64}N_6O_8S_2$; found $[M+H]^+$ 929.4314.

3-(6-(3-(3',6'-Dihydroxy-3-oxo-3*H*-spiro[isobenzofuran-1,9'-xanthen]-5-yl)thioureido)hexanamido)-*N*-(2-(2-oxoindolin-4-yl)ethyl)-*N*-propylpropan-1-aminium 2,2,2-trifluoroacetate (17e).

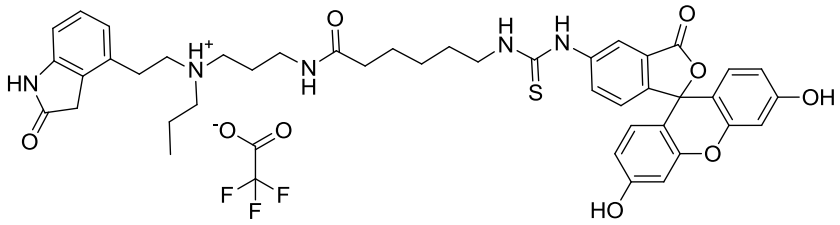

Yellow solid (2 mg, 20%). ^{1}H NMR (d_6-DMSO) δ 0.94 (t, *J* 7.3 Hz, 3H), 1.31 (m, 2H), 1.52-1.71 (m, 6H), 1.81 (m, 2H), 2.12 (t, *J* 7.5 Hz, 2H), 2.55 (s, 2H), 2.88 (m, 2H), 3.08-3.17 (m, 6H), 3.26 (m, 2H), 3.56 (s, 2H), 6.55-6.61 (m, 4H), 6.68 (d, *J* 2.1 Hz, 2H), 6.73 (d, *J* 7.8 Hz, 1H), 6.86 (d, *J* 7.5 Hz, 1H), 7.14-7.19 (m, 2H), 7.73 (d, *J* 8.1 Hz, 1H), 7.99 (t, *J* 5.5 Hz, 1H), 8.18 (br s, 1H),

8.24 (s, 1H), 9.38 (br s, 1H), 9.98 (br s, 1H), 10.15 (br s, 2H), 10.43 (s, 1H). HPLC purity (λ= 214 nm): 100%, t_R = 5.53 min. HRMS (ESI)-TOF (*m/z)*: $[M+H]^+$ 778.3274 calcd for $C_{43}H_{47}N_5O_7S$; found $[M+Na]^+$ 800.3002.

Synthesis of SB269252 fluorescently labelled ligands.

Ethyl 5-hydroxy-1*H*-indole-2-carboxylate (19).[31]

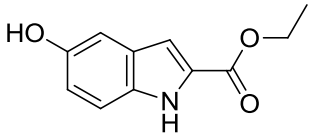

5-Hydoxy-indole-2-carboxylic acid (**18**, 900 mg, 5.08 mmol) is added to ethanol (40 mL) and a catalytic amount of H_2SO_4 (0.10 mL, 1.78 mmol). After 24 h reflux, the solvent was removed in vacuo and the resulting residue dissolved in DCM (20 mL) and washed with $NaHCO_3$ (3 × 20 mL) and brine (20 mL). The organic layer was dried over Na_2SO_4 and evaporated to dryness to give the product as a beige-brown solid (or white needles) (822 mg, 79%). ^{1}H NMR ($CDCl_3$) δ 1.41 (t, *J* 7.1 Hz, 3H) 4.40 (q, *J* 7.1 Hz, 2H), 4.82 (br s, 1H, NH), 6.93 (dd, *J* 8.8, 2.4 Hz, 1H), 7.06 (d, *J* 2.4 Hz, 1H), 7.10 (dd, *J* 2.1, 0.9 Hz, 1H), 7.29 (dt, *J* 8.8, 0.9 Hz, 1H), 8.84 (br s, 1H, OH). ^{13}C NMR ($CDCl_3$) δ 14.5 (CH_3), 61.2 (CH_2), 106.1 (CH), 108.0 (CH), 112.9 (CH), 116.3 (CH), 128.3 (C), 132.5 (C), 148.3 (C), 150.3 (C), 162.1 (C).

1-*tert*-Butyl 2-ethyl 5-hydroxy-1*H*-indole-1,2-dicarboxylate (20).[32]

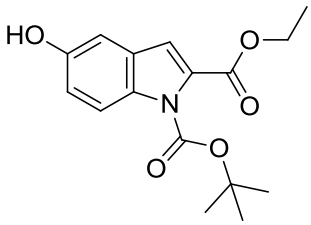

Compound **19** (750 mg, 3.65 mmol) was added to 1, 4-dioxane (8 mL). Triethylamine (0.76 mL, 5.48 mmol) and BOC_2O (1.2 g, 5.48 mmol) were also added slowly to the reaction mixture which is then heated up to reflux for 3 h. The solvent is then removed in vacuo and the resulting residue dissolved in ethyl acetate (20 mL). The organic layer is then washed with 1M $KHSO_4$

(50 mL), water (50 mL), brine (50 mL) and dried over anhydrous Na_2SO_4 before evaporating to dryness to give a beige solid that was not purified any further (1.09 g, 97%). ^{1}H NMR ($CDCl_3$) δ 1.42 (t, *J* 7.1 Hz, 3H), 1.57 (s, 9H), 4.41 (q, *J* 7.1 Hz, 2H), 7.13 (dd, *J* 8.9, 2.3 Hz, 1H), 7.19 (dd, *J* 2.1, 0.9 Hz, 1H), 7.39 (dt, *J* 8.9, 0.8 Hz, 1H), 7.47 (m, 1H), 9.03 (br s, 1H, OH). ^{13}C NMR ($CDCl_3$) δ 14.5 (CH_3), 27.9 (CH_3), 61.3 (CH_2), 83.5 (C), 108.9 (CH), 112.5 (CH), 114.2 (CH), 119.9 (CH), 127.7 (C), 128.9 (C), 134.7 (C), 145.5 (C), 152.8 (C), 161.9 (C).

1-*tert*-Butyl 2-ethyl 5-(2-((*tert*-butoxycarbonyl)amino)ethoxy)-1*H*-indole-1,2-dicarboxylate (21).

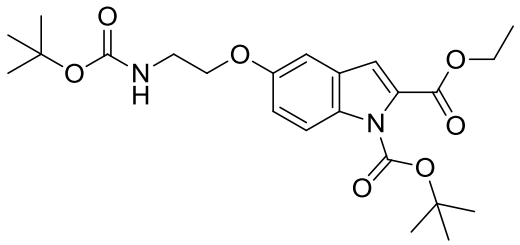

Compound **20** (800 mg, 2.62 mmol) is added to dry DMF (15 mL) under N_2. Sodium hydride (60% in mineral oil dispersion, 157 mg, 3.93 mmol) is added slowly and the reaction stirred at room temperature for 1 h. *tert*-Butyl (3-bromopropyl)carbamate (686 mg, 2.88 mmol) was then dissolved in DMF (1 mL) and added dropwise to the reaction mixture which was left to stir overnight. The DMF was then removed in vacuo and the resulting residue dissolved in ethyl acetate. The organic layer was washed with water (2 × 20 mL) and brine (2 × 20 mL), dried over Na_2SO_4, filtered and evaporated to dryness. Further purification via column chromatography (gradient 4:1 to 2:1 petroleum spirits: ethyl acetate) gave the product as a colourless oil (952 mg, 78%). ^{1}H NMR ($CDCl_3$) δ 1.41 (t, *J* 7.1 Hz, 3H), 1.45 (s, 9H), 1.57 (s, 9H), 1.99 (p, *J* 6.8 Hz, 2H), 3.12 (m, 2H), 4.38 (q, *J* 7.1 Hz, 2H), 4.61 (t, *J* 7.0 Hz, 2H), 4.96 (br s, 1H, NH), 7.16 (dd, *J* 9.0, 2.3 Hz, 1H), 7.28 (d, *J* 0.7 Hz, 1H), 7.36 (d, *J* 9.0 Hz, 1H), 7.45 (d, *J* 2.1 Hz, 1H). ^{13}C NMR ($CDCl_3$) δ 14.4 (CH_3), 27.8 (CH_3), 28.5 (CH_3), 30.8 (CH_2), 37.8 (CH_2), 42.3 (CH_2), 60.9 (CH_2), 79.3 (C), 83.4 (C), 110.8 (CH), 110.9 (CH), 114.2 (CH), 119.6 (CH), 125.9 (C), 128.5 (C), 136.8 (C), 145.4 (C), 152.7 (C), 156.1 (C), 162.1 (C).

1-(*tert*-Butoxycarbonyl)-5-(3-((*tert*-butoxycarbonyl)amino)propoxy)-1*H*-indole-2-carboxylic acid (22).

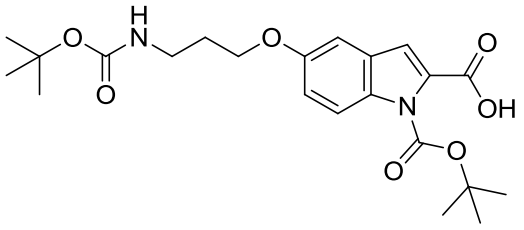

Compound **21** (952 mg, 2.06 mmol) dissolved in THF (15 mL). LiOH (148 mg, 6.17 mmol) was dissolved in water (5 mL) and then added to the reaction mixture which was left to stir at RT overnight. After this time, the pH was adjusted to ~2 and extracted with ethyl acetate (3 × 20 mL). The combined organic layers were then washed with water (50 mL), brine (50 mL), dried over anhydrous Na_2SO_4, filtered and evaporated to dryness to give a brown foam (831 mg, 93%). The product was confirmed only via ^{1}H NMR and used as the crude as further purification results in multiple degradation products. ^{1}H NMR ($CDCl_3$) δ 1.46 (s, 9H), 1.58 (s, 9H), 2.01 (m, 2H), 4.62 (t, *J* 7.1 Hz, 2H), 4.90 (m, 1H, NH), 7.18 (dd, *J* 9.0, 2.2 Hz, 1H), 7.36-7.40 (m, 2H), 7.48 (d, *J* 2.2 Hz, 1H).

Ethyl 2-((*trans*)-4-((*tert*-butoxycarbonyl)amino)cyclohexyl)acetate (24).[33]

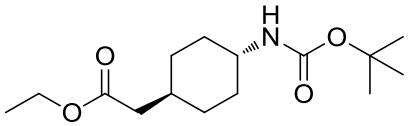

Compound **23** (984 mg, 3.82 mmol) was taken up in DCM (15 mL) and to the mixture at RT was added *N*-(3-dimethylaminopropyl)-*N*′-ethylcarbodiimide hydrochloride (806 mg, 4.21 mmol) followed by a catalytic amount of 4-(dimethylamino)pyridine (23 mg, 0.19 mmol). The colourless solution was allowed to stir at RT for 15 min, then absolute EtOH (15 mL) was added, and the mixture was allowed to stir at RT for 24 h. The mixture was then concentrated in vacuo and taken up in EtOAc (30 mL) causing a precipitate to emerge. The organic layer was washed with 1 M $KHSO_4$ (2 × 20 mL), brine (20 mL), dried over anhydrous Na_2SO_4 and evaporated to dryness to reveal a colourless oil which later started to solidify (646 mg, 59%). ^{1}H NMR ($CDCl_3$)

δ 1.03-1.17 (m, 4H), 1.25 (t, *J* 7.1 Hz, 3H), 1.44 (s, 9H), 1.69-1.79 (m, 3H), 1.98-2.01 (m, 2H), 2.18 (d, *J* 6.8 Hz, 2H), 3.37 (br s, 1H), 4.12 (q, *J* 7.1 Hz, 2H), 4.37 (br s, 1H). ^{13}C NMR ($CDCl_3$) δ 14.4 (CH_3), 28.6 (CH_3), 31.7 (CH_2), 33.3 (CH_2), 34.2 (CH), 41.6 (CH_2), 49.6 (CH), 60.4 (CH_2), 79.3 (C), 155.4 (C), 173.1 (C).

***tert*-Butyl ((*trans*)-4-(2-oxoethyl)cyclohexyl)carbamate (25).[33]**

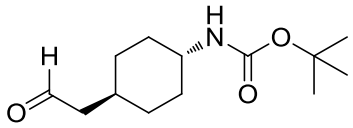

Compound **24** (631 mg, 2.21 mmol) was taken up in toluene (25 mL), degassed with nitrogen bubbling for 15 min, then cooled to -78 °C on a dry ice/acetone bath for a further 10 min. To the stirring colourless solution under nitrogen, was slowly added diisobutylaluminium hydride (1 M in toluene, 0.86 mL, 4.42 mmol) dropwise over 15 min. The mixture was then allowed to stir at -78 °C until foaming of the reaction mixture stopped (1 h). The mixture was then quenched slowly with methanol (10 mL) in toluene (10 mL), and warmed to RT with stirring for 15 min. Saturated potassium sodium tartrate solution (30 mL) was added and the mixture stirred vigorously for 30 min. The product was then extracted with diethyl ether (3 × 30 mL), and the combined organic extracts dried over anhydrous Na_2SO_4 and evaporated to dryness to give the crude compound. The product was further purified by column chromatography (5:1 petroleum spirits/ethyl acetate) to give a white waxy solid (485 mg, 91%). ^{1}H NMR ($CDCl_3$) δ 1.05-1.19 (m, 4H), 1.44 (s, 9H), 1.77-1.84 (m, 3H), 2.00-2.05 (m, 2H), 2.33 (dd, *J* 6.6, 2.0 Hz, 2H), 3.38 (br s, 1H), 4.39 (br s, 1H), 9.76 (t, *J* 2.01 Hz, 1H). ^{13}C NMR ($CDCl_3$) δ 28.5 (CH_3), 31.8 (CH), 31.9 (CH_2), 33.3 (CH_2), 49.5 (CH), 50.8 (CH_2), 79.3 (C), 155.3 (C), 202.4 (CH).

***tert*-Butyl ((*trans*)-4-(2-(7-cyano-3,4-dihydroisoquinolin-2(1*H*)-yl)ethyl)cyclohexyl)carbamate (28).[33]**

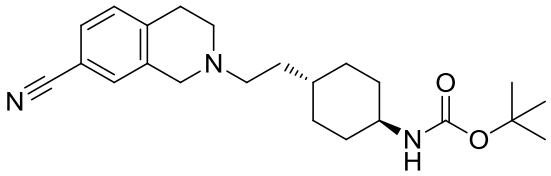

Compound **25** (1.29 g, 5.34 mmol) and 1,2,3,4-tetrahydroisoquinoline-7-carbonitrile (**26**, 845 mg, 5.34 mmol) were taken up in 1,2-DCE (30 mL). $NaBH(OAc)_3$ (1.70 g, 8.01 mmol) was added to the stirred solution at RT under nitrogen. After 24 h, the reaction mixture was diluted with DCM (15 mL), washed with 1 M K_2CO_3 solution (3 × 20 mL), brine (20 mL), dried over anhydrous Na_2SO_4 and evaporated to dryness. The crude material was purified by flash column chromatography (1:1 Petroleum spirits/ethyl acetate) to give the title compound as a yellow solid (1.13 g, 55%). ^{1}H NMR ($CDCl_3$) δ 1.00-1.13 (m, 4H), 1.25 (m, 1H), 1.44 (s, 9H), 1.48-1.60 (m, 2H), 1.80 (m, 2H), 1.99 (m, 2H), 2.55 (m, 2H), 2.75 (m, 2H), 2.96 (m, 2H), 3.37 (br s, 1H), 3.63 (s, 2H), 4.38 (d, *J* 6.3 Hz, 1H), 7.19 (d, *J* 7.9 Hz, 1H), 7.32 (s, 1H), 7.41 (dd, *J* 7.9, 1.5 Hz, 1H). ^{13}C NMR ($CDCl_3$) δ 28.4 (CH_3), 29.4 (CH_2), 31.9 (CH_2), 33.3 (CH_2), 34.0 (CH_2), 35.1 (CH), 49.8 (CH), 50.2 (CH_2), 55.5 (CH_2), 56.0 (CH_2), 78.8 (C), 109.2 (C), 119.0 (C), 129.4 (CH), 129.5 (CH), 130.3 (CH), 136.3 (C), 140.3 (C), 155.2 (C).

***tert*-Butyl ((*trans*)-4-(2-(4-(2-methoxyphenyl)piperazin-1-yl)ethyl)cyclohexyl)carbamate (29).**

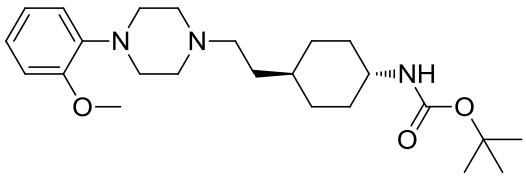

2-Methoxyphenylpiperazine hydrochloride (**27**, 701 mg, 3.06 mmol), DIPEA (0.53 mL, 3.06 mmol) and **25** (740 mg, 3.06 mmol) was added to 1,2-dichloroethane (20 mL) under N_2 at rt. $NaBH(OAc)_3$ (396 mg, 3.06 mmol) was added and the reaction stirred for several hours before an additional 2 equivalents were added. After 24 h, the reaction mixture was diluted with DCM

(15 mL), washed with 1 M K_2CO_3 solution (3 × 20 mL), brine (20 mL), dried over anhydrous Na_2SO_4 and evaporated to dryness. The crude material was purified by column chromatography (gradient: 100% chloroform : 2% methanol) to give the title compound as a pale yellow solid (928 mg, 55%). ^{1}H NMR ($CDCl_3$) δ 1.00-1.09 (m, 4H), 1.20-1.24 (m, 1H), 1.41-1.47 (m, 11H), 1.75-1.8 (m, 2H), 1.97-2.01 (m, 2H), 2.39-2.43 (m, 2H), 2.64 (m, 4H), 3.10 (m, 4H), 3.37 (br s, 1H), 3.86 (s, 3H), 4.36 (m, 1H), 6.86 (dd, *J* 7.9, 1.3 Hz, 1H), 6.89-7.02 (m, 3H). ^{13}C NMR ($CDCl_3$) δ 28.6 (CH_3), 32.1 (CH_2), 33.6 (CH_2), 34.0 (CH_2), 35.7 (CH), 50.03 (CH), 50.8 (CH_2), 53.7 (CH_2), 55.5 (CH_3), 56.9 (CH_2), 79.2 (C), 111.3 (CH), 118.3 (CH), 121.1 (CH), 123.0 (CH), 141.5 (C), 152.4 (C), 155.4 (C).

2-(2-((*trans*)-4-Aminocyclohexyl)ethyl)-1,2,3,4-tetrahydroisoquinoline-7-carbonitrile (30).[33]

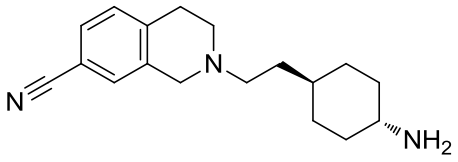

Compound **28** (1.13 g, 2.94 mmol) was taken up in DCM (10 mL) and trifluoroacetic acid (2 mL) was added dropwise at room temperature. After 2 h, the reaction mixture was diluted with DCM (10 mL) and water (10 mL) and ammonium hydroxide solution (5 mL). The pH was adjusted to approximately 10 and the aqueous layer was extracted with further with DCM (2 × 20 mL). The organic extracts were then combined and washed with brine (20 mL) and dried over anhydrous Na_2SO_4, then evaporated to dryness to furnish the free base (717 mg, 86%). The resulting residue was then added to 1 equivalent of 1 M HCl in diethyl ether and stirred vigorously for 5 minutes. The solvent was then removed in vacuo to leave the dihydrochloride product as a yellow solid in quantitative yield. ^{1}H NMR ($CDCl_3$) δ 0.84-1.03 (m, 4H), 1.13-117 (m, 1H), 1.34-1.39 (m, 2H), 1.65-1.74 (m, 4H), 2.42-2.46 (m, 3H), 2.63 (t, *J* 5.8 Hz, 2H), 2.85 (t, *J* 5.6 Hz, 2H), 3.05 (br s, 2H, NH_2), 3.54 (s, 2H), 7.29 (d, *J* 8.5 Hz, 1H), 7.54-7.56 (m, 2H). ^{13}C NMR ($CDCl_3$) δ 28.9 (CH_2), 31.8 (CH_2), 33.7 (CH_2), 34.8 (CH), 36.0 (CH_2), 49.8 (CH_2), 50.5

(CH), 54.8 (CH_2), 55.4 (CH_2), 108.2 (C), 119.1 (C), 129.4 (CH), 129.6 (CH), 130.3 (CH), 136.7 (C), 140.7 (C).

(*trans*)-4-(2-(4-(2-Methoxyphenyl)piperazin-1-yl)ethyl)cyclohexanamine (31).

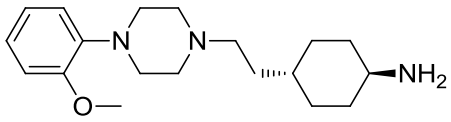

Compound **29** (920 mg, 2.20 mmol) was added to DCM (5 mL) and TFA (2 mL) and stirred at RT for several hours. After this time the reaction mixture was diluted with DCM (10 mL) and the pH adjusted to 10-14 using 1 M NaOH. The organic layer was removed, the aqueous layer further extracted with 3 × 10 mL portions of DCM and the combined organic extracts washed with saturated brine, dried over anhydrous Na_2SO_4, filtered and evaporated to dryness to give a yellow solid (677 mg, 97%). ^{1}H NMR ($CDCl_3$) δ 0.98-1.09 (m, 4H), 1.23 (m, 1H), 1.36 (br s, 2H), 1.41-1.47 (m, 2H), 1.76 (m, 2H), 1.85 (m, 2H), 2.40-2.44 (m, 2H), 2.60 (m, 1H), 2.65 (m, 4H), 3.10 (m, 4H), 3.86 (s, 3H), 6.86 (dd, *J* 7.9, 1.3 Hz, 1H), 6.89-7.02 (m, 3H). ^{13}C NMR ($CDCl_3$) δ 32.3 (CH_2), 34.2 (CH_2), 35.8 (CH_2), 36.9 (CH), 50.8 (CH), 50.9 (CH_2), 53.7 (CH_2), 55.5 (CH_3), 57.0 (CH_2), 111.2 (CH), 118.3 (CH), 121.1 (CH), 123.0 (CH), 141.5 (C), 152.4 (C).

t*ert*-Butyl 5-(3-((*tert*-butoxycarbonyl)amino)propoxy)-2-(((*trans*)-4-(2-(7-cyano-3,4-dihydroisoquinolin-2(1*H*)-yl)ethyl)cyclohexyl)carbamoyl)-1*H*-indole-1-carboxylate (32).

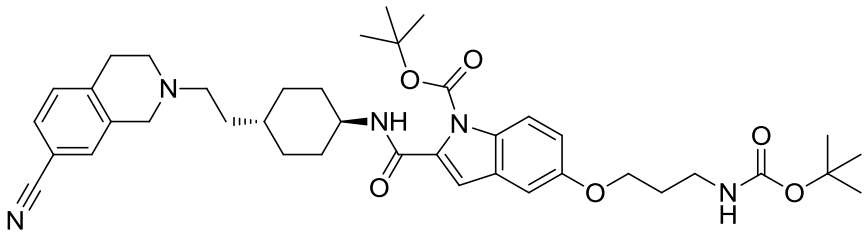

Compound **30** (181 mg, 0.42 mmol) and *N*,*N*-diisopropylethylamine (0.08 mL, 0.45 mmol) was added to *N*,*N*-dimethylformamide (5 mL) under N_2 at room temperature. BOP (1934 mg, 0.44 mmol) was then added and the reaction left to stir for 5-10 mins. 2-(2-((*trans*)-4-aminocyclohexyl)ethyl)-1,2,3,4-tetrahydroisoquinoline-7-carbonitrile dihydrochloride (164 mg, 0.46 mmol) was dissolved in 2 mL of dimethylformamide and *N*,*N*-diisopropylethylamine (1

equiv.) was added to convert to the free amine. The amine was then added slowly to the reaction mixture and stirred at room temperature for 7 h. The solvent was then removed in vacuo and the resulting residue dissolved in dichloromethane (50 mL) and partitioned between sodium bicarbonate (50 mL). The aqueous phase was further extracted with 3 × 50 mL portions of dichloromethane. The organic layers were then collected and washed with water (50 mL), brine (50 mL), dried over anhydrous Na_2SO_4, filtered and concentrated to give the crude product. To remove excess HMPA, the crude product was dissolved in ethyl acetate and washed with 3 × 50 mL portions of 2M brine. Purification of the product was done by column chromatography (2:1 ethylacetate/petroleum spirits) to give the product as a white solid (168 mg, 57%). ^{1}H NMR ($CDCl_3$) δ 1.13-1.36 (m, 5H), 1.44 (s, 9H), 1.54 (m, 2H), 1.57 (s, 9H), 1.86 (m, 2H), 1.98 (m, 2H), 2.10 (m, 2H), 2.55 (m, 2H), 2.74 (m, 2H), 2.95 (m, 2H), 3.06 (m, 2H), 3.62 (s, 2H), 3.89 (m, 1H), 4.54 (t, *J* 6.6 Hz, 2H), 5.39 (m, 1H, NH), 6.16 (d, *J* 8.1 Hz, 1H, NH), 6.76 (s, 1H), 7.10 (dd, *J* 9.0, 2.3 Hz, 1H), 7.19 (d, *J* 7.9 Hz, 1H), 7.30-7.34 (m, 2H), 7.37-7.40 (m, 2H). ^{13}C NMR ($CDCl_3$) δ 27.8 (CH_3), 28.5 (CH_3), 29.5 (CH_2), 30.5 (CH_2), 31.9 (CH_2), 33.0 (CH_2), 34.1 (CH_2), 35.3 (CH), 37.5 (CH_2), 42.2 (CH_2), 49.0 (CH), 50.3 (CH_2), 55.7 (CH_2), 56.1 (CH_2), 79.0 (C), 83.4 (C), 103.9 (CH), 109.4 (C), 110.9 (CH), 113.5 (CH), 118.4 (CH), 119.2 (C), 126.3 (C), 129.6 (CH), 129.7 (CH), 130.5 (CH), 133.2 (C), 135.9 (C), 136.4 (C), 140.4 (C), 145.4 (C), 152.7 (C), 156.2 (C), 161.8 (C). HRMS (ESI)-TOF (*m/z*): $[M+H]^+$ 700.4074 calcd for $C_{40}H_{53}N_5O_6$; found $[M+H]^+$ 700.4084.

***tert*-Butyl 5-(3-((tert-butoxycarbonyl)amino)propoxy)-2-(((*trans*)-4-(2-(4-(2-methoxyphenyl)piperazin-1-yl)ethyl)cyclohexyl)carbamoyl)-1*H*-indole-1-carboxylate (33).**

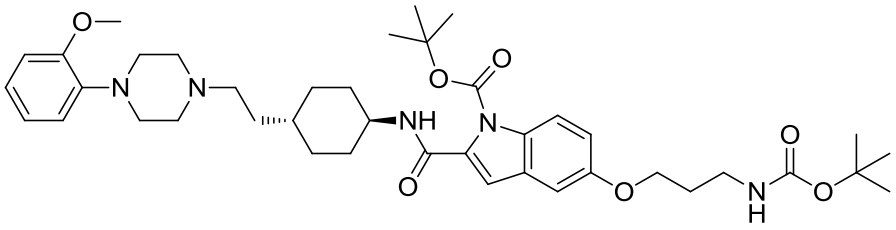

Compound **31** (248 mg, 0.57 mmol) and *N*,*N*-diisopropylethylamine (0.10 mL, 0.60 mmol) was added to dimethylformamide (5 mL) under N_2 at room temperature. BOP (266 mg, 0.60 mmol) was then added and the reaction left to stir for 5-10 mins. (*trans*)-4-(2-(4-(2-methoxyphenyl)piperazin-1-yl)ethyl)cyclohexanamine (200 mg, 0.63 mmol) was then added slowly to the reaction mixture and stirred at room temperature for overnight. The solvent was then removed in vacuo and the resulting residue dissolved in dichloromethane (50 mL) and partitioned between sodium bicarbonate (50 mL). The aqueous phase was further extracted with 3 × 50 mL portions of dichloromethane. The organic layers were then collected and washed with water (50 mL), brine (50 mL), dried over anhydrous Na_2SO_4, filtered and concentrated to give the crude product. To remove excess HMPA, the crude product was dissolved in ethyl acetate and washed with 3 × 50 mL portions of 2M brine. Purification of the product was done by column chromatography ($CHCl_3$/MeOH: 2-10%) to give the product as a beige solid (247 mg, 59%). ^{1}H NMR ($CDCl_3$) δ 1.11-1.32 (m, 5H), 1.48 (s, 9H), 1.50 (m, 2H), 1.57 (s, 9H), 1.86 (m, 2H), 2.00 (m, 2H), 2.11 (m, 2H), 2.45 (m, 2H), 2.66 (m, 4H), 3.07-3.11 (m, 6H), 3.87 (s, 3H), 3.90 (m, 1H), 4.57 (t, *J* 6.7 Hz, 2H), 5.37 (m, 1H), 6.03 (d, *J* 8.1 Hz, 1H), 6.76 (s, 1H), 6.86 (dd, *J* 8.0, 1.3 Hz, 1H), 6.90-7.02 (m, 3H), 7.11 (dd, *J* 9.0, 2.3 Hz, 1H), 7.34 (d, *J* 9.0 Hz, 1H), 7.39 (d, *J* 2.2 Hz, 1H). ^{13}C NMR ($CDCl_3$) δ 27.9 (CH_3), 28.6 (CH_3), 30.6 (CH_2), 32.1 (CH_2), 33.2 (CH_2), 34.0 (CH_2), 35.6 (CH), 37.6 (CH_2), 42.3 (CH_2), 49.1 (CH), 50.8 (CH_2), 53.7 (CH_2), 55.5 (CH_3), 56.8 (CH_2), 79.1 (C), 83.5 (C), 103.9 (CH), 111.0 (CH), 111.3 (CH), 113.6 (CH), 118.3 (CH), 118.6 (CH), 121.1 (CH), 123.1 (CH), 126.3 (C), 133.3 (C), 136.0 (C), 141.5 (C), 145.5

(C), 152.4 (C), 152.8 (C), 156.3 (C), 161.8 (C). HRMS (ESI)-TOF (*m/z*): $[M+H]^+$ 734.4493 calcd for $C_{41}H_{59}N_5O_7$; found $[M+H]^+$ 734.4495.

3-((*E*)-4-(2-((6-((3-((2-(((*trans*)-4-(2-(7-Cyano-1,2,3,4-tetrahydroisoquinolin-2-ium-2-yl)ethyl)cyclohexyl)carbamoyl)-1*H*-indol-5-yl)oxy)propyl)amino)-6-oxohexyl)amino)-2-oxoethoxy)styryl)-5,5-difluoro-7-(thiophen-2-yl)-5*H*-dipyrrolo[1,2-c:2',1'-*f*][1,3,2]diazaborinin-4-ium-5-uide 2,2,2-trifluoroacetate (34a).

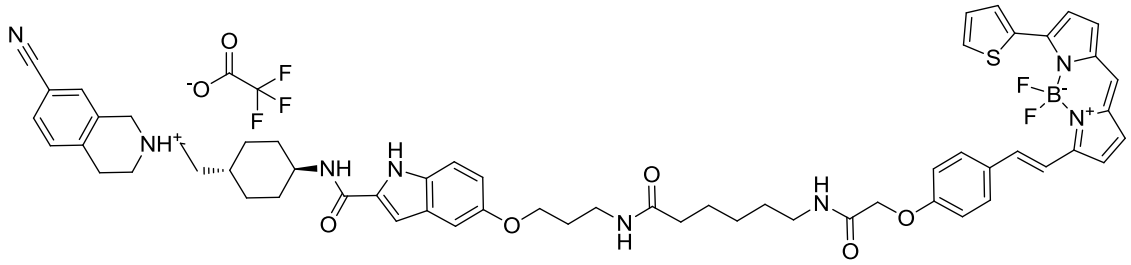

Fluffy blue solid (3 mg, 32%).^{1}H NMR (d_6-DMSO) δ 1.06-1.12 (m, 2H), 1.21-1.52 (m, 10H), 1.66 (m, 2H), 1.76-1.79 (m, 4H), 1.89 (m, 2H), 2.05 (t, *J* 7.4 Hz, 2H), 2.99 (m, 2H), 3.10-3.19 (m, 4H), 3.28 (m, 2H), 3.74 (m, 2H), 4.32 (m, 1H), 4.46 (t, *J* 6.8 Hz, 2H), 4.53 (s, 2H), 4.62 (d, *J* 15.9 Hz, 1H), 6.78 (dd, *J* 8.9, 2.3 Hz, 1H), 6.88 (br s, 1H), 6.89 (d, *J* 2.3 Hz, 1H), 6.96 (d, *J* 4.2 Hz, 1H), 7.07 (d, *J* 8.8 Hz, 2H), 7.27-7.30 (m, 3H), 7.33 (br s, 1H), 7.38 (d, *J* 4.3 Hz, 1H), 7.42 (br s, 1H), 7.49 (d, *J* 8.0 Hz, 1H), 7.60-7.62 (m, 3H), 7.72 (br s, 1H), 7.75-7.80 (m, 3H), 7.83 (dd, *J* 5.1, 1.0 Hz, 1H), 8.04 (dd, *J* 3.8, 1.0 Hz, 1H), 8.15 (t, *J* 5.8 Hz, 1H), 8.20 (d, *J* 8.0 Hz, 1H), 8.89 (br s, 1H), 9.84 (br s, 1H). HPLC purity (λ= 214 nm): 95%, t_R = 7.64 min. HRMS (ESI)-TOF (*m/z*): $[M+H]^+$ 1045.4781 calcd for $C_{59}H_{63}BF_2N_8O_5S$; found $[M+H]^+$ 1045.4787.

1-(6-((3-((2-(((*trans*)-4-(2-(7-Cyano-1,2,3,4-tetrahydroisoquinolin-2-ium-2-yl)ethyl)cyclohexyl)carbamoyl)-1*H*-indol-5-yl)oxy)propyl)amino)-6-oxohexyl)-2-((1*E*,3*E*,5*E*)-5-(1-ethyl-3,3-dimethyl-5-sulfoindolin-2-ylidene)penta-1,3-dien-1-yl)-3,3-dimethyl-3*H*-indol-1-ium-5-sulfonate 2,2,2-trifluoroacetate (34b).

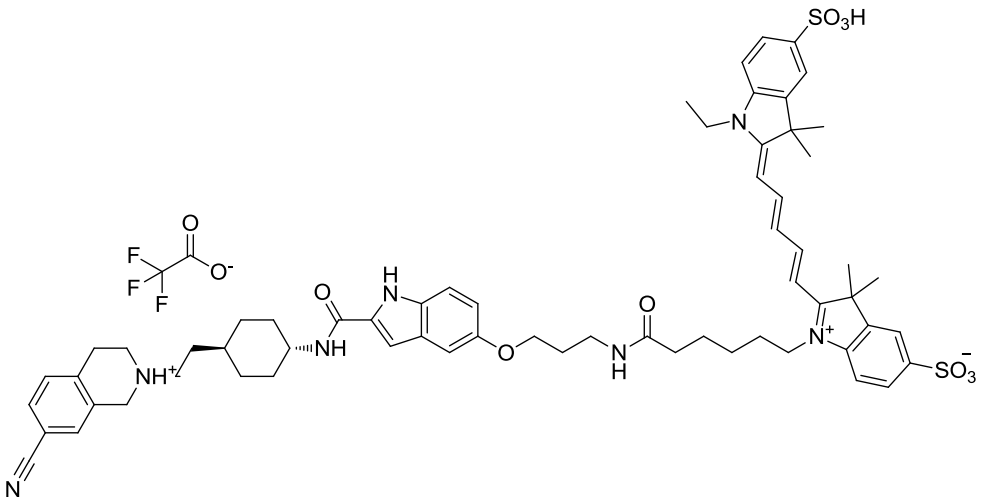

Fluffy blue solid (3 mg, 16%). ^{1}H NMR (d_6-DMSO) δ 0.89 (m, 2H), 1.18-1.37 (m, 9H), 1.55-1.57 (m, 4H), 1.64-1.79 (m, 20H), 2.04-2.08 (m, 2H), 2.98 (m, 2H), 3.21 (m, 4H), 3.63 (m, 2H), 3.75 (m, 1H), 4.11 (m, 4H), 4.34 (m, 1H), 4.45 (m, 2H), 4.63-4.67 (m, 1H), 6.26-6.32 (t, *J* 12.7 Hz, 2H), 6.77 (dd, *J* 8.9, 2.3 Hz, 1H), 6.87 (s, 1H), 6.87 (s, 1H), 7.30-7.35 (m, 3H), 7.51 (d, *J* 8.5 Hz, 1H), 7.66 (dt, *J* = 8.1, 2.2 Hz, 2H), 7.77-7.82 (m, 3H), 7.84 (dd, *J* 3.2, 1.4 Hz, 2H), 8.15 (d, *J* 8.1 Hz, 1H), 8.36 (t, *J* 13.2 Hz, 2H), 8.87 (br s, 1H), 9.80 (br s, 1H). HPLC purity (λ= 214 nm): 100%, t_R = 5.18 min. HRMS (ESI)-TOF (*m/z*): $[M+H]^+$ 1138.5146 calcd for $C_{63}H_{75}N_7O_9S_2$; found $[M+H]^+$ 1138.5140.

1-(6-((3-((2-(((*trans*)-4-(2-(7-Cyano-1,2,3,4-tetrahydroisoquinolin-2-ium-2-yl)ethyl)cyclohexyl)carbamoyl)-1*H*-indol-5-yl)oxy)propyl)amino)-6-oxohexyl)-3,3-dimethyl-2-((1*E*,3*E*)-3-(1,3,3-trimethyl-5-sulfoindolin-2-ylidene)prop-1-en-1-yl)-3*H*-indol-1-ium-5-sulfonate 2,2,2-trifluoroacetate (34c).

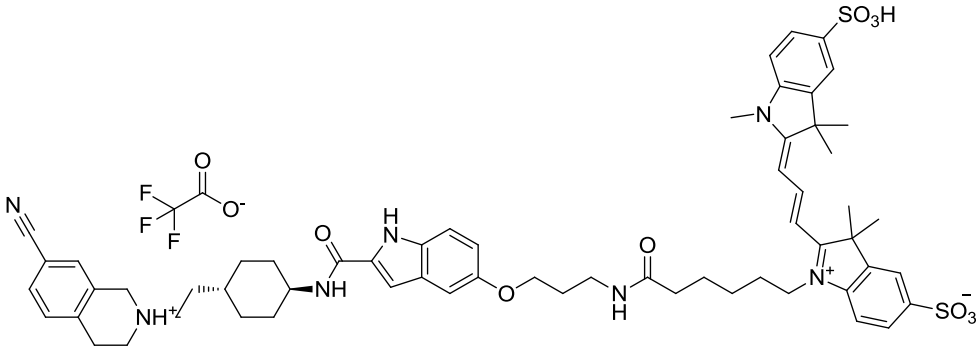

Pink solid (5 mg, 31%). ^{1}H NMR (d_6-DMSO) δ 0.89 (m, 2H), 1.26 (m, 3H), 1.40 (m, 2H), 1.58 (m, 4H), 1.68 (d, *J* 1.0 Hz, 12H), 1.75 (m, 4H), 2.07 (t, *J* 7.3 Hz, 2H), 2.98 (m, 2H), 3.17-3.51 (m, 11H; under H_2O peak), 3.64 (s, 3H), 3.77 (m, 1H), 4.11 (t, *J* 6.9 Hz, 2H), 4.35 (m, 1H), 4.45 (t, *J* 6.7 Hz, 2H), 4.66 (d, *J* 15.1 Hz, 1H), 6.48 (dd, *J* 3.5, 2.9 Hz, 2H), 6.77 (dd, *J* 8.9, 2.3 Hz, 1H), 6.86 (s, 2H), 7.32 (d, *J* 8.9 Hz, 1H), 7.38-7.41 (m, 2H), 7.51 (d, *J* 8.5 Hz, 1H), 7.70 (ddd, *J* 8.0, 6.4, 1.6 Hz, 2H), 7.77-7.83 (m, 4H), 8.16 (d, *J* 8.0 Hz, 1H), 8.33 (t, *J* 13.5 Hz, 1H), 8.90 (br s, 1H), 9.77 (br s, 1H). HPLC purity (λ= 214 nm): 100%, t_R = 4.92 min. HRMS (ESI)-TOF (*m/z*): $[M+H]^+$ 1098.4833 calcd for $C_{60}H_{71}N_7O_9S_2$; found $[M+H]^+$ 1098.4834.

5-(*N*-(3-((2-(((*trans*)-4-(2-(7-Cyano-1,2,3,4-tetrahydroisoquinolin-2-ium-2-yl)ethyl)cyclohexyl)carbamoyl)-1*H*-indol-5-yl)oxy)propyl)sulfamoyl)-2-(6-(diethylamino)-3-(diethyliminio)-3*H*-xanthen-9-yl)benzenesulfonate 2,2,2-trifluoroacetate (34d).

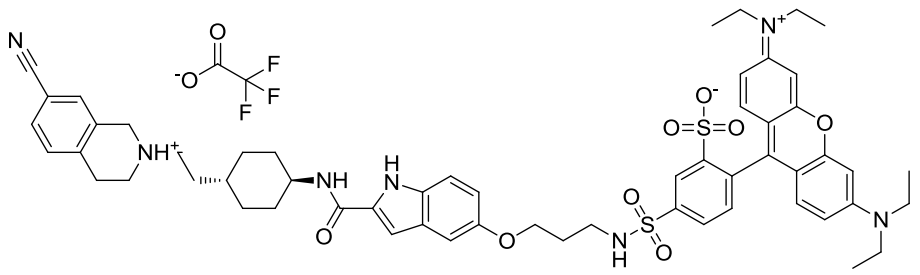

Purple solid (3 mg, 23%). ^{1}H NMR (d_6-DMSO) δ 1.09 (m, 2H), 1.22 (t, *J* 7.1 Hz, 12H), 1.33-1.38 (m, 3H), 1.65 (m, 2H), 1.83-1.90 (m, 6H), 2.83 (m, 2H), 3.18 (m, 2H), 3.28 (m, 2H), 3.60-3.70 (m, 9H), 3.73 (m, 2H), 4.33 (m, 1H), 4.45 (t, *J* 6.8 Hz, 2H), 4.62 (m, 1H), 6.78 (dd, *J* 8.9, 2.3 Hz, 1H), 6.88- 6.99 (m, 8H), 7.33 (d, *J* 9.1 Hz, 1H), 7.43 (d, *J* 8.0 Hz, 1H), 7.50 (d, *J* 7.9 Hz, 1H), 7.75-7.79 (m, 2H), 7.88 (dd, *J* 7.9, 1.9 Hz, 1H), 7.97 (t, *J* 5.7 Hz, 1H), 8.25 (d, *J* 8.1 Hz, 1H), 8.41 (d, *J* 1.9 Hz, 1H), 8.88 (br s, 1H), 9.80 (br s, 1H). HPLC purity (λ= 214 nm): 99% t_R 6.19 min. HRMS (ESI)-TOF (*m/z*): $[M+H]^+$ 1040.4414 calcd for $C_{57}H_{65}N_7O_8S_2$; found $[M+H]^+$ 1040.4424.

7-Cyano-2-(2-((*trans*)-4-(5-(3-(3-(3',6'-dihydroxy-3-oxo-3*H*-spiro[isobenzofuran-1,9'-xanthen]-5-yl)thioureido)propoxy)-1*H*-indole-2-carboxamido)cyclohexyl)ethyl)-1,2,3,4-tetrahydroisoquinolin-2-ium 2,2,2-trifluoroacetate (34e).

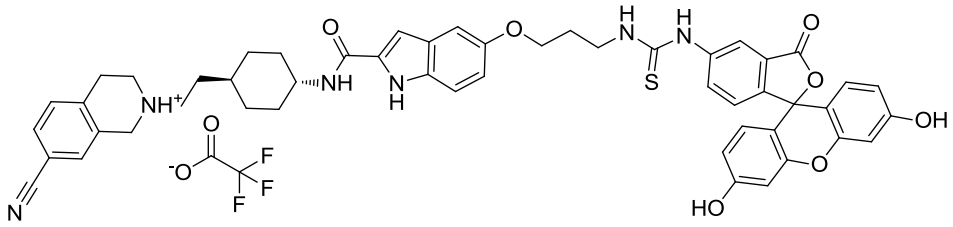

Orange solid (1.5 mg, 9%). ^{1}H NMR (d_6-DMSO) δ 1.06 (m, 2H), 1.28-1.41 (m, 3H), 1.64 (m, 2H), 1.78 (m, 2H), 1.89 (m, 2H), 1.98 (m, 2H), 3.17 (m, 2H), 3.24-3.78 (m, 7H; under H_2O peak), 4.33 (m, 1H), 4.45 (t, *J* 6.8 Hz, 2H), 4.62 (m, 1H), 6.55 (d, *J* 2.3 Hz, 1H), 6.57 (d, *J* 2.3 Hz, 1H), 6.60 (s, 1H), 6.62 (br s, 1H), 6.68 (d, *J* 2.3 Hz, 2H), 6.80 (dd, *J* 8.9, 2.3 Hz, 1H), 6.90-

6-91 (m, 2H), 7.20 (d, *J* 8.2 Hz, 1H), 7.38 (d, *J* 9.0 Hz, 1H), 7.50 (d, *J* 8.0 Hz, 1H), 7.74-7.78 (m, 3H), 8.19-8.23 (m, 3H), 8.89 (br s, 1H), 9.86 (br s, 1H), 10.01 (br s, 1H), 10.14 (br s, 2H). HPLC purity (λ= 214 nm): 100%, t_R = 6.15 min. HRMS (ESI)-TOF (*m/z*): $[M+H]^+$ 889.3383 calcd for $C_{51}H_{48}N_6O_7S$; found $[M+H]^+$ 889.3390.

5,5-Difluoro-3-((*E*)-4-(2-((6-((3-((2-(((*trans*)-4-(2-(4-(2-methoxyphenyl)piperazin-1-ium-1-yl)ethyl)cyclohexyl)carbamoyl)-1*H*-indol-5-yl)oxy)propyl)amino)-6-oxohexyl)amino)-2-oxoethoxy)styryl)-7-(thiophen-2-yl)-5*H*-dipyrrolo[1,2-c:2',1'-*f*][1,3,2]diazaborinin-4-ium-5-uide 2,2,2-trifluoroacetate (35a).

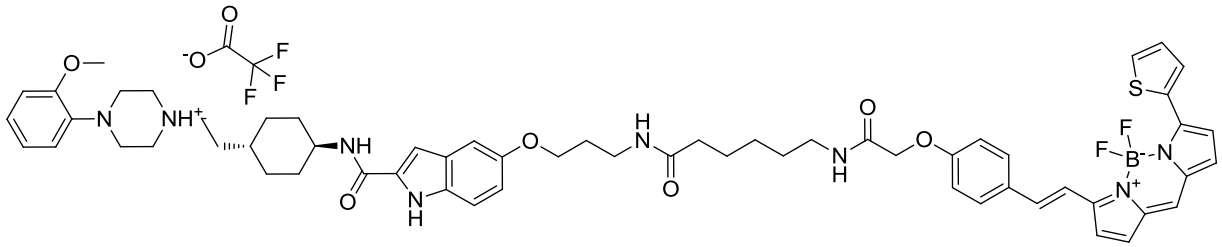

Blue solid (1 mg, 11%). ^{1}H NMR (d_6-DMSO) δ 1.08 (m, 2H), 1.24-1.52 (m, 10H), 1.59 (m, 2H), 1.76-1.79 (m, 4H), 1.86 (m, 2H), 2.05 (t, *J* 7.4 Hz, 2H), 2.90 (m, 2H), 3.00 (m, 2H), 3.10-3.20 (m, 6H), 3.50-3.58 (m, 4H), 3.79 (s, 3H under H_2O peak), 4.46 (t, *J* 6.6 Hz, 2H), 4.54 (s, 2H), 6.78 (dd, *J* 8.9, 2.2 Hz, 1H), 6.89-7.09 (m, 9H), 7.27-7.42 (m, 6H), 7.60-7.62 (m, 3H), 7.74 (d, *J* 16.3 Hz, 1H), 7.80 (t, *J* 5.4 Hz, 1H), 7.83 (dd, *J* 5.0, 0.8 Hz, 1H), 8.05 (dd, *J* 3.7, 0.7 Hz, 1H), 8.16 (t, *J* 5.6 Hz, 1H), 8.21 (d, *J* 8.0 Hz, 1H), 8.89 (br s, 1H), 9.51 (br s, 1H). HPLC purity (λ= 214 nm): 100%, t_R = 7.88 min. HRMS (ESI)-TOF (*m/z*): $[M+H]^+$ 1079.5200 calcd for $C_{60}H_{69}BF_2N_7O_9S$; found $[M+H]^+$ 1079.5223.

1-(6-((3-((2-(((*trans*)-4-(2-(4-(2-Methoxyphenyl)piperazin-1-ium-1-yl)ethyl)cyclohexyl)carbamoyl)-1*H*-indol-5-yl)oxy)propyl)amino)-6-oxohexyl)-3,3-dimethyl-2-((1*E*,3*E*,5E)-5-(1,3,3-trimethyl-5-sulfoindolin-2-ylidene)penta-1,3-dien-1-yl)-3*H*-indol-1-ium-5-sulfonate 2,2,2-trifluoroacetate (35b).

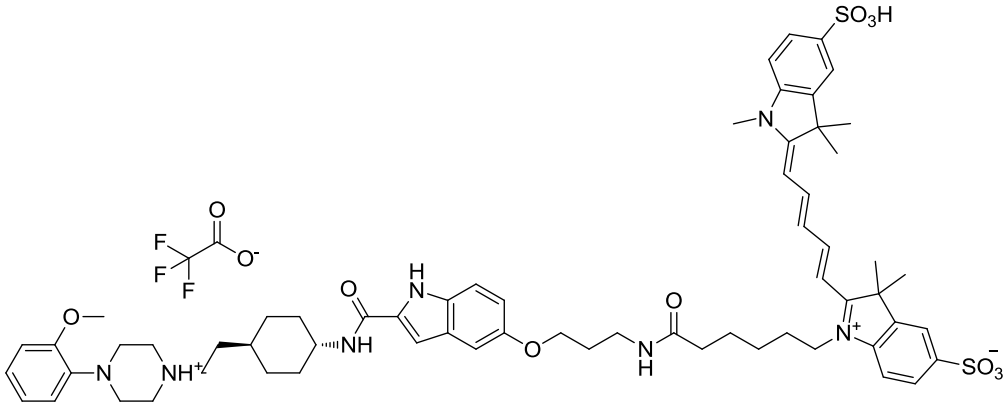

Blue solid (2 mg, 21%). ^{1}H NMR (d_6-DMSO) δ 0.85 (m, 2H), 1.16-1.81 (m, 30H), 2.06 (t, *J* 7.2 Hz, 2H), 2.94-3.00 (m, 4H), 3.16 (m, 2H), 3.29-3.44 (m, 6H under H_2O peak), 3.58 (s, 3H), 3.80 (s, 3H), 4.09 (m, 2H), 4.46 (m, 2H), 6.22 (d, *J* 13.3 Hz, 1H), 6.31 (d, *J* 13.3 Hz, 1H), 6.54 (m, 2H), 6.77 (dd, *J* 8.9, 2.2 Hz, 1H), 6.86-6.88 (m, 2H), 6.91-7.06 (m, 4H), 7.31-7.34 (m, 3H), 7.65-7.67 (m, 2H), 7.81-7.84 (m, 2H), 8.16 (d, *J* 8.2 Hz, 1H), 8.32-8.38 (m, 2H), 8.89 (br s, 1H), 9.36 (br s, 1H). HPLC purity (λ= 214 nm): 100%, t_R = 5.31 min. HRMS (ESI)-TOF (*m/z)*: $[M+H]^+$ 1158.5408 calcd for $C_{63}H_{79}N_7O_{10}S_2$; found $[M+H]^+$ 1158.5381.

1-(6-((3-((2-(((*trans*)-4-(2-(4-(2-Methoxyphenyl)piperazin-1-ium-1-yl)ethyl)cyclohexyl)carbamoyl)-1*H*-indol-5-yl)oxy)propyl)amino)-6-oxohexyl)-3,3-dimethyl-2-((1*E*,3*E*)-3-(1,3,3-trimethyl-5-sulfoindolin-2-ylidene)prop-1-en-1-yl)-3*H*-indol-1-ium-5-sulfonate 2,2,2-trifluoroacetate (35c).

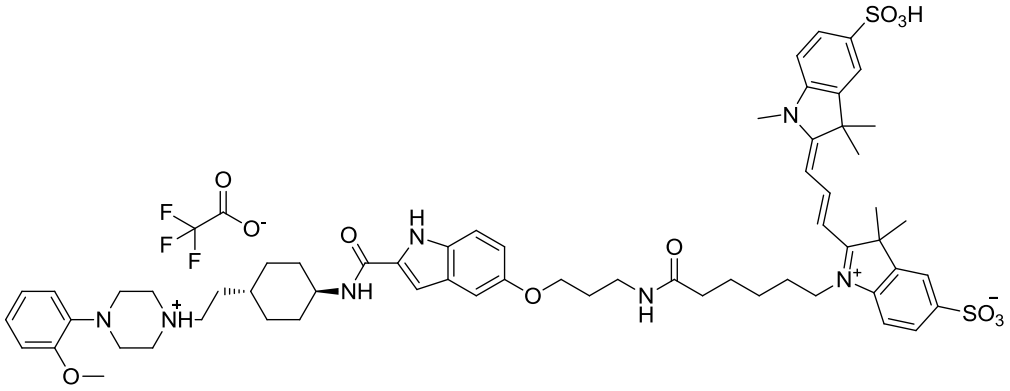

Pink solid (6 mg, 41%). ^{1}H NMR (d_6-DMSO) δ 0.80 (m, 2H), 1.08-1.25 (m, 3H), 1.32 (m, 2H), 1.41 (m, 2H), 1.52 (m, 2H), 1.61-1.73 (m, 19H), 2.00 (t, *J* 7.1 Hz, 2H), 2.86-2.92 (m, 4H), 3.05-3.14 (m, 4H), 3.48 (m, 6H under water peak), 3.56 (s, 3H), 3.74 (s, 3H), 4.04 (t, *J* 7.2 Hz, 2H), 4.38 (t, *J* 6.6 Hz, 2H), 6.41 (d, *J* 13.5 Hz, 1H), 6.42 (d, *J* 13.4 Hz, 1H) 6.70 (dd, *J* 8.9, 2.3 Hz, 1H), 6.79-6.80 (m, 2H), 6.83-6.99 (m, 4H), 7.25 (d, *J* 9.0 Hz, 1H), 7.32 (d, *J* 8.4 Hz, 1H), 7.33 (d, *J* 8.3 Hz, 1H), 7.60-7.64 (m, 2H), 7.74-7.76 (m, 3H), 8.09 (d, *J* 8.1 Hz, 1H), 8.26 (t, *J* 13.4 Hz, 1H), 8.79 (br s, 1H), 9.27 (br s, 1H). HPLC purity (λ= 214 nm): 100%, t_R = 5.17 min. HRMS (ESI)-TOF (*m/z*): $[M+H]^+$ 1132.5252 calcd for $C_{61}H_{77}N_7O_{10}S_2$; found $[M+H]^+$ 1132.5233.

2-(6-(Diethylamino)-3-(diethyliminio)-3*H*-xanthen-9-yl)-5-(*N*-(3-((2-(((*trans*)-4-(2-(4-(2-methoxyphenyl)piperazin-1-ium-1-yl)ethyl)cyclohexyl)carbamoyl)-1*H*-indol-5-yl)oxy)propyl)sulfamoyl)benzenesulfonate 2,2,2-trifluoroacetate (35d).

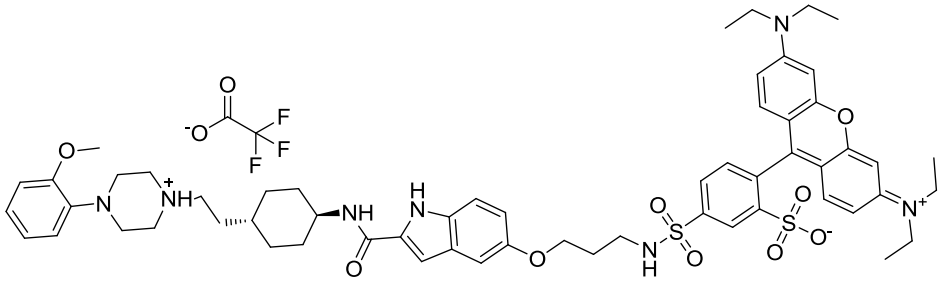

Purple solid (5 mg, 29%). ^{1}H NMR (d_6-DMSO) δ 1.02-1.11 (m, 2H), 1.22 (t, *J* 7.0 Hz, 12H), 1.28-1.39 (m, 3H), 1.59 (m, 2H), 1.76-1.90 (m, 6H), 2.81-2.93 (m, 4H), 3.13-3.20 (m, 4H), 3.32-3.77 (m, 13H under H_2O peak), 3.80 (s, 3H), 4.45 (t, *J* 6.9 Hz, 2H), 6.77 (dd, *J* 8.9, 2.3 Hz, 1H), 6.88-7.04 (m, 12H), 7.33 (d, *J* 9.0 Hz, 1H), 7.44 (d, *J* 8.0 Hz, 1H), 7.88 (dd, *J* 8.0, 1.9 Hz, 1H), 7.98 (t, *J* 5.6 Hz, 1H), 8.25 (d, *J* 8.0 Hz, 1H), 8.41 (d, *J* 1.9 Hz, 1H), 8.90 (br s, 1H), 9.41 (br s, 1H). HPLC purity (λ= 214 nm): 95%, t_R = 6.99 min HRMS (ESI)-TOF (*m/z*): $[M+H]^+$ 1074.4833 calcd for $C_{58}H_{71}N_7O_9S_2$; found $[M+H]^+$ 1074.4843.

1-(2-((*trans*)-4-(5-(3-(3-(3',6'-Dihydroxy-3-oxo-3*H*-spiro[isobenzofuran-1,9'-xanthen]-5-yl)thioureido)propoxy)-1*H*-indole-2-carboxamido)cyclohexyl)ethyl)-4-(2-methoxyphenyl)piperazin-1-ium 2,2,2-trifluoroacetate (35e).

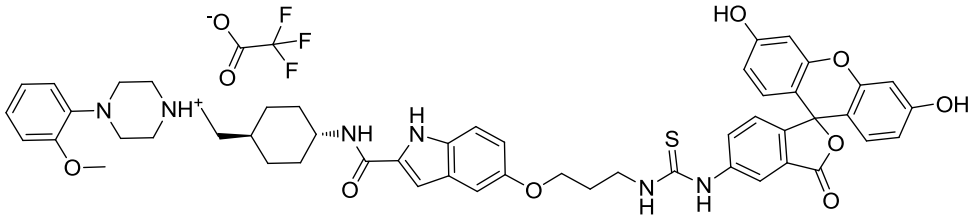

Yellow solid (6 mg, 39%). ^{1}H NMR (d_6-DMSO) δ1.06 (m, 2H), 1.24-1.37 (m, 3H), 1.57 (m, 2H), 1.76-1.79 (m, 2H), 1.87 (m, 2H), 1.98 (m, 2H), 2.90 (m, 2H), 3.13-3.20 (m, 4H), 3.32-3.74 (m, 4H, under H_2O peak), 3.80 (s, 3H), 4.55 (t, *J* 6.9 Hz, 2H), 6.55-6.22 (m, 4H), 6.69 (d, *J* 2.2 Hz, 2H), 6.80 (dd, *J* 8.9, 2.2 Hz, 1H), 6.90-7.06 (m, 6H), 7.20 (d, *J* 8.3 Hz, 1H), 7.38 (d, *J* 8.9 Hz, 1H), 7.76 (d, *J* 7.9 Hz, 1H), 8.20-8.24 (m, 3H), 8.92 (br s, 1H), 9.44 (br s, 1H), 10.05 (br s,

1H), 10.17 (br s, 2H). HPLC purity (λ= 214 nm): 100%, t_R = 6.42 min. HRMS (ESI)-TOF (*m/z*): $[M+H]^+$ 923.3802 calcd for $C_{52}H_{54}N_6O_8S$; found $[M+H]^+$ 923.3795.

1-(2-((*trans*)-4-(5-(3-(4-((6-Methoxy-1,2,4,5-tetrazin-3-yl)oxy)butanamido)propoxy)-1*H*-indole-2-carboxamido)cyclohexyl)ethyl)-4-(2-methoxyphenyl)piperazin-1-ium 2,2,2-trifluoroacetate (35f).

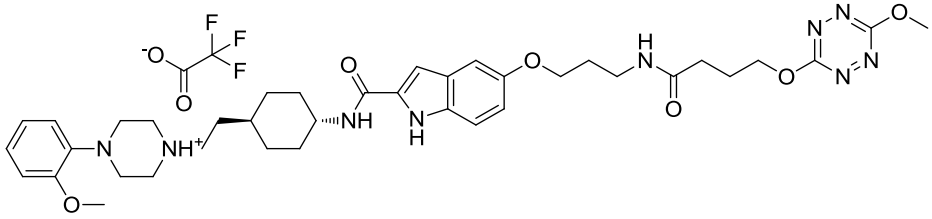

Peach/pale pink solid (2 mg, 17%). ^{1}H NMR (d_6-DMSO) δ 1.02 (m, 2H), 1.17-1.32 (m, 3H), 1.53 (m, 2H), 1.69-1.73 (m, 4H), 1.80 (m, 2H), 1.99 (m, 2H), 2.22 (m, 2H), 2.82 (m, 2H), 2.93 (m, 2H), 3.07-3.14 (m, 4H), 3.24-3.49 (m, 4H, under H_2O peak), 3.65 (m, 1H), 3.73 (s, 3H), 4.06 (s, 3H), 4.37-4.45 (m, 4H), 6.70 (dd, *J* 8.9, 2.3 Hz, 1H), 6.81-6.97 (m, 6H), 7.25 (d, *J* 9.0 Hz, 1H), 7.85 (t, *J* 5.4 Hz, 1H), 8.13 (d, *J* 8.0 Hz, 1H), 8.81 (br s, 1H), 9.35 (br s, 1H). HPLC purity (λ= 214 nm): 100%, t_R = 6.08 min HRMS (ESI)-TOF (*m/z*): $[M+H]^+$ 730.4041 calcd for $C_{38}H_{51}N_9O_6$; found $[M+H]^+$ 730.4066.

Pharmacology.

[^{3}H]Raclopride Binding Assays. FlpIn CHO cells stably expressing the human D_{2L} receptor were grown and maintained in DMEM supplemented with 10% fetal bovine serum (FBS), and 200 μg/mL of Hygromycin-B, at 37 °C in a humidified incubator containing 5% CO_2. Radioligand binding experiments were performed with receptors expressed on intact cells, which were seeded at 40,000 cells/well and grown overnight at 37 °C. Assays were performed in a total volume of 200 μL in binding buffer (10 mM HEPES, 146 mM NaCl, 10 mM D-glucose, 5 mM KCl, 1 mM $MgSO_4.7H_2O$, 2 mM $CaCl_2$, 1.5 mM $NaHCO_3$, pH 7.4) containing 0.32 nM [^{3}H]Raclopride, in the absence or presence of the competing compounds, and incubated for 1

hour at 37 °C. Assays were terminated by removal of the binding reaction mixture, followed by rapid washing, twice, with ice-cold 0.9% NaCl (100 μL/well). OptiPhase Supermix scintillation cocktail (100 μL) was added, plates were sealed (TopSeal^{TM}), and radioactivity was measured in a MicroBeta^2 LumiJET microplate counter.

Confocal Microscopy. FlpIn CHO cells stably expressing the human D_{2L} receptor were grown and maintained in DMEM (containing 25 mM HEPES and no phenol red) supplemented with 10% fetal bovine serum (FBS), and 200 μg/mL of Hygromycin-B, at 37°C in a humidified incubator with 5% CO_2. Cells were plated at 25,000 cells/well in an Ibidi 8-chamber u-slide slide and allowed to grow overnight. Prior to experiments cells were washed twice with 100 μL of DMEM. For the control 50 μL of the fluorescently labelled ligands **35b-e** were added to the cells (total volume 200 μL) and incubated for 30 mins at 37 °C in a humidified incubator with 5% CO_2. For displacement experiments cells were pre-incubated with 1 μM of haloperidol for 30 mins before the fluorescently ligand was added and incubated for a further 30 mins. Cells were then imaged using a Leica SP8 confocal microscope using a ×63 PLApo CS2 NA1.4 oil immersion objective. A pinhole diameter of 3 Airy Unit was used and the laser power, gain and offset was kept constant for all ligands and experimental conditions.

Data Analysis. Computerized nonlinear regression was performed using Prism 6.0 (GraphPad Software, San Diego, CA).

References

1. Catapano, L. A.; Manji, H. K. G protein-coupled receptors in major psychiatric disorders. *Biochim. Biophys. Acta Biomembr.* **2007,** *1768*, 976-993.

2. Brooks, D. J. Dopamine agonists: Their role in the treatment of Parkinson's disease. *J. Neurol., Neurosurg. Psychiatry* **2000,** *68*, 685-689.

3. Vernall, A. J.; Hill, S. J.; Kellam, B. The evolving small-molecule fluorescent-conjugate toolbox for class a GPCRs. *Brit. J. Pharmacol.* **2014,** *171*, 1073-1084.

4. Cottet, M.; Faklaris, O.; Zwier, J. M.; Trinquet, E.; Pin, J.-P.; Durroux, T. Original fluorescent ligand-based assays open new perspectives in G-protein coupled receptor drug screening. *Pharmaceuticals* **2011,** *4*, 202-214.

5. Vernall, A. J.; Stoddart, L. A.; Briddon, S. J.; Hill, S. J.; Kellam, B. Highly potent and selective fluorescent antagonists of the human adenosine A_3 receptor based on the 1,2,4-triazolo[4,3-a]quinoxalin-1-one scaffold. *J. Med. Chem.* **2012,** *55*, 1771-1782.

6. Stoddart, Leigh A.; Vernall, Andrea J.; Denman, Jessica L.; Briddon, Stephen J.; Kellam, B.; Hill, Stephen J. Fragment screening at adenosine-A_3 receptors in living cells using a fluorescence-based binding assay. *Chemistry & Biology* **2012,** *19*, 1105-1115.

7. Giepmans, B. N. G.; Adams, S. R.; Ellisman, M. H.; Tsien, R. Y. The fluorescent toolbox for assessing protein location and function. *Science* **2006,** *312*, 217-224.

8. Gonçalves, M. S. T. Fluorescent labeling of biomolecules with organic probes. *Chem. Rev.* **2008,** *109*, 190-212.

9. Middleton, R. J.; Briddon, S. J.; Cordeaux, Y.; Yates, A. S.; Dale, C. L.; George, M. W.; Baker, J. G.; Hill, S. J.; Kellam, B. New fluorescent adenosine A_1-receptor agonists that allow quantification of ligand−receptor interactions in microdomains of single living cells. *J. Med. Chem.* **2007,** *50*, 782-793.

10. Daval, S. B.; Valant, C.; Bonnet, D.; Kellenberger, E.; Hibert, M.; Galzi, J.-L.; Ilien, B. Fluorescent derivatives of AC-42 to probe bitopic orthosteric/allosteric binding mechanisms on muscarinic M_1 receptors. *J. Med. Chem.* **2012,** *55*, 2125-2143.

11. Alonso, D.; Vázquez-Villa, H.; Gamo, A. M.; Martínez-Esperón, M. F.; Tortosa, M.; Viso, A.; Fernández de la Pradilla, R.; Junquera, E.; Aicart, E.; Martín-Fontecha, M.; Benhamú, B.; López-Rodríguez, M. L.; Ortega-Gutiérrez, S. Development of fluorescent ligands for the human 5-$HT1_A$ receptor. *ACS Med. Chem. Lett.* **2010,** *1*, 249-253.

12. Madras, B. K.; Canfield, D. R.; Pfaelzer, C.; Vittimberga, F. J.; Difiglia, M.; Aronin, N.; Bakthavachalam, V.; Baindur, N.; Neumeyer, J. L. Fluorescent and biotin probes for dopamine receptors: D_1 and D_2 receptor affinity and selectivity. *Mol. Pharmacol.* **1990,** *37*, 833-839.

13. Monsma, F. J.; Barton, A. C.; Chol Kang, H.; Brassard, D. L.; Haugland, R. P.; Sibley, D. R. Characterization of novel fluorescent ligands with high affinity for D_1 and D_2 dopaminergic receptors. *J. Neurochem.* **1989,** *52*, 1641-1644.

14. Bakthavachalam, V.; Baindur, N.; Madras, B. K.; Neumeyer, J. L. Fluorescent probes for dopamine receptors: Synthesis and characterization of fluorescein and 7-nitrobenz-2-oxa-1,3-diazol-4-yl conjugates of D-1 and D-2 receptor ligands. *J. Med. Chem.* **1991,** *34*, 3235-3241.

15. Barton, A. C.; Kang, H. C.; Rinaudo, M. S.; Monsma Jr, F. J.; Stewart-Fram, R. M.; Macinko Jr, J. A.; Haugland, R. P.; Ariano, M. A.; Sibley, D. R. Multiple fluorescent ligands for dopamine receptors. I. Pharmacological characterization and receptor selectivity. *Brain Res.* **1991,** *547*, 199-207.

16. Seeman, P. Targeting the dopamine D_2 receptor in schizophrenia. *Expert Opin. Ther. Targets* **2006,** *10*, 515-531.

17. Bohme, I.; Beck-Sickinger, A. Illuminating the life of GPCRs. *Cell Commun. Signaling* **2009,** *7*, 16.

18. Seeman, P. Atypical antipsychotics: Mechanism of action. *Focus* **2004,** *2*, 48-58.

19. Meltzer, H. Y. The role of serotonin in antipsychotic drug action. *Neuropsychopharmacology* **1999,** *21*, 106S-115S.

20. Whone, A. L.; Watts, R. L.; Stoessl, A. J.; Davis, M.; Reske, S.; Nahmias, C.; Lang, A. E.; Rascol, O.; Ribeiro, M. J.; Remy, P.; Poewe, W. H.; Hauser, R. A.; Brooks, D. J. Slower progression of Parkinson's disease with ropinirole versus levodopa: The real-pet study. *Ann. Neurol.* **2003,** *54*, 93-101.

21. McRobb, F. M.; Crosby, I. T.; Yuriev, E.; Lane, J. R.; Capuano, B. Homobivalent ligands of the atypical antipsychotic clozapine: Design, synthesis, and pharmacological evaluation. *J. Med. Chem.* **2012,** *55*, 1622-1634.

22. Jorg, M.; Kaczor, A. A.; Mak, F. S.; Lee, K. C. K.; Poso, A.; Miller, N. D.; Scammells, P. J.; Capuano, B. Investigation of novel ropinirole analogues: Synthesis, pharmacological evaluation and computational analysis of dopamine D_2 receptor functionalized congeners and homobivalent ligands. *MedChemComm* **2014,** *5*, 891-898.

23. Stemp, G.; Ashmeade, T.; Branch, C. L.; Hadley, M. S.; Hunter, A. J.; Johnson, C. N.; Nash, D. J.; Thewlis, K. M.; Vong, A. K. K.; Austin, N. E.; Jeffrey, P.; Avenell, K. Y.; Boyfield, I.; Hagan, J. J.; Middlemiss, D. N.; Reavill, C.; Riley, G. J.; Routledge, C.; Wood, M. Design and synthesis of *trans*-N-[4-[2-(6-cyano-1,2,3,4-tetrahydroisoquinolin-2- yl)ethyl]cyclohexyl]-4-quinolinecarboxamide (SB-277011): A potent and selective dopamine D_3 receptor antagonist with high oral bioavailability and CNS penetration in the rat. *J. Med. Chem.* **2000,** *43*, 1878-1885.

24. Silvano, E.; Millan, M. J.; la Cour, C. M.; Han, Y.; Duan, L.; Griffin, S. A.; Luedtke, R. R.; Aloisi, G.; Rossi, M.; Zazzeroni, F.; Javitch, J. A.; Maggio, R. The tetrahydroisoquinoline derivative SB269,652 is an allosteric antagonist at dopamine D_3 and D_2 receptors. *Mol. Pharmacol.* **2010,** *78*, 925-934.

25. Lane, J. R.; Donthamsetti, P.; Shonberg, J.; Draper-Joyce, C. J.; Dentry, S.; Michino, M.; Shi, L.; López, L.; Scammells, P. J.; Capuano, B.; Sexton, P. M.; Javitch, J. A.; Christopoulos, A. A new mechanism of allostery in a G protein–coupled receptor dimer. *Nat. Chem. Biol.* **2014,** *10*, 745-752.

26. Mistry, S. N.; Valant, C.; Sexton, P. M.; Capuano, B.; Christopoulos, A.; Scammells, P. J. Synthesis and pharmacological profiling of analogues of benzyl quinolone carboxylic acid (BQCA) as allosteric modulators of the M_1 muscarinic receptor. *J. Med. Chem.* **2013,** *56*, 5151-5172.

27. Brady, A. E.; Jones, C. K.; Bridges, T. M.; Kennedy, J. P.; Thompson, A. D.; Heiman, J. U.; Breininger, M. L.; Gentry, P. R.; Yin, H.; Jadhav, S. B.; Shirey, J. K.; Conn, P. J.; Lindsley, C. W. Centrally active allosteric potentiators of the M_4 muscarinic acetylcholine receptor reverse amphetamine-induced hyperlocomotor activity in rats. *J. Pharmacol. Exp. Ther.* **2008,** *327*, 941-953.

28. Sharma, S.; Rodriguez, A. L.; Conn, P. J.; Lindsley, C. W. Synthesis and SAR of a $mGluR_5$ allosteric partial antagonist lead: Unexpected modulation of pharmacology with slight structural modifications to a 5-(phenylethynyl)pyrimidine scaffold. *Bioorg. Med. Chem. Lett.* **2008,** *18*, 4098-4101.

29. Baker, J. G.; Middleton, R.; Adams, L.; May, L. T.; Briddon, S. J.; Kellam, B.; Hill, S. J. Influence of fluorophore and linker composition on the pharmacology of fluorescent adenosine A_1 receptor ligands. *Brit. J. Pharmacol.* **2010,** *159*, 772-786.

30. Briddon, S. J.; Hill, S. J. Pharmacology under the microscope: The use of fluorescence correlation spectroscopy to determine the properties of ligand–receptor complexes. *Trends Pharmacol. Sci.* **2007,** *28*, 637-645.

31. Frecentese, F.; Fiorino, F.; Perissutti, E.; Severino, B.; Magli, E.; Esposito, A.; De Angelis, F.; Massarelli, P.; Nencini, C.; Viti, B.; Santagada, V.; Caliendo, G., Efficient microwave combinatorial synthesis of novel indolic arylpiperazine derivatives as serotoninergic ligands. *Eur. J. Med. Chem.* **2010,** *45* (2), 752-759.

32. Deaton, D., Norman; Navas, F., III; Spearing, P., Kenneth Farnesoid x receptor agonists WO2008/157270 A1, 13th June, **2008**.

33. Shonberg, J.; Herenbrink, C. K.; López, L.; Christopoulos, A.; Scammells, P. J.; Capuano, B.; Lane, J. R., A structure–activity analysis of biased agonism at the dopamine D_2 receptor. *J. Med. Chem.* **2013,** *56* (22), 9199-9221.

Supporting Information- Chapter 5

Supporting Table 1. Functional ERK1/2 phosphorylation data for fluorescently labelled ligands **11a-e**, **17a-e**, **34a-e** and **35a-f** at the D_2R[a]

Parent Compd	Fluorophore used	Compd	pK_B ± SEM (K_B, μM)[b]	pEC_{50} ± SEM (EC_{50}, μM), E_{max} ± SEMc
Clozapine	BODIPY	**11a**	n/a	-
	Cy5	**11b**	5.81 ± 0.05 (1.5)	-
	Cy3	**11c**	6.04 ± 0.06 (0.9)	-
	LRB	**11d**	6.26 ± 0.15 (0.5)	-
	FITC	**11e**	5.76 ± 0.06 (1.7)	-
Ropinirole	BODIPY	**17a**	-	5.64 ± 0.06 (2.3), 67 ± 3
	Cy5	**17b**	-	6.61 ± 0.14 (0.2), 68 ± 6
	Cy3	**17c**	-	6.77 ± 0.17 (0.2), 60 ± 6
	LRB	**17d**	-	6.09 ± 0.17 (0.8), 57 ± 6
	FITC	**17e**	-	6.00 ± 0.11 (0.9), 47 ± 3
SB269652	BODIPY	**34a**	n/a	-
	Cy5	**34b**	6.94 ± 0.09 (0.1)	-
	Cy3	**34c**	6.62 ± 0.06 (0.2)	-
	LRB	**34d**	5.74 ± 0.07 (1.8)	-
	FITC	**34e**	6.63 ± 0.10 (0.2)	-
2-MPP-SB269652	BODIPY	**35a**	5.66 ± 0.29 (2.2)	-
	Cy5	**35b**	6.71 ± 0.05 (0.2)	-
	Cy3	**35c**	6.93 ± 0.06 (0.1)	-
	LRB	**35d**	6.19 ± 0.46 (0.6)	-
	FITC	**35e**	7.07 ± 0.09 (0.1)	-
	Tetrazine	**35f**	6.66 ± 0.04 (0.2)	-

[a]Data represent the mean ± SEM of one experiment performed in duplicate. [b]Compounds are interacted with varying concentrations of dopamine and fit to a Gaddum Schild analysis. [c]Compounds are tested at a concentration range of 10 μM- 0.01 nM at a stimulation time of 5 mins. n/a= compound not active.

Supporting Figure 1. Fluorescence profile of fluorescently labelled ligands **35b-e** in aqueous buffers (HBSS, HEPES, PBS, DMEM; top) and methanol (bottom) at 10 μM measured in a spectrometer.

Cy5
(**35b**)

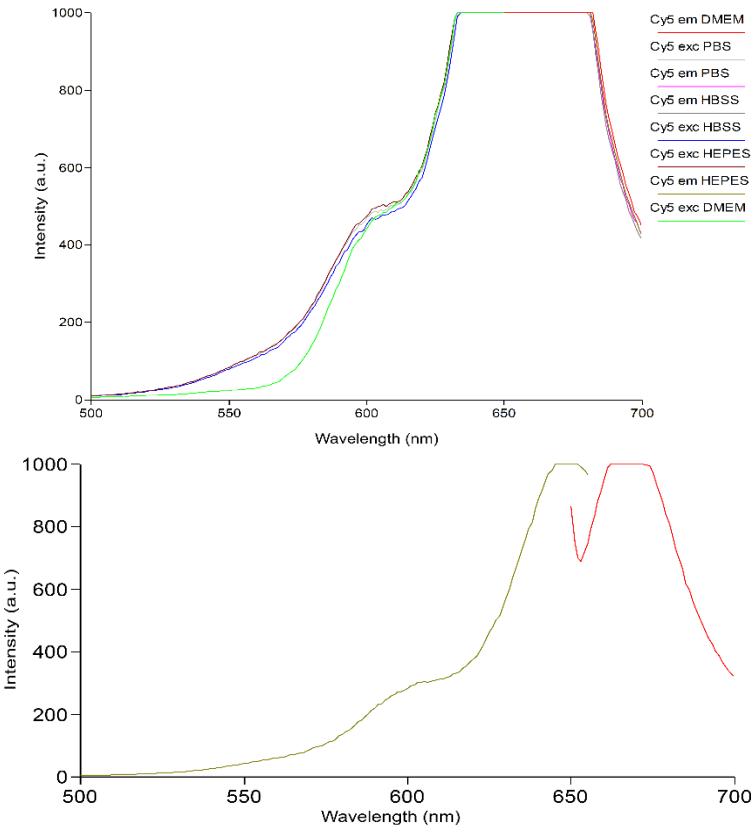

Cy3
(**35c**)

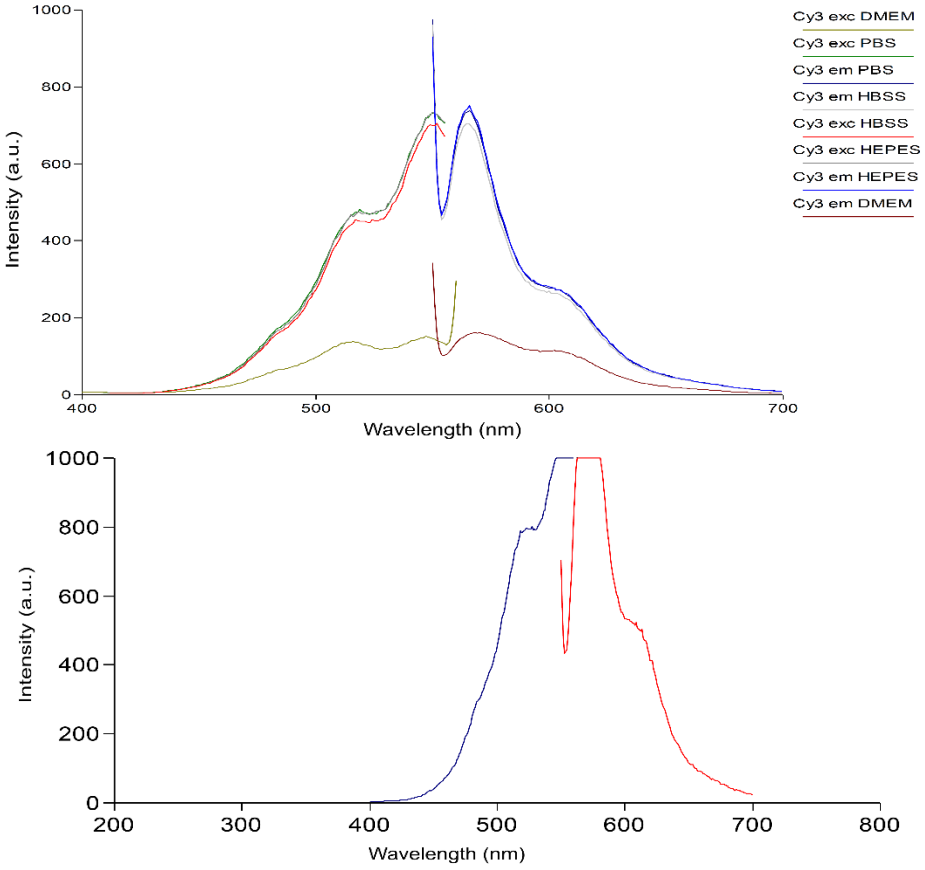

LRB
(**35d**)

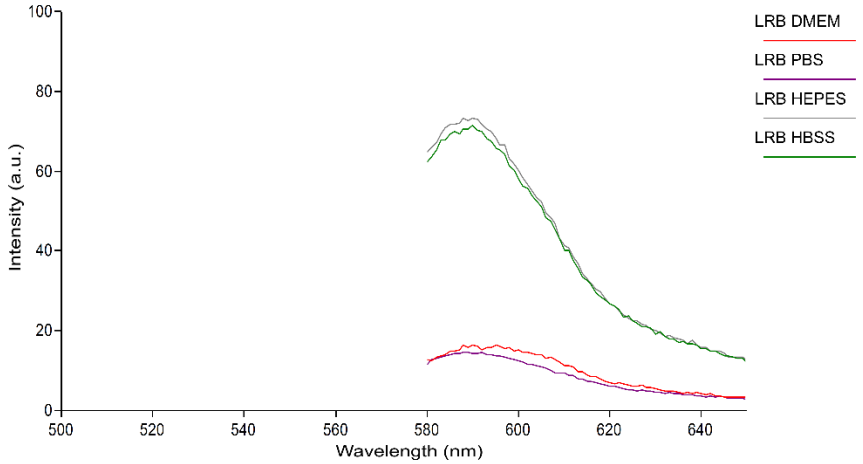

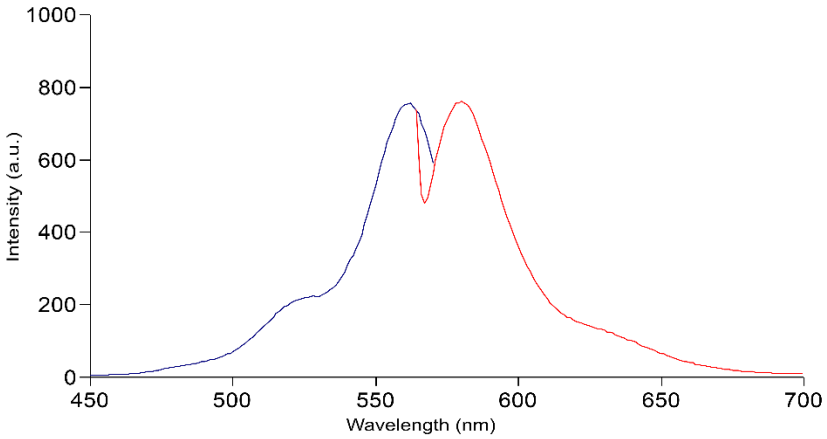

FITC
(**35e**)

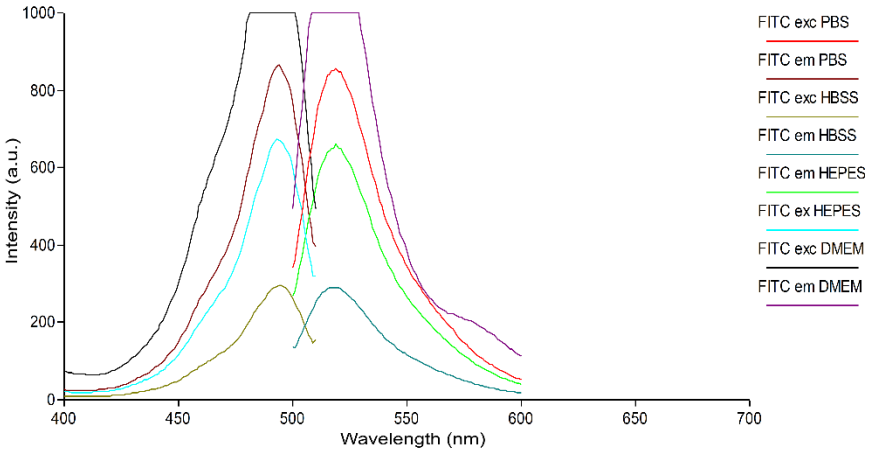

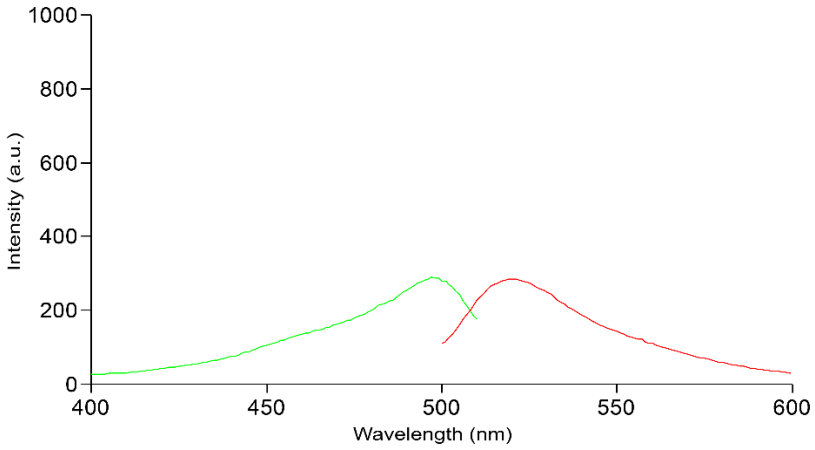

Supporting Figure 2. Confocal images of 2-MPP-SB269252 fluorescently labelled ligand **35d** at 1 μM and 300 nM.

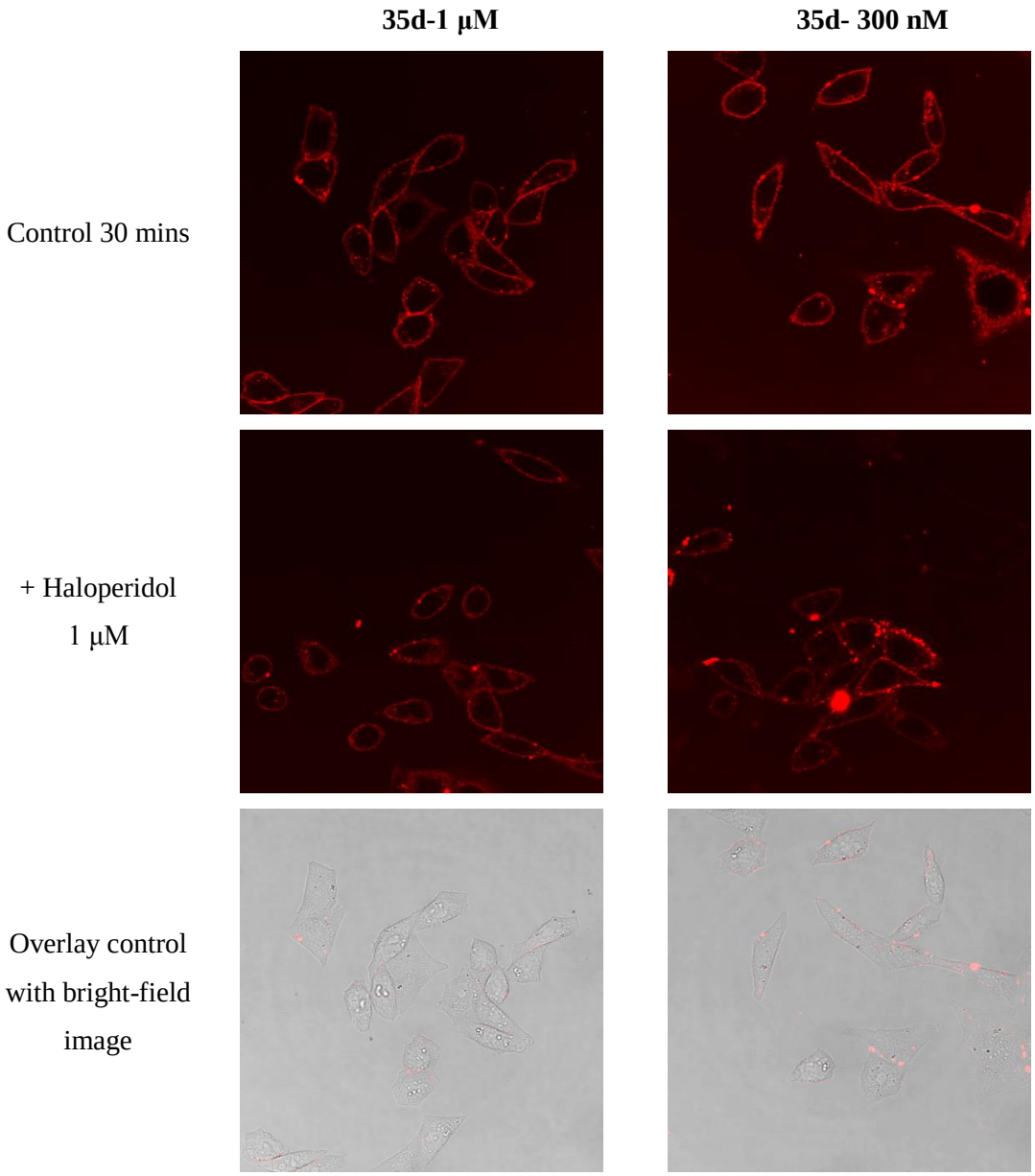

Chapter 6- Thesis Outcomes and Future Prospects

Thesis outcomes

This thesis has explored medicinal chemistry techniques to gain selectivity at GPCRs targeting the CNS. Specifically we designed, synthesised and pharmacologically evaluated numerous series of compounds that investigated PAMs targeting the M_4 mAChR as a way of achieving subtype selectivity and D_2R biased ligands as a way of obtaining pathway specific selectivity. Privileged structures were also utilised in a merged DML approach to design in a favourable polypharmacological profile targeting the M_1 mAChR, D_2R and 5-$HT_{2A}R$. Last, the synthesis and pharmacological evaluation of fluorescently labelled ligands for the D_2R allowed a "toolbox" of ligands to be devised for use in a variety of different applications.

Chapter 2, which is formatted for submission to *ACS Medicinal Chemistry Letters*, reported the development of a series of PAMs based on LY2033298 for the M_4 mAChR. These ligands were profiled using an operational model of allosterism to determine values of functional affinity (K_B), cooperativity ($\alpha\beta$) and intrinsic agonism (τ_B). Profiling PAMs using this model is useful for separating out the different parameters in order to probe the effects that each has towards the overall modulatory properties of the compounds. Key SAR findings include that the thienopyridine scaffold was able to tolerate a variety of small structural changes, however the addition of larger and more lipophilic groups was not tolerated and detrimental to the allosteric properties of the ligand. As such, the possibility of synthesising dual-acting ligands, i.e. an M_4 PAM linked to a D_2/5-HT_{2A} orthosteric ligand is a challenging undertaking.

Chapter 3, which is published in the *Journal of Medicinal Chemistry*, centred on the utilisation of privileged structures and extracting useful SAR about the relationship between biased agonism at the D_2R and antipsychotic efficacy. Differing from chapter 2, it explored means of obtaining pathway specific analogues as opposed to receptor subtype selective analogues. In terms of bias, small structural changes to both the phenylpiperazine (2-methoxy vs 2,3-dichloro) and

heterocyclic units resulted in different bias patterns. The findings confirmed that small structural changes to ligands can have a large impact on the conformational changes of the D_2R that result in the bias of certain signaling pathways over others. Therefore whether exploring subtype selectivity through allosteric ligands or pathway specificity through biased ligands, evidently in both cases minor structural changes can have a large effect globally at the GPCR of interest.

Chapter 4 is currently submitted to the *Journal of Medicinal Chemistry* and uses privileged structures in combination with a merged DML approach. This chapter highlights the advantage of using privileged structures to aid in "designing in" a desired pharmacological profile. We were able to use these approaches to obtain a key compound which displayed activity at all three intended receptors (M_1R, D_2R and 5-$HT_{2A}R$).

Chapter 5, which is formatted for submission to the *Journal of Medicinal Chemistry*, explored the development of fluorescently labelled ligands targeting the D_2R. Due to the lack of fluorescent tools for the D_2R, the final series of compounds represent ideal starting points for further optimization in addition to three key fluorescently labelled ligands based on the high affinity antagonist 2-MPP-SB269652. The three fluorescently labelled ligands identified, showed specific cell membrane binding for the D_2R and very weak non-specific binding. Due to time constraints the ligands were not optimised into a competition based binding assay. Despite this, their use in such an application would allow the possibility of a HTS approach to identify novel ligands for the D_2R that could be used to design new drugs for the D_2R or to develop further DMLs.

Overall, this thesis studied four key receptors (D_2R, M_1/M_4 mAChRs and 5-$HT_{2A}R$) that are all directly involved in schizophrenia and also have implications in other CNS disorders. A variety of different medicinal chemistry techniques were explored and often in combination with each

other. The chapters in this thesis, whilst all revolve around similar themes, all stand alone and are either published, submitted or prepared manuscripts for submission as research papers.

Future prospects

Chapter 2

As the literature for PAMs targeting the M_4 mAChR is currently dominated by analogues with a thienopyridine core (refer to overview in chapter 1), future work may involve synthesising new scaffolds. Particularly since no PAMs based on the thienopyridine scaffold have managed to progress through to clinical trials due to encountering difficulties in selectivity, species variability and problems with ADME, there is likely a need to move away from this core. There is currently no solved x-ray crystal structure for the M_4 mAChR with an allosteric ligand. Consequently, there is only speculation about the location of the allosteric pocket, the mechanism of action of allosteric ligands at this receptor and whether it is similar to the other receptor subtypes in this family. Therefore, further developments of new PAMs at this receptor may help to gain more SAR knowledge about the allosteric pocket and the way allosteric ligands bind to this receptor.

Chapter 3

As a direct follow up to the series of partial agonists published in chapter 3, the bias profile of some of the key compounds could be further profiled in other signalling pathways. This may help to further elucidate what pathways are important for bias at the D_2R. The ligands could also be tested *in vivo* in models for schizophrenia to confirm their usefulness as antipsychotics, and to further probe the relationship between antipsychotic efficacy and bias. Additionally, by following the model pharmacophore outlined in chapter 3, there is also the possibility of exploring other D_2R privileged structures which could be used for the development of new antagonists and partial agonists.

Chapter 4

The privileged structures explored in chapter 4 represent a small proportion of scaffolds common to the D_2 or D_2/5-HT_{2A} receptors. Since the orthosteric site at the D_2R is able to tolerate a variety of different structural modifications to ligands and still maintain relatively good activity in most cases, there are numerous antipsychotics that could be utilised in the DML approach that may be better tolerated at the M_1 mAChR. An obvious component that needs optimisation is the putative M_1 allosteric agonist LuAE51090. Not all compounds retained agonism at the M_1 mAChR and for the compound that did, it was a weak partial agonist compared to LuAE51090. Therefore it may be essential to incorporate other structural aspects of LuAE51090 that may have been missed during the merging process. Alternatively, bitopic ligands such as AC-42, TBPB or 77-LH-28-1 (chapter 1) may be suitable ligands for further development into DMLs. Strategies for combining two separate fragments should look at merging at both ends of a single molecule. For example the M_1 mAChR bitopic agonist TBPB could be merged with the privileged structures derived from the antipsychotics ziprasidone and risperidone (which displayed high binding affinities at the D_2R and 5-$HT_{2A}R$ in chapter 4) at both ends (Figure 1). This may give the molecule a better chance of retaining any M_1 activity rather than investigating one side only.

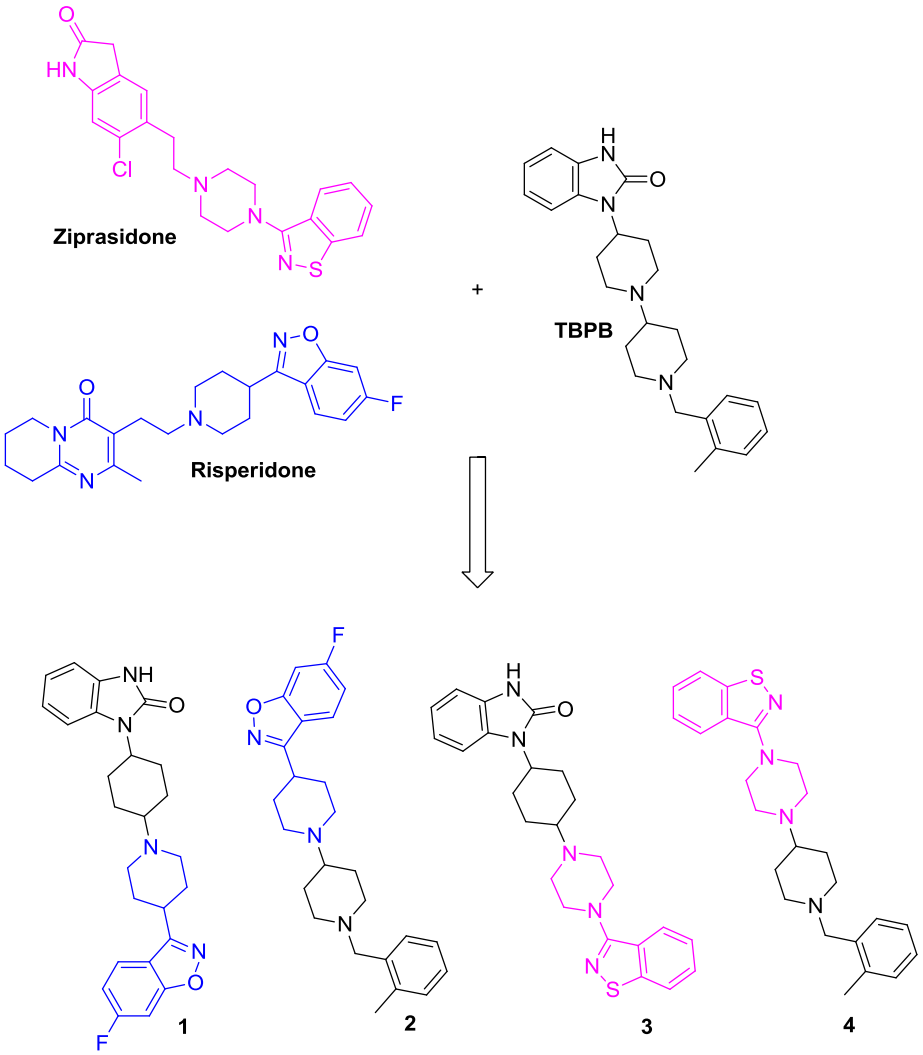

Figure 1. Merging antipsychotics ziprasidone and risperidone with the M_1 mAChR bitopic agonist TBPB to give potential DMLs **1-4**.

Chapter 5

The results represented in chapter 5 are an initial SAR study for fluorescently labelled ligands targeting the D_2R, therefore the ligands used may need further refinement. As it has been demonstrated in the literature and through work in this thesis (chapter 2) that small structural changes to allosteric modulators can have a large impact on their modulatory properties, it may be difficult to make a fluorescent derivative of SB269652. A variety of congeners would need to be synthesised first to get an indication if simple alkyl chains are tolerated at different positions on the indole before fully functionalising with a fluorophore. Furthermore, clozapine and ropinirole derivatives were all synthesised to occupy a certain chemical space, however as nearly

all fluorescent derivatives encountered a loss in binding affinity, it would suggest that either the fluorophores may require a longer or shorter linker to either maintain the affinity or enhance it. Additionally, in cases where a particularly long alkyl linker is required, the use of PEG linkers may prove useful to assist in the water solubility of the drugs for pharmacological testing.

Exploring other D_2 ligands for development as fluorescently labelled ligands is also viable future work. Although, this will require a great deal of SAR around the initial compounds first to find suitable linking points before functionalising with a fluorophore. For instance aripiprazole could be used as a different functionality to the previous ligands explored (partial agonist). It could be assumed that the 2,3-dichlorophenylpiperazine moiety present in aripiprazole resides in the orthosteric pocket at the D_2R due to possessing the crucial ionisable nitrogen. Therefore linking a fluorophore through the dihydroquinolinone motif could provide a suitable tethering point (Figure 2). Notable ligands may also be optimised as fluorescently labelled ligands for the M_1 mAChR to be used in a competition based binding assay to screen for new chemical compounds and scaffolds.

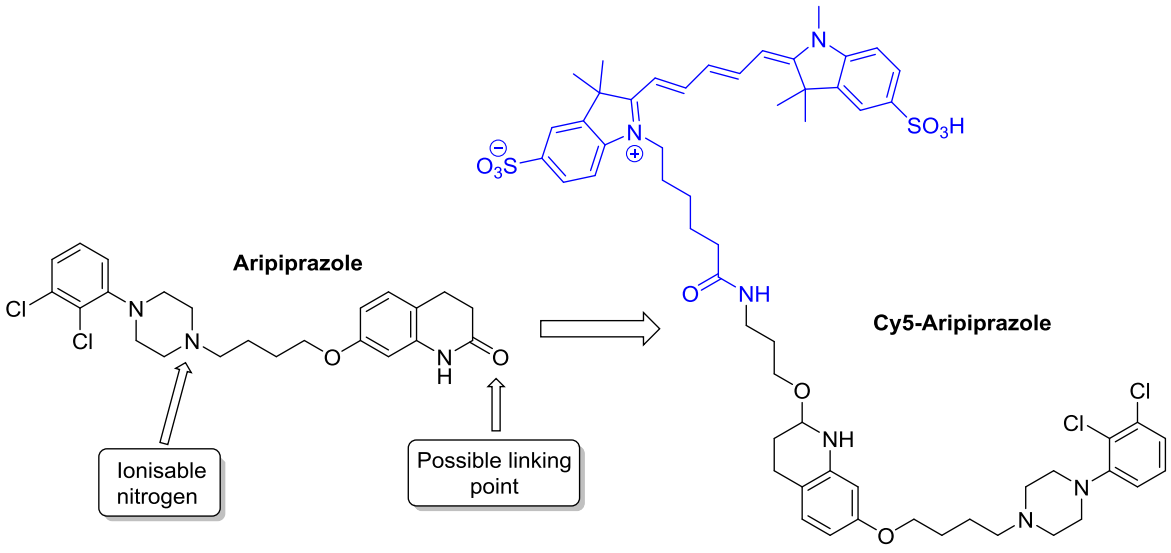

Figure 2. Functionalising aripiprazole with the fluorophore Cy5.

Appendices

Appendix 1- Chapter 3 unpublished Supporting Information

Synthesis, characterization and testing of methoxy substituted derivatives of SB269652

General procedure work up: The solvent was removed in vacuo and the resulting residue dissolved in dichloromethane (20 mL) and partitioned between sodium bicarbonate (30 mL). The aqueous phase was further extracted with 3 × 10 mL portions of dichloromethane. The organic layers were then collected and washed with water (30 mL), brine (30 mL), dried over anhydrous sodium sulfate, filtered and concentrated to give the crude product. To remove excess HMPA, the crude product was dissolved in ethyl acetate and washed with 3 × 20 mL portions of 2 M brine. Purification of the product was achieved via column chromatography ($CHCl_3$/MeOH: 2%).

***N*-((*trans*)-4-(2-(7-Cyano-3,4-dihydroisoquinolin-2(1*H*)-yl)ethyl)cyclohexyl)-4-methoxy-1*H*-indole-2-carboxamide (1).**

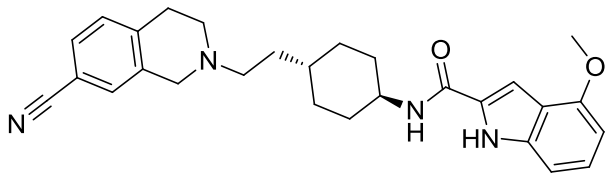

4-Methoxy-1*H*-indole-2-carboxylic acid (35 mg, 0.18 mmol) and *N*,*N*-diisopropylethylamine (0.04 mL, 0.20 mmol) was added to dimethylformamide (5 mL) under N_2 at room temperature. BOP (85 mg, 0.19 mmol) was then added and the reaction left to stir for 5-10 mins. 2-(2-((*trans*)-4-Aminocyclohexyl)ethyl)-1,2,3,4-tetrahydroisoquinoline-7-carbonitrile (57 mg, 0.20 mmol) was then added slowly to the reaction mixture and stirred at room temperature for overnight. Workup according to the general procedure gave the product as a beige solid (47 mg,

56%). ^{1}H NMR (d_6-DMSO) δ 1.06 (m, 2H), 1.28-1.34 (m, 3H), 1.45 (dd, *J* 14.4, 6.8 Hz, 2H), 1.79-1.88 (m, 4H), 2.48 (m, 2H), 2.67 (m, 2H), 2.88 (m, 2H), 3.58 (s, 2H), 3.74 (m, 1H), 3.87 (s, 3H), 6.49 (d, *J* 7.4 Hz, 1H), 6.99-7.09 (m, 2H), 7.24 (m, 1H), 7.31 (d, *J* 8.4 Hz, 1H), 7.56-7.57 (m, 2H), 8.13 (d, *J* 8.1 Hz, 1H), 11.50 (d, *J* 1.7 Hz, 1H). ^{13}C NMR (d_6-DMSO) δ 28.9 (CH_2), 31.7 (CH_2), 32.3 (CH_2), 33.6 (CH_2), 34.7 (CH), 48.2 (CH), 49.8 (CH_2), 54.8 (CH_2), 55.0 (CH_3), 55.3 (CH_2), 99.2 (CH), 100.1 (CH), 105.4 (CH), 108.2 (C), 118.1 (C), 119.1 (C), 124.1 (CH), 129.5 (CH), 129.7 (CH), 130.4 (CH), 130.6 (C), 136.7 (C), 137.7 (C), 140.6 (C), 153.6 (C), 160.1 (C). HPLC purity (λ= 214 nm): 100% t_R 6.32 min. HRMS (ESI)-TOF (*m/z*): $[M+H]^+$ 457.2604 calcd for $C_{28}H_{32}N_4O_2$; found $[M+H]^+$ 457.2614.

***N*-((*trans*)-4-(2-(7-Cyano-3,4-dihydroisoquinolin-2(1*H*)-yl)ethyl)cyclohexyl)-5-methoxy-1*H*-indole-2-carboxamide (2).**

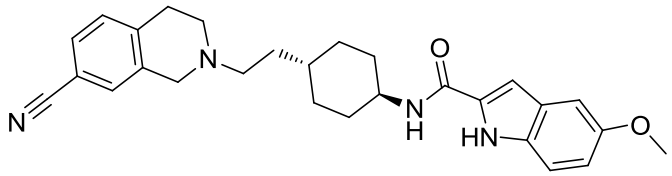

5-Methoxy-1*H*-indole-2-carboxylic acid (29 mg, 0.15 mmol) and *N*,*N*-diisopropylethylamine (0.03 mL, 0.17 mmol) was added to dimethylformamide (5 mL) under N_2 at room temperature. BOP (70 mg, 0.16 mmol) was then added and the reaction left to stir for 5-10 mins. 2-(2-((*trans*)-4-Aminocyclohexyl)ethyl)-1,2,3,4-tetrahydroisoquinoline-7-carbonitrile (47 mg, 0.17 mmol) was then added slowly to the reaction mixture and stirred at room temperature for overnight. Workup according to the general procedure gave the product as a white solid (39 mg, 56%). ^{1}H NMR (d_6-DMSO) δ 1.06 (m, 2H), 1.28-1.37 (m, 3H), 1.44 (dd, *J* 14.5, 6.8 Hz, 2H), 1.80-1.89 (m, 4H), 2.48 (m, 2H), 2.67 (m, 2H), 2.88 (m, 2H), 3.58 (s, 2H), 3.74 (m, 1H), 3.75 (s, 3H), 6.82 (dd, *J* 8.9, 2.5 Hz, 1H), 7.04-7.06 (m, 2H), 7.31 (d, *J* 9.0 Hz, 2H), 7.56-7.57 (m, 2H), 8.13 (d, *J* 8.1 Hz, 1H), 11.35 (d, *J* 1.7 Hz, 1H). ^{13}C NMR (d_6-DMSO) δ 28.9 (CH_2), 31.7 (CH_2), 32.3 (CH_2), 33.6 (CH_2), 34.8 (CH), 48.2 (CH), 49.8 (CH_2), 54.8 (CH_2), 55.3 (CH_3), 55.4 (CH_2),

101.9 (CH), 102.2 (CH), 108.2 (C), 113.1 (CH), 114.2 (CH), 119.1 (C), 127.4 (C), 129.4 (CH), 129.7 (CH), 130.4 (CH), 131.6 (C), 132.3 (C), 136.7 (C), 140.7 (C), 153.7 (C), 160.2 (C). HPLC purity (λ= 214 nm): 100% t_R 5.98 min. HRMS (ESI)-TOF (*m/z)*: $[M+H]^+$ 457.2604 calcd for $C_{28}H_{32}N_4O_2$; found $[M+H]^+$ 457.2620.

***N*-((*trans*)-4-(2-(7-Cyano-3,4-dihydroisoquinolin-2(1*H*)-yl)ethyl)cyclohexyl)-6-methoxy-1*H*-indole-2-carboxamide (3).**

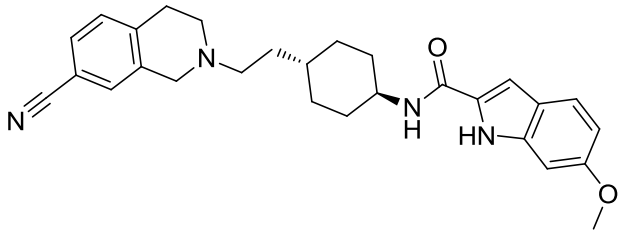

6-Methoxy-1*H*-indole-2-carboxylic acid (35 mg, 0.18 mmol) and *N*,*N*-diisopropylethylamine (0.04 mL, 0.20 mmol) was added to dimethylformamide (5 mL) under N_2 at room temperature. BOP (85 mg, 0.19 mmol) was then added and the reaction left to stir for 5-10 mins. 2-(2-((*trans*)-4-Aminocyclohexyl)ethyl)-1,2,3,4-tetrahydroisoquinoline-7-carbonitrile (57 mg, 0.20 mmol) was then added slowly to the reaction mixture and stirred at room temperature for overnight. Workup according to the general procedure gave the product as a white solid (40 mg, 47%). ^{1}H NMR (d_6-DMSO) δ 1.07 (m, 2H), 1.29-1.35 (m, 3H), 1.45 (dd, *J* 14.4, 6.8 Hz, 2H), 1.79-1.88 (m, 4H), 2.48 (m, 2H), 2.66 (m, 2H), 2.88 (m, 2H), 3.57 (s, 2H), 3.74 (m, 1H), 3.76 (s, 3H), 6.68 (dd, *J* 8.7, 2.3 Hz, 1H), 6.88 (d, *J* 2.2 Hz, 1H), 7.07 (d, *J* 1.5 Hz, 1H), 7.31 (d, *J* 8.4 Hz, 1H), 7.46 (d, *J* 8.7 Hz, 1H), 7.56-7.57 (m, 2H), 8.06 (d, *J* 8.1 Hz, 1H), 11.32 (d, *J* 1.6 Hz, 1H). ^{13}C NMR (d_6-DMSO) δ 28.9 (CH_2), 31.8 (CH_2), 32.4 (CH_2), 33.6 (CH_2), 34.8 (CH), 48.1 (CH), 49.8 (CH_2), 54.8 (CH_2), 55.1 (CH_3), 55.4 (CH_2), 94.2 (CH), 102.7 (CH), 108.2 (C), 110.8 (CH), 119.1 (C), 121.3 (C), 122.2 (CH), 129.4 (CH), 129.7 (CH), 130.4 (CH), 130.9 (C), 136.7 (C), 137.3 (C), 140.7 (C), 156.9 (C), 160.3 (C). HPLC purity (λ= 214 nm): 93% t_R 6.25 min. HRMS (ESI)-TOF (*m/z)*: $[M+H]^+$ 457.2604 calcd for $C_{28}H_{32}N_4O_2$; found $[M+H]^+$ 457.2606.

***N*-((*trans*)-4-(2-(7-Cyano-3,4-dihydroisoquinolin-2(1*H*)-yl)ethyl)cyclohexyl)-7-methoxy-1*H*-indole-2-carboxamide (4).**

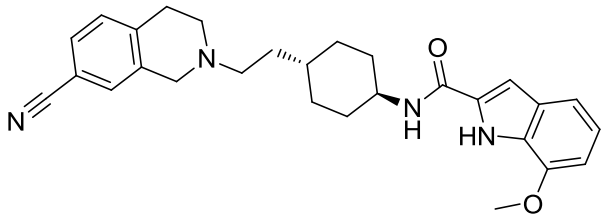

7-Methoxy-1*H*-indole-2-carboxylic acid (30 mg, 0.16 mmol) and *N*,*N*-diisopropylethylamine (0.03 mL, 0.17 mmol) was added to dimethylformamide (5 mL) under N_2 at room temperature. BOP (73 mg, 0.16 mmol) was then added and the reaction left to stir for 5-10 mins. 2-(2-((*trans*)-4-Aminocyclohexyl)ethyl)-1,2,3,4-tetrahydroisoquinoline-7-carbonitrile (49 mg, 0.17 mmol) was then added slowly to the reaction mixture and stirred at room temperature for overnight. Workup according to the general procedure gave the product as pale yellow solid (53 mg, 74%). ^{1}H NMR ($CDCl_3$) δ 1.16-1.30 (m, 4H), 1.35 (m, 1H), 1.57 (dd, *J* 15.1, 6.8 Hz, 2H), 1.87 (m, 2H), 2.13 (m, 2H), 2.61 (m, 2H), 2.81 (m, 2H), 3.00 (m, 2H), 3.69 (s, 2H), 3.96 (m, 1H), 3.97 (s, 3H), 6.05 (d, *J* 8.2 Hz, 1H), 6.71 (d, *J* 7.3 Hz, 1H), 6.81 (d, *J* 2.3 Hz, 1H), 7.06 (t, *J* 7.9 Hz, 1H), 7.23 (t, *J* 7.6 Hz, 2H), 7.35 (m, 1H), 7.43 (dd, *J* 7.9, 1.6 Hz, 1H), 9.34 (s, 1H). ^{13}C NMR ($CDCl_3$) δ 29.2 (CH_2), 32.0 (CH_2), 33.2 (CH_2), 33.8 (CH_2), 35.3 (CH), 48.9 (CH), 50.2 (CH_2), 55.4 (CH_2), 55.5 (CH_3), 56.03 (CH_2), 102.3 (CH), 103.6 (CH), 109.7 (C), 114.2 (CH), 119.2 (C), 121.2 (CH), 127.4 (C), 128.9 (C), 129.7 (CH), 129.9 (CH), 130.5 (CH), 130.8 (C), 136.1 (C), 140.3 (C), 146.7 (C), 160.7 (C). HPLC purity (λ= 214 nm): 94% t_R 6.39 min. HRMS (ESI)-TOF (*m/z*): $[M+H]^+$ 457.2604 calcd for $C_{28}H_{32}N_4O_2$; found $[M+H]^+$ 457.2602.

Table 1. Compounds **1-4** tested in pERK1/2 assays at the D_2R[a]

Compound	pK_B ± SEM (K_B, nM)	Log α ± SEM
SB269652[b]	6.31 ± 0.25 (490)	-0.98 ± 0.14
1[b]	6.21 ± 0.27 (617)	-0.52 ± 0.11
2[c]	8.70 ± 0.32 (2.0)	-
3[c]	7.60 ± 0.17 (25.1)	-
4[c]	7.29 ± 0.13 (51.3)	-

[a]Data are the mean of three experiments ± SEM performed in duplicate. All compounds are tested at a concentration range between 10 µM- 1 nM or 30 µM- 300 nM for SB269652 and interacted with varying concentrations of dopamine (10 µM- 0.01 nM). Compounds are fit to an allosteric model[b] or Gaddum Schild plot[c]

Appendix 2

List of publications

Szabo, M.; Klein Herenbrink, C.; Christopoulos, A.; Lane, J. R.; Capuano, B., Structure–activity relationships of privileged structures lead to the discovery of novel biased ligands at the dopamine D_2 receptor. *J. Med. Chem.* **2014,** *57* (11), 4924-4939.

Szabo, M.; Agostino, M.; Malone, D. T.; Yuriev, E.; Capuano, B., The design, synthesis and biological evaluation of novel URB602 analogues as potential monoacylglycerol lipase inhibitors. *Bioorg. Med. Chem. Lett.* **2011,** *21* (22), 6782-6787.

Awards

Oct 2014	Postgraduate Publication Award
May 2012	CTx Post-Graduate and MRGS Student Travel Award
Jan 2010	Monash Honours Jubilee Scholarship

Conference presentations

Szabo, M et al. *Designed Multiple Ligands Targeting Dopamine D_2 and Muscarinic M_1 Receptors*, MIPS advisory board. Monash University, Parkville, Melbourne, Australia. 30th June 2014. (Poster presentation)

Szabo, M et al. *Designed Multiple Ligands Targeting Dopamine D_2 and Muscarinic M_4 Receptors*:

- Lundbeck Pharmaceutical Company. Copenhagen, Denmark. 30th August 2012. (Oral presentation)

- EFMC-ISMC 22nd International Symposium on Medicinal Chemistry. Berlin, Germany. 2-6th September, 2012. (Poster presentation)
- Faculty of Pharmacy and Pharmaceutical Sciences 7th Annual Postgraduate Research Symposium. Monash Institute of Pharmaceutical Sciences, Melbourne, Australia. 26th September, 2012. (Poster presentation)
- Cancer Therapeutics CRC (CTx) Annual Postgraduate Student Symposium. Walter and Eliza Hall Insitute, Melbourne Australia. 16th October 2012. (Poster presentation)
- Molecular Pharmacology of G Protein-Coupled Receptor. Monash University, Parkville, Melbourne, Australia. 6-8th December 2012. (Poster presentation)

Szabo, M et al. *URB602 Analogues as Potential Monoacylglycerol Lipase Inhibitors*, RACI Biomolecular Division Conference: Biomolecular at the Beach. Torquay, Australia. 4-8th December, 2011. (Poster presentation)